Integrin-Ligand Interactions and Cytokine Production by Monocytic Cells

Adrienne Lesley Edkins
Division of Biochemistry and Molecular Biology, IBLS
University of Glasgow
May 2008

A thesis submitted for award of the degree of
Doctor of Philosophy

Abstract

CD23 is a Type II glycoprotein that exists in both membrane-bound (mbCD23) and soluble (sCD23) forms and functions as the low affinity receptor for IgE. CD23 interacts with a range of proteins to fulfil its function *in vivo*. Through interactions with its ligands IgE and CD21, CD23 regulates the levels of IgE in serum. Soluble CD23 also interacts with members of the integrin family of membrane receptors. Integrins are heterodimeric transmembrane receptors that participate in bidirectional signalling across membranes and have a critical role in cellular adhesion reactions. CD23 interacts with four integrins, αVβ3 and αVβ5 from the αV integrin family, and αMβ2 and αXβ2, from the β2 family of integrins.

Using peptide array technology, we identified set of overlapping peptides derived from the soluble CD23 sequence that interact with integrins expressed on the surface of monocytic cells and with purified αVβ3 and αVβ5 integrins in *in vitro* Biacore assays. These peptides all contained a common basic tripeptide motif, termed the Arg-Lys-Cys (RKC) motif. Integrins traditionally recognise and bind the Arg-Gly-Asp (RGD) tripeptide in their ligands in a cation-dependent manner. However, the *in vitro* interaction between RKC-containing peptides and purified integrins was determined to be cation-independent, salt-sensitive and independent of RGD binding. The interaction was blocked by full length CD23. Substitution of the residues in the RKC motif reduced or abolished binding of the peptides to integrins expressed on cells and *in vitro*, as measured by Biacore analysis, and abolished the competition with CD23. Taken together, these data suggest that the RKC motif is the site in CD23 that is recognised and bound by αVβ3 and αVβ5 integrins. The RKC motif can be considered a novel recognition motif for integrins, as it is cation-independent, and its binding is not blocked by the presence of RGD-containing integrin ligands. Therefore it is likely that the RKC motif interacts with integrins at a site other than that used for RGD-binding, similar to the interactions that have been described for the binding of the HIV Tat protein.

The interaction between sCD23 and its integrin receptors is important in the regulation of cytokine production by monocytic cells. Most monocytic cells will express a combination of the different CD23-binding integrins simultaneously and, therefore, the cytokine output of that cell will be the net result of the

interaction of CD23 with a combination of integrins. We used monoclonal antibodies to investigate the role of individual integrins in cytokine production. Antibodies were selected to allow comparision of the cytokine response between, a) integrin families, b) integrin subunits, and c) integrin epitopes.

The cytokine profile induced by integrin ligation did not differ between the αV and ß2 integrin families, although the concentration of cytokines produced varied depending on the heterodimer targeted. However, within a particular family, cytokine production induced by integrin ligation was specific and relied on the recognition of a precise epitope on the integrin. Cytokine production by CD23-binding integrins appears to require the ligation of the α subunit of the integrin heterodimer. We identified an antibody directed against the αVß3 integrin that induced high levels of cytokine production. Cytokine production following ligation of the integrin with this antibody was dependent on activation of the ERK/MAPK pathway in cells. This production of cytokines and phosphorylation of ERK was enhanced by the addition of macrophage colony stimulating factor (M-CSF) and partially inhibited by an anti-TLR-2 antibody. Chronic stimulation (<3 days) of THP-1 cells with the anti-αVβ3 antibody in the presence of M-CSF led to morphological changes in the cell line associated with the development of a more macrophage-like phenotype and the continued production of cytokines. Analysis of the changes in cell surface marker expression and cytokine profiles suggested that the THP-1 cells had undergone an M2b programme of macrophage activation in response to αVß3 ligation. Data presented herein reinforce the importance of the role of integrins in the control of adhesion-independent signalling pathways in suspension cells.

Table of Contents

List of Tables

List of Figures

Acknowledgements

I gratefully acknowledge the support and assistance of the following people, all of whom have been indispensable to the completion of this research and thesis.

- Professor Bill Cushley, my supervisor, for his dedication, diligence and continued support, encouragement and guidance.

- Professors Brad Ozanne, Gordon Lindsay and Richard Cogdell for their support and encouragement.

- Dr Sharon Kelly, for the assistance with the Biacore experiments and data analysis.

- Dr Gillian Borland for her guidance and support over the last four years

- Dr Mridu Acharya, who has been a daily source of support and encouragement. Thank you for being a true friend, never being too busy to discuss a new idea and always being ready to help whenever required. I look forward to establishing the Zimbo-Nepali Research Initiative and to future bad-hair days!

- Dr Lindsay MacLellan for her support and friendship during the time we shared in Lab 232.

- To all the other members of Lab 232/233, past and present, for their support and friendship.

- The Wellcome Trust PhD group of 2003, Dr Christine Kohlhaas, Dr Alex Segref, Dr Jana Vavrova, Dr Elizabeth Rideout, Dr Colm Nestor, Dr Theo Kantidakis and Dr Mridu Acharya, for your friendship and support throughout the last 4 years. It has been a truly unique environment and I count myself very lucky to have had the opportunity to know and work with you all. I will cherish the memories and I look forward to our continued contact, socially and scientifically, in the future.

For Fraser and Maureen, thank you for everything

Declaration

I hereby declare that the work presented in this thesis is my own, except where otherwise cited or acknowledged. No part of this thesis has been presented for any other degree.

Adrienne Edkins

Abbreviations

ADAM	A Disintegrin and Metalloproteinase Protein
ADMIDAS	Adjacent to metal ion dependent adhesion site
Akt/PKB	Protein Kinase B
ALL	Acute lymphoblastic leukaemia
AML	Acute myelogenous leukaemia
BSA	Bovine serum albumin
βTD	Beta tail domain
CLL	Chronic lymphocytic leukaemia
DAPI	4',6-Diamidino-2-Phenylindole
Db-cAMP	Dibutryl-cyclic adenosine monophosphate
E.coli	*Escherichia coli*
ECM	Extracellular matrix
EBV	Epstein-Barr virus
ECL	Enhanced chemiluminescence
EDTA	Ethylenediaminetetraacetic Acid
EGF-like	Epidermal growth factor-like
ERK	Extracellular signal-regulated kinase
ELISA	Enzyme linked immunosorbent assay

ELR	Glu-Leu-Arg motif
EMSA	Electrophoretic mobility shift assay
ACS	Fluorescence-activated cell sorting
FAK	Focal adhesion kinase
FCS	Foetal calf serum
FITC	Fluorescein-isothiocyanate
FN	Fibronectin
FBGN	Fibrinogen
GEF	Guanine exchange factor
GF	Growth factor
GFR	Growth Factor Receptor
GM-CSF	Granulocyte/Macrophage colony stimulating factor
GPCR	G-protein-coupled receptor
I-domain	Inserted-domain
Ig	Immunoglobulin
ICAM-1	Intracellular cell adhesion molecule
IL	Interleukin
IFN	Interferon
IkB	Inhibitory kB
IκK	IκB kinase

IRAK-1	Interleukin Receptor Associated Kinase-1
LP	Long peptide
LPS	Lipopolysaccharide
LIMBS	Ligand induced metal binding site
M-CSF	Macrophage colony stimulating factor
MAb	Monoclonal antibody
Mal	MyD88 adapter-like
MAPK	Mitogen Activated Protein Kinase
mbCD23	Membrane-bound CD23
MHC	Major Histocompatibility Complex
MIDAS	Metal ion dependent adhesion site
MIP-1ß	Macrophage inflammatory protein-1beta
MyD88	Myeloid differentiation factor 88
NFkB	Nuclear factor-kB
NO	Nitric oxide
PBS	Phosphate buffered saline
PBST	Phosphate buffered saline with Tween-20
PCR	Polymerase chain reaction
PDGF	Platelet-derived growth factor
PE	Phycoerythrin

PI3K	Phosphatidyl inositol-3-kinase
PSI	Plexin-Semaphorin-Integrin
RA	Rheumatoid arthritis
RANKL	Receptor activator for NFκB ligand
RANTES	Regulated on Activation Normal T cell Expressed and Secreted
RGD	Arg-Gly-Asp
RKC	Arg-Lys-Cys
RIPA	Radio-immunoprecipitation assay
RT-PCR	Reverse transcriptase-polymerase chain reaction
RTK	Receptor tyrosine kinase
sCD23	Soluble CD23
SDF-1	Stromal cell-derived factor-1
SDS-PAGE	Sodium-Dodecyl-Sulphate Polyacrylamide Gel Electrophoresis
SFK	Src-family kinase
SI	Stimulation Index (equivalent to fold stimulation)
SLE	Systemic lupus erythematosus
SPR	Surface plasmon resonance
TAM	Tumour-associated macrophage
TBS	Tris-buffered Saline
TBST	Tris-buffered Saline with Tween-20

TIR	Toll/IL-1 receptor
TIRAP	TIR domain-containing adapter protein
TLR	Toll-like receptor
TNF	Tumor necrosis factor
TRACP	Tartrate-resistant acid phosphatase
TRAF-6	TNF receptor-associated factor-6
TRIF	TIR-domain-containing adapter inducing interferon-β
TAK-1	Transforming growth factor-b-activated kinase-1
TLR	Toll-like receptor
VCAM-1	Vascular cell adhesion molecule
VEGF	Vascular endothelial growth factor
VN	Vitronectin

1 LITERATURE REVIEW

1.1 The Immune System

The immune system is the term used to describe the collection of mechanisms used by an organism to protect itself from injury and disease. It is composed of the innate and adaptive immune systems which work in conjunction to defend and heal the body. The adaptive immune system is a collection of highly specialised cells and processes that combat infections. The adaptive immune response is specialised, and recognises and mounts a specific immune response against a particular pathogen and also stores a memory of that infection for later challenges. The major effector cells of the adaptive immune response are B and T lymphocytes, which have distinct roles in cell-mediated adaptive immunity. The adaptive immune system is activated by the non-specific innate immune response, which often forms the first line of defence against infection [1].

The innate immune system is an evolutionarily conserved mechanism of defence against pathogens and is capable of being activated in a non-specific manner. This means that the response to infection is rapid and does not rely on prior encounter with a pathogen to mount an innate immune response against it. The innate immune system, unlike the adaptive immune system, does not confer long-lasting or protective immunity to the host. It is comprised of cellular components, such as monocytes and neutrophils, and non-cellular components, such as the complement system, which work in conjunction to mount the innate defense against infection [1].

1.1.1 Cells of the Innate Immune System

The innate immune system is comprised of a number of leukocytes, with defined functions. These include basophils, eosinophils, neutrophils, mast cells and monocytes, each of which has a specific role in innate immunity. Neutrophils defend the body against bacterial or fungal infection and are usually first responders to microbial infection. Eosinophils are primarily involved in combating parasitic infections and are also the predominant cells in allergic reactions. Basophils are chiefly responsible for allergic and antigen responses by the release of the inflammatory mediator, histamine. Of particular interest in this thesis, is the role of monocytes and macrophages in innate immunity and inflammation [2].

1.1.2 Monocytic cells

Monocytes are leukocytes that play a major role in the innate immune system. Monocytes are the precursors for a number of terminally-differentiated cells of the body, including cells such as macrophages [3], dendritic cells [4], and osteoclasts [5]. Monocytes develop in the bone marrow from a pluripotent stem cell via the common myeloid progenitor cell, which is the precursor for all cells of the granulocyte lineage. The earliest stage is the monoblast, which develops into a mature monocyte in the blood via a promonocyte stage. Mature monocytes circulate in the blood, where they constitute about 3-8% of the total leukocyte population. Monocytes also migrate into the tissues where they differentiate into macrophages, depending on the local environment [2]. They are phagocytic cells, which bind and engulf pathogens directly or via opsonising antibodies or complement. They also present antigen to T cells and produce a range of cytokines and chemokines. In the presence of specific stimuli, macrophages undergo regulated programmes of activation that give rise to either pro-inflammatory or anti-inflammatory macrophages (discussed further in Chapter 5) [6-8].

1.1.3 Cytokines

Cytokines are small (8-30kDa), water-soluble proteins that are secreted by a wide variety of cells and play an important role in cellular communication. Cytokines mediate their effects by binding to their cognate receptors and are critical mediators of both the innate and adaptive immune responses [9]. In certain cases, cytokines will share receptors and receptor subunits and have overlapping functions. They are important in the recruitment, development and maturation or differentiation of cell types, as well as playing a role in a range of immunological situations. Cytokines can be broadly classified as either pro-inflammatory or anti-inflammatory, although often this is misleading, as the net effect of the inflammatory response will be a result of the balance between pro- and anti-inflammatory mediators. The nature, duration and extent of cellular activities induced by a certain cytokine will be affected by the individual cytokine concentration and the combinations of other cytokines present. The target cell type, the micro-environment of that cell and the characteristics of neighbouring cells will also govern the effect of a particular cytokine [10].

1.1.3.1 Pro-inflammatory Cytokines

Pro-inflammatory cytokines are those that generally favour the development of an inflammatory state. The group includes cytokines such as tumour necrosis factor-alpha (TNF-α), interferon-gamma (IFN-γ), interleukin-6 (IL-6) and interleukin-1 alpha/beta (IL-1α/β), which are responsible for early inflammatory responses. Other inflammatory cytokines include transforming growth factor-beta (TGF-β), interleukin-12 (IL-12) and interleukin-8 (IL-8). Pro-inflammatory cytokines induce the inflammatory state and also modulate the production of secondary mediators and the recruitment of immune cells [11].

1.1.3.2 Anti-inflammatory Cytokines

Anti-inflammatory cytokines are those immunomodulatory cytokines that control or counter-act the magnitude of inflammatory responses *in vivo*. They act by inhibiting the production or biological effects of pro-inflammatory cytokines. The major anti-inflammatory cytokines are interleukin-4 (IL-4), interleukin-10 (IL-10) and interleukin-13 (IL-13), but the group also includes interleukin-16 (IL-6), interferon-alpha (IFN-α), transforming growth factor-beta (TGF-β), and interleukin-1 receptor A (IL-1RA) [11].

1.1.3.3 Chemokines

Chemokines are chemotactic cytokines that regulate the migration of different cell types [12]. Chemokines are generally small polypeptides (8-10 kDa) and often exhibit a degree of sequence similarity. All chemokines contain a number of conserved cysteine residues involved in intramolecular disulphide bond formation. Chemokines can be further classified as CXC-chemokines (α-chemokines), CC-chemokines (ß-chemokines), C-chemokines (γ-chemokines) or CX_3C-chemokines (δ chemokines) depending on their structural features and genomic location. Certain α-chemokines also possess an additional Glu-Leu-Arg (ELR) sequence at the N-terminal end. The biological activities of chemokines are mediated by specific receptors, many of which have overlapping ligand specificities and can bind several of different chemokines. These transmembrane receptors belong to the large group of seven transmembrane domain receptors

that contain seven hydrophobic alpha-helical segments, which mediate signalling via coupling to heterotrimeric G-proteins [13].

Chemokines have been shown to exert their effects on distinct subsets of cells. Some chemokines have been shown to induce selective migration of subsets of leukocytes. Chemokines containing the ELR motif are especially chemotactic for neutrophils, while chemokines lacking the ELR motif are chemotactic for other cell types (including monocytes, B-cells, basophils and eosinophils). The combined effects of multiple chemokines will affect the cellular composition at inflammatory sites. The existence of clearly defined subgroups of chemokines on the basis of structural and functional properties illustrates the importance of chemoattractant diversity in the regulation of the leukocytes migration *in vivo* [14, 15].

In addition to mediating cell recruitment, chemokines influence a number of cellular processes, under both physiological and pathological circumstances. Chemokines, such as IL-8, are multi-functional cytokines that influence and enhance inflammation through chemotaxis and activation of cells at inflammatory sites [13]. Certain chemokines activate granulocytes and/or monocytes, induce degranulation and lysosomal enzyme release. Others have a priming effect on immune cells, allowing them to respond to sub-optimal amounts of inflammatory mediators [16]. Chemokines are important during the infection of cells by pathogens, such as the use of the chemokine receptors CXCR-4 and CCR5 as co-receptors for the HIV virus [17-19]. The natural ligands (SDF-1 and RANTES/MIP-1β, respectively) and antagonists of CXCR-4 and CCR5 compete with HIV for binding to these receptors [20]. SDF-1 also has a role in the development and trafficking of cells during haematopoesis [21]. Many chemokines are correlated with a number of pathological conditions including autoimmune diseases [22], chronic inflammatory diseases [23], atherosclerosis and cancer [24].

1.1.4 Inflammation and Disease

Inflammation is the complex vascular response of the body to a biological insult, such as an infection. The successful conclusion of inflammation is the removal of the harmful agent and healing of the wounded tissues. Inflammation can be classified as either acute or chronic. Appropriate inflammation is necessary to

establish the environment required to combat an infection, including factors such as the activation of the complement system, and the recruitment of phagocytic cells and B and T lymphocytes to the inflamed area [13, 25]. However, in certain circumstances, inflammation can arise either due to an inappropriate stimulus or may be altered such that it leads to a disease state. Examples of such inflammatory diseases include disorders such as rheumatoid arthritis (RA), system lupus erythematosis (SLE), Sjogren's syndrome, Crohn's disease and certain cancers [9, 26-28]. A common characteristic connecting a number of the inflammatory disorders described above is the high levels of the low affinity receptor for IgE, CD23 [29, 30].

1.2 The Low Affinity Receptor for IgE (FCεRII / CD23)

CD23 (Blast-2, FcεRII) is a 45 kDa, Type II membrane glycoprotein [31, 32]. CD23 is the only known Ig receptor that is not a member of the immunoglobulin superfamily [32]. Membrane bound CD23 (mbCD23) is cleaved by membrane-associated metalloproteases to yield soluble CD23 (sCD23) fragments of 37kDa, which are subsequently cleaved to yield CD23 species of 33kDa, 29kDa, 25kDa and 16kDa [33, 34]. All fragments contain the C-type lectin domain of CD23 and varying portions of the stalk region. Cleavage of the mbCD23 to yield the 37 kDa species occurs at a site close to the membrane and the single site of N-glycosylation [35]. CD23 can exist as a monomer and trimer in both membrane-bound and soluble forms. These soluble fragments retain many of the activities of membrane associated CD23 and also possess cytokine-like activity [36-41].

CD23 is normally expressed on mature B cells, particularly activated cells, although its expression is significantly altered in a number of pathological conditions [42-54]. The normal levels of CD23 detected in human serum range from 0.5 – 5 ng/mL, with children and neonates having higher levels than adults [42]. In some disorders, such as chronic lymphocytic leukaemia (CLL), elevated levels of CD23 may have prognostic value and may correlate with the progression of the disease [43-47]. Elevated CD23 levels are also observed in disorders such as rheumatoid arthritis, where the levels of $CD23^+$ B cells are increased, as is the level of sCD23 in the serum and synovial fluid [48-56].

In addition to being a marker for certain diseases, sCD23 possesses cytokine-like activities. Soluble CD23 acts as a growth factor for Epstein-Barr transformed cell lines [57, 58], prevents apoptosis of germinal centre B cells [59] and induces differentiation of prothymocytes [60]. These combined activites make CD23 an interesting molecule in the regulation of cell growth and differentiation.

1.2.1 CD23 Structure

At the structural level, CD23 is comprised of a number of distinctive functional domains and motifs that define its activities (Figure 1-1) [32, 61, 62]. The C terminal extracellular domain of CD23 shares structural similarity with the C-type lectin family. The 3-dimensional structure of the lectin head of CD23 has been determined by NMR spectroscopy [62] and X-ray crystallography [63]. The CD23 domain contains two α helices orientated at right angles relative to each other and two antiparallel ß sheets, each made up of four β strands. The structure has a hydrophobic core, containing 7 tryptophans and other highly conserved residues, with 4 disulphide bridges maintaining the tertiary structure. The CD23 lectin domain exhibits a polarity with respect to the distribution of its electrostatic charges. The positive and negative residues of the highly charged surface are located on different faces of the molecule. The authors postulate that this is essential for the interaction of CD23 with itself and its ligands [62].

The stalk domain of CD23 contains 7 hydrophobic repeats that form an alpha helical coiled-coil structure [64]. This region connects the lectin domain to the transmembrane domain and is the site of oligomerisation of CD23 into trimers. The leucine zipper region is near the transmembrane domain and has a 7 amino acid motif, beginning with a Leu or Ile residue, which is repeated 5 times in human CD23 [61]. The stalk is the site of proteolytic cleavage that generates sCD23 species [33, 34]. The N terminus of CD23 is cytoplasmic and associated with the cytoskeleton. There are two forms of CD23, CD23a and CD23b, which differ in the sequence of this region. CD23a contains the sequence 'Met-Glu-Glu-Gly-Gln-**Tyr-Ser-Glu-Ile-Glu**' (MEEGQ**YSEIE**) at the N terminus, while CD23b contains the sequence 'Met-Asn-Pro-Pro-**Ser-Gln-Glu-Ile-Glu**' (MNPP**SQEIE**) [65]. The residues in bold represent the consensus N terminal pentameric sequence for the two splice variants of CD23.

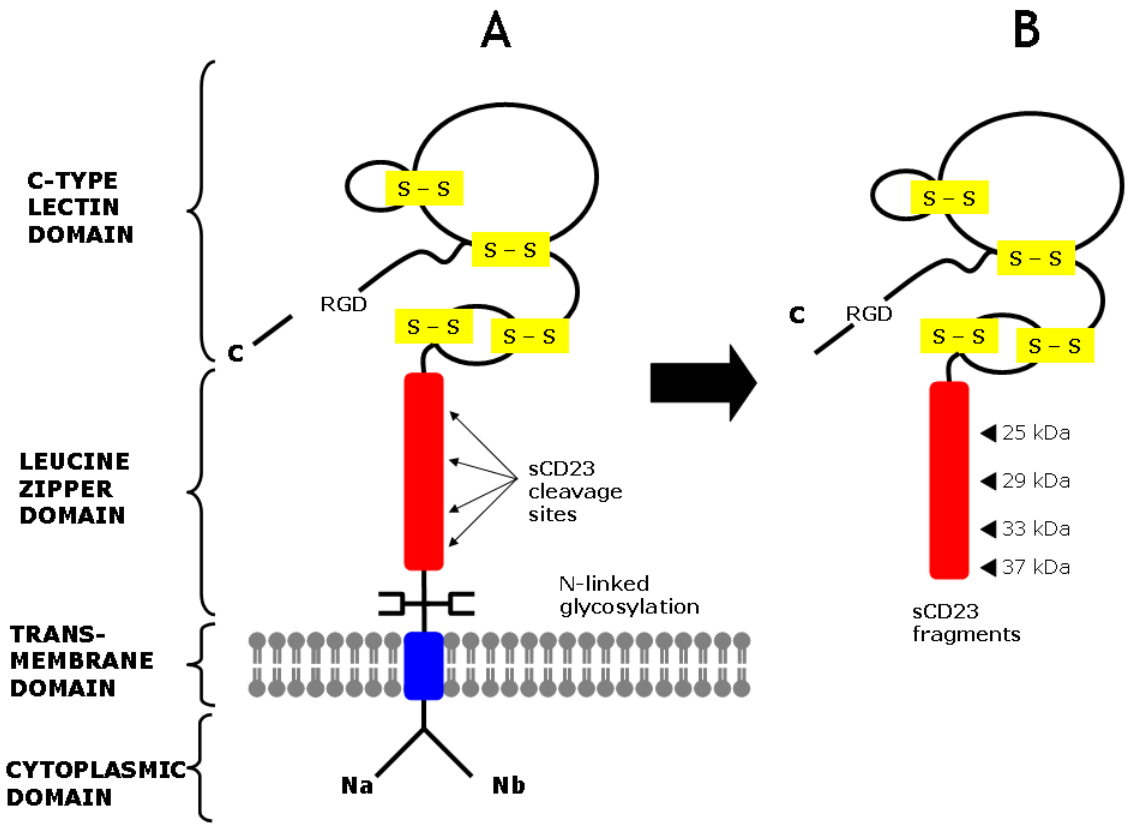

Figure 1-1 Schematic representation of CD23 structure

Membrane-bound (A) and soluble (B) CD23 species are comprised of a number of domains which define their function. Cytoplasmic sequence of mbCD23 can be comprised of either the a or b N terminal sequence.

CD23a is constitutively expressed and confined to certain cell types. CD23b is upregulated by exposure to IL-4 and expressed on a wide range of cell types [66]. The a and b forms of human CD23 have different functions. The Asn-Pro motif of CD23b is associated with phagocytosis, while the Tyr based motif of CD23a is involved in endocytosis [65].

Human CD23 contains an inverse RGD (DGR) sequence near the C terminus. The RGD sequence is a common recognition motif for integrin-mediated binding and is found in a wide range of diverse proteins that are involved in cell adhesion (discussed fully later) [67]. The conformation of this DGR-containing region is not known. The DGR sequence is only found in human CD23 and not in CD23 from other species, although the role of this motif remains undefined. One suggestion is that this DGR sequence (inverse RGD) in CD23 may interact with an inverse 'RGD-binding inhibitory sequence'. This suggestion is based on a similar interaction with respect to the integrin gpIIb/IIIa. In this case, an RGD-binding inhibitory sequence in the platelet integrin gpIIb/IIIa blocks the binding of RGD-containing ligand fibrinogen. Indeed, CD23 contains a possible 'DGR-binding inhibitory motif' in the stalk region near the membrane. Complete definition of the role of the DRG motif will rely on further information on the mechanism of RGD recognition and binding by integrins [61, 68].

1.2.2 CD23 Function

CD23 participates in both protein-protein interactions and protein-carbohydrate interactions. To date, CD23 has been shown to form partnerships with IgE [62, 69], CD21 [62, 70-73], αXß2 and αMß2 [74] (leukocyte integrins) and the vitronectin receptors αVß3 [40] and αVß5 [75] (Figure 1-2). The interaction of mbCD23 and sCD23 with these ligands results in specific events in the cell, particularly in the context of allergy, inflammation and cytokine production.

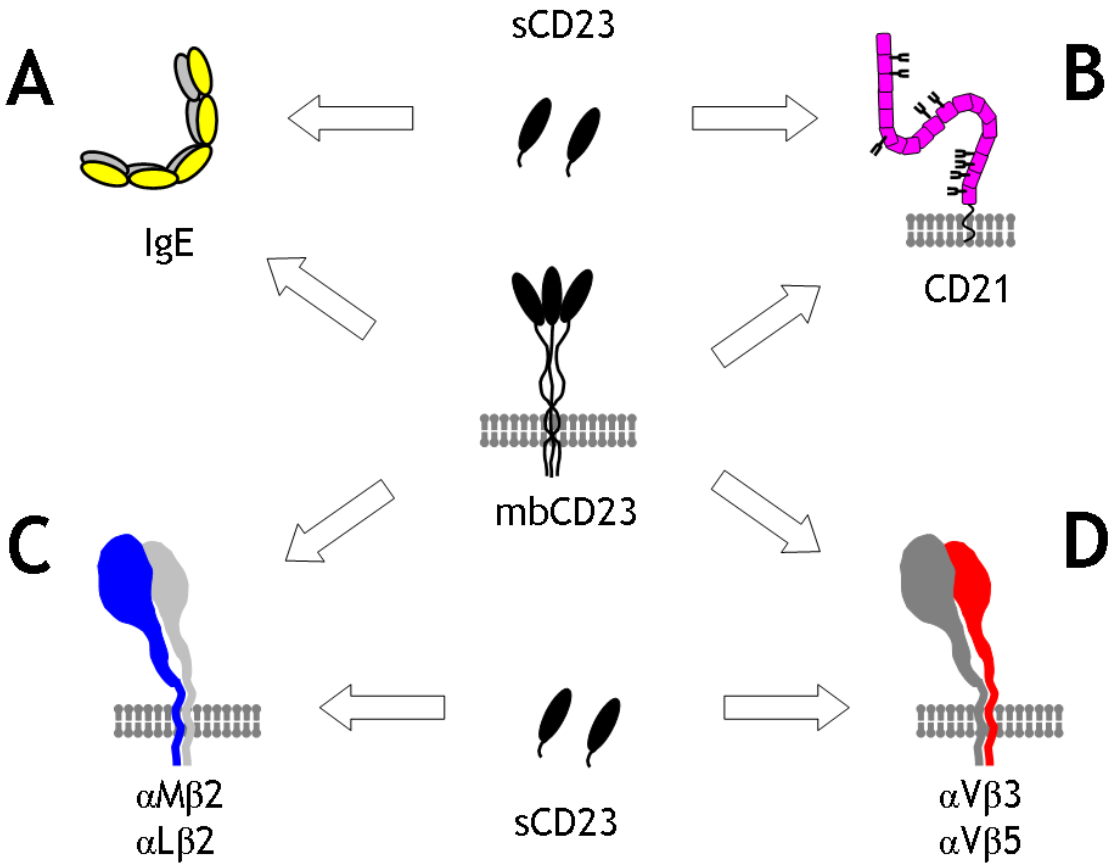

Figure 1-2 Interactions of CD23 and its ligands
Membrane-bound and soluble CD23 interact with a number of ligands, including (A) IgE, (B) CD21, (C) αMβ2 and αXβ2 integrins, and (D) αVβ3 and αVβ5 integrins. The interaction with CD21 and IgE is important in the regulation of serum levels of IgE, while the interaction of CD23 with its integrin receptors induces cytokine production (αMβ2, αXβ2, αVβ3) and cell proliferation (αVβ5).

1.2.2.1 CD23 interaction with IgE

IgE is one of the classes of human antibodies and is produced exclusively in mammals. IgE is particularly effective in defending the body against parasitic infections and as such, B cells secreting IgE are found in high concentrations in areas of the body most susceptible to parasitic invasion (skin, lungs and gut). Allergy is caused by the over-expression of IgE in response to common environmental allergens found in a variety of substances. Although IgE comprises a very small fraction of the total antibody in human serum, its action is amplified significantly by the interaction between IgE and its receptors.

CD23 is the low affinity receptor for IgE, binding IgE with an affinity of Ka ~10^7 M^{-1}. CD23 recognises the Cε3 domain of IgE, with Lys352 on IgE shown to be essential for CD23 binding [76]. The site of interaction between CD23 and IgE has been determined from the recent NMR solution structure of the CD23 C-type lectin domain, which suggests a continuous interaction surface for IgE comprising selected CD23 amino acids in the region between residues Trp184 and Ala279 [62]. All of the fragments of sCD23 retain the ability to bind IgE, although only fragments greater than 28kDa promote IgE synthesis and the 16kDa species can in fact inhibit this activity [42].

The CD23/IgE interaction is important in the regulation of IgE levels. The membrane-bound and soluble forms of CD23 have different roles in the regulation of IgE expression and associated activities [42] (Figure 1-3). Ligation of trimeric mbCD23 by IgE results in negative regulation of IgE synthesis, reducing serum levels of IgE [32, 77, 78]. IgE binding to mbCD23 inhibits the release of sCD23 from the membrane by stabilising the stalk region of CD23 and preventing proteolytic cleavage, thereby further repressing IgE synthesis. In contrast, ligation of IgE by soluble CD23 species leads to an upregulation in IgE synthesis. The ability of sCD23 trimers to enhance IgE production is thought to be through its ability to cross-link IgE and CD21, another CD23 ligand, on cells [32, 62, 79].

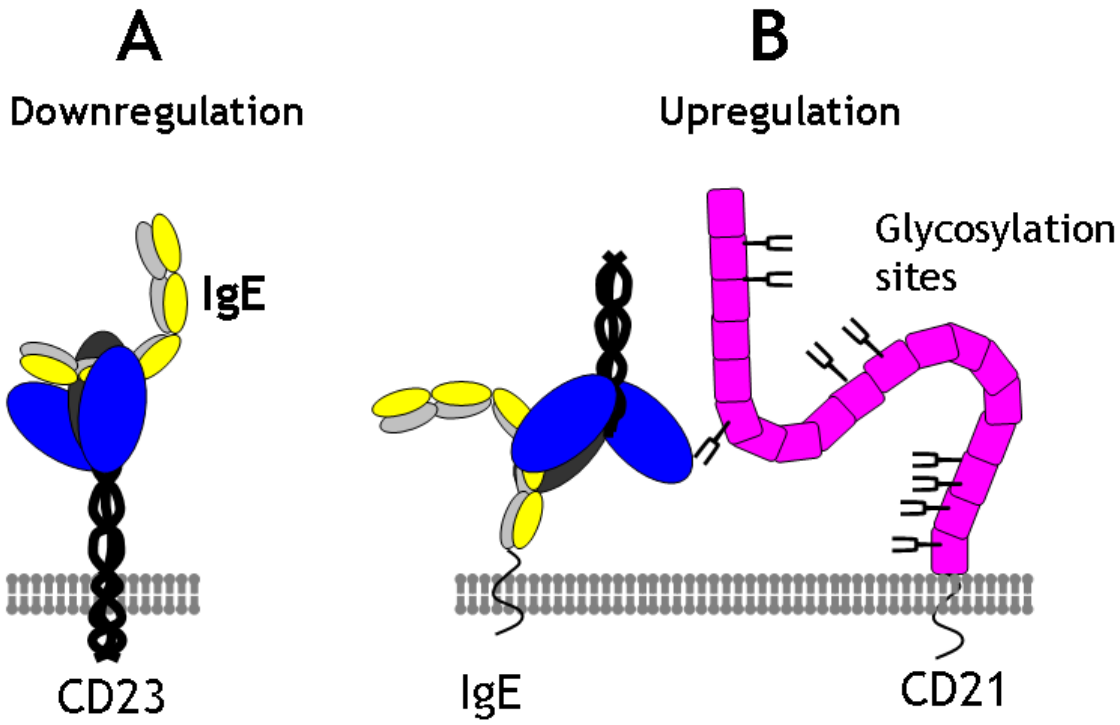

Figure 1-3 Regulation of IgE Synthesis by CD23
The interaction of mbCD23 and sCD23 with its ligands CD21 and IgE differentially regulates IgE synthesis. (A)The interaction between mbCD23 and IgE leads to downregulation in the production of IgE. (B) The complex of CD21 and IgE with sCD23 upregulates the production of serum levels of IgE.

1.2.2.2 CD23 interaction with CD21

CD21 is a 145 kDa, Type I transmembrane glycoprotein, also known as the complement receptor type 2 (CR2) that plays a major role in human B cell activation and proliferation [72]. CD21 and CD23 interact in both their membrane-bound and soluble forms and these interactions are mediated via protein-protein interactions and via N-linked sugar chains on CD21. The interaction site on CD23 for CD21 is found in the C-type lectin head and involves residues Glu294, Gly295, Ser296 and Glu298 [62].

Binding sites for CD21 and IgE on CD23 are distinct from each other [37, 62]. sCD21 and sCD23 form a complex composed of a sCD23 trimer, sCD21 and IgE [42, 62]. This soluble complex is similar to the trimeric CD23/IgE structure formed at the membrane, although the ability of sCD23 to form trimers remains contentious [80]. In this case, two of the CD23 lectin heads bind IgE, leaving the third domain available for interaction with CD21. This interaction between sCD21 with sCD23 was shown to be biologically relevant in inhibiting the production of IgE in IL-4 stimulated B cell cultures [79]. In addition the CD23/CD21 interaction is relevant in the regulation of IgE production, the survival of germinal centre B cells and B cell presentation of antigens to T cells. These results suggest a role for the sCD21/sCD23 interaction in the context of inflammation and allergy.

1.3 Integrins

CD23 is important in the regulation of IgE serum levels through its interaction with CD21 and IgE [73, 79, 81, 82]. These interactions have been the focus of a significant quantity of research. In addition to these effects, CD23, and in particular sCD23, is able to induce the production of proinflammatory cytokines. It is the interactions between CD23 and members of the integrin family of cell adhesion molecules that may play a role in mediating these cytokine functions [40, 41, 83, 84]. The interaction between CD23 and integrins may therefore be a potential point of intervention for the treatment of inflammatory disorders in which overproduction of cytokines is a hallmark [85, 86].

Integrins mediate cell adhesion in a number of biological processes, including cell migration, morphogenesis and differentiation [87, 88]. Cell adhesion is a fundamental event that is essential for a number of processes, such as embryonic development [89], tumour cell metastasis [90], wound healing [91] and monocyte extravasation [92]. Integins physically link the extracellular environment with the cellular cytoskeleton. They participate in both the transmission of signals from the extracellular matrix (ECM) to the inside of the cell ('outside in' signalling) and from the cell to the ECM ('inside out' signalling) [88]. They are a diverse family of receptors that mediate cell-matrix, cell-cell and cell-pathogen interactions [87].

1.3.1 Integrin Structure

Integrins are membrane-associated heterodimeric molecules formed by a non-covalent interaction between two Type I transmembrane glycoproteins, named the alpha (α) and beta (ß) subunit. To date, 18 α and 8 ß subunits have been identified. These subunits associate to form 24 different αß integins, each of which has defined functions and cellular expression patterns and levels (Figure 1-4). These features of integrins result in a large network of molecules that control cell adhesion and related events [93].

The integrins are predominantly extracellular, with short cytoplasmic tails (with the exception of the ß4 integrin). The overall assembly of the structure represents an extracellular globular headpiece supported by two 'legs', one from each subunit, anchored in the membrane. The N-terminal extracellular region of the heterodimeric integrins contains 12 structural domains (Figure 1-5). The headpiece is the site of the majority of interactions between the two subunits and is comprised of 4 domains from the α subunit and 8 from the ß subunit. The headpiece is made up of the ß-propeller domain from the α subunit and the ß subunit hybrid and ßA domains. The α subunit leg is made up of the Thigh and Calf-1 and Calf-2 domains. The ß subunit leg comprises the plexin/semaphorin/integrin (PSI) domain, 4 epidermal growth factor (EGF)-like domains and a ß tail domain. A flexible region between the globular headpiece and legs, known as the 'genu', is the site of bending during integrin activation. The main interactions between the two subunits are found in the globular head region, between the α subunit ß-propeller and the ß subunit ßA domain [93, 94].

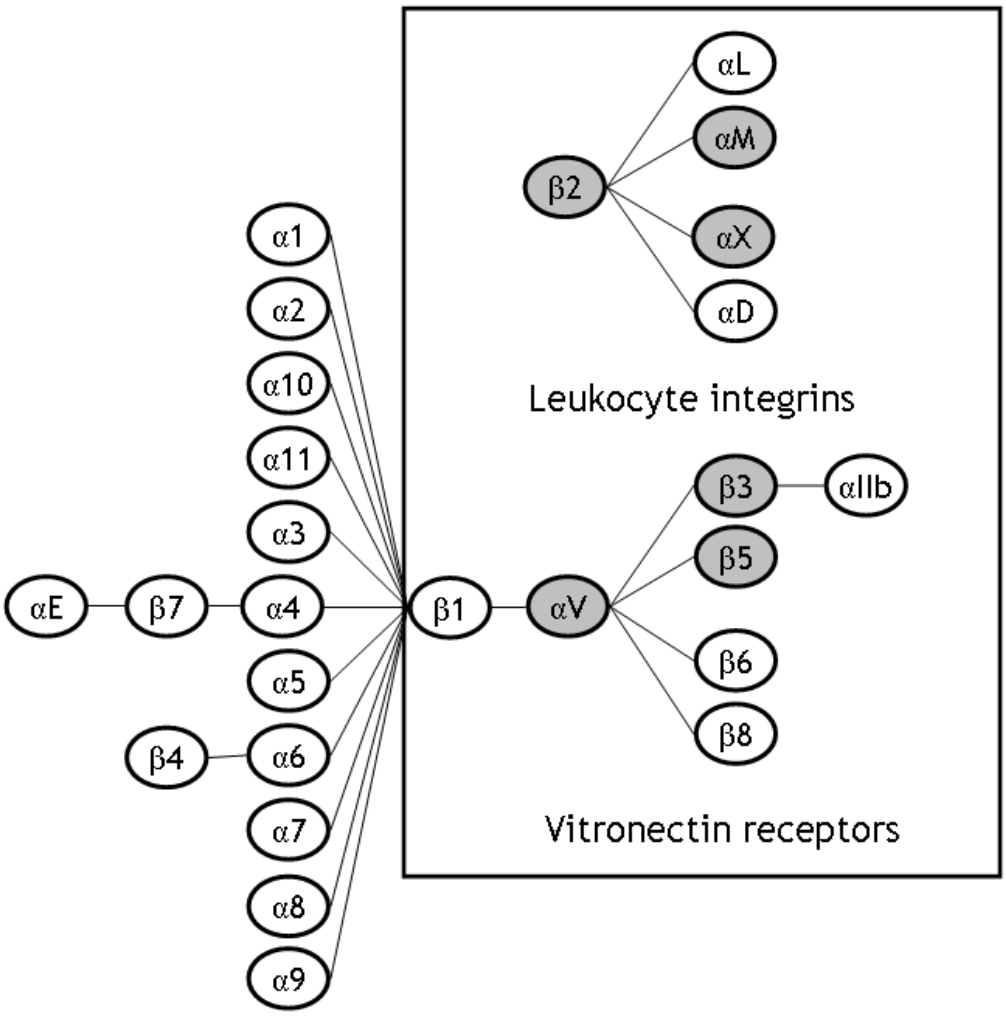

Figure 1-4 Association of α and β subunits to form integrin heterodimers
18 α and 8 β subunits associate to form 24 different integrin heterodimers with different cellular functions and distributions. The vitronectin family of integrins contain the common αV subunit and can all bind the ECM protein vitronectin. The leukocyte integrins all contain the common β2 subunit and are expressed on leukocytes. The integrins known to bind CD23 are shaded grey.

1.3.1.1 Alpha Subunit

The α subunit is comprised of four or five domains. There are two types of α subunit, differentiated by the presence or absence of a domain known as the inserted (I)-domain. The I-domain contains 200 amino acids, inserted between ß sheets 2 and 3 of the ß-propeller domain. It is also known as the von Willebrand A domain due to similarities to this structure. The I-domain is only found in certain α subunits, although its presence has been predicted in other α subunits. This domain is the major ligand recognition and binding site in I-domain-containing α subunits, via a metal ion-dependent adhesion site (MIDAS). Residues from this site (DXSXS) are integral for the coordination of metal ions, in conjunction with complementary sites on the ß subunit, during cation-dependant ligand binding by integrins [95].

The N-terminal ß-propeller domain forms a seven-bladed ß-propeller structure, comprised of seven segments of approximately 60 amino acids that share weak homology. The ß propeller contains the 'active site' amino acids that, in conjunction with amino acids from the ß subunit, participate in ligand binding in integrins that lack an I-domain. In I-domain-containing α subunits, the ß-propeller domain may cooperate with the I-domain residues during ligand binding. Ligand binding residues cluster at the top and side of the ß-propeller. At the base of the ß-propeller, opposite the αß interface, are four solvent-exposed calcium binding sites. The coordination of calcium at these sites and other numerous contacts between the ß-propeller and the Thigh domain suggests that the ß-propeller is structurally rigid [94].

The remaining C terminus of the extracellular domain of the α subunit contains stalk-like structures of the Thigh and Calf-1 and Calf-2 domains. These are 3 β-sandwich domains. The Thigh region adopts an Ig-like structure, although it is significantly larger. The interface between the Thigh and ß-propeller is relatively large and elongated (about 700Å^2) and is suggestive of possible interdomain movement. This movement may be rotation and may be mediated by the binding of calcium at the base of the ß-propeller [94].

The two Calf domains share structural similarity. Both contain two antiparallel ß sheets, Calf-1 domains contain four ß strands and Calf-2 contains 5. Calf-2 also

contains the Arg860 residue that is the site of proteolytic cleavage that generates the heavy and light chains of αV. The interface between the Thigh and Calf-1 domain occupies approximately 200Å^2. The base of the Thigh and the top of the Calf-1 domain that form the genu are rich in acidic residues that coordinate a calcium ion. This ion may stabilise these acidic residues when the integrin is in the open conformation [94].

1.3.1.2 Beta Subunit

The N-terminal 50 amino acids of the ß subunit are predicted to form a plexin-semaphorin-integrin (PSI)-like domain. Despite being encoded at the N-terminus, structurally, this domain forms part of the ß subunit leg. The region is cysteine-rich, 6 of which are common to other PSI domains. The first of the cysteines forms a long range disulphide bridge with the C terminal cysteine rich region of the ß subunit, which restrains the integrin in an inactive state [96].

The highly conserved ßA domain, also known as the I-like domain, comprises a domain of approximately 240 residues (residues 100 – 340). The ßA domain adopts a Rossman fold and, aside from the presence of two extra loop regions, is identical to that observed in the integrin I-domain. It comprises a central ß sheet of 6 strands, surrounded by 8 α helices. This domain donates the majority of residues involved in ligand binding and contains two metal coordination sites that participate in ligand binding – the MIDAS (Metal Ion Dependent Adhesion Site) and LIMBS (Ligand Induced Metal Binding Site). The MIDAS is formed by the side chains of residues Asp112, Ser121, Ser123 (DXSXS motif), Glu220 and Asp251. The MIDAS is located in a crevice at the top of the central ß strand. The LIMBS is defined by residues Asp158, Asn215, Asp217, Pro219 and Glu220. The Mn^{2+} ion coordinated by LIMBS does not directly contact the ligand, but ligand binding is reliant on the presence of the Mn^{2+} ion [94, 97].

The Hybrid domain is formed from two stretches of linear sequence on either side of the ßA domain that fold into an Ig-like structure. The Hybrid and ßA domains form a relatively large, circular interface (approximately 650Å^2) of mixed hydrophobic and hydrophilic nature. The numerous interactions between the Thigh and ßA domains suggest that interdomain movement is minimal [94].

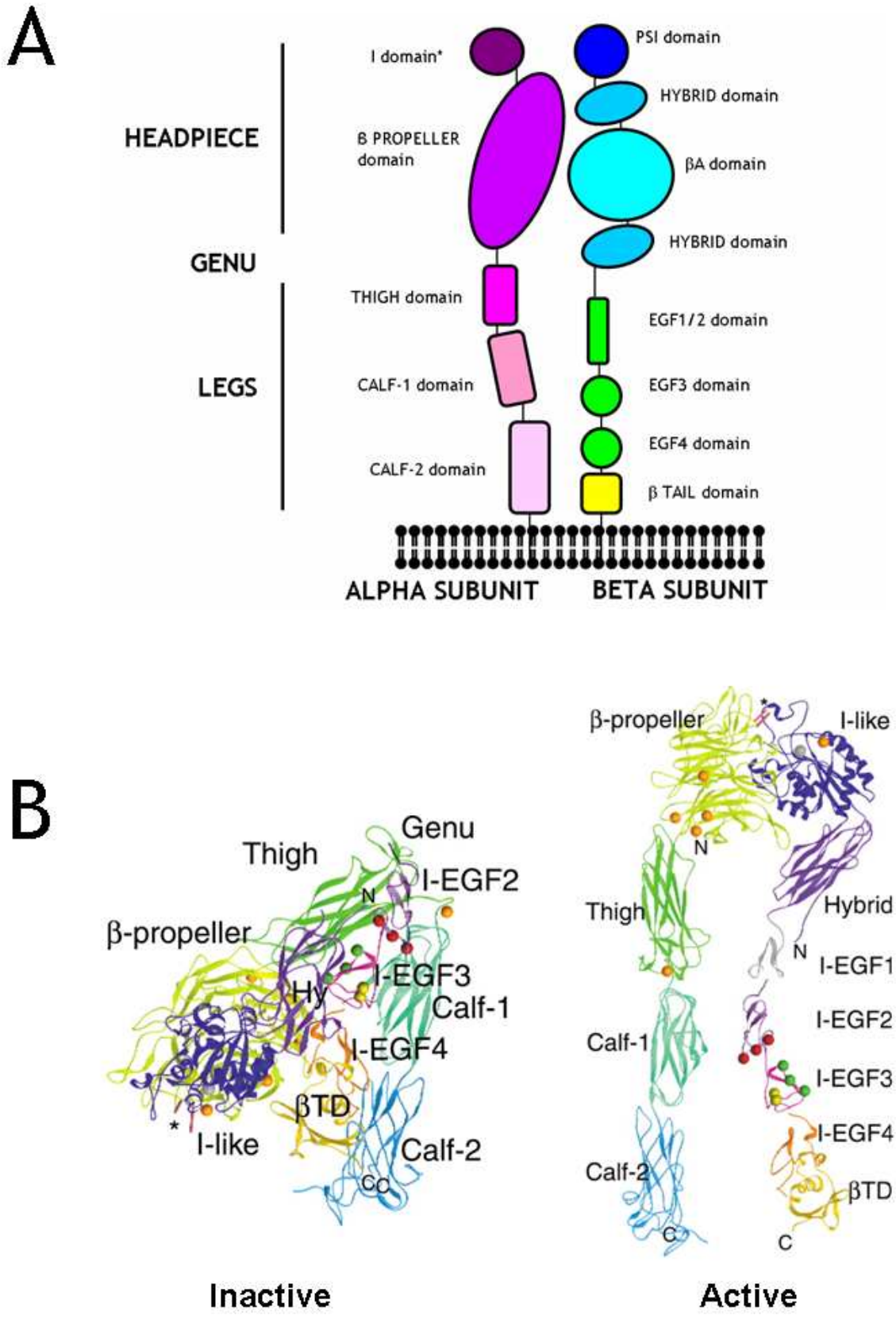

Figure 1-5 Structural feature and conformational activation of αVβ3 integrin
(A) Schematic representation of the domains comprising the α and β integrin subunits. (B) Bent (inactive) and extended (active) conformations of integrins as proposed by the switchblade model of integrin activation [98].

The Epidermal Growth Factor-like (EGF) domains (EGF1/2, EGF3 and EGF4) are contained in residues 340 to 700 of the ß subunit. Each domain contains 3 disulphide bridges that are necessary for the integrin EGF structure. A fourth disulphide bridge links the domains. EGF1/2 is largely unstructured in the crystal structure, although the predicted sequence predicts a high degree of structural similarity with EGF3 and 4. These domains are one of 3 structural subtypes of EGF-like domain that occur in proteins. The EGF domains lie in the genu region and the lack of resolution may be a result of the movement in this area. EGF3 and 4 are similar in structure and together form an extended rod-shaped unit. The interface between EGF3 and 4 is small (200Å^2) and probably rigid due to extensive interdomain contacts, including a disulphide bridge, main chain hydrogen bonds and hydrophobic interactions. Antibodies that selectively recognise activated integrins have been shown to bind epitopes that map to these EGF domains [95]. These ß subunit regions correspond to the α subunit stalk region and are considered important for signal transduction [99, 100].

The very C-terminal region contains the ß tail domain (ßTD). The ßTD is comprised of a ß sheet of 4 antiparallel and parallel ß strands. Facing it is an α helix, that interacts hydrophobically with the ß sheet. The ßTD does not share any significant homology with other known domains and may be considered a new fold. This domain forms two weak hydrophobic interactions with the EGF domains, suggesting that this interface may be flexible [94].

1.3.2 Ligand recognition by Integrins

Binding of ligands by integrin is dependent on the presence of a particular motif within that ligand. The Arg-Gly-Asp (RGD) peptide was first discovered in fibronectin and is now widely recognised as the classical recognition sequence for most integrins [101]. This sequence is found in a diverse range of receptors and integrin ligands. The presence of a small motif in a range of functionally diverse ligands creates an extensive system for recognition by cell adhesion molecules. Introduction of the RGD sequence to lysozyme and hirudin gave the proteins the ability to function in cell adhesion [102].

1.3.2.1 The Classical Recognition Sequence, 'RGD'

The RGD tripeptide is the smallest unit that can be recognised and bound by integrins and in some cases is sufficient to mimic (when attached to a surface) or block (when in solution) the adhesive action of the natural ligand [103]. The effect elicited by the RGD peptide is generally less than that mediated by its natural ligand. The sequence is specific and even conservative changes (such as Gly to Ala) significantly reduce the activity of the peptide. The conformation of the amino acid residues in the peptide is important for activity, with an RGD peptide containing D-arginine being inactive [101]. Although the minimal unit necessary for activity is the RGD motif, there is a requirement for a further residue at the C-terminal end, to block the carboxyl group of Asp. The C terminal sequence affects the affinity and selectivity of the RGD peptide binding. Peptides with Gly, Trp or Phe residues C terminal to the RGD have higher binding affinities for the α5ß1 integrin, while the αVß3 and αVß5 integrins prefer Ser or Ala, and αIIBß3 requires a Tyr or Arg [104]. The rigidity or flexibility of RGD containing loops has been linked in NMR studies to a narrow or wide range of recognition profile, respectively. Cyclisation of the RGD containing peptides increases interaction with vitronectin receptors, but not fibronectin receptors [105].

Proteins containing RGD motifs and participating in cell adhesion include fibronectin, vitronectin, fibrinogen, von Willebrand factor, thrombospondin, laminin, entactin, tenascin, osteopontin, bone sialoprotein and under certain conditions collagens [106]. Some proteins that do not naturally mediate cell attachment, such as Gamma II crystallin and *Escherichia coli* (*E.coli*) lambda receptor, are capable of binding integrins *in vitro*. This is most likely due to the recognition of the specific conformations of the RGD motif in these proteins by integrins (especially αVß3). The recognition of the RGD tripeptide is also exploited by pathogens to gain entry into the cell. Adenovirus penton protein, foot and mouth virus coat protein and *Bordetella pertussis* surface protein all contain RGD motifs capable of being bound by cell surface integrins. The RGD site is evolutionarily conserved in other organisms and may mediate attachments in *Drosophila* and certain plants [101].

Recent interrogation of sequence databases revealed 7182 proteins containing RGD sequences. Of these 7182, 404 are membrane proteins, 120 of which have the RGD peptide located in their extracellular domain. These proteins contain a number of known cell adhesion proteins, in addition to 48 well-characterised receptors. In most cases the authors determined that the RGD motifs form or are predicted to lie in a loop structure similar to that observed in cell adhesion complexes. In addition, RGD motifs from receptors with known crystal structures were shown to assume a similar conformation, with the Arg and Asp residues pointing away from each other, to that observed in cell adhesion complexes. Receptors have not been considered as having cell adhesion properties before this study and the significance of these RGD sequences will need to be determined experimentally [102].

While the RGD peptide is the smallest recognisable unit, the conformation in which the peptide is presented is essential for its function. The conformation of the peptide will influence binding by different integrins. α5ß1 preferred binding larger, RGD-containing fibronectin polypeptides, while αVß3 was more efficient at binding smaller RGD-containing fibronectin fragments [107]. This could suggest that the presence of surrounding sequence will influence the peptide recognition and binding ability [104]. Alternatively, while the RGD motif is the basic unit of recognition, binding specificity may also rely on the presence of synergistic sites. The presence of synergistic sites has been suggested for ligands of integrins αIIbß3, α5ß1, αVß3 and αVß5 [75, 108, 109].

Insights into the binding of RGD containing ligands have been provided by the crystal structure of the extracellular domain of αVß3 integrin alone and in complex with a cyclic RGD-containing pentapeptide. The availability of both ligand-bound and ligand-free structures allows analysis of both the fundamental residues involved in the interaction and conformational changes that arise due to ligand binding [94, 98].

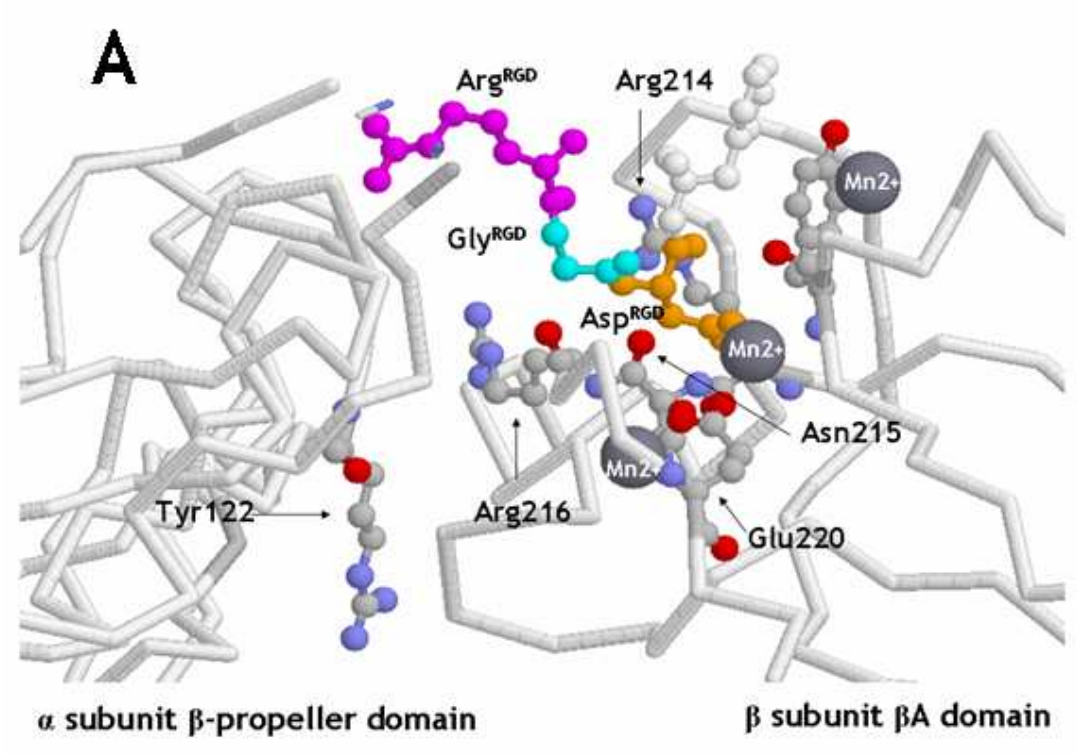

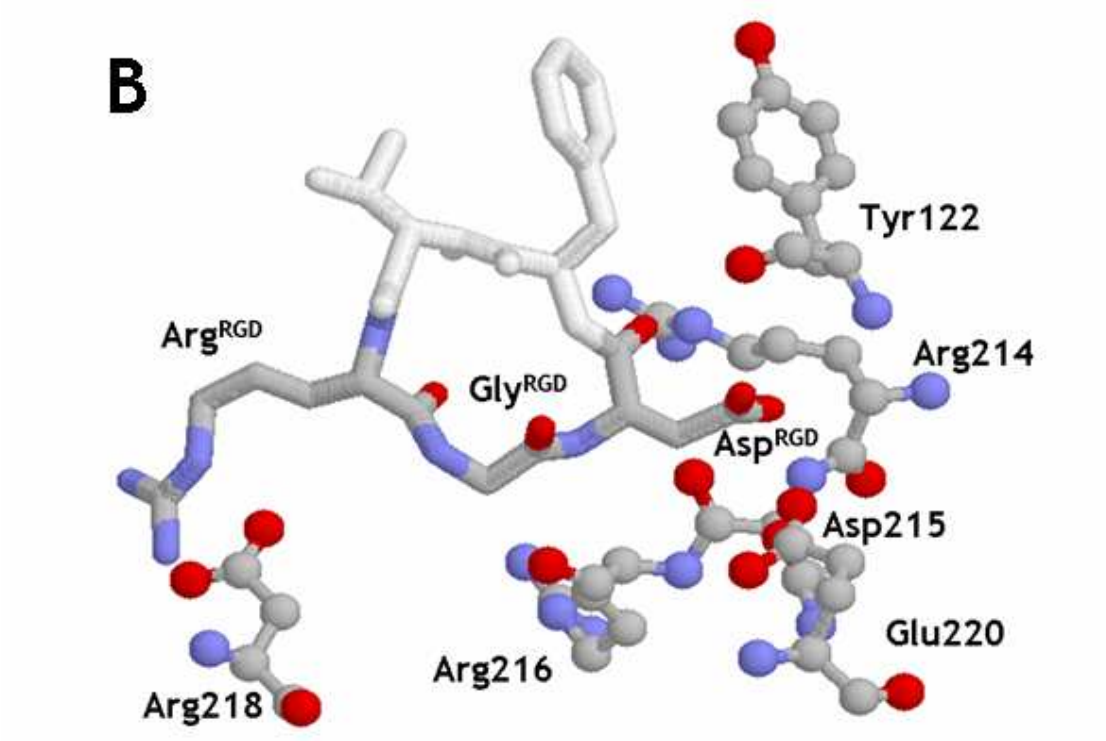

Figure 1-6 Binding of cyclic RGD containing peptide by αVβ3
(A) Binding of the cyclic RGD containing peptide by αVβ3 involves residues from both subunits.
(B)The conformation of the cyclic RGD containing peptide in complex with αVβ3.

Ligand binding is cation-dependent and mediated by residues from both the α and ß subunit. The Asp of the RGD sequence is coordinated by a divalent cation bound by the MIDAS on the α subunit. In I-containing α subunits the MIDAS is located in the I-domain and in non I-domain containing integrins there is a corresponding MIDAS on the ß subunit. In certain cases, the ß-propeller domain from the α-subunit also donates residues to bind the ligand. The ß subunit contains two sites capable of coordinating metal ions, the MIDAS and LIMBS, which participate in ligand binding. ADMIDAS (adjacent to MIDAS) coordinates either Ca^{2+} or Mn^{2+} in the presence and absence of ligand, while the LIMBS contains a Mn^{2+} when ligand is present, but not in the absence of ligand [98].

The RGD peptide binds a shallow groove at the interface of the ß-propeller of the α subunit and the ßA domain of the ß subunit. The Arg^{RGD} residue is bound by the ß-propeller groove. The Arg^{RGD} guandinium group forms a bidentate salt bridge with Asp218 and another salt bridge with Asp150. These ß propeller residues are located at the base and rear of the groove, respectively. In this conformation, the majority of the upper Arg^{RGD} sidechain is solvent-exposed, making it likely that the interaction is further stabilised by interactions with water molecules. The interaction with the ß subunit ßA domain is mediated primarily by the Asp carboxylate group. This group forms the centre of a network of polar interactions with the ßA residues and the MIDAS. One of the carboxylate oxygen atoms is coordinated by a Mn^{2+} ion at MIDAS, while the second hydrogen bonds with backbone amides of Tyr122 and Asn 215 and the Arg214 sidechain. The Asp^{RGD} residue is completely buried within its binding pocket, with the remainder of the chain forming hydrophobic contacts with the beta carbon of Asn215. The central Gly^{RGD} projects into the interface between the α and ß subunits. It interacts with the αV subunit, primarily via the carbonyl oxygen of Arg216. The main chain conformation of the RGD peptide in the structure is identical to that observed in the natural integrin ligand Echistatin [98] (Figure 1-6).

The binding to the ßA domain is similar to that observed with the αA integrin-ligand interaction. In both cases, an acidic residue contacts a metal ion at MIDAS. ßA differs from αA in that a ligand is required for divalent cation binding, however the αA domain can bind a metal ion in the presence or absence of ligand. This is explained by the conformation of the side chain of Glu220 in the unliganded ßA domain. Glu220 intrudes into the MIDAS, restricting cation binding

possibly through steric hindrance. The structure of the ligand-bound ßA domain shows a change in the conformation of the Glu220 sidechain, allowing access to the MIDAS for cations. The ßA domain also contains a second cation binding site termed LIMBS. At this site, the metal ion is coordinated by the other carboxylate oxygen of Glu220, the side chains of Asp158, Asn215 and Asp217, the carbonyl oxygens of Asp217 and Pro219. Although this site does not directly contact the ligand, it is required for metal ion coordination, as the coordination sphere is absent in the unliganded structure. Its most likely role is to stabilise the orientation of Glu220 and provide structural stability to the ligand binding region [98] (Figure 1-6).

Changes in the overall structure between the ligand-free and ligand-bound integrin are observed, despite the binding of only the small simple recognition sequence. At the tertiary level, there is a change in the conformation of some of the loops in the ßA domain. Quaternary changes are observed in the head region, with the ßA and ß-propeller domains coming closer together at the peptide-binding site. The ß propeller is slightly rotated at the propeller-thigh interface, with a corresponding rotation observed from the ßA domain. These changes are analogous to the change observed with G proteins, where the ßA alters its orientation relative to the ß propeller. It is likely that this change is going to be more pronounced when the integrin is bound by one of the larger and structurally diverse natural ligands [98].

1.3.2.2 Other Recognition Sequences

Integrins also recognise sequences other than the RGD motif in their ligands. In certain cases, these recognition sequences are slight variations on the RGD motif. The Gly position of the RGD may be occupied by a number of residues or in certain cases by two residues and still be bound by integrins [101]. A peptide containing the sequence NGR binds with low affinity to integrins, although the inverse RGD sequence, DGR, does not have any measurable integrin binding activity. This is interesting in the context of CD23, as it contains a DGR sequence and is known to interact with RGD-binding integrins. Whether the interaction is via this DGR sequence remains to be fully determined [67].

αIIbß3 also binds the sequence KQAGDV, an interaction that is blocked by RGD containing peptides and so presumably occurs at the same binding site. α4ß1 and α4ß7 recognise the LDV peptide [110]. This motif is found in a splice variant of fibronectin. α4ß1 also recognises the IDA(PS) and REDV sequences in fibronectin. IDA could be regarded as a version of LDV and REDV as a version of RGD. α2ß1 has been shown to recognise the DGEA motif, YGYYGDALR from laminin and FYFDLR from type IV collagen. The α1ß1 integrin recognises a motif composed of Arg and Asp residues on type I collagen. The αMß2 integrin recognises the sequence KRLDGS from fibrinogen and sequences containing L/IET in I-CAMs are recognised by ß2 integrins [101, 104].

Despite the range of sequences recognised by integrins, in most cases, those alternative motifs described thus far all include an Asp, or the closely related, Glu residue. This requirement for the Asp may be due to its ability to coordinate metal ions essential for integrin-based ligand recognition. The group of snake proteins, the disintegrins, contain RGD motifs and can interact with integrins [111]. In some cases the RGD sequence is replaced by KGD. The ADAM (a distintegrin and metalloproteinase) family of mammalian proteins is homologous to the disintegrins, although they do not contain the RGD motif. The recognition site determined for one ADAM, fertilin, was found to be TDE, which may be analogous to the disintegrin RGD [112, 113].

The recognition of the RGD binding motif was fully determined by the solution of the structure of αVß3 bound to an RGD-containing pentapeptide. As such, full elucidation of the mechanism of recognition of these alternative motifs will rely on the future crystallisation of integrin-ligand complexes.

1.3.2.3 Alternate Binding Sites

In addition to the recognition of different sequences at the 'RGD-recognition site' of integrins, the existence of an additional, distinct ligand binding site on the $\alpha V\beta 3$ and $\alpha V\beta 5$ integrins has been suggested. These alternate binding sites have been suggested by the binding of ligands, such as tumstatin [114], HIV Tat protein [109] and entactin [115], to these integrins at RGD-independent sites. These studies have proposed either the existence of an additional distinct binding site or a synergistic ligand recognition site that cooperates with the RGD binding

site. Analysis of the binding of Type IV collagen indicates that this protein contains additional αVβ5 and αVβ3 binding sites [108]. These sites, however, are recognised more efficiently when in the context of the intact protein (and potentially the RGD site), than as individual peptides. This may suggest a synergistic relationship or a requirement for a specific conformation during the binding of the non-RGD collagen-derived peptides. Similarly, studies with the HIV Tat protein have suggested the presence of a synergistic binding site in αVβ5 [109]. A 9 residue basic peptide derived from Tat was shown to bind the αVβ5 integrin in an RGD and divalent cation-independent fashion. This basic peptide was highly specific with respect to sequence and capable of mediating cell attachment. The authors postulate that, although Tat contains an RGD motif, it is not presented in a context that allows it to bind αVβ5. They suggest that the basic peptide binds a synergistic site on αVβ5 to mediate specific interactions. Studies on the binding of tumstatin-derived peptides to αVβ3 indicated that the protein contains an RGD-independent αVβ3 binding site, as the binding of the peptides was not inhibited by the presence of cyclic RGD peptides [114]. Entactin was also shown to contain two distinct RGD-independent cell attachment peptides. Mutants of entactin lacking the RGD motif were still capable of mediating cell attachment, although identification of the integrin involved in binding still requires elucidation [115].

1.3.3 Integrin Activation and Signalling

Integrins are capable of transmitting signals bidirectionally across the membrane. They form a mechanical link between the cytoskeleton and the extracellular matrix and activate intracellular signalling pathways [116, 117]. They are capable of transmitting signals from the ECM to the interior of the cell ('outside-in' signalling) and from the interior of the cell to the external environment ('inside-out' signalling) [88]. Formation of mechanically stable integrin complexes is essential for the transduction of mechanical signals between the cell and ECM. Integrins are physically associated with the contractile cytoskeleton in the cytoplasm of cells and form transient interactions with ligands through their extracellular domains. Except for the β4 subunit, which is connected to intermediate filaments of the cytoskeleton, all of the cytoplasmic tails of integrins are linked to the actin-based microfilament system of the cell [118-120].

The transmission of a signal from a ligand-binding site, across the membrane and to the cytoskeleton (or *vice versa*), requires long-range conformational changes and cooperation between integrin domains. Many integrins are not constitutively active, but require activation prior to ligand binding and signalling. The signal for activation or inhibition may come from interactions between different integrins [95]. The current model for integrin activation is based on the recently solved structure of the extracellular domains of the αVβ3 integrin [94, 97, 98]. This model is referred to as the 'Switchblade model' and suggests the integrin changes between active and inactive forms by conformational rearrangement (Figure 1-5). The inactive form of the αVβ3 integrin has a bent shape, with the protein anchored in the membrane and the extracellular domains bent over to create a V-shape. The site of bending is the genu between the headpiece and stalk regions of the heterodimer. This structure was determined in the presence of Ca^{2+} ions, known to promote the inactive form of integrins. In addition, the lack of ligand or Mg^{2+} ions supports the interpretation that this is the inactive conformation of the integrin. Structural analysis of integrins in the presence of ligand indicates an open extended conformation is the active structure. Thus the 'Switchblade' model proposes that that activation of the integrin results in an extension of the headpiece away from the membrane, in a manner analogous to the opening of a switchblade knife. This conformational change makes the activation and functional binding residues accessible [94, 121].

1.3.3.1 Inside-out signalling

Inside-out signalling relates to the transmisson of signals from the interior of the cell to the ECM. For example, integrins on leukocytes and platelets will need to be activated by internal signals or agonists to bind their ligands. The current hypothesis is that the α subunit blocks the ß subunit contacts with the cytoskeleton when the integrin is in an inactive state. The activation of integrins by inside-out signalling is regulated by the movement apart of the areas of the α and β subunit domains in response to a stimulus [100, 122, 123]. This is thought to supply the trigger for the upward switchblade movement of the extracellular headpiece, leading to activation of the integrin from within the cell. In addition to these changes in affinity, it has been suggested that changes in integrin avidity (clustering) affect signalling. Many studies report an increase in integrin activity and signalling due to receptor clustering. This would obviously lead to

improved efficiency of ligand binding, particularly in the case of multivalent ligands [95]. It is difficult, however, to distinguish whether integrin clustering is the stimulus for, or the consequence of, an increase in ligand binding affinity. Despite this, changes in avidity are generally regarded as important for inside-out signalling, not least because of the difficulties in direct quantitation of binding of soluble ligands that affect integrin affinity. The most likely situation of integrin activation will include a combination of changes in affinity and avidity, depending on the integrin and cell type of its expression [124].

1.3.3.2 Outside-in signalling

Integrin-mediated 'outside-in' signalling refers to the transduction of signals generated by ligand binding to the extracellular domains of integrins, across the membrane to activate intracellular signal pathways. The activation of integrins for 'outside in' signalling is also dependent on changes in integrin avidity, although avidity alone is not enough to stimulate complete outside-in signalling [95]. Concurrent changes in affinity will also affect the ability of an integrin to participate in outside-in signalling. Using electron microscopy, Takagi and collegues showed that gross conformational changes occur when an inactive integrin (αVß3) is exposed to a high affinity ligand mimetic and Mn^{2+} ions. The inactive integrin opened in a switchblade-like manner, with an accompanying swinging out of the hybrid domain. The authors propose that integrin activation occurs in two stages. In the first stage, ligand or Mn^{2+} binding induces the opening of the inactive integrin and subsequent conformational changes in the integrin result in high affinity binding of the ligand [125]. This suggests there are three activation states for the integrin- the closed conformation when the integrin is inactive, the extended conformation with a 'closed' headpiece due to ligand or Mn^{2+} binding and the high affinity state, where the integrin headpiece is open due to conformational changes and the ligand is bound. The susceptibility of individual integrins to activation will differ according to their ligand binding capabilities, requirements for divalent cations and biological function [126, 127].

1.3.3.3 Integrin cytoplasmic signalling cascades

Outside-in signalling by integrins in response to binding of external ligands results in the activation of a number of signalling pathways within the cell, the ultimate consequence of which is a change in gene expression and behaviour of that cell depending on the nature of the particular stimulus. Integrin signalling controls a range of cellular functions including adhesion, cytokine production, cell growth and differentiation [128].

The cytoplasmic tails of integrins are short and lack any inherent enzyme activity. Signal transduction from integrins is via a series of adaptor proteins, which link the integrin to the cytoskeleton, cytoplasmic kinases and transmembrane growth factor receptors. Integrins directly activate cytoplasmic kinase signalling pathways themselves and are also able to modulate the signalling pathways that arise from growth factor receptors. The major signalling pathways activated by integrins are summarised in Figure 1-7 [90].

1.3.3.3.1 Src-family kinases (SFKs) and Focal Adhesion Kinase (FAK) signalling by integrins

Integrin-mediated signalling occurs predominantly through the activation of Src-family kinases (SFK) and focal adhesion kinase (FAK) [128]. FAK activation is most important in adhesion-based signalling mechanisms for integrins and controls the activation of a number of downstream pathways. FAK interacts with the ß subunit cytoplasmic domains of integrins, either directly or via an interaction with the cytoskeletal proteins paxillin and talin. Activation results in the autophosphorylation of FAK on Tyr^{397} and acts as a scaffold for SFKs (Src and Fyn) in focal adhesions, leading to the phosphorylation of $p130^{CAS}$ and paxillin, recruitment of Crk-DOCK180n complex and activation of Rac. Active Rac can subsequently activate the NFκB transcription factors directly or lead to the PAK-dependent activation of JNK (c-jun N-terminal kinase). Active Crk is also capable of activating C3G, leading to the Rap1/B-Raf/ERK (extracellular-regulated kinase) activation cascade. FAK can also directly or indirectly (via SFKs) activate the signalling molecule PI3K (phosphatidyl inositol-3-kinase), which in turn leads to the activation of the serine/threonine kinase Akt/PKB and GEF (guanine exchange factor) via the synthesis of phosphatidylinositol-3,4,5-triphosphate

(PtdIns(3,4,5,)P_3). Cross talk between FAK and TLR signalling pathways (via MyD88) has also been shown to enhance of the activation of NFκB and transcription of NFκB-controlled genes, such as IL-6 [129].

1.3.3.3.2 Mitogen Activated Protein Kinase (MAPK) signalling by integrins

Integrins can activate ERK via the GTPase-dependent Ras/Raf/MEK/ERK mitogen-activated protein kinase (MAPK) pathway through a FAK dependent or independent mechanism [117]. Integrin ligation can lead to the activation of SFKs or FAK, both of which lead to the activation of Shc, Grb2, and Sos and results in the phosphorylation of the Ras GTPase. Active Ras phosphorylates Raf, which activates MEK, which in turn activates ERK [130]. The MAPK cascade which results in the activation of the ERK is a key regulator of a number of cellular processes. The effects of this pathway, activated by both adhesive and growth factor signals, are mediated by the dynamics of the magnitude and duration of ERK activation. Both FAK-dependent and Shc-dependent mechanisms of activating ERK are likely to be important during integrin mediated signalling. Shc, which activates rapidly, is most likey responsible for the initial high levels of ERK phosphorylation, while FAK, which is activated more slowly, may contribute to sustaining this ERK activation [128].

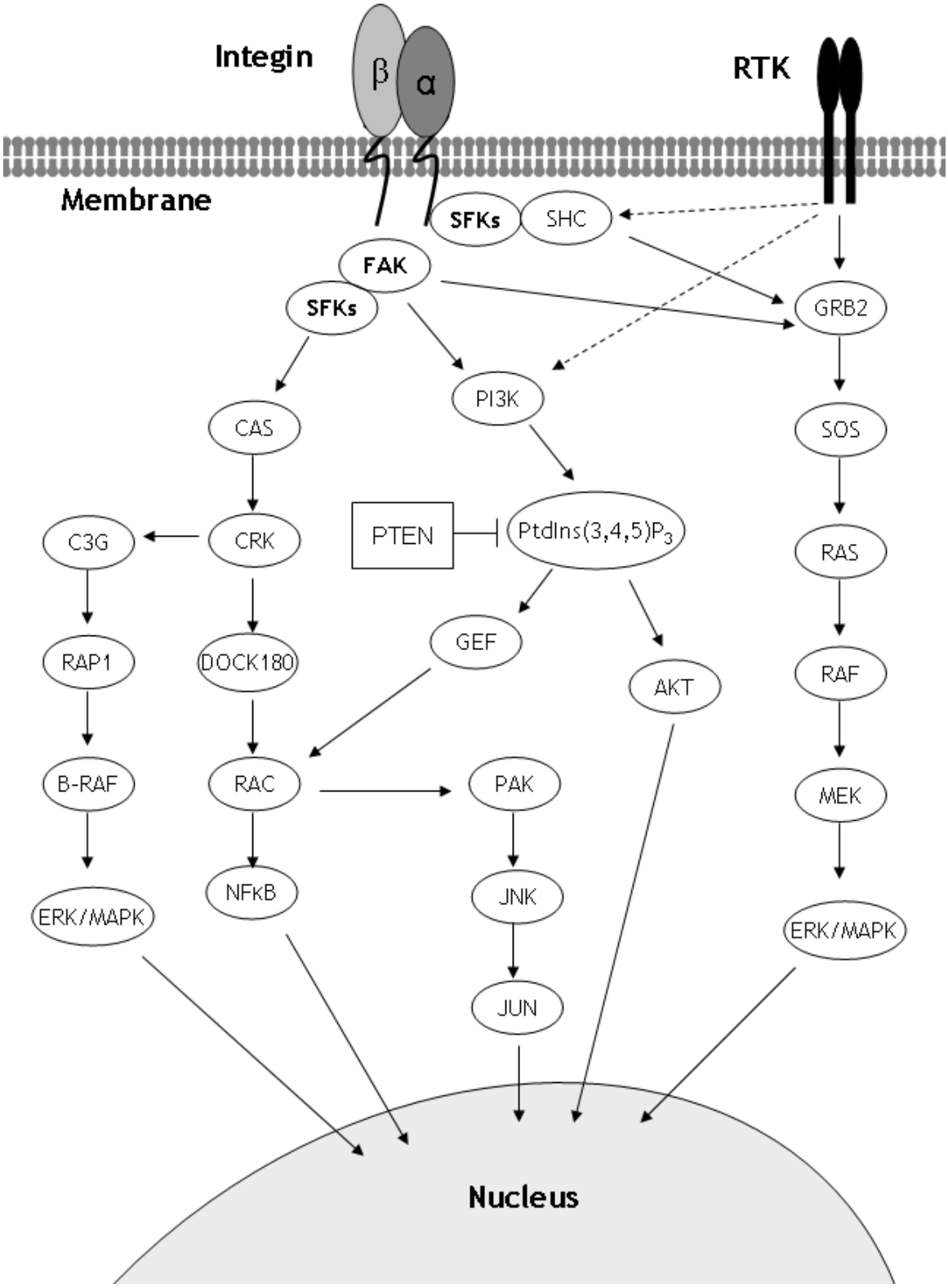

Figure 1-7 Cytoplasmic signalling cascades from integrins
Integrin-mediated signalling can lead to the activation of a number of cytoplasmic signalling cascades that result in a change in gene expression. Integrin-mediated signalling can arise directly from the integrin itself or from the association between an integrin and growth factor receptor.

1.3.3.3.3 Nuclear Factor Kappa B (NFκB) signalling by integrins

NFκB is the collective name given to the family of dimeric transcription factors (made up of combinations of the monomeric p50, p52 and p60 subunits) which control the transcription of a range of pro-inflammatory genes [131]. The proteins are held in an inactive form in the cytoplasm by their association with the IκB (inhibitory κB) protein inhibitor. The targeted phosphorylation of IκB protein by the IκK (inhibitory κ kinase) and subsequent IκB degradation releases the active NFκB complex, which translocates to the nucleus and induces the transcription of target genes. NFκB activation has been implicated in many biological processes, including inflammation, apoptosis and cell proliferation. Integrin ligation leading to the production of cytokines, including TNF-α and IL-1, involves the activation of NFκB (p50:p65 dimer) via the activation of the Rac GTPase. FAK can either activate Rac via the Cas/Crk/Dock180 cascade or via PI3K and GEF [90].

There is also evidence for cross-talk between FAK and MyD88 (myeloid differentiation factor 88) pathways. MyD88 is an adaptor protein that controls signalling from a number of Toll-like receptors (TLRs), which are a major group of surface receptors that activate NFκB and play an essential role in innate immune signalling and detection of pathogens (Figure 1-8). Signalling arising from different TLRs is either MyD88-dependent or MyD88-independent. MyD88 is associated with TLR cytoplasmic tails and activation leads to a signalling cascade involving TIRAP/Mal, IRAK and TRAF-6 signalling molecules, leading to NFκB activation [132].

MyD88 and FAK are key adaptors involved in signalling downstream of TLR-2, TLR-4, and integrin α5β1, linking pathogen detection to the initiation of an inflammatory response. FAK activation leads to activation of the downstream components of the MyD88 signalling pathway and subsequent activation of MAPK and NFκB and synthesis of cytokines. The MyD88 and integrin pathways are interlinked, but the mechanism of this cross-talk is poorly understood at present [129]. The αMβ2 integrin was shown to signal using TLR pathway intermediates during the activation of NFκB in THP-1 cells. The αMβ2 integrin was shown to bind to IRAK and to activate the TRAF-6 and TAK signalling molecules. Interestingly, this αMβ2-mediated activation of NFκB was determined to be

MyD88-independent. The most recent study has identified a role for FAK in integrin-mediated activation of NFκB. FAK induced the activation of Etk (a member of the Tec family of kinases) and TIRAP/Mal (a TLR adaptor protein). FAK was shown to be associated with the Etk, MyD88, and TIRAP/Mal molecules in the cell [133].

1.3.3.4 Integrin modulation of other receptors

In addition to direct adhesion-based signalling, integrins modulate signalling from other receptors [116, 134, 135]. Growth factors (GF) induce their activity through binding their cognate receptors on the surface of cells. In most cases, the interaction between integrin and growth factor receptor (GFR) is a synergistic one and leads to an enhancement of GFR signalling and an amplification of the response of the cell to the presence of the GF [116]. The ability of integrins to activate ERK may be especially important when the concentrations of GF in the cell are low. Under these circumstances, the synergy between integrins and GFR leading to ERK activation will be essential for cell proliferation and differentiation. Activation of ERK in this case is usually via the Grb2/Sos/Ras/Raf/MEK/ERK pathway [136]. Integrins can also modulate the GFR activity by influencing its localisation and/or internalisation and degradation [134].

Integrin modulation of GFR activity has been described for a number of GFR including, basic fibroblast growth factor receptor (bFGFR) [137], vascular endothelial growth factor receptor (VEGFR) [138], platelet derived growth factor receptor (PDGFR) [139], insulin growth factor receptor (IGFR) [140, 141], and c-FMS (M-CSF receptor) [142]. The β2 integrins also play an important role as part of the endotoxin signalling complex, which contains CD14, TLR-4 and β2 integrins [143].

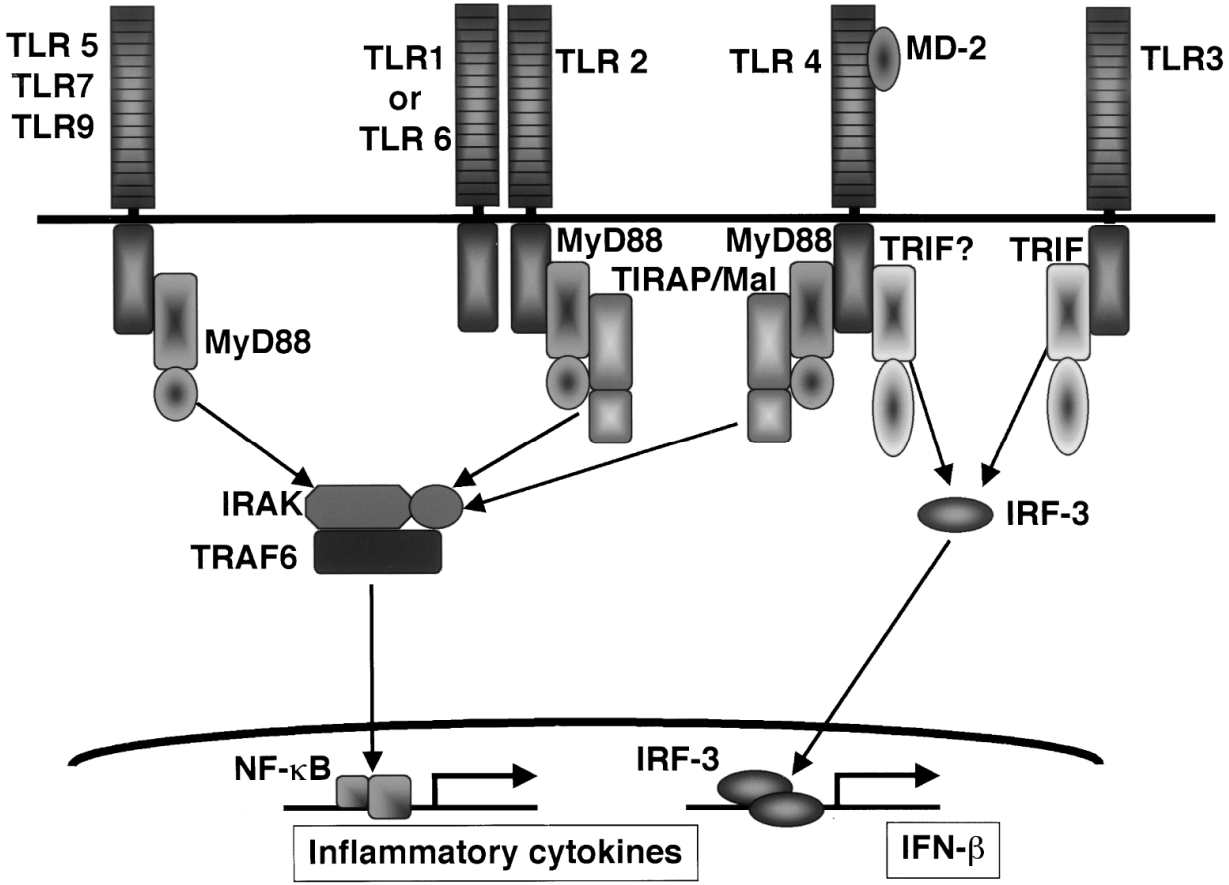

Figure 1-8 Toll-like Receptor (TLR) signalling pathways
TLR receptors are an evolutionarily conserved group of receptors with important roles in the innate immune sensing of pathogens. Signalling from TLR dimeric receptors may be depedent or independent of the MyD88 molecule.

1.3.4CD23/Integrin Interactions

1.3.4.1 CD23 interaction with beta-2 (CD18) Integrins.

The ß2 integrins are exclusively expressed on leukocytes (and are often referred to as 'the leukocyte intergrins'). They are heterodimeric αß integrins, formed by the association of one of 4 α chains (αD, αL, αM or αX) with the ß2 integrin. αMß2 and αXß2 bind a number of ligands, including CD54, fibrinogen, factor X, lipopolysaccharide (LPS), concanavalin A and zymosan [144]. Integrins are proteins that play a critical role in cell adhesion and signalling across membranes. They control cell-cell and cell-extracellular matrix contacts and participate in signalling both from the cytoplasm to the exterior of the cell and *vice versa*. Cell adhesion is essential for cell migration, proliferation and differentiation. Thus, integrins are crucial for correct cell development and function and are implicated in a number of pathologies [124]. An absence of the ß2 integrin results in impairment of a variety of immune functions, including macrophage oxidative burst and phagocytosis and lymphocyte proliferation. The ß2 integrins control a number of leukocyte functions. The αMß2 and αXß2 integrins are responsible for regulation of functions in myeloid cells (aggregation, adhesion and spreading, phagocytosis and oxidative burst), while αLß2 predominates in lymphocytes (lymphocyte proliferation, T and B cell aggregation and cell killing) [145].

CD23 interacts with the alpha chains of the leukocyte integrins αMß2 (CD11b/CD18) and αXß2 (CD11c/CD18). Membrane-bound CD23 incorporated into liposomes was shown to interact with αXß2 and αMß2 expressed on the surface of monocytes. The interaction between CD23 and αMß2/αXß2 was determined to be cation-dependent and was inhibited by factor X, but not by the presence of fibrinogen. The interaction was reduced after tunicamycin treatment and increased in with the presence of calcium ions, supporting this hypothesis that this interaction between CD23 and these ß2 integrins is, at least in part, via carbohydrate moeties on αMß2 and αXß2. This suggests that the C-type lectin domain of CD23 is involved in this interaction. The lack of inhibition by fibrinogen also supports the fact that CD23 is unlikely to bind αMß2 or αXß2 at the RGD recognition site [74].

sCD23 was shown to bind αMß2 and αXß2 and induce production of the pro-inflammatory cytokines IL-1ß, IL-6 and TNFα. This cytokine production was NOS dependent although, unlike the sCD21/sCD23 interaction that stimulates the inducible form of NOS, this interaction resulted in the activation of Type III constitutive NOS (cNOS). The induction of cNOS was due to increased catalytic activity due to an increase in intracellular calcium, as opposed to an upregulation of expression of cNOS. The nitric oxide produced by this interaction increased the levels of cGMP by the stimulation of guanylate cyclase, similar to the increase observed during sCD21/sCD23 interaction. cNOS stimulation is tightly regulated and declines rapidly after activation. This stimulation of cNOS, with a subsequent induction in pro-inflammatory cytokines supports the role for sCD23 in the early events of inflammatory responses [146].

The exact signalling pathways of sCD23/ß2 integrin-stimulated cytokine production in monocytes are not well characterised. The pathway for the production of IL-1ß, a key pro-inflammatory cytokine, has been described. Expression of IL-1ß was controlled at the transcriptional level and the pathway shown to involve the activation of members of the mitogen-activated protein kinase (MAPK) family [84].

1.3.4.2 CD23 interaction with alpha-V (αV) Integrins.

The αV family of integrins includes the αV subunit in complex with one of ß1, ß3, ß5, ß6 or ß8 subunits. All members of the aV group of integrins recognise and bind the RGD motif in substrates. Substrates for these integrins include vitronectin [147], fibronectin [148], osteopontin [149], fibrinogen [150], collagen [108], von Willebrand factor [151], tenascin [152] and thrombospondin [153]. Apart from αVß6, all the integrins bind vitronectin. Their ligand specificity is quite varied, although only αVß1 and αVß3 bind more than two different extracellular matrix proteins. However, the substrate preference for members of the αV integrin family is also influenced by the cell type of expression. αV integrins are expressed on a range of cells, including smooth muscle cells, fibroblasts, keratinocytes and endothelial cells. Expression of different isoforms will also change during developmental stages. There is evidence for redundancy between the different αV isoforms. Many cells will express more than one receptor for a specific ECM protein (the best example is vitronectin). The expression of a number of

receptors for the same substrate may indicate a link to different pathways in the cell, culminating in different effector functions. αVβ3 and αVβ5 both bind vitronectin. FG carcinoma cells expressing αVβ5 bind but do not migrate on vitronectin, while cell variants expressing αVβ3 migrate on vitronectin. Addition of epidermal growth factor (EGF) to αVβ3-deficient FG carcinoma cells enabled these cells to spread on vitronectin in a PKC-mediated αVβ5-dependent manner [154]. This indicates that αV integrins are capable of acting independently or in cooperation with each other to fulfil specific functions [155].

The lack of reagents has prevented the investigation of the cellular roles of some of the members of the αV family. The best described members in terms of function of the αV family are the αVβ3 and αVβ5 integrin isoforms. αVβ5 can only mediate spreading on vitronectin [156, 157]. In contrast to this, αVβ3 can mediate spreading on several substrates such as vitronectin [158], fibronectin [148], fibrinogen [159], laminin [160], osteopontin [161] and collagen [108]. The modified expression and function of αV integrins on many tumour cells has indicated a possible role for these proteins in tumour metastasis and progression. αV integrins are expressed on a variety of tumourogenic cell lines. αVβ3 expressed on melanoma cells mediates cell invasion [162]. αV integrins have a role in formation of tumours in nude mice, demonstrating that they contribute to malignancy. Preliminary data indicate that αVβ1, αVβ6 and αVβ8 expression is altered during tumour progression. These isoforms show differing expression levels at specific stages of differentiation, restricted tissue expression and improve growth of transfected cells [118, 163]. Elevated levels of αVβ3 are noted in infiltrating cells of breast carcinoma and renal cell carcinoma, while reduced levels are associated with angiosarcomas. In addition, αVβ3 expression is involved in tumour progression, with more advanced tumours containing higher levels of the protein [155, 164].

CD23 interacts with the vitronectin receptor αVß3. αVβ3 is associated with CD47, a 50kDa multispan transmembrane protein, to form the αVβ3 integrin signalling complex. This complex regulates leukocyte activation and mediates the phagocytosis of aging apoptotic leukocytes. This latter function is mediated by proinflammatory cytokines such as GM-CSF, TNF-α, IL-1 and IFN-γ [40]. The highest level of expression of αVβ3 *in vivo* is the osteoclast, cells responsible for the resorption of bone. It is also expressed at lower levels in other cells, such as

megakaryocytes, kidney, smooth muscle and endothelium. Expression of αVβ3 is upregulated in certain malignancies and cultured cell lines. αVβ3 binds a wide range of RGD-containing ligands, particular bone proteins, and has a critical role in promoting cell migration and controlling the balance between cell proliferation and differentiation. αVβ3 also plays an important role in mediating heterotypic cell adhesion, analogous to the VCAM/α4β1 and ICAM-1/αMβ2 interactions. αVβ3 plays a role in cytokine production through its interaction with CD23 [155].

Our laboratory has recently determined an interaction between CD23 and αVß5 [75]. The interaction between sCD23 and αVß5 is implicated in prevention of apoptosis of pre-B cells and shown to be independent of the classical RGD recognition site on the integrin, as it was not inhibited by the presence of an RGDS peptide. The region of CD23 binding to αVß5 contains the motif RKC. Peptides containing this RKC motif were able to bind αVß5 and αVß3. This interaction motif may be relevant to the interaction of CD23 with its other receptors [75]. This suggests an alternate interaction and recognition site for CD23 and signifies an additional, undefined role for this multifunctional molecule.

1.4 Research Aims

The interaction between CD23 and specific integrins is important in the production of cytokines by monocytic cells. We hypothesise that integrin-mediated cytokine production occurs via an interaction distinct from that used in adhesion-based integrin interactions. We hypothesise that the interaction is highly specific and will be influenced by the individual characteristics of the integrin(s) involved.

The specific aims of this project were as follows:

1. To analyse the nature of interaction between commercially-available purified αVβ3 and αVβ5 integrins and CD23 *in vitro*.

2. To analyse if the newly identified CD23 integrin receptor, αVβ5, plays a role in cytokine production by monocytic cells.

3. To analyse the importance of integrin ligation to cytokine production by CD23-binding integrins. The effect of targeting different integrin heterodimers, different integrin subunits and different integrin epitopes will be investigated.

4. To investigate the roles of the different CD23-binding integrins, namely αVβ3, αVβ5, αMβ2 and αXβ2, with respect to cytokine production and monocyte biology, and attempt to identify any potential hierarchy of importance that exists.

2 METHODS AND MATERIALS

2.1 Chemicals and Reagents

All routine chemicals used were purchased from Sigma Chemical Co, Poole, UK unless otherwise stated. The details of purchase of speciality chemicals are indicated in the sections pertaining to their use.

2.2 Antibodies, Oligonucleotides and Peptides

Eighty-three (83) overlapping nonameric peptides derived from the 25kDa form of the human CD23a sequence were synthesised by Mimitopes, Victoria, Australia. The peptides were numbered according to their position in the original CD23 sequence [75] and were synthesised as biotinylated peptides (with a common SGSG linker and N-terminal biotin) and/or as unlabelled peptides (lacking the linker and N-terminal biotin moiety). The details and sequences of the unlabelled peptides used in this study are described in Table 2-1. The primary and secondary antibodies used for flow cytometry, immunofluorescence, Western analysis, neutralisation and stimulation assays are detailed in Table 2-2. Olignucleotides used in RT-PCR, PCR or EMSAs in this study are detailed in Table 2.4. The details of commonly used buffers are in Table 2-3.

In addition to the CD23-derived peptides, a peptide inhibitor of MyD88 signalling was purchased from Imgenex (CA, USA) and used in the analysis of TLR-2 signalling. The details of this peptide and its control peptide are also detailed in Table 2-1.

2.3 Cell lines and culture

Dulbecco's Modified Eagle's Medium (DMEM), Trypan Blue, 200mM L-Glutamine and Penicillin-Streptomycin solution were purchased from Sigma Chemicals, Poole, UK. OptiMEM and RPMI-1640 media were from Invitrogen, Paisley, UK. Foetal Calf Serum (FCS) was supplied by TCS Cellworks, Buckingham, UK. Recombinant human cytokines M-CSF and GM-CSF were from Peprotech, UK.

Table 2-1 Table of Peptides used in this study

PEPTIDE	ABBREVIATION	SEQUENCE	SUPPLIER
Peptide 8	P8	PEKWINFQR	Mimitopes, Victoria, Australia
Peptide 9*	P9	KWINFQ**RKC**	
Peptide 10*	P10	INFQ**RKC**YY	
Peptide 11*	P11	FQ**RKC**YYFG	
Peptide 12*	P12	**RKC**YYFGKG	
Peptide 13	P13	CYYFGKGTK	
Long Peptide*	LP	KWINFQ**RKC**YYFGKG	
Peptide 58	P58	GSGRWNDAF	
Anti-MyD88**		DRQIKIWFQNRRMKWKK**RDVLPGT**	Imgenex, CA, USA
Control anti-MyD88		DRQIKIWFQNRRMKWKK	

* Common active RKC tripeptide motif is shown in bold
** TIR homodimerisation sequence is in bold

THP-1 [165], U937[166], Jurkat[167] and IB4[168] cell lines used in these analyses were from laboratory stocks. Purified primary human CD14+ monocytes from peripheral blood and bone marrow were purchased from Lonza, UK and cultured with or without 10ng/mL M-CSF (Peprotech) in RPMI-1640 medium supplemented with 10% (v/v) FCS, 2mM glutamine and 1% (v/v) penicillin/streptomycin. Unless otherwise stated, all stimulation experiments were conducted in OptiMEM lacking FCS but supplemented with 2mM glutamine and 1% (v/v) penicillin/streptomycin.

Table 2-2 Antibodies used in this study

ANTIGEN*	SOURCE	CLONE	ISOTYPE	SUPPLIER	CONJUGATE	DILUTION OR WORKING CONCENTRATION	USED IN
Actin	Rabbit polyconal	-	IgG1	Sigma Chemicals Co, Poole, UK		1/1000	WB
Av	Mouse Monoclonal	AMF7	IgG1	Millipore, MA, USA		1 µg/mL	FACS, STIM
Av	Mouse Monoclonal	LM142	IgG1	Millipore, MA, USA		1 µg/mL	STIM
Av	Rabbit Polyclonal	-	IgG1	Millipore, MA, USA		1/500	WB
αVβ3	Mouse Monoclonal	23C6	IgG1	Millipore, MA, USA		1 µg/mL	FACS, STIM
αVβ3	Mouse Monoclonal	LM609	IgG1	Millipore, MA, USA		1 µg/mL	FACS, STIM
αVβ5	Mouse Monoclonal	P1F6	IgG1	Millipore, MA, USA		1 µg/mL	FACS, STIM
αVβ5	Mouse Monoclonal	15F11	IgG2a	Millipore, MA, USA		1 µg/mL	FACS, STIM
αVβ6	Mouse Monoclonal	10D5	IgG2a	Millipore, MA, USA		1 µg/mL	FACS
β1	Mouse Monoclonal	47BR	IgG1	Autogen Bioclear, Buckinghamshire, UK		1/500	WB
β2	Mouse Monoclonal	PAH9	IgG3	Millipore, MA, USA		1 µg/mL	FACS, STIM
β2	Mouse Monoclonal	MEM48	IgG1	Millipore, MA, USA		1 µg/mL	FACS,STIM
αMβ2	Mouse Monoclonal	44	IgG1	Millipore, MA, USA		1 µg/mL	FACS, STIM
αMβ2	Mouse Monoclonal	ICO-GMI	IgG2a	Millipore, MA, USA		1 µg/mL	FACS, STIM
αXβ2	Mouse Monoclonal	3.9	IgG1	Millipore, MA, USA		1 µg/mL	FACS,STIM
αXβ2	Mouse Monoclonal	HC1/1	IgG1	Millipore, MA, USA		1 µg/mL	FACS, STIM
Phospho-p44/42 MAP kinase(Thr202/Tyr204)	Rabbit polyclonal		-	Cell Signalling Technologies, MA, USA		1/1000	WB
p44/42 MAP kinase	Rabbit polyclonal		-	Cell Signalling Technologies, MA, USA		1/1000	WB
Phospho-Beta3 (Tyr785)	Rabbit polyclonal		-	Millipore, MA, USA		1/1000	WB
Phospho-Beta3 (Tyr773)	Rabbit polyclonal		-	Millipore, MA, USA		1/1000	WB
CD1a	Mouse Monoclonal	NA1/34	IgG2a	Abcam, Cambridge, UK	PE	1 µg/mL	FACS, IFA
CD14	Mouse Monoclonal		IgG2a	Millipore, MA, USA	FITC	1 µg/mL	FACS,IFA
CD23	Mouse Monoclonal		IgG3	Autogen Bioclear		1 µg/mL	FACS
CD25	Mouse Monoclonal	ACT-1	IgG1	DAKO, Glostrup, Denmark		1 µg/mL	FACS
CD86	Mouse monoclonal	B-T7	IgG1	Diaclone, Besancon,France		1 µg/mL	FACS
HLA-DR	Mouse Monoclonal	B-F1	IgG1	Abcam, Cambridge, UK	Biotin	1 µg/mL	FACS,IFA

Table 2.2 contiuned.

ANTIGEN*	SOURCE	CLONE	ISOTYPE	SUPPLIER	CONJUGATE	DILUTION OR WORKING CONCENTRATION	USED IN
CCR5	Mouse Monoclonal		IgG1	R&D Systems, Abingdon, UK		1 µg/mL	FACS
cFMS	Rabbit polyclonal		-	Santa Cruz Biotechnology, CA, USA		1/1000	WB, NEUT
TLR2	Mouse monoclonal	TL2.1	IgG2a	Santa Cruz Biotechnology, CA, USA		1/500	WB, NEUT
IRAK-1	Rabbit polyclonal	H-273	-	Santa Cruz Biotechnology, CA, USA		1/500	WB,IFA
TRAF-6	Mouse monoclonal	D-10	IgG1	Santa Cruz Biotechnology, CA, USA		1/500	WB,IFA
p65	Rabbit polyclonal		-	Cell Signalling Technologies, MA, USA		1/500	WB,IFA,EMSA
IFN-γ receptor subunit 1	Mouse monoclonal	92101	IgG1	R&D Systems, Abingdon, UK		1/500	WB,IFA,NEUT
IgG1	Mouse isotype control		-	Sigma Chemicals Co, Poole, UK		1/1000	FACS,STIM
IgG2a	Mouse isotype control		-	Sigma Chemicals Co, Poole, UK		1/1000	FACS,STIM
IgG3	Mouse isotype control		-	Sigma Chemicals Co, Poole, UK		1/1000	FACS,STIM
Streptavidin-HRP			-	BD Bioscience, Oxford, UK.	HRP	1/1000	WB
Anti-mouse IgG HRP			-	Sigma Chemicals Co, Poole, UK	HRP	1/1000	WB
Anti-rabbit IgG HRP			-	Sigma Chemicals Co, Poole, UK	HRP	1/1000	WB
Secondary PE			-	BD Bioscience, Oxford, UK.	PE	1/1000	FACS,IFA
Secondary FITC			-	BD Bioscience, Oxford, UK.	FITC	1/1000	FACS,IFA

*All antibodies are against human antigens unless otherwise stated. Abbreviations used: FITC-fluorescein isothyanate; PE-phycoerythrin; WB-Western Blotting; FACS – flow cytometry; IFA-immunofluorescence assay; STIM-stimulation assays, NEUT-neutralisation assays, EMSA-electromobility shift assays

2.4 Flow cytometry

Expression of surface markers on cells and cell lines was measured by indirect immunofluorescent staining (flow cytometry). Cells were harvested by centrifugation and washed twice with ice-cold phosphate-buffered saline (PBS). 100 µL of cell suspension in ice-cold PBS ($5x10^6$ cells/mL) was incubated with primary antibody and isotype-matched controls (Table 2-2) or biotinylated CD23-derived peptides and controls (Table 2-1) for 30 – 60 mins at 4^0C. The cells were washed twice with ice-cold PBS and incubated with secondary antibody (for unlabelled primary antibodies) or streptavidin (for biotinylated primary antibodies and CD23-derived peptides) conjugated to either a FITC or PE fluorescent label. After 30 – 60 mins incubation at 4^0C, cells were washed twice with ice-cold PBS and resuspended in PBS/formaldehyde for flow cytometry using the Becton Dickinson FACScan machine and CellQuest software (BD Bioscience, NJ, USA).

2.5 Biotinylation of Antibodies and Proteins

Antibodies and CD23 were biotinylated using N-hydroxysuccinimidobiotin (NHS-Biotin) treatment. NHS-biotin was purchased from Sigma Chemicals Co, Poole, UK. CD23 (0.1mg/mL) or antibodies (1mg/mL) were incubated with 1mg/mL NHS-Biotin/DMSO on a rotator overnight at 4^0C. Uncongujated biotin was removed by dialysis against PBS.

2.6 Sodium Dodecyl Sulphate-Polyacrylamide Gel Electrophoresis (SDS-PAGE), Western Blotting and chemiluminescent based detection of proteins

Western analysis and chemiluminescence-based immunodetection was used to detect the presence of specific proteins. Discontinuous SDS-PAGE using the Invitrogen NuPage system was conducted according to the manufacturer's instructions (Invitrogen, Paisley, UK). Buffers used are described in Table 2-3.

Cells (1 x 10^6) in OptiMEM were stimulated with integrin-specific antibodies, CD23, CD23-derived peptides, LPS or Zymosan at 37 ºC at concentrations and time periods indicated in figure legends. Cells were harvested by centrifugation, lysed in radio immunoprecipitation assay (RIPA) buffer (50mM Tris-HCl pH7.4, 150mM NaCl, 1mM EGTA, 1mM Na_3VO_4, 1% (w/v) NP40, 1mM Na deoxycholate, 1mM PMSF and 2μg/mL Leupeptin) and the lysate cleared by centrifugation at 13,000 x *g* for 15 min. Protein concentrations were measured by Bradford Assay (BioRad Laboratories Ltd, Hampstead, UK), using BSA as a standard. Equal quantities of total protein (20-40μg) were loaded per lane and resolved on a 4-12% NuPAGE Novex Bis-Tris gradient gels (Invitrogen, Paisley, UK) according to manufacturer's instructions (based on the standard SDS-PAGE method [169]).

Proteins on the gel were transferred to nitrocellulose (Amersham, Buckinghamshire, UK) and non-specific sites on the membrane blocked for 1 h in 5% (w/v) bovine serum albumin (BSA) in Tris-buffered Saline with Tween-20 (TBST). Proteins on the membrane were detected by incubation overnight at 4ºC with specific primary antibodies (1/200 – 1/1000 dilution in TBST with 5% (w/v) BSA). Membranes were washed extensively in TBST and incubated with secondary antibodies for 1 h (1/10000 dilution in TBST with 5% (w/v) BSA) conjugated to HRP. The chemiluminescent signal was detected by exposure of the membrane to Kodak MXB film, after a 5min incubation period with the SuperSignal Pico Western Chemiluminescence Substrate (Pierce, Rockford, USA). The membrane was subsequently stripped and total protein in each lane quantified (to standardise any signals for loading inaccuracies) using matched primary and secondary antibodies to actin according to the above mentioned procedure. Bands were recorded and quantified by densitometry using the *ImageJ* program.

2.7 Cell Migration Assays

The migration of cell lines in response to conditioned media from integrin-stimulated THP-1 cells was assessed using disposable transwell plates (Corning NY, USA). The plates consisted of a polycarbonate membrane insert, with a pore size of 5μm, separating the upper and lower chambers. Cells were washed twice and resuspended in OptiMEM (Invitrogen, Paisley, UK). 5x10^5 cells were placed in the upper chamber and 500uL of cleared supernatant (undiluted or diluted as

stated in figure legends) from stimulated THP-1 cells was placed in the lower chamber. The plates were incubated at 37^0C in 5% CO_2 for 3 hours, after which, cells that had migrated to the lower chamber were harvested by centrifugation, washed in PBS and resuspended in equal volumes of PBS/formaldehyde. Unstained total cell counts were collected by flow cytometry over a defined time period (30-60 sec). The effect of proteins on migration across the membrane was tested by coating the polycarbonate membrane with FCS, vitronectin (VN), fibronectin (FN), fibrinogen (FBGN) or BSA (control) for 1 hour at 37^0C or overnight at 4^0C prior to setting up the migration experiments. All these coating proteins were purchased from Sigma, Poole, UK.

Table 2-3 Composition of buffers in routine use

BUFFERS	ABBREVIATION	COMPOSTION
Phosphate-buffered saline	PBS	13mM NaCl, 27mM KCl, 4.3mM Na_2HPO_4, 1.4mM KH_2PO_4, pH 7.2
Tris-buffered saline	TBS	50mM Tris-HCl pH 7.4, 150mM NaCl
Tris-buffer saline with Tween-20	TBST	50mM Tris-HCl pH 7.4, 150mM NaCl, 0.1% w/v Tween20,
Tris-Acetate-EDTA buffer	TAE	40mM Tris-Acetate pH 8.5, 2mM Na_2EDTA
Tris-Borate-EDTA buffer	TBE	45mM Tris-Borate pH 8.3, 1mM EDTA
Western transfer buffer		25mM Tris, 192mM Glycine , 20% v/v methanol
Nitrocellulose stripping buffer		62.5 mM Tris HCl pH 6.7, 2% w/v SDS, 100mM ß-mercaptoethanol
NuPAGE MOPS buffer	MOPS	Invitrogen proprietry information

2.8 Cell stimulation and Analysis of Cytokine Production

The antibodies used for cell stimulation are indicated in the figure legends and described fully in Table 2-2. DerCD23 [62] was a kind gift of Dr. Jim McDonnell (Oxford, UK). Bacterial LPS, dibutryl cyclic AMP (db-cAMP) and yeast zymosan A were purchased from Sigma, Poole, Greiss reagent was purchased from Promega, WI, USA and the nitroblue tetrazolium assay (NBT) was from Sigma Chemicals Co, Poole.

Cells were stimulated with antibodies against specific integrins (0.5µg/mL – 10µg/mL), bacterial lipopolysaccharide (LPS) (1ng/mL – 1µg/mL), zymosan (10ng/mL – 20ug/mL), derCD23 (0.1µg/mL – 1µg/mL), CD23-derived peptides (0.5µg/mL – 20µg/mL), either alone or in conjunction with cytokines/growth factors (M-CSF at 5ng/mL and GM-CSF at 1ng/mL). After incubation 37^0C for 24 to 72 hours, supernatants were collected, cleared by centrifugation and stored at -20^0C until analysis.

Cytokines in cell supernatants were detected using sandwich ELISA assays and Cytokine protein array techniques (Biosource, UK). The cytokine arrays Human Cartesian Array Set II, and ELISAs for detection of IL-8, IL-12, IL-4, VEGF, RANTES, and MIP-1ß were from Biosource, Invitrogen, Paisley, UK. ELISA kits for TNF-α detection were from R&D Systems and those for detection of IL-10 and IFN-γ were from Peprotech. All cytokine protein arrays and ELISAs were performed as per manufacturer's instructions.

2.9 Analysis of mechanisms of cell signalling and cytokine production

The activation of MAPK signalling pathways was analysed by Western blotting over time and in response to different stimuli, as indicated in figure legends. The importance of ERK phosphorylation to cytokine production was analysed by ELISA (enzyme-linked immunosorbent assay) after incubation with the specific MEK inhibitor, U0126. The MEK inhibitor U0126 was purchased from Sigma, Poole, UK.

2.10 Differentiation of monocytes

THP-1 cells or $CD14^+$ primary human monocytes were grown in OptiMEM supplemented with M-CSF (5ng/mL), GM-CSF (2ng/mL) or db-cAMP (100μM) for 4 days. The effect of these differentiating agents on the cytokine production and integrin expression profile was determined by ELISA and flow cytometry, respectively. Morphological changes observed in THP-1 cells treated with antibodies and M-CSF (5ng/mL) were recorded by phase contrast microscopy using the Zeiss Axiovert 135 microscope. M-CSF and GM-CSF were from Peprotech and dibutryl cyclic AMP (db-cAMP) was purchased from Sigma Chemicals (Poole, UK).

2.11 RNA extraction and Reverse Transcription-Polymerase Chain Reaction (RT-PCR)

Total RNA was extracted using the Trizol reagent (Invitrogen, Paisley, UK) according to the manufacturer's instructions. Briefly, 10^6-10^7 cells were harvested and resuspended in 1mL Trizol/10^7 cells. Chloroform (0.2mL/1mL Trizol) was added and the sample shaken vigorously for 15 seconds by hand. Phase separation was achieved by centrifugation at 12 000 x g at 4^0C for 15 min and the colourless aqueous phase collected and RNA precipitated by addition of isopropanol (0.5mL/1mL Trizol) for 10 min at room temperature, followed by centrifugation at 12 000 x g at 4^0C for 10 min. The RNA pellet was washed with 75% (v/v) ethanol (1mL/1mL Trizol), air-dried and resuspended in 50μl of nuclease free water (Sigma, Poole, UK). RNA concentration and purity were determined spectrophotometrically by absorbance at 260nm and 280nm.

Table 2-4 Table of Primers for RT-PCR and PCR

TARGET	SUPPLIER	AMPLICON SIZE (BP)
CXCL8	R&D Systems	158
GAPDH	R&D Systems	576
M-CSF	R&D Systems	464
IFN-γ	R&D Systems	453

Total RNA extracted was used for RT-PCR reactions. First strand cDNA synthesis was performed at 37 ºC for 1 hour using the M-MLV reverse transcriptase enzyme and random primers (Promega, Southampton, UK) according to the manufacturer's instructions. Subsequent PCR reactions were performed using Taq polymerase (Promega, Southampton, UK) and the transcript specific primers (Table 2.4) and cycling parameters described below.

Initial denaturation	94 ºC / 2min	1 cycle
Denaturation	94 ºC / 45 sec	30 cycles
Annealing	55 ºC / 45 sec	
Extension	72 ºC / 45 sec	
Final extension	72ºC / 5 min	1 cycle
Hold	4 ºC / hold	

2.12 Indirect Immunofluorescence Assay (IFA) and Confocal Microscopy

Primary and secondary antibodies used in IFA are described in Table 2.2. The DAPI nuclear stain (4',6-diamidino-2-phenylindole) was from Sigma, Poole, UK. Stimulated cells were prepared for confocal microscopy using the acetone/methanol method. Subsequent to stimulation as indicated in figure legends, cells (1 x 10^6/mL) were washed in PBS and 50µL spread on multiwell microscope slide. Cells were fixed with ice-cold acetone/methanol (1:1) solution for 5min and air dried. Cells were permeablised with 0.02% (w/v) Triton-X100/PBS solution for 30min at room temperature and blocked with 3% (w/v) BSA in PBS for 15min, before incubation with primary antibody (1/50 dilution in 3% (w/v) BSA in PBS) for 30 - 60 min at 37^0C. Cells were washed with 0.1% (w/v) BSA/PBS and incubated for 30 – 60 min at 37^0C with the appropriate secondary antibody conjugated to a fluorescent label (FITC, Cy5 or PE). Cells were washed with 0.1% (w/v) BSA/PBS, nuclei stained with DAPI solution (1ug/mL), and the slides air-dried and mounted in Citifluor before analysis using the Zeiss LSM 510 confocal microscope.

2.13 Electrophoretic Mobility Shift Assays (EMSA)

The activation of NFκβ transcription factors was performed using the radioactively labelled NFκβ consensus oligonucleotide (Santa Cruz Biotechnology, CA, USA) in EMSA reactions. The [γ-^{32}P] ATP was purchased from Perkin-Elmer (MA, USA) and polynucleotide kinase oligonucleotide end labelling kit was from Promega. The antibodies used are described in Table 2-2.

Nuclear extracts were prepared from 1x10^7 cells stimulated with agents as indicated in figure legends. Cells were collected by centrifugation and resuspended on ice in Sucrose Buffer with NP-40 (0.32M sucrose, 10mM Tris-HCl, pH 8.0, 3mM $CaCl_2$, 2mM MgOAc, 0.1 mM EDTA, 0.5% (w/v) NP-40, 1mM DTT, 0.5mM PMSF). Nuclei were harvested by centrifugation at 500 x *g* at 4^0C for 5 min. The nuclear pellet washed with Sucrose Buffer without NP-40 (0.32M sucrose, 10mM Tris-HCl, pH 8.0, 3mM $CaCl_2$, 2mM MgOAc, 0.1 mM EDTA, 1mM DTT, 0.5mM PMSF), collected by centrifugation at 500 x *g* at 4^0C for 5 min and resuspended in Low Salt Buffer (20mM HEPES-KOH pH 7.9, 1.5 mM $MgCl_2$, 20 mM KCl, 0.2 mM EDTA, 25% (v/v) glycerol, 0.5 mM DTT, 0.5 mM PMSF). An equal volume of High Salt Buffer (20mM HEPES-KOH pH 7.9, 1.5 mM $MgCl_2$, 800 mM KCl, 0.2 mM EDTA, 25% (v/v) glycerol, 1% (w/v) NP-40, 0.5 mM DTT, 0.5 mM PMSF) was added in small aliquots and the samples incubated on a rotary shaker at 4^0C for 45 min. Samples were cleared by centrifugation at 14 000 x *g* at 4^0C for 15 min and the protein content of the resultant supernatant containing the nuclear fraction quantitated by Bradford's assay prior to use in EMSA assays.

Olginucleotides were labelled with [γ-^{32}P] ATP using the polynucleotide kinase oligonucleotide end labelling kit according to manufacturer's instructions. The labelled oligonucleotides were purified by ethanol precipitation. 1ng of radioactively labelled ("hot") oligonucleotide was incubated with 10 μg of nuclear extracts for 30 mins at room temperature, prior to resolution on a 5% polyacrylamide gel in 0.5 x TBE. The gel was dried and exposed to X-ray film at -80^0C for various lengths of time (overnight-2 weeks) until an acceptable signal was obtained. Specificity of reactions was confirmed by addition of 2ng of competing unlabelled NFkappaB consensus oligonucleotide ("cold" oligo) and the inclusion of 1μg of antibodies to specific NFκβ signalling proteins (supershift).

2.14 Surface Plasmon Resonance (SPR) analysis using the BIACORE System

Interactions between CD23-derived peptides and αVβ3 and αVβ5 integrins were performed at 25^0C using the automated Biacore 2000 machine (Biacore AB). The integrins were immobilised at approximately 4000 response units on a C1 chip using amine coupling chemistry. An underivatised reference cell was employed as a control surface. CD23-derived peptides in HBS-EP buffer (0.01 M HEPES-KOH pH 7.4, 0.15 M NaCl, 3 mM EDTA, 0.005% (v/v) Surfactant P20) were injected over the test and control chip surfaces at a flow rate of 40μL.min-1 and allowed a 3min association phase followed by a 6 min dissociation phase. The sensor surfaces were regenerated to baseline by injection of 0.2M glycine-HCL, pH2.5, where necessary. In all experiments, peptides bound exclusively to the test cell, there was no non-specific binding to the control reference cell and regeneration of a stable baseline was readily achieved. Data collected was standarised using control and blank injections prior to kinetic analysis, according to standard double referencing data subtraction methods [170]. All kinetic analysis was performed using BIAevaluation 3.0.2 software (Biacore AB).

2.15 Ellman's Assay for free Sulphydryl groups in CD23-derived peptides

CD23 derived peptides contain a single cysteine, so the moles of total sulphydryl (SH) can be determined from the peptide concentration (i.e. equivalent to the moles of peptide contained in the sample). The proportion of this total sulphydryl (SH) existing as free SH was determined by reaction with Ellman's Reagent (5,5'-Dithio-bis 2-nitrobenzoic acid/DTNB) [171]. DNTB was purchased from Sigma Chemicals Co, Poole, UK. 50μL of CD23-derived peptides were incubated with 200μL of DNTB for 30mins and the absorbance at 415nm recorded. The moles of free SH were calculated and the data represented as a percentage of total SH.

3 ANALYSIS OF THE CD23-αV INTEGRIN INTERACTION

3.1 INTRODUCTION

3.1.1 The Classical Recognition Sequence 'RGD'

Binding of ligands by integrins is dependent on the presence of a particular motif within that ligand. The Arg-Gly-Asp (RGD) peptide was first discovered in fibronectin and is now widely recognised as the classical recognition sequence for most integrins [101]. This sequence is found in a diverse range of receptors and integrin ligands. The presence of a small motif in a range of functionally diverse ligands creates an extensive system for recognition by cell adhesion molecules [102].

3.1.2 Integrin ligand recognition

Insights into the binding of RGD-containing ligands have been provided by the crystal structure of the extracellular domain αVß3 integrin alone [94] and in complex with a cyclic RGD-containing peptide [98]. The availability of both ligand-bound and ligand-free structures allows analysis of both the fundamental residues involved in the interaction and conformational changes that arise due to ligand binding. Ligand binding is cation-dependent and mediated by residues from both the α and ß subunit of the integrin heterodimer (Figure 1.6). The RGD peptide binds a shallow groove at the interface of the ß-propeller of the α subunit and the ßA domain of the ß subunit. The central Gly^{RGD} projects into the interface between the α and ß subunits. It forms hydrophobic interactions with the αV subunit, primarily via the carbonyl oxygen of Arg216. The main chain conformation of the RGD peptide in the structure is identical to that observed in the natural integrin ligand Echistatin [98].

In addition to the recognition of different sequences at this 'RGD-recognition site' of integrins, the existence of an additional, distinct ligand binding site, for ligands such as tumstatin, HIV Tat protein and entactin, on the $\alpha V\beta 3$ and $\alpha V\beta 5$ integrins has been suggested. These studies have proposed either the existence of an additional distinct binding site or a synergistic ligand recognition site that cooperates with the RGD binding site.

3.1.3 CD23-integrin interactions

CD23 exists in both membrane-bound and soluble forms. Soluble CD23 binds four members of the integrin superfamily of proteins, in addition to its ligands CD21 and IgE. CD23 has been shown to bind the αMß2 (CD11b/CD18), αXß2 (CD11c/CD18) [83] and αVß3[40] integrins on monocytic cells. Our laboratory has recently identified αVß5 as a new integrin ligand for CD23 [75]. The interaction between CD23 and these integrins on monocytes is functionally important in the production of pro-inflammatory cytokines, including IL-1ß, IL-6 and TNFα[40, 41, 83], but the site of interaction between CD23 and these integrins remains to be fully elucidated.

3.2 RESULTS

3.2.1 Macrophage cell lines express integrin receptors for CD23

CD23 interacts with four members of the integrin family of receptors – two members of the ß2 family (αMß2 and αXß2) and two members of the αV family (αVß3 and αVß5) [40, 75, 172]. The expression of these integrins on the surface of model cell lines, THP-1 and U937, was determined by flow cytometry (Figure 3-1). The antibody staining for individual integrins is shown as black lines with the isotype matched controls shown in grey shading.

Both THP-1 and U937 cell lines showed high levels of surface expression of αVß3, αVß5 and αXß2 integrins, shown by an increase in staining compared to the isotype control staining. Of these integrins, the αVß3 and αVß5 heterodimers were expressed at higher levels on the surface of cells than the αXß2 heterodimer. Both THP-1 and U937 expressed only low levels of the αMß2 integrin heterodimer. Overall, there was no major difference in the levels or relative ratios of expression of different integrin isoforms between the two cell lines, THP-1 and U937.

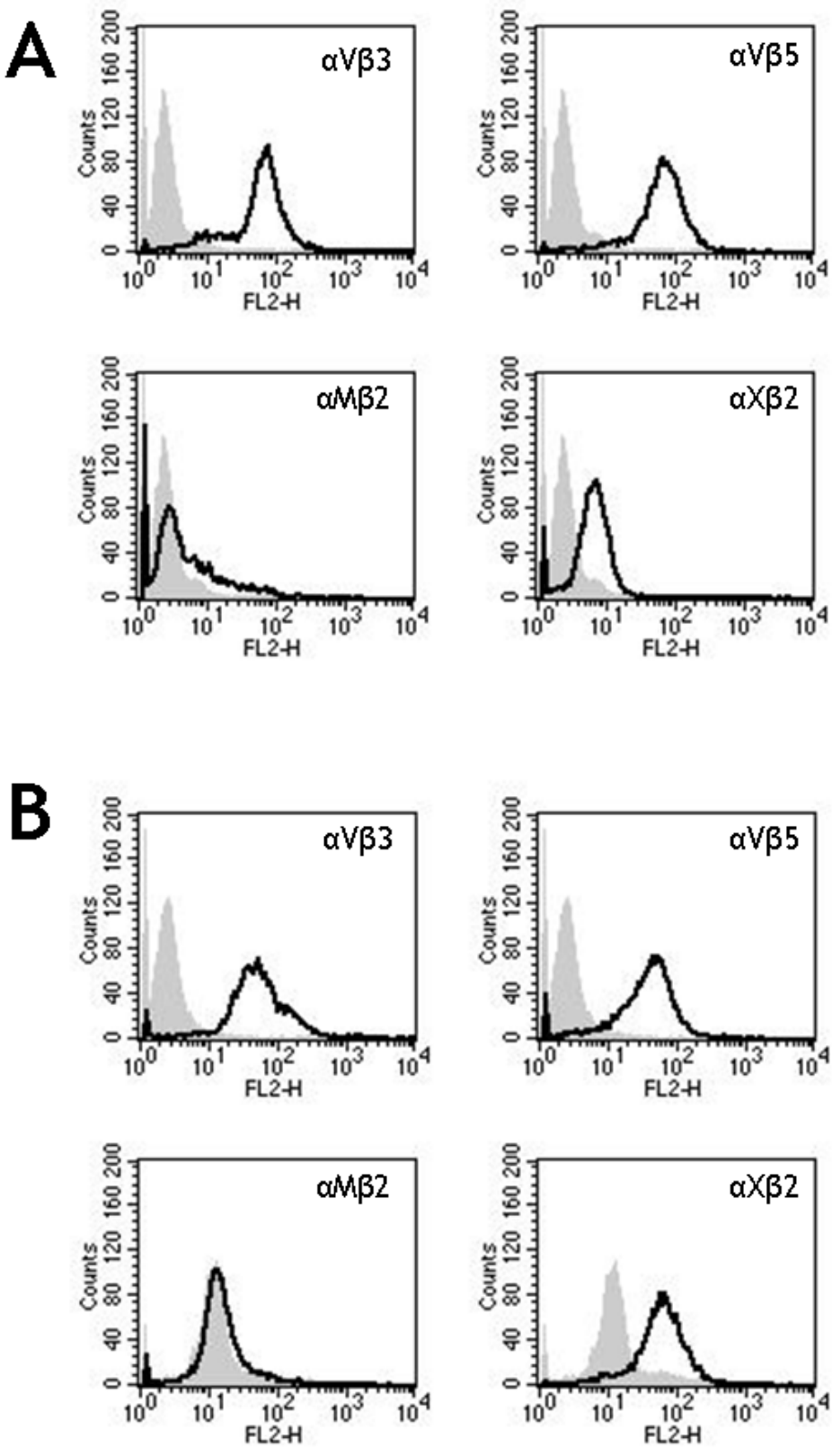

Figure 3-1 Expression of CD23 binding integrins on monocytic cell lines
Surface expression of CD23-binding integrins on U937 (A) and THP-1 (B) cell lines was determined by flow cytometry. Cells were incubated with antibodies against specific integrins, as indicated in the right hand corner of the plots. Primary antibody binding was detected using secondary antibody conjugated to PE. The binding of isotype matched controls is shown as grey shading and the integrin staining shown as a bold black line.

3.2.2 Identification of the recognition sequence in CD23 for αV integrins

The classical sequence recognised and bound by integrins is the RGD motif. This RGD (or a closely related sequence) is found in most integrin ligands. CD23 has been shown to bind integrins, but it does not contain a classical RGD motif. CD23 does, however, contain a DGR motif (inverted RGD motif) near the C terminus (Figure 1-1). There has been much debate as to whether this DGR motif is functionally equivalent to an RGD motif and is the site of integrin recognition of CD23 [61, 67, 173].

In order to define the integrin binding motif on CD23, we generated a library of 83 overlapping nonameric peptides derived from residues 131-321 of the 25kDa soluble CD23 sequence. The peptides are numbered sequentially as they occur in the CD23 sequence (starting with P1 from residue 131) and included an SGSG linker and an N-terminal biotin label [75]. The biotinylated CD23-derived peptides were assessed, for their ability to bind to the surface of SMS-SB cells by flow cytometry (Figure 3-2). SMS-SB cells express the αVβ5 integrin as the only CD23 receptor [174]. The binding of CD23-derived peptides was detected using streptavidin-conjugated PE, which was used to detect the biotin label on the peptides. Figure 3-2 shows the mean fluorescence values for the binding of the 83 biotinylated peptides to the surface of SMS-SB cells.

A peak in binding was observed for four peptides, named P9 - P12, which corresponded to residues Lys^{166} to Gly^{180} in the soluble CD23 sequence. Interrogation of the sequence of the CD23-derived peptides identified a common RKC motif in these peptides (Figure 3-3). A low level of binding was observed with peptides P60 - P63. These peptides (P60-P63) all contain a common sequence, which includes a RK dipeptide. This is similar to the RK dipeptide in the RKC containing CD23 peptides and may account for the low levels of binding. Peptides P78 - P80, which contain the DGR motif, did not bind to SMS-SB cells.

The preliminary screening for binding was conducted using SMS-SB cells, a pre-B cell line which expressed only a single CD23 binding integrin (αVβ5). It was therefore necessary to establish whether the RKC containing peptides were capable of binding other cell types expressing CD23 binding integrins. Binding of

P9 - P12 to the established model monocytic cell lines THP-1 and U937 was tested by flow cytometry. THP-1 and U937 cells did not express CD23 (*data not shown*). Figure 3.3 shows the binding of CD23 and RKC containing CD23-derived peptides to THP-1 cells. CD23/CD23-derived peptide binding is shown as a solid black line and background staining shown as grey shading. CD23 and CD23-derived P9 - P12 bound to THP-1 cells, as indicated by an increase in fluorescence (Figure 3-3A). All these species contain a common RKC motif (Figure 3-3B). CD23-derived P8, which does not contain the RKC motif but does have some sequence similarity with P9, did not bind to THP-1 cells. An identical binding pattern was observed for the second monocytic cell line, U937 (*data not shown*). Subsequent to identification of the RKC motif, an additional peptide, named LP (long peptide), was also synthesised. The LP contained 15 residues spanning the entire sequence from the beginning of P9 to the end of P12 and contained the entire putative CD23 binding sequence.

Cell binding analysis represents the overall binding of the CD23-derived peptides to multiple integrins on the cell surface. Most cells will express more than one CD23 ligand (Figure 3-1) and, therefore, to establish these peptides as *bone fide* integrin ligands, it was essential to analyse their binding characteristics with respect to individual purified integrins. Binding of peptides to purified αVß3 and αVß5 integrins, which are commercially available, was measured by surface plasmon resonance (SPR), using the BIACORE system. Interactions between CD23-derived peptides and immobilised $\alpha V\beta 3$ and $\alpha V\beta 5$ integrins were performed at 25^0C using the automated Biacore 2000 machine. In all experiments, peptides bound exclusively to the test cell, there was no non-specific binding to the control reference cell and regeneration of a stable baseline was readily achieved. Data collected were standarised using control and blank injections, according to standard double referencing data subtraction methods [170]. Figure 3-4 shows the sensorgram for the binding of CD23-derived peptides (Figure 3-4A) and CD23 (Figure 3-4B) to the purified αVß5 integrin. Both CD23 and the RKC containing CD23-derived peptides showed characteristic binding curves over time, with association and dissociation phases indicative of a specific interaction. The control P58, which is derived from the CD23 sequence but does not contain the RKC motif, did not bind to the purified integrin, as shown by the lack of any association or dissociation curves on the sensorgram. This binding trace appears as a flat line on the sensorgram (Figure 3-4A, black line).

A qualitative hierarchy of the strength of binding can be obtained by observation of the amplitude of the binding response for equivalent concentrations of different peptides. This suggested that under these conditions the LP interacted most strongly with the immobilised αVß5 integrin, as this peptide gave the largest binding response, even at a ten-fold lower concentration than the other peptides (1μM for LP compared to 10μM for the other CD23 derived peptides). In this manner, the peptides were ranked in order of highest to lowest binding as follows; LP > P11 > P12 > P9 > P10. Equivalent traces and qualitative binding hierarchy data was obtained for the immobilised αVß3 integrin (*data not shown*).

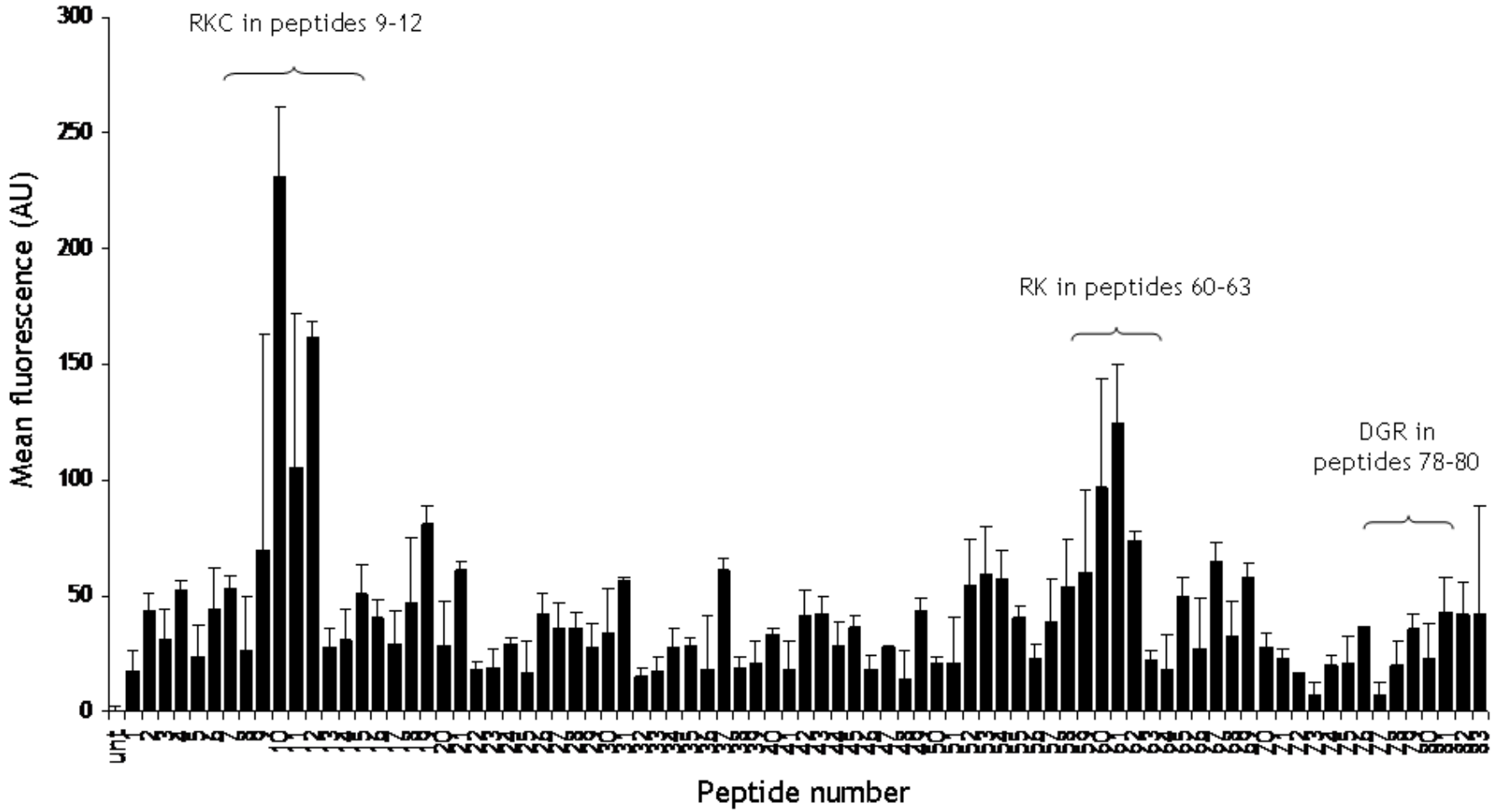

Figure 3-2 Binding of biotinylated CD23-derived peptides to SMS-SB cells

The binding of biotinylated CD23-derived nonameric peptides was determined by flow cytometry analysis. Biotinylated peptides were incubated on ice with SMS-SB cells and peptide binding detected using streptavidin conjugated to the fluorescent label PE. The mean fluorescence intensity for each peptide binding is plotted against peptide number in the bar chart. Data are representative of at least 3 separate experiments. The error bars indicate standard deviations (SD).

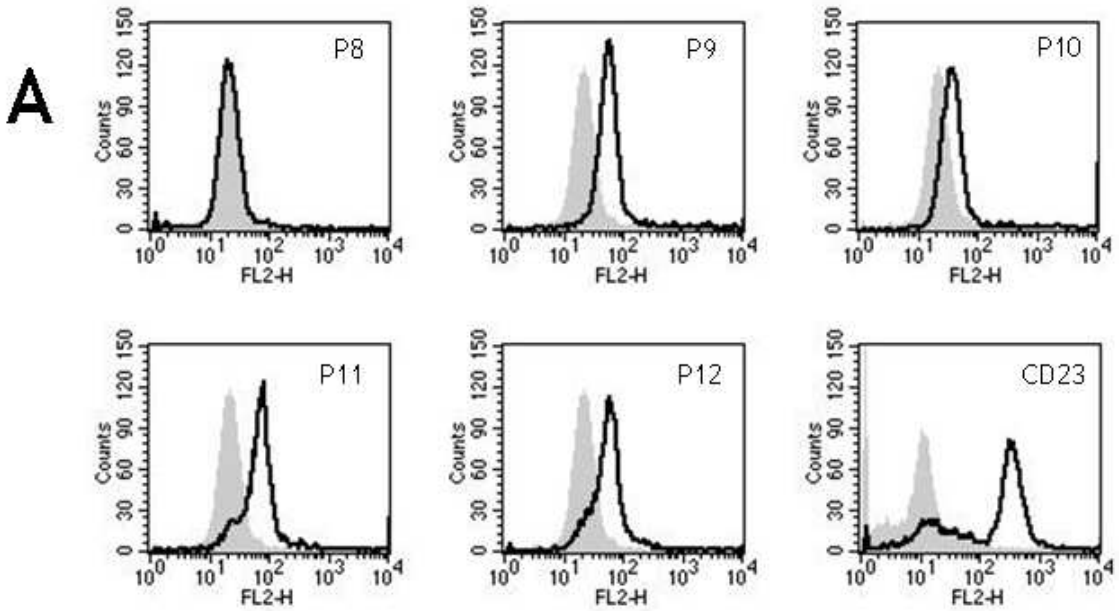

B

8		T	C	P	E	K	W	I	N	F								
9						K	W	I	N	F	Q	**R**	**K**	**C**				
10								I	N	F	Q	**R**	**K**	**C**	Y	Y		
11										F	Q	**R**	**K**	**C**	Y	Y	F	G
12												**R**	**K**	**C**	Y	Y	R	G	K	G
LP						K	W	I	N	F	Q	**R**	**K**	**C**	Y	Y	R	G	K	G*

Figure 3-3 Binding of CD23 and CD23-derived peptides to THP-1 cells
The binding of CD23 and CD23-derived peptides P9-P12 to THP-1 cells was determined by flow cytometry. The grey shading indicates autofluorescence and peptide binding is show as a black line. (A). Cells were incubated on ice with biotinylated peptides or CD23. Binding of biotinylated peptides was detected using streptavidin conjugated to PE. CD23 binding was detected by anti-CD23 antibody conjugated to PE. Analysis of the sequence of CD23-derived peptides which bind to cells reveals a common RKC motif (B). *Long peptide (LP) was synthesized subsequent to the identification of P9-P12 and contains the entire CD23-derived sequence spanning P9-P12.

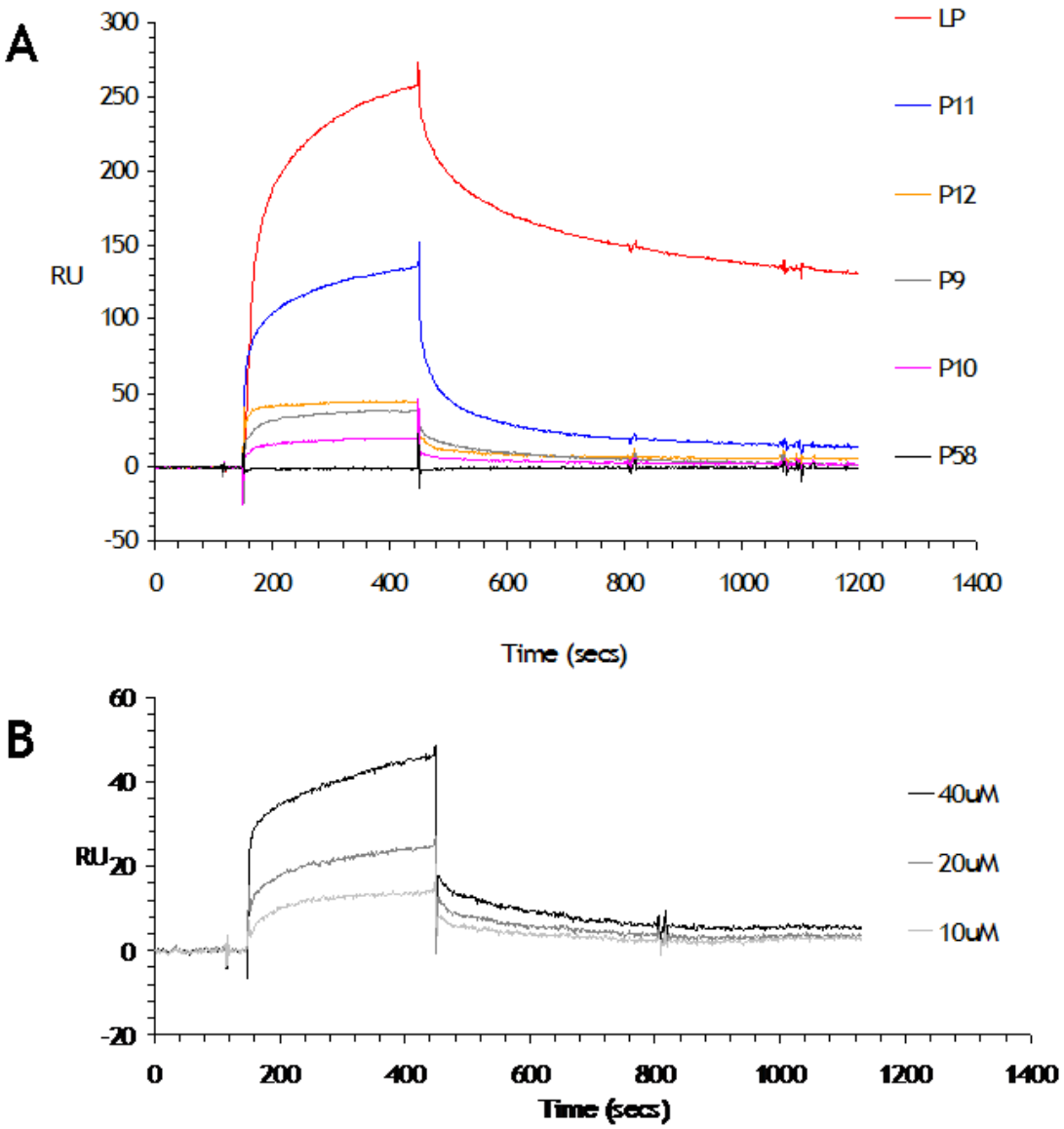

Figure 3-4 BIACORE analysis of binding of CD23-derived peptides and CD23 to purified αVβ5 integrin

Interactions between (A) CD23-derived peptides, (B) derCD23 and integrins were performed at 25^0C using the automated Bicore 2000 machine (Biacore AB). Purified αVβ5 integrin was immobilized on the chip surface and CD23-derived peptides (10μM) or derCD23 in solution were injected over the chip surface. An underivatised reference cell was employed as a control surface. In Panel A, the different peptides are shown as distinct line colours as indicated in the legend, and in Panel B the different colours indicate different concentrations of soluble derCD23 injected over the integrin surface. Data collected were standarised using control and blank injections prior to kinetic analysis, according to standard double referencing data subtraction methods [170], using BIAevaluation 3.1 software (Biacore AB).

3.2.3 CD23-derived peptides compete with CD23 for binding

Integrins are known to recognise the tripeptide RGD motif in their ligands at the interface of the α and ß subunit of the heterodimer. As the RKC motif is also a tripeptide motif, we examined whether this RKC motif was a variant of the RGD motif and would therefore compete with RGD-containing ligands and/or CD23 for integrin binding.

The RKC-containing peptides compete with CD23 for binding to the cells, as shown by the inhibition of binding of one species by the other in flow cytometric binding assays (Figure 3-5A). These assays showed that CD23 was capable of blocking the binding of P11 to THP-1 cells, when incubated with cells prior to CD23 binding and, *vice versa*, P11 was capable of blocking the binding of CD23 to THP-1 cells. (Figure 3-5A). However, preincubation with RGD-containing integrin extracellular matrix proteins vitronectin and fibronectin, failed to prevent the binding of biotinylated P11 to THP-1 cells (Figure 3-5B).

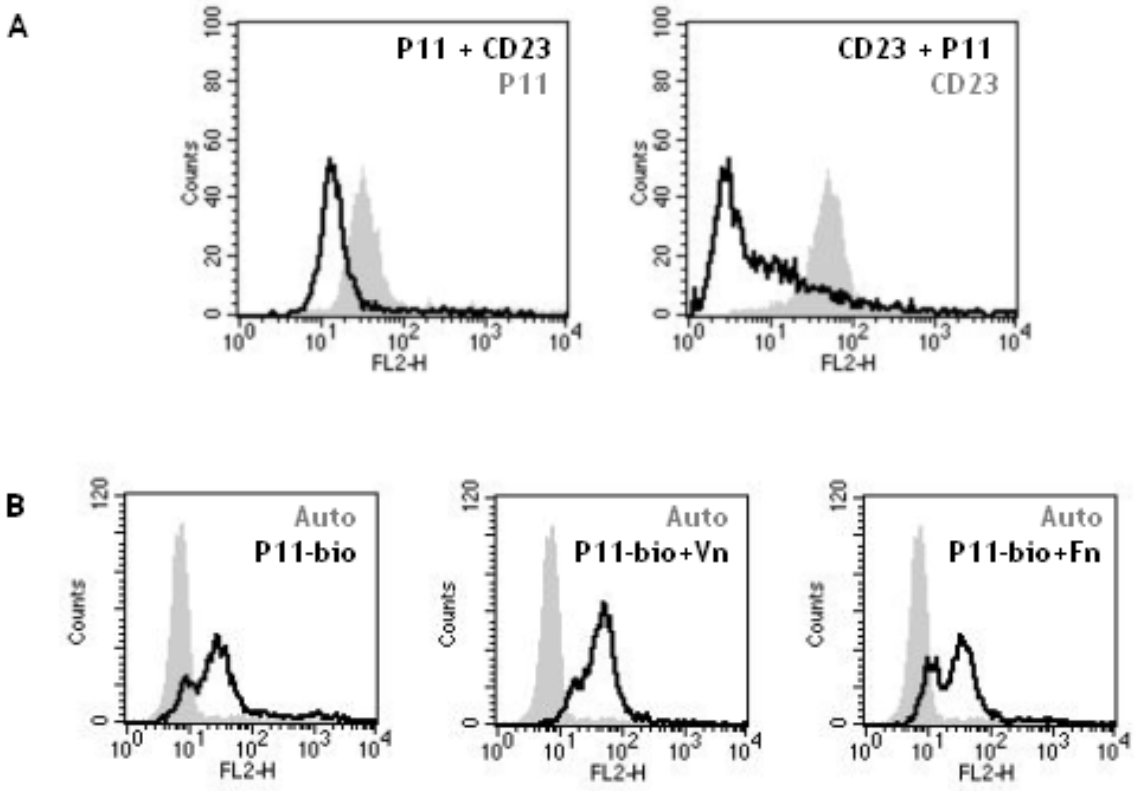

Figure 3-5 CD23 but not RGD containing ligands compete with CD23-derived peptides for binding

CD23, CD23-derived peptides, vitronectin (Vn) and fibronectin (Fn) were assessed for the ability to compete for binding to THP-1 cells by flow cytometry. Binding of biotinylated peptides and CD23 was detected using streptavidin conjugated to PE. The identity of the staining is indicated on the histograms.(A) THP-1 cells were incubated with P11 or CD23 prior to binding of biotinylated CD23 or P11, respectively. (B) THP-1 cells were incubated with vitronectin (Vn) or fibronectin (Fn) prior to binding of biotinylated P11. In Panel A, the binding of CD23 or P11 alone is shown as grey shading and the competiion binding is shown as black line. In Panel B, the autofluorescence (auto) of cells is shown as grey shading and the binding of P11 with or without RGD-containing ligands is shown as a black line.

3.2.4 Substitution of RKC motif abolishes both integrin binding and competition with CD23

The importance of the RKC motif to integrin binding was determined using peptides carrying substitutions in the residues comprising the RKC motif. Peptides with mutations in the RKC motif were synthesised to exactly the same specifications as the previous peptides and assessed for their ability to bind monocytic cell lines by flow cytometry and purified integrins by Biacore analysis. Figure 3-6A shows the binding of P9 to THP-1 cells (grey shading), as measured by flow cytometry. Background binding and the binding of mutant peptides is shown as a solid black line. Mutation of any of the residues in the RKC (R→A, R→Q, K→A, RK→AA and C→S) abrogated peptide binding to cells and resembled the background staining. The analysis of the binding of these mutant peptides to purified αVß3 and αVß5 integrins was extended using Biacore analysis.

Figure 3-7 shows the binding of P9 and mutants in solution to immobilised integrin αVß5. Mutation of any of the residues affects the binding of the peptides to the immobilised αVß5 integrin. Peptides carrying the RK→AA and C→S substitutions showed no binding to the immobilised αVβ5 integrin. Mutant peptides P9RK, P9KA and P9RQ showed some residual binding, although the binding was reduced compared to wild type P9. The binding of mutants P9RK and P9RA was reduced by approximately 50% and 75%, respectively. The P9RQ mutant showed only a very low level of residual binding, approximately one-tenth of the wild type P9 binding. Equivalent binding traces were obtained for the binding of mutants of P11 to αVß5; and for the binding of mutants of P9 and P11 to the αVß3 integrin (*data not shown*).

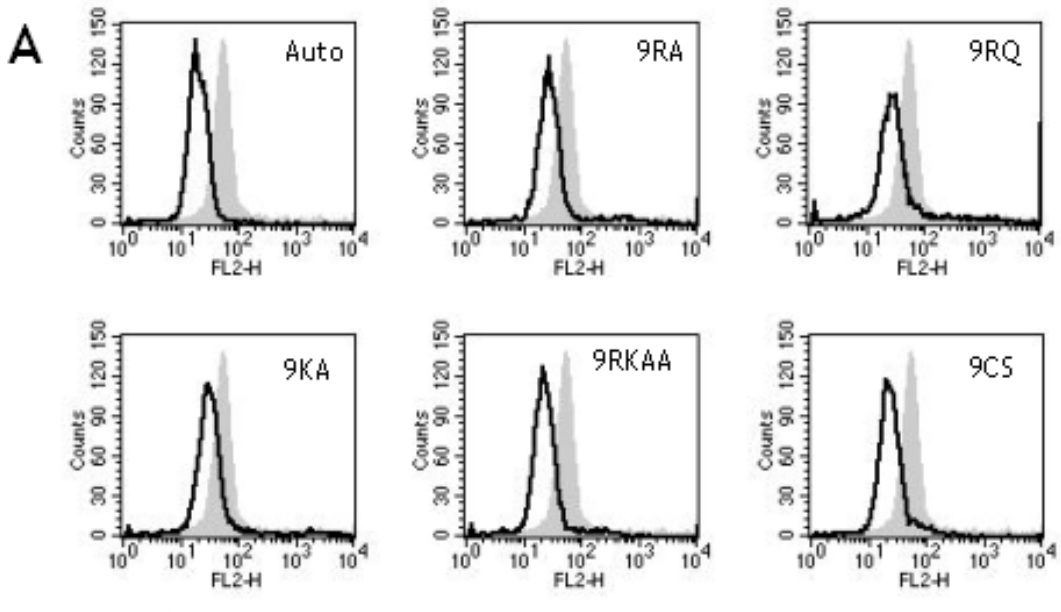

C

Peptide Name	Sequence	Peptide Name	Sequence
P9	KWINFQ**RKC**	P9RKAA	KWINFQ**AAC**
P9RA	KWINFQ**AKC**	P9CS	KWINFQ**RKS**
P9RQ	KWINFQ**QKC**	P11	FQ**RKC**YYFG
P9KA	KWINFQ**RAC**	P11RKAA	FQ**AAC**YYFG

Figure 3-6 Mutation of the RKC motif abrogates cell binding and competition
(A) Mutation of residues of the RKC motif abolishes binding of P9 to cells. The cells were incubated with biotinylated peptides and peptide binding detected by streptavidin conjugated to PE. The autofluoresence of cells (auto) is shown as grey shading and binding of biotinylated P9 mutants is shown as a bold line. The particular mutation is indicated in the top right corner of the plot. (B) Mutation of the RKC motif abolishes the ability of CD23-derived P11 to compete with CD23 for binding. Cells were incubated with CD23 with or without non-biotinylated P11, prior to detection of CD23 binding by anti-CD23 antibody conjugated to PE. The binding of CD23 alone is shown in grey shading and the binding of CD23 in the presence of P11 or P11RKAA is shown as a bold black line. (C) Sequences of CD23-derived peptides and mutants thereof (with substitutions indicated in bold).

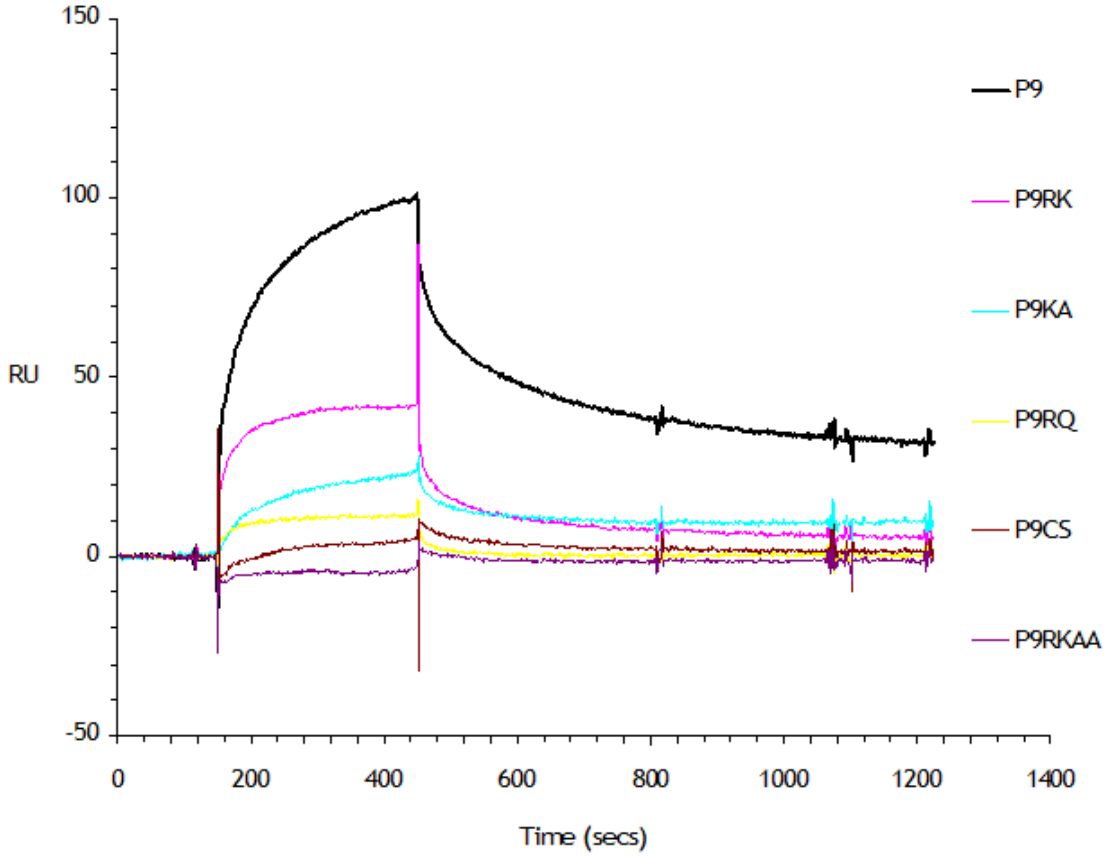

Figure 3-7 Mutation of the RKC motif abrogates binding to purified integrins
Binding of CD23-derived peptides in solution to immobilized αVβ5 integrin was measured by BIACORE analysis. Purified αVβ5 integrin was immobilized on the chip surface and CD23-derived P9 and mutants (10μM) in solution injected over the chip surfaces. An underivatised reference cell was employed as a control surface. Data collected were standarised using control and blank injections prior to kinetic analysis, according to standard double referencing data subtraction methods [170], using BIAevaluation 3.1 software. The colour coding used for identification of each injected peptide is shown in the the panel itself.

3.2.5 *In vitro* kinetic analysis of interaction between CD23 or CD23-derived peptides and αV integrins

Figures 3-4 and 3-7 demonstrate the type of qualitative information that can be obtained from the Biacore sensorgram. Extending this analysis using kinetic modelling and a range of analyte concentrations allows the calculation of quantitative parameters to define the interaction.

Figures 3-8 and 3-9 show the Biacore sensorgrams for the binding of a range of concentrations of CD23-derived peptides to immobilised αVβ3 and αVβ5 integrins, respectively. For both integrins, the RKC containing peptides (P9-P12 and LP) show characteristic association and dissociation curves. As the concentration of the peptides increases, so does the amplitude of the interaction. The control P58, which is derived from CD23 but does not contain the RKC motif, does not bind at any concentration. These data were used to quantify the interaction between the αVβ3 and αVβ5 integrins and derCD23 and CD23-derived peptides.

As the exact site and mechanism of interaction between the integrins and CD23/CD23-derived peptides remains to be identified fully, we applied a simple 1:1 binding model to the kinetic analysis. The Langmuir binding model is based on the fact that the interaction involves the Analyte A (in this case the peptide in solution) binding to a Ligand B (in this case the immobilised integrin).

The kinetic constants derived from the analyses are shown in Table 1-1. All constants were generated using BIAevaluation 3.1 Software. For both the αVβ3 and the αVβ5 integrin, the qualitative hierarchy of binding (LP > P11 > P12 > P9 > P10) noted by visual observation of the sensorgram is confirmed by the values obtained for the dissociation constants (K_D) for peptides binding to integrins. DerCD23 binds with an affinity similar to P11, so the hierarchy for binding affinities under these conditions for both αVβ3 and αVβ5 integrins including derCD23 is LP > P11 and derCD23 > P12 > P9 > P10.

The affinities of the individual peptides for the different integrins are similar, for example, derCD23 binds to αVβ3 with a K_D of 6.00 x 10^{-6}M and to αVβ5 with a K_D of 6.04 x 10^{-6}M and LP binds to αVβ3 with a K_D of 2.33 x 10^{-7}M and to αVβ5

with a K_D of 3.68 x 10^{-7}M. Only P9 and P10 have K_D values that differ significantly for αVβ3 and αVβ5 (two orders of magnitude). The K_D values determined in this study are in a similar range to those determined for the interaction between derCD23 and its other ligands CD21 and IgE [62].

3.2.5.1 Potential role for disulphide bond in CD23 derived peptides during integrin binding

The integrin-binding CD23-derived peptides contain a cysteine residue which may be capable of forming an inter-peptide disulphide bond. To test the ability of the RKC containing peptides to form disulphides, peptide solutions were prepared and stored at 4^0C for up to 30 days. Samples were removed at intervals and reacted with Ellman's reagent to detect the molar concentration of free sulphydryl groups.

Reaction of Ellman's reagent with free sulphydryl groups can be followed by an increase in absorbance at 405nm and the concentration determined using Beer's Law [171]. As P9-P12 and LP contain only a single cysteine, the molar concentration of total sulphydryl can be calculated from the peptide concentration. The percentage disulphide for each peptide over time was calculated by determining the molar concentration of free sulphydryl by reaction with Ellman's reagent.

All of the peptides exhibited some degree of disulphide formation (reduction in free sulphydryl concentration) over time (Figure 3-10). Peptide P9-P12 had a significant proportion (between 80-90%) disulphide after 1 day of storage at 4^0C. The LP exhibited a lower percentage of disulphide (approximately 30%) after 1 day of storage at 4^0C. After 10 days storage, all peptides displayed increased levels of disulphide formation. P58, which does not contain any cysteines, was used as a control and did not produce any change in absorbance at 405nm with Ellman's reagent.

3.2.5.2 Effect of cations and salt concentrations on CD23-αV integrin binding

As RGD binding is cation dependent, we tested if CD23-derived peptide binding to αV integrins required divalent cations. Magnesium, supplied as chloride salts, was spiked into the Biacore running HSB buffer and the effect on peptide binding determined.

After testing the binding of the peptides in the presence of the magnesium chloride, fresh buffer containing EDTA (ethylenediaminetetraacetic acid) was added, the system equilibrated and the binding of the same CD23-derived peptides tested. The data for the binding of selected peptides to immobilised αVβ3 and αVβ5 integrins in the absence (black lines) and presence of magnesium chloride (red lines) are shown in Figure 3-11. In all cases, the peptides bound to the integrins in the absence of divalent cations and the presence of the chelating agent EDTA. Addition of magnesium chloride to the system prevented binding of peptides to both αVβ3 and αVβ5 integrins, as shown by the lack of characteristic association and dissociation curves. The sensorgram traces for the binding of LP and P9 in the presence of chloride (red lines) resembles the binding traces for the control peptide P58, which does not bind to the integrins (grey lines).

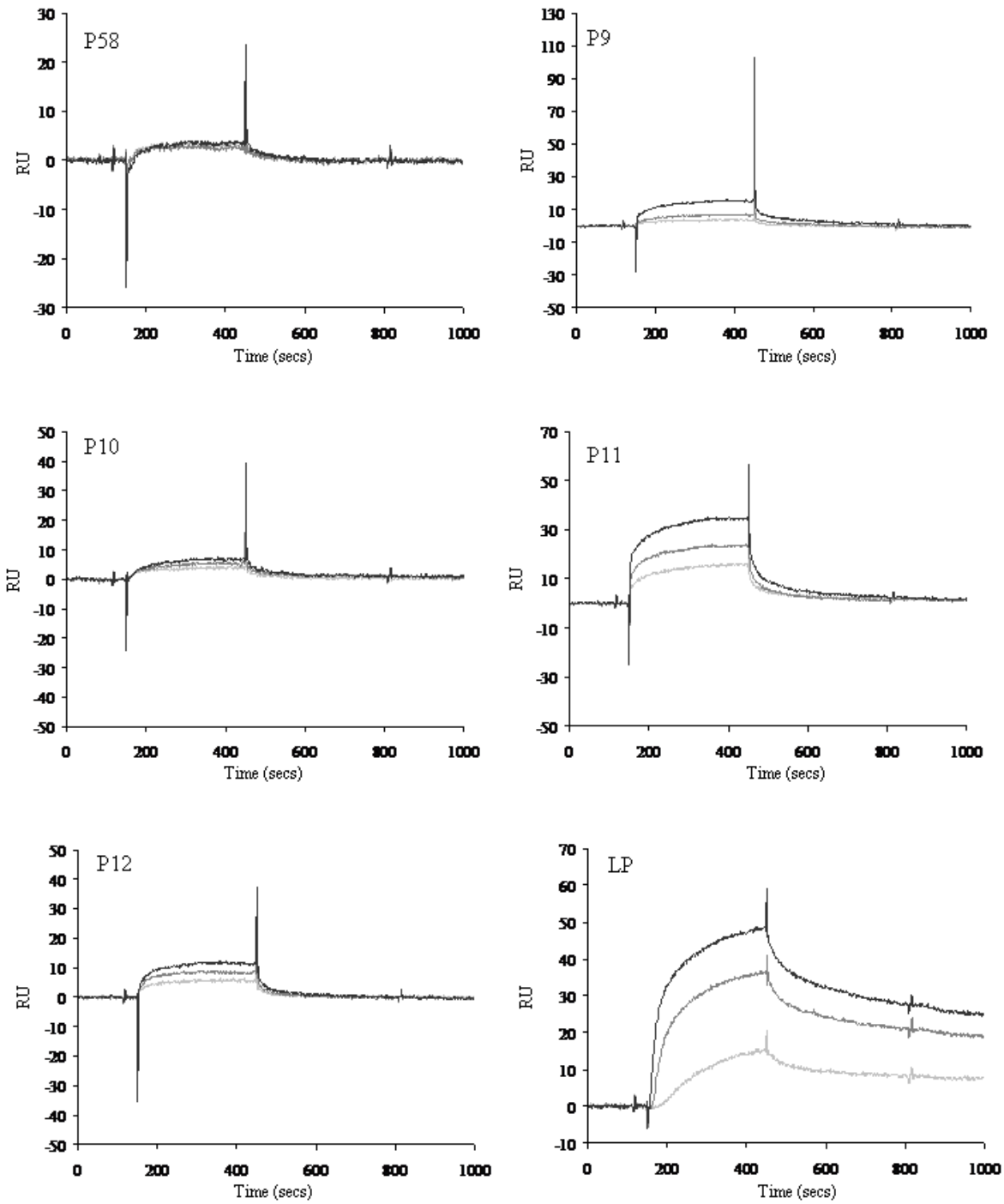

Figure 3-8 BIACORE analysis of binding of CD23-derived peptides to purified αVβ3 integrin

Purified αVβ3 integrin was immobilized on the chip surface. CD23-derived peptides at different concentrations in solution were injected over the test and control chip surfaces. Data collected were standarised using control and blank injections prior to kinetic analysis, according to standard double referencing data subtraction methods [170], using BIAevaluation 3.1 software (Biacore AB). For P9-P12 and P58, the light grey line is 5μM, the dark grey line is 10μM and the black line is 20μM. For the LP, the light grey line is 0.25μM, the dark grey line is 0.5μM and the black line is 1μM.

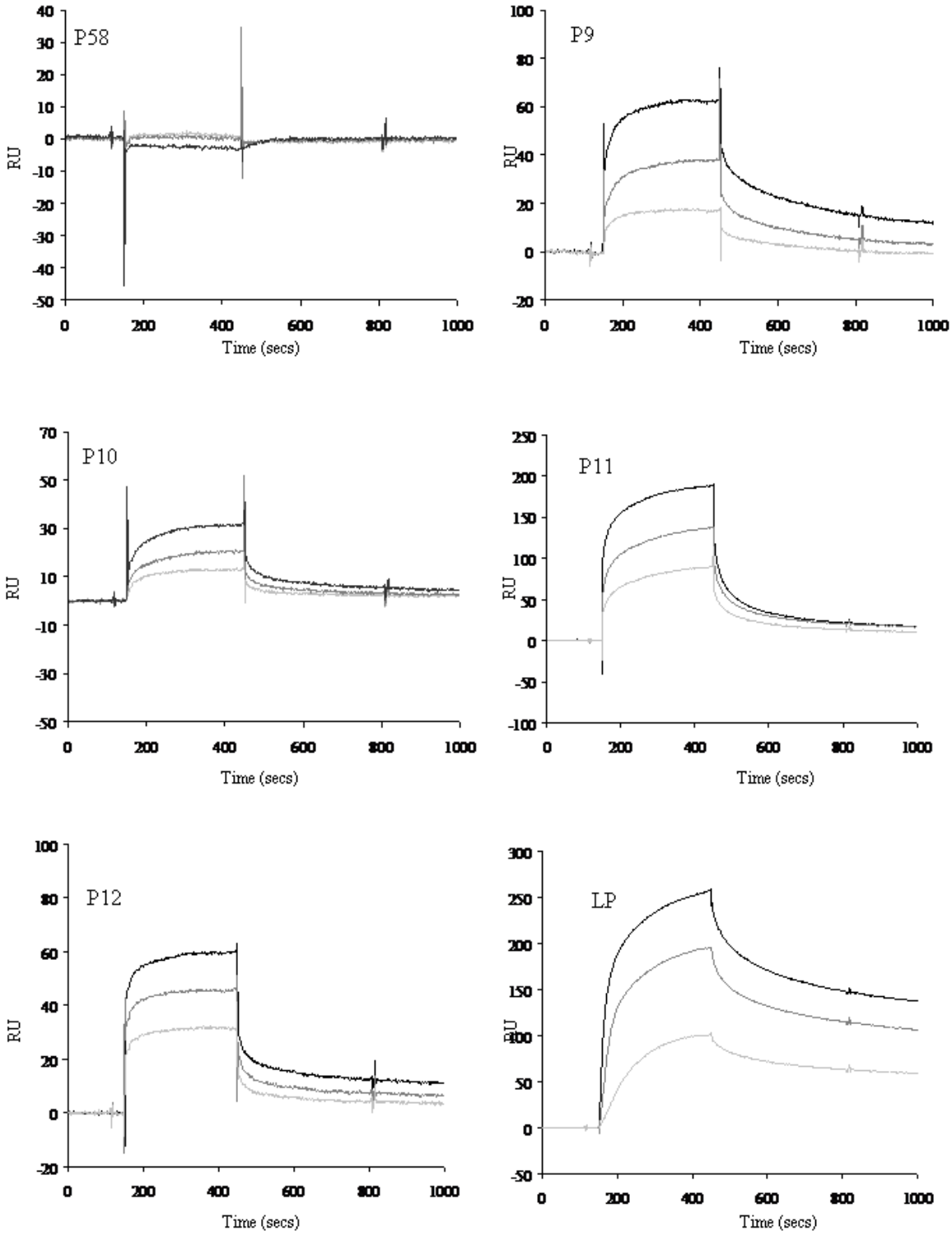

Figure 3-9 BIACORE analysis of the binding of CD23-derived peptides to purified αVβ5 integrin

Purified αVβ5 integrin was immobilized on the chip surface. CD23-derived peptides at different concentrations in solution were injected over the test and control chip surfaces. Data collected were standarised using control and blank injections prior to kinetic analysis, according to standard double referencing data subtraction methods [170], using BIAevaluation 3.1 software (Biacore AB). For P9-P12 and P58, the light grey line is 5μM, the dark grey line is 10μM and the black line is 20μM. For the LP, the light grey line is 0.25μM, the dark grey line is 0.5μM and the black line is 1μM.

Table 3-1 Kinetic Constants determined for the binding of derCD23 and CD23-derived peptides to immobilised integrins

Ligand	αVβ3	αVβ5
	K_d (M)	K_d (M)
P9	$8.98 \pm 3.14 \times 10^{-4}$	$1.30 \pm 0.08 \times 10^{-6}$
P10	$8.13 \pm 6.19 \times 10^{-4}$	$1.55 \pm 0.76 \times 10^{-6}$
P11	$9.87 \pm 0.12 \times 10^{-6}$	$8.92 \pm 0.2 \times 10^{-6}$
P12	$1.07 \pm 0.14 \times 10^{-5}$	$3.73 \pm 0.35 \times 10^{-6}$
LP	$2.33 \pm 0.068 \times 10^{-7}$	$3.68 \pm 0.04 \times 10^{-7}$
derCD23	$6.00 \pm 4.21 \times 10^{-6}$	$6.04 \pm 3.59 \times 10^{-6}$
Published constants for derCD23 and its other ligands[62]		
Ligand	**K_d (M)**	
CD21	$8.70 \pm 0.9 \times 10^{-7}$	
IgE	$1.3 \pm 0.3 \times 10^{-6}$	

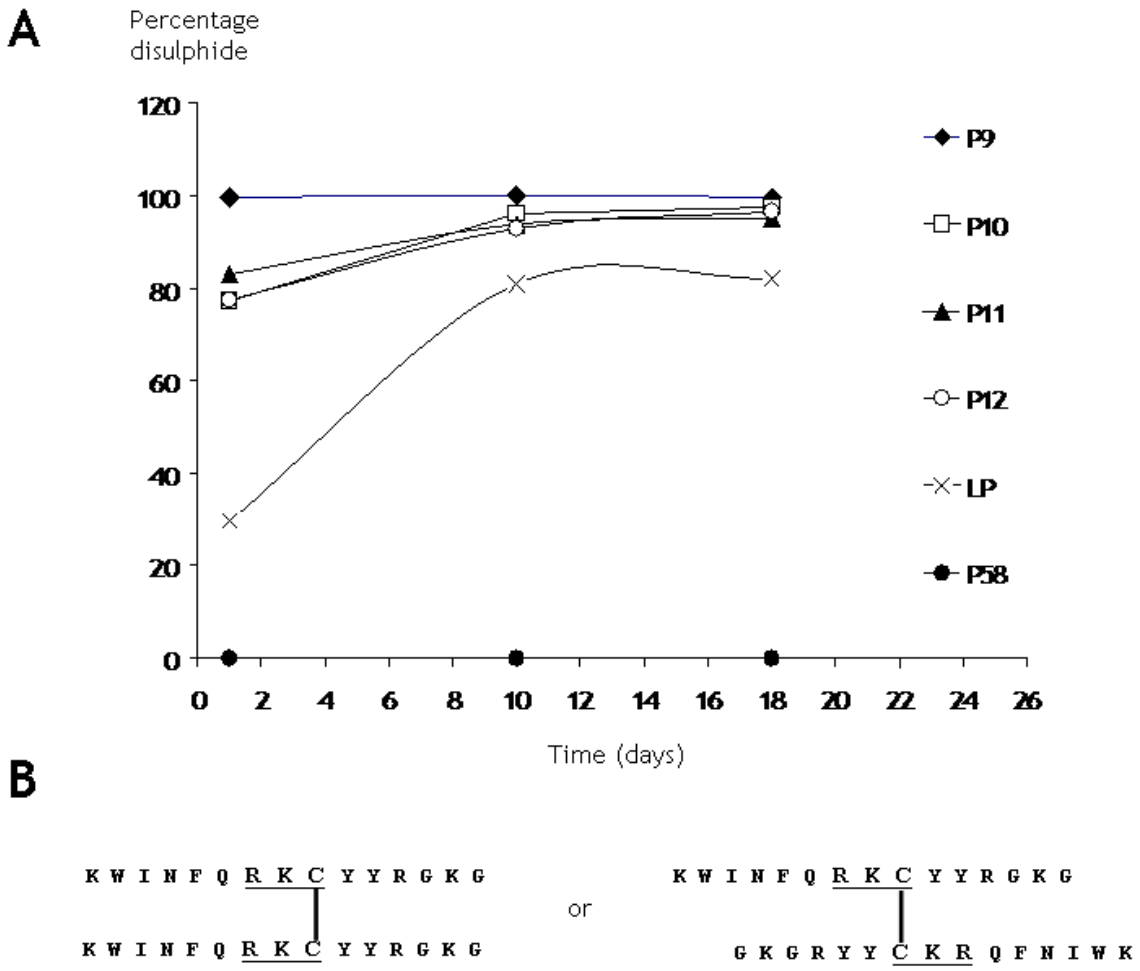

Figure 3-10 Analysis of disulphide formation in CD23-derived peptides by Ellman's Assay

(A) Ellman's reagent was used to determine disulphide bond formation in CD23-derived peptides. Peptide solutions at 10µM were prepared and stored at 4^0C for a month. The percentage disulphide was determined at specified time points by incubation with Ellman's Reagent and measurement of absorbance at 450nm. (B) RKC-containing CD23 long peptide sequence contains a single cysteine, possibly capable of forming two disulphide-bonded dipeptide species.

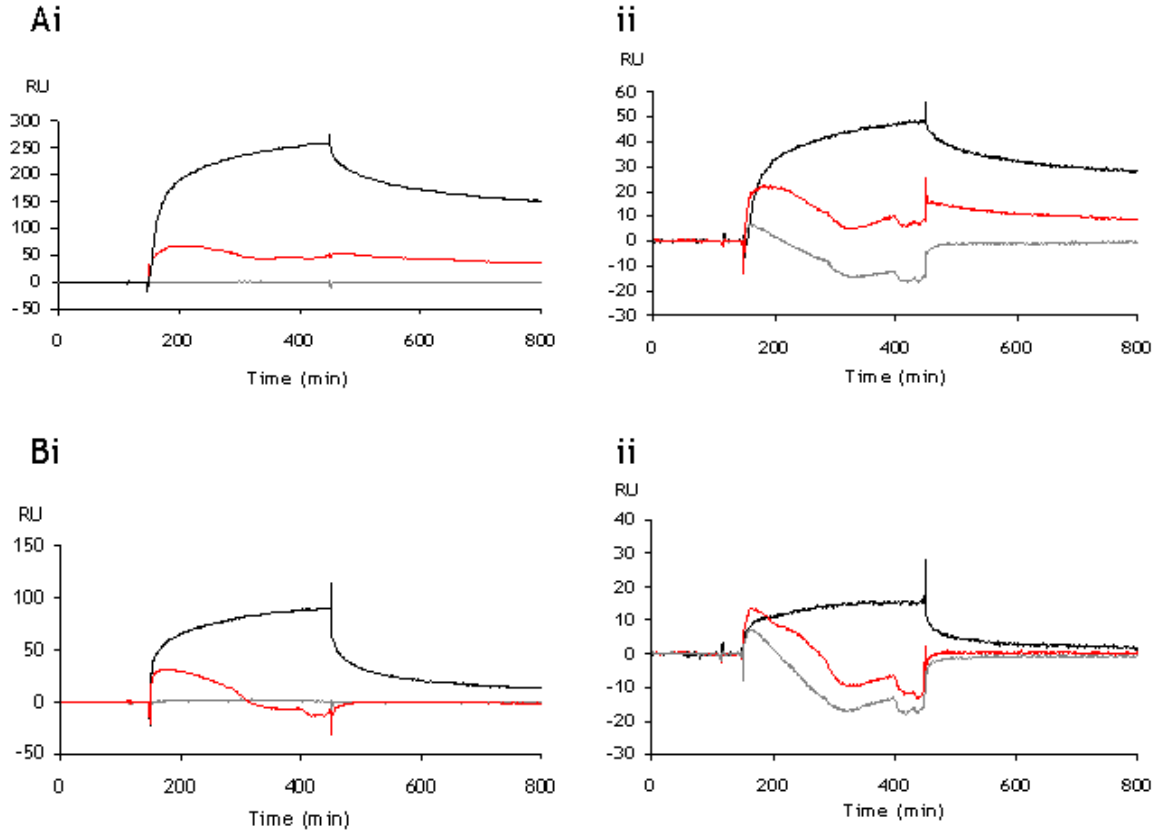

Figure 3-11 BIACORE analysis of effect of salt concentration on binding of CD23-derived peptides

Panel A shows the binding of CD23-derived peptide LP to the purified αVβ3 (Ai) and αVβ5 (Aii) integrins. Panel B shows the binding of CD23-derived peptide P9 to the purified αVβ3 (Bi) and αVβ5 (Bii) integrins. In all graphs, the black line shows the binding sensorgram for the specific peptide in the absence of divalent cations or chloride ions. The grey line shows the binding of CD23-derived P58. This peptide P58 did not bind the purified integrins and therefore is considered a control for absence of binding. The red line shows the binding of the specific peptide in the presence of divalent cations and chloride ions. Data collected were standardized using control and blank injections prior to kinetic analysis, according to standard double referencing data subtraction methods [170], using BIAevaluation 3.1 software.

3.3 DISCUSSION

CD23 binds to four members of the integrin family of proteins, αMß2, αXß2, αVß3 and αVß5. Using cell lines that express CD23-binding integrins and commercially-available purified αVß3 and αVß5 integrins, we investigated the interaction between CD23 and these integrins. We generated a library of nonameric peptides derived from the CD23 sequence (residues 131-321) and identified a set of peptides (P9-P12) which bound to integrins expressed on the surface of cells and purified αVß3 and αVß5 integrins in *in vitro* Biacore analysis. Although many protein recognition motifs are cryptic and non-linear, this protein array technique was determined suitable for our purposes as integrins are well known to bind small, linear peptide motifs (RGD) [175].

3.3.1 RKC is a new integrin recognition motif

Those CD23-derived peptides that bound cells and integrins were found to contain a common, linear tripeptide recognition sequence, termed the RKC motif. Peptides containing this motif bound to cells expressing integrins in flow cytometry assays and to purified αVß3 and αVß5 integrins in Biacore analysis. The interaction between RKC-containing peptides was determined to be independent of divalent cations, salt sensitive and not inhibited by the presence of RGD-containing integrin ligands. Mutation of residues in the RKC motif abolished the interaction with cells and purified integrins as judged by Biacore. These data suggest that the RKC is a new recognition motif for αV integrins and that the sequence is recognised and bound by the integrin at a site distinct from that used for RGD binding.

The classical integrin recognition motif is the tripeptide RGD motif, found in numerous integrin ligands. Initial observations suggested that the RKC motif might be a new variant of the RGD motif, given that it was a tripeptide motif and that CD23 does not contain an RGD sequence, but is known to bind integrins. Integrins do bind variations of the RGD tripeptide motif at the site usually bound by RGD-containing ligands, for example the KQAGDV sequence is bound by αIIbβ3, the LDV is bound by α4β1 and α4β7 and REDV sequence from fibronectin is bound by α4β1 [101, 110].

3.3.2 RKC binding is independent of RGD binding

All of the alternative integrin recognition sequences described previously are considered variants of the RGD motif and are bound at the same site on the integrin at the RGD-binding site. The inverse RGD sequence, DGR, does not have any measurable integrin binding activity. This is important in the context of CD23, as it contains a DGR sequence and is known to interact with RGD-binding integrins [67]. Our data support the fact that DGR is not an integrin recognition motif, as peptides from the CD23 sequence containing this DRG motif (P60-63) failed to bind to cells in our assays.

Despite the range of sequences recognised by integrins, in most cases, those alternative motifs described thus far all include an Asp, or the closely related, Glu residue. The RGD peptide binds a shallow groove at the interface of the ß-propeller of the α subunit and the ßA domain of the ß subunit (Figure 1.6). The requirement for the Asp may be due to its ability to coordinate metal ions essential for integrin-based ligand recognition. In addition to binding the metal ion at the MIDAS site, the Asp^{RGD} side chain makes contacts with residues Tyr122 from the α subunit and Arg214 and Asn215 from the ßA domain on the ß subunit. The Arg^{RGD} residue is bound by the ß-propeller groove from the α subunit, where the guanidinium group forms a bidentate salt bridge with Asp218 and another salt bridge with Asp150 (Figure 1-6). This group forms the centre of a network of polar interactions with the ßA residues and the MIDAS. The central Gly^{RGD} residue projects into the interface between the α and ß subunits. It interacts with the αV subunit, primarily via the carbonyl oxygen of Arg216.

In view of this binding information obtained from the crystal structure of the αVß3 integrin in complex with a cyclic RGD containing peptide, the characteristics of the RKC make it improbable that the RKC would be bound at the RGD site. The RKC motif lacks the acidic residue and therefore would be unable to coordinate the divalent cation; indeed our data show that the RKC binding is independent of divalent cations and can occur in the presence of the chelating agent EDTA. CD23-derived peptides do not compete for binding with RGD containing ligands. In addition, a predicted conflict between the Arg216 carbonyl group integral to RGD binding and the large, charged lysine group of the RKC means the Lys^{RKC} is unlikely to be accommodated in the Gly^{RGD} position

at the interface of the two subunits. Taken together, these data suggest that the RKC is a novel recognition sequence and is bound at a site distinct from that used for RGD binding.

Although the RGD-binding site is the most extensively studied interaction site on integrins, there are precedents for the existence of an alternative binding site from other studies. These alternate binding sites have been suggested by the binding of ligands, such as tumstatin [114], HIV Tat protein [109] and entactin [115], to the αVß3 and αVß5 integrins at RGD-independent sites. These studies have proposed either the existence of an additional distinct binding site or a synergistic ligand recognition site that cooperates with the RGD binding site [109, 176, 177]. In most cases, this additional non-RGD site recognises basic sequences.

Analysis of the binding of Type IV collagen indicates that this protein contains additional αVβ5 and αVβ3 binding sites [108]. Studies on the binding of tumstatin-derived peptides to αVβ3 indicated that the protein contains two RGD-independent αVβ3 binding sites, as the binding of these peptides was not inhibited by the presence of cyclic RGD peptides [114]. Entactin was also shown to contain two distinct RGD-independent cell attachment peptides. Mutants of entactin lacking the RGD motif were still capable of mediating cell attachment, although the integrin involved in binding remains to be identfied [115]. The α2ß1 integrin also recognises a basic tetrapeptide RKKH site in the protein jararhagin[177] and α3ß1 recognises a basic sequence in laminin [176].

3.3.3 Substitution of the RKC affects integrin binding

The interaction of CD23/CD23-derived peptides and integrins required the presence of the RKC motif. Substitution of residues in the RKC tripeptide affected the interaction between the peptides and both the αVß3 and αvB5 integrins. Mutation of any of the residues in the RKC motif abolishes the interaction of these peptides with cells, while the Biacore analysis was more sensitive and reveals that some of the mutant peptides retain some binding ability. P9 carrying a mutation of the Arg^{RKC} to a similarly charged Lys residue shows a reduction in binding to approximately half of that of the wild type P9, but did not completely prevent binding in our assays. Mutation of the same residue to a Gln almost completely abolished any binding to the purified

integrin. Mutation of the Lys^{RKC} to Ala also results in a significant reduction in binding. These three mutations highlight the importance of the basic nature of the RKC motif in the binding to integrins. Any mutation that reduces the basic nature of the motif reduces the interaction. The double mutant RK→AA mutant displays no binding in the context of either P9 (Figure 3-7) or P11 (*data not shown*).

Interestingly, the P9C→S mutant completely ablates the binding between the RKC containing peptides and the integrins. Analysis of the structure of the RKC motif in complete CD23 reveals that this residue is part of a disulphide bond (Figure 3-12). We investigated the abilty of the CD23-derived peptides to form inter-peptide disulphide bonds using Ellman's reagent. Our analysis revealed that the peptides did appear to form disulphides, as indicated by a lower concentration of free sulphydryl groups than total sulphydryls over time. This disulphide bonding may be important for peptide binding, indicated by the lack of binding in the P9C→S mutant (which cannot form an inter-peptide disulphide bond). Work from another member of the laboratory has highlighted the importance of the Cys^{RKC} to the biological role of the CD23 derived peptides in B cells. RKC containing peptides stimulate the proliferation of B cell precursors [75]. A specific murine cell line, BAF03 requires ß-mercaptoethanol in the growth medium for survival. This fact was exploited to examine the role of the disulphide bond in RKC containing peptides. P9 was boiled with ß-mercaptoethanol to reduce the disulphide bond and then tested for its ability to stimulate the growth of BAF03 cultures (including ß-mercaptoethanol in the medium). Untreated P9 was capable of stimulating cell growth, but the ß-mercaptoethanol treated P9 was not (*Dr. Mridu Acharya, unpublished data*). These data support the important role of the Cys^{RKC} in the binding and activity of these peptides. The mechanism underlying this characteristic remains to be determined. It is possible that the disulphide provides a degree of structural rigidity to the peptides that is required for binding or activity. Alternatively, the dimeric peptide may cause dimerisation of the integrins to which it bound. These are only theories at present and will need to be determined conclusively by crystallisation/structural analyses.

Although the RKC motif is the core unit important for binding, the hierarchy of binding obtained from the Biacore analysis (both qualitative and in K_D values)

reveals that other regions of the peptides must be important for binding. Were it only the RKC motif that was the critical determinant for binding, all peptides containing that tripeptide should bind with equivalent affinities. We observed, however, that peptides bound with different affinities, suggesting an important role for the flanking sequence in integrin binding (Table 1-1). The LP (2.33 x 10^{-7}M and 3.68 x 10^{-7}M for the αVβ3 and αVβ5 integrin, respectively) shows the highest affinity binding, higher than any of the other P9-P12 and in fact higher that obtained for CD23 (K_D 6 x 10^{-6}M and 3 x 10^{-7}M for the αVβ3 and αVβ5 integrin, respectively, from which all the peptides were derived). The fact that the LP binds more strongly to both αVβ3 and αVβ5 than the other CD23-derived peptides indicates that, although the RKC is required for binding, the flanking sequence influences the strength of that interaction. The LP contains the whole sequence encompassing those peptides which bind the integrins and therefore must contain the majority of the complete binding sequence. The increased affinity of the LP for the integrin is interesting, as the natural ligand (CD23) binds with lower affinity than the LP derived from it. It may be that there is some structural arrangement or induced-fit conformation that the LP is capable of achieving that the full length CD23 is prevented from by steric hindrance. Whether this is true or has physiological relevance remains to be determined.

The hierarchy of binding determined from the kinetic analysis is also observed qualitatively by looking at the relative responses of equivalent concentrations of CD23-derived peptides in the Biacore sensorgrams (Figure 3-4). It is worth noting, however, that the kinetic parameters determined for this interaction are only relevant in the context of our experiment and the interaction model used to fit the data. In the absence of knowledge of the exact mechanism of the interaction between CD23/CD23-derived peptides and αV integrins, we applied a simple 1:1 interaction model to calculate kinetic parameters. This may not be the most accurate method of fitting the data. We determined by Ellman's assay that these CD23-derived peptides are capable of forming disulphide bonds. Given that the peptides contain only a single disulphide bond, the only possible disulphide bonded species would be an inter-peptide bond. Mutation of the C→S abolishes the potential to form a disulphide and prevents binding; a peptide treated with the reducing agent ß-mercaptoethanol loses its functional activity (*Dr Mridu Acharya, unpublished data*). This suggests that a dipeptide, which possibly might contain 2 recognition sites (RKC) for the integrin, may be the

active conformation. Visual observation of the shape of the association and dissociation curves suggests a biphasic reaction (Figure 3-4). If this were correct, a model that incorporated this would give more accurate kinetic data. This model would need to address the different binding scenarios that could arise from this, possibilities that include a ligand in solution with two binding sites for a single integrin molecule or a single dipeptide binding two integrin molecules.

Further investigation of the interaction will allow re-analysis of these data as more information regarding the interaction between these species becomes available. Care should be taken therefore when making assumptions about *in vivo* binding, although it does not, however, detract from the value of these data in comparing the *in vitro* interaction characteristics of the different CD23 derived peptides and mutants thereof.

3.3.4 RKC binding is cation independent and salt sensitive

A 9 residue basic peptide derived from the HIV Tat protein was shown to bind the αVβ5 integrin in an RGD and divalent-cation independent fashion. This basic peptide was highly specific with respect to sequence and capable of mediating cell attachment [109]. The authors postulate that, although Tat contains an RGD motif, it is not presented in a context that allows it to bind αVβ5. They suggest that the basic peptide binds a synergistic site on αVβ5 to mediate specific interactions [109]. The binding of this peptide may give a clue to the binding of the RKC motif, as there are similarities with the CD23-derived peptides. In CD23 the DGR is not presented in a format that can be recognised and the interaction was rather mediated by an interaction of the RKC with a basic domain binding site on the integrin. Moreover, the interaction between the basic peptide from Tat and the αVβ5 integrin was cation independent and salt sensitive (chloride), similar to that observed for the binding of RKC peptides to the αVβ3 and αVβ5 integrins in the Biacore analysis. The addition of the magnesium to the Biacore buffer as a chloride salt would have elevated the salt concentration above physiological levels, as the buffer contained 150mM sodium chloride prior to addition of 100mM magnesium chloride. Other similar salt-sensitive interactions involving integrins have been described, including the interaction of collagen and fibronectin by the α3β1 integrin [178].

3.3.5 Analysis of the structures of CD23

Two structures of the soluble C-type lectin-like head of CD23, both of which contain the RKC motif, have been published in the literature [62, 63]. Examination of the structures shows that the binding sites for the three CD23 ligands, CD21, IgE and integrins (RKC), are independent of each other (Figure 3-12A).

Whereas a crystal structure gives a single set of coordinates, the NMR structure is an average of a number of structural coordinates, due to the dynamic nature of proteins in solution. It is possible therefore to isolate each individual structural file and analyse them individually. Figure 3-12B shows an image of the 20 individual structure files that comprise the NMR structure of CD23 overlaid on each other using the Pymol graphics program (Delano Scientific, CA). The C-type lectin head is displayed as ribbons and the RKC motif rendered as sticks. The RKC motif is located on a solvent-exposed disulphide-bonded loop at the N-terminal end of the C-lectin head domain, between the ß0 and ß1 strands. The $Cys174^{RKC}$ forms a disulphide bond with Cys163 and therefore is restricted and maintains its position in all of the 20 structures comprising the NMR average structure. Similarly, the $Lys173^{RKC}$ does not show much movement, other than a slight apparent rotation of the side chain. In contrast, the $Arg172^{RKC}$ side chain is shown to sample a number of positions in the different NMR structure files which make up the final structure. Comparison of the relative positions of the RKC motif in the averaged NMR structure and crystal structure indicates that in the crystal structure (Figure 3.12B) the $Arg172^{RKC}$ and $Lys173^{RKC}$ appear less solvent-exposed than in the averaged NMR structure (Figure 3-12A). However, as the crystal structure represents a single defined structure ("snapshot in time"), it is possible that this less solvent-exposed conformation is also observed during dynamic movements of the solution CD23. The fact that it is not reflected in the averaged CD23 NMR structure suggested that in solution this residue is more likely to be solvent exposed than not. This apparent flexibilty in the $Arg172^{RKC}$ may have important consequences for the binding of CD23 to its integrin ligands. It does not preclude the possibility of an induced-fit model for CD23 binding. The relevance of this to the interaction will rely on the solution of a structural model of the interaction prior to making any conclusions in this regard.

Data collected in this study suggested that the interaction between CD23-derived peptides and αV integrins occurs via an RKC motif in CD23 and that this motif is bound at an alternate binding site to that which recognises the RGD motif. Attempts to identify this site during this investigation were hampered by technical problems and it remains to be identified. Work is continuing to extend the analysis of this interaction. Our priority is to identify the location of the basic site for ligand binding on the αV integrins and to analyse the substitutions of the RKC motif in the full length CD23 protein.

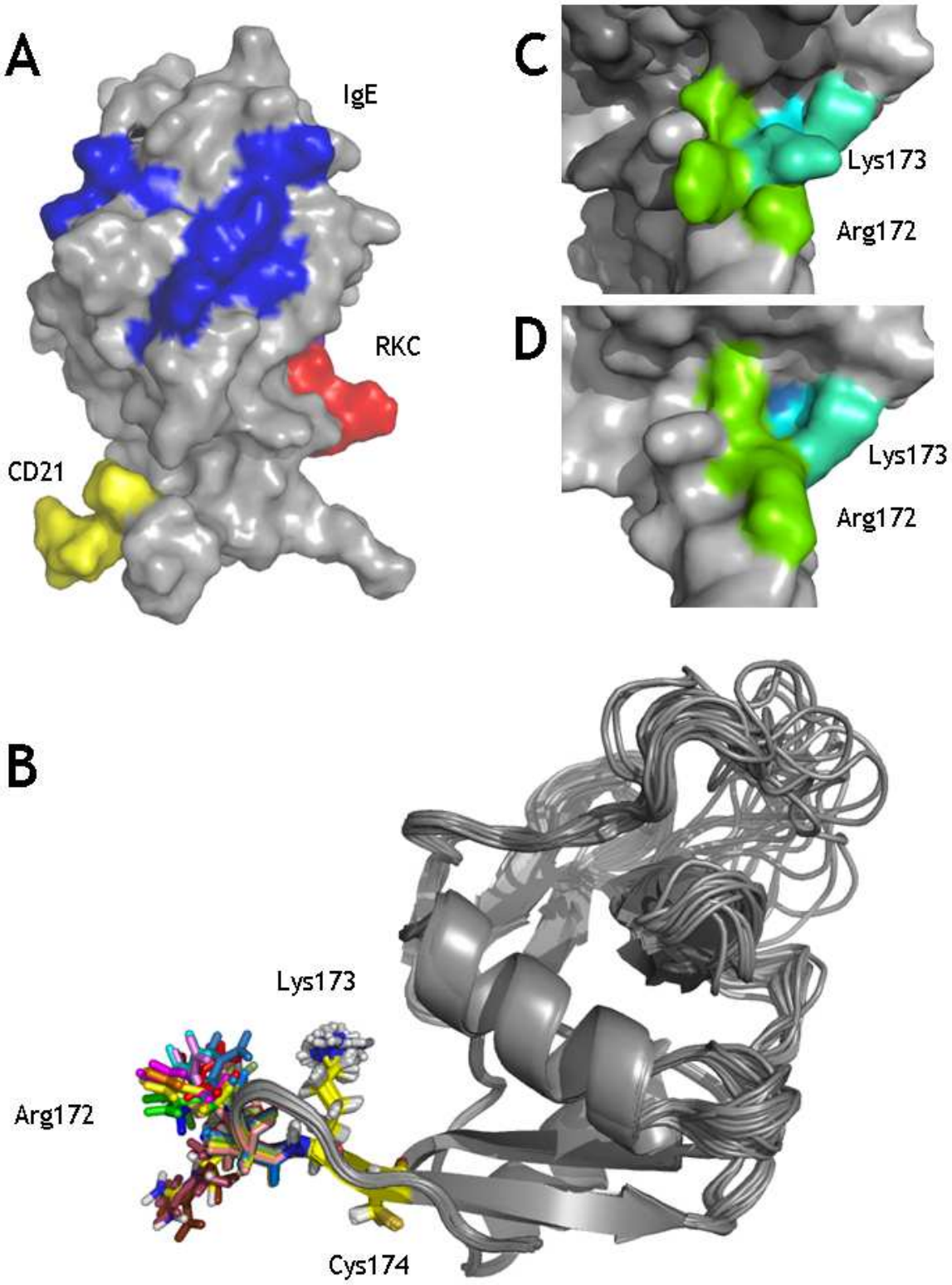

Figure 3-12 Analysis of RKC motif in CD23 crystal and NMR structures
Crystal [94, 98] and NMR [62, 63] structures of the C-lectin like domain of CD23 have been solved. (A) The binding sites for IgE (blue), CD21 (red) and integrins/RKC (yellow) on CD23 are distinct from each other. (B) CD23 solution structure, showing the position of the RKC motif in the 27 individual coordinate files that comprise the NMR structure file. The RKC motif (shown as sticks) is located on a solvent-exposed loop at the base of the C-lectin like head domain of CD23. The Lys^{RKC} and Cys^{RKC} retain similar positions in all the files, while the Arg^{RKC} is shown to sample a number of positions. RKC motif is shown in the NMR solution (C) and crystal (D) structures of CD23. Figures were generated using Pymol (DeLano Scientific); NMR structure PDB code is 1T8C and Crystal structure PDB code is 2H2R.

4 INTEGRIN-REGULATED CYTOKINE PRODUCTION BY MONOCYTIC CELLS

4.1 Introduction

4.1.1 CD23-Integrin interactions and cytokine production

CD23 (Blast-2, FcεRII) is a 45 kDa, Type II transmembrane glycoprotein, which exists in both membrane bound and soluble forms [32]. Membrane bound CD23 (mbCD23) is cleaved by membrane-associated metalloproteases to yield soluble CD23 (sCD23) fragments of 37kDa, which are subsequently cleaved to yield CD23 species of 33kDa, 29kDa, 25kDa and 16kDa [35, 179]. These sCD23 species possess cytokine-like activities, which may be induced by interactions with partner proteins. Of particular interest in this thesis is the interaction between sCD23 and integrins, which is important in the stimulation the production of cytokines by monocytes [40, 41, 83, 84, 180]. Integrins are proteins that play a critical role in cell adhesion and signalling across membranes. They control cell-cell and cell-extracellular matrix contacts and participate in signalling both from the cytoplasm to the exterior of the cell and *vice versa*. CD23 interacts with two classes of integrin (αV and β2) to induce cytokine synthesis in monocytes.

4.1.1.1 CD23 and β2 integrins

The ß2 integrins are exclusively expressed on leukocytes. They are heterodimeric αß integrins, formed by the non-covalent association of one of 4 α chains (αD, αL, αM or αX) with the ß2 integrin [88, 144]. An absence of the ß2 integrin results in impairment of a variety of immune functions, including reductions in macrophage oxidative burst and phagocytosis and lymphocyte proliferation [181]. CD23 interacts with the alpha chains of the leukocyte integrins αMß2 (CD11b/CD18) and αXß2 (CD11c/CD18) [74]. Membrane-bound CD23 incorporated into liposomes has been shown to interact with αXß2 and αMß2 expressed on the surface of monocytes. Soluble CD23 was demonstrated to induce the synthesis by monocytes of the pro-inflammatory cytokines IL-1ß, IL-6 and TNF-α through interaction with αMß2 and αXß2 [41, 74, 83, 84].

4.1.1.2 CD23 and αV integrins

The αV family of integrins, also known as the vitronectin receptors, include the αV subunit in complex with one of ß1, ß3, ß5, ß6 or ß8 subunits. CD23 interacts

with the vitronectin receptors αVß3 and αVβ5, with αVβ3 having an important role in cytokine production in monocytes. Integrin αVß3 is associated with CD47, a 50kDa tetraspan transmembrane protein, to form the αVß3 integrin signalling complex [182, 183]. The αVß3 integrin plays a role in cytokine production through its interaction with sCD23, which leads to the production of TNF-α and IL-1 [40]. Our laboratory has recently identified an interaction between CD23 and αVß5, which is implicated in prevention of apoptosis of pre-B cells [75]. The potential role of αVβ5 in cytokine production remains to be established.

4.1.2 Hierarchy of integrin activity in cytokine production by monocytic cells

The role of CD23 in initiating cytokine production by monocytic cells via an interaction with one or more of its integrin receptors has been described by a number of groups [40, 41, 83, 84]. However, the relative importance of each of the individual integrin isoforms to this process has not been studied in detail. We aimed to extend the analysis of the role of individual integrins in cytokine production by monocytic cells and to identify any relative hierarchy of importance of the individual integrins with respect to cytokine production. This analysis included the first investigation of the role of the αVβ5 integrin in promoting cytokine synthesis by monocytic cells.

4.2 Results

4.2.1 CD23 drives cytokine production by monocytic cells

The interaction between CD23 and integrins expressed on monocytic cells has been shown to induce the synthesis of cytokines, including TNF-α, IL-1β, MIP-1α/β and nitric oxide [40, 41, 83, 84, 180]. We tested our model monocytic cell line, THP-1, for the ability to produce cytokines in response to treatment with CD23 (Figure 4-1A). Supernatant from THP-1 cells stimulated overnight with CD23 was tested for the presence of RANTES, IL-8 and MIP-1β using ELISA. CD23 stimulated the production of all of these cytokines by THP-1 cells (Figure 4.1A), albeit to different extents.

However, CD23 binds to four members of the integrin family of proteins (αVβ3, αVβ5, αMβ2 and αXβ2) and often more than a single integrin isoform will be expressed on the surface of monocytic cells at the same time. The cytokine output of a cell, therefore, will be the net result of the interaction of CD23 with the range of interacting integrins expressed on that particular cell. In order to assess the contribution of individual integrins to the cytokine output, we used antibodies against specific integrin isoforms to attempt to identify a hierarchy of importance amongst the different CD23-binding integrins with respect to monocyte stimulation (Figure 4-1B).

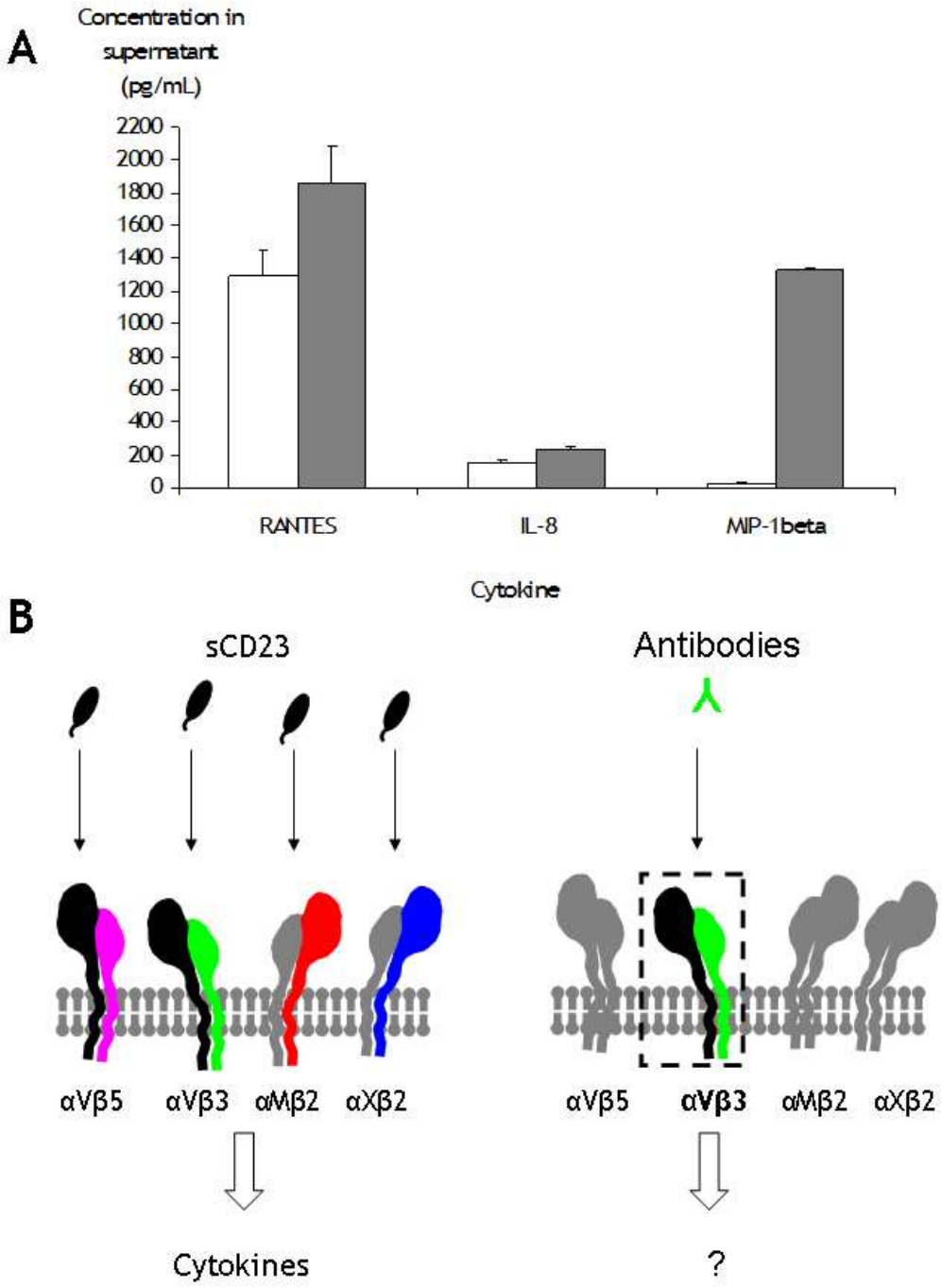

Figure 4.1 Cytokine production by CD23-integrin interaction in monocytes
(A) THP-1 cells were incubated overnight alone (white bars) or with 5µg/mL sCD23 (grey bars) Cytokines released into the supernatant were detected by ELISA. (B) The response of a monocytic cell to CD23 treatment is due to the combined effect of binding to any of 4 possible CD23 binding integrins. The use of antibodies raised against specific integrins allowed identification of the contribution of individual integrin isoforms and/or subunits to the cytokine output of the monocyte.

4.2.2 Qualitative analysis of the cytokine output in response to integrin binding

In order to investigate the global cytokine production profile induced by stimulating integrins on monocytic cells, we used a commercially available cytokine array technique (Figure 4-2). This method uses a combination of sandwich ELISA, Western blotting and chemiluminescent-based detection to simultaneously analyse a sample for the presence of 36 different cytokines in duplicate. The protein array itself comprises a nitrocellulose membrane with antibodies conjugated to it at defined locations in a grid (Figure 4-2B). This membrane was incubated with the sample (in our case cleared supernatant from stimulated cells) and then non-specific sites on the membrane were blocked with BSA. Cytokines in the sample/supernatant bound to their corresponding antibody on the membrane. The bound cytokines were then detected with a biotinylated primary antibody against that specific cytokine (to form the antibody "sandwich"). The binding of biotinylated primary antibody was detected using streptavidin-conjugated to HRP, the nitrocellulose membrane incubated with chemiluminescent substrate and a signal pattern recorded on X-ray film. The membrane is orientated by the location of the positive and negative samples and the location of the signal relative to that identifies a particular cytokine, as indicated by the grid (Figure 4-2B and C). The global cytokine output for a particular stimulus can be determined semi-quantitatively using densitometry and standardisation of the signal strength of individual cytokines against the positive control signals (Figure 4-2D).

We selected a specific cytokine array that would allow us to analyse the production of a range of inflammatory cytokines. We validated the use of this technique for our purposes by first investigating the response of THP-1 cells to stimulation with IgG1, LPS and CD23. LPS and CD23 are known inducers of cytokine production [41, 184-186] and IgG1 was used as a negative control for ligating (but not cross-linking) of Fcγ receptors (certain members of which are known to induce cytokine production in phagocytes). Figure 4-2C shows the cytokine array membrane for cleared supernatants from untreated THP-1 cells and THP-1 cells treated overnight with IgG1, LPS and CD23. All of these arrays displayed the expected patterns for the positive and negative control signals on the membranes. These are shown as a block of four signal dots at the top right and

bottom right of each of the blots (positive controls), separated by a space that shows no signal (negative control), indicating that the array had performed according to manufacturer's instructions.

The blot using the supernatant from untreated THP-1 cells showed positive signals in certain positions. These signals correspond to cytokines that are produced constitutively by the cell line, such as the chemokine RANTES. THP-1 cells are derived from a patient suffering from acute myelogenous leukaemia and therefore the changes associated with this disease may be responsible for this constitutive production of certain cytokines. IgG1-treated THP-1 cells showed a similar profile in cytokine production as the untreated cells and in some cases lower levels of constitutive cytokine production. LPS and CD23, both known to induce cytokine production by monocytes, produced a number of positive signals, indicating the presence of a range of cytokines in the THP-1 supernatant. Strong positive signals were obtained for RANTES, MIP-1α/β, IL-8, VEGF, IL-4 and IL-12p40 in response to LPS and sCD23 treatment.

The array technique is, however, qualitative and therefore could only be used to illustrate the presence or absence of a certain cytokine but not to determine its concentration. Additionally, the chemiluminescent based signal detection meant that there was the potential for membrane-to-membrane variation in signal intensity due to exposure times. As such, the signal intensity for each cytokine was standardised against the positive control signals on each individual blot. The positive and negative control signal intensities are independent of concentration and therefore ideal for use as an internal standard to normalise cytokine signal intensity for exposure differences. This produced a set of data that could be used for comparison between different blots. The standardised data for the signal intensity of 36 cytokines produced in response to negative (untreated and IgG1) and positive (LPS and IgG1) treatments are shown in Figure 4-2D. This chart shows the cytokine signal intensity determined by densitometry and represented as a ratio relative to the signal intensity of the positive control signal intensity on that same membrane. The signal ratios of the 36 cytokines produced in response to a particular treatment are shown together on the chart. This gives a *global* view of the effect of the particular treatment; allowing identification of those treatments which are most stimulatory with respect to cytokine production. The chart shows that although there is some constitutive

production of cytokines observed in the untreated supernatant or the IgG1-treated cells, there is a large increase in the number of positive signals when the THP-1 cells are treated with LPS or CD23.

Using this semi-quantitative approach, we analysed the response of THP-1 cells to antibodies directed against individual CD23-binding integrins (Figures 4-3 and 4-4). THP-1 cells express high levels of the αVβ3, αVβ5 and αXβ2 integrins but only low levels of the αMβ2 integrin. The difference in expression levels of the different CD23-binding integrins with respect to cytokine production is discussed later in the chapter (Figure 4-8). We selected pairs of antibodies against the four CD23-binding integrins (αVβ3, αVβ5, αMβ2 and αXβ2) and the two common integrin chains (αV and β2). The antibodies were selected to recognise the different families of integrin (αV or β2), distinct heterodimer isoforms within those families (αV, αVβ3 or αVβ5) or different epitopes on a specific heterodimer (Table 4-1). We used these antibodies to determine the difference in the cytokine response to binding of the αV integrins as opposed to the β2 integrins, to analyse the role of different isoforms within a particular family (αV or β2), and to investigate the role of different epitopes on a specific integrin.

Figure 4-3 shows the global cytokine profile for THP-1 cells treated with antibodies against CD23-binding integrins from the αV family. The cytokine array membrane signal pattern is shown in Figure 4-3B and the associated densitometry data are displayed in the bar chart in Figure 4-3C. The untreated and IgG1-treated THP-1 supernatants did not produce significantly different signals, other than certain cytokines, such as RANTES, which were constitutively expressed by the THP-1 cell line. LPS treatment led to the expression of a number of cytokines, leading to a large change of signals represented in the densitometry chart. This indicated that LPS induced the production of a range of cytokines by THP-1 cells, including TNF-α, RANTES, IL-8 and MIP-1β. Comparing the cytokine arrays for the treatment of THP-1 cells with antibodies (Figure 4-3Bii) showed that THP-1 cells produced cytokines, including RANTES, IL-8 and MIP-1β, in response to anti-αV antibodies. Stimulation of THP-1 cells with antibodies against αV (using AMF7) and αVβ3 (23C6) and αVβ5 (15F11) produced a similar qualitative cytokine profile, although αV and αVβ5 ligation were less effective than αVβ3. The anti-αVβ3 antibody was the most effective at

stimulating cytokine production by THP-1 cells and induced the greatest range of cytokines of the anti-αV antibodies (Figure 4-3C).

Figure 4-4 shows the equivalent data for the global cytokine profile for THP-1 cells treated with antibodies against CD23 binding integrins from the β2 family. Stimulation of THP-1 cells with antibodies to members of the β2 family of integrins resulted in the production of a range of cytokines. Ligation of the β2 subunit using the antibody MEM48 did not produce a change in the profile compared with untreated or IgG1-treated THP-1 cells. Treatment with the anti-αMβ2 antibody Clone44 and anti-αXβ2 antibody HC1.1 induced the production of a similar range of cytokines to that observed with LPS treatment. Of the two treatments, the anti-αXβ2 antibody produced the greater cytokine response and was most similar to the LPS induced response (Figure 4-4D).

Analysis of the qualitative cytokine data collected for stimulation of the αV and β2 integrins indicated that a similar profile of cytokines is produced, irrespective of the family of integrin targeted. Rather than a change in the identity of the cytokines, the concentration of individual cytokines produced in response to stimulation of integrins was seen to vary. Using the qualitative information obtained from the global cytokine arrays, a number of cytokines that had been secreted as a consequence of integrin binding were selected for quantitative analysis. The chemokines MIP-1β, IL-8 and RANTES were selected for the majority of further analysis. In certain cases the production of other cytokines and growth factors, including but not limited to IL-4 or VEGF, were analysed.

A

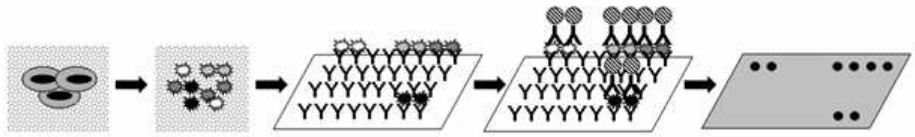

B

	a	b	c	d	e	f	g
1	Apo1/Fas	Leptin	RANTES	ICAM-1	IL-12	IL-7	Positive* (***)
2	CTLA	MIP-1α	TGF-β	VCAM-1	IL-3	IL-8	Positive*
3	Eotaxin	MIP-1β	IFN-γ	VEGF	IL-1	IL-10	Negative**
4	GM-CSF	MIP-1	TNF-α	IL-1α	IL-5	IL-12p40	Negative**
5	EGF	MIP-5	TNF-RI	IL-1β	IL-6	IL-15	Positive*
6	IP-10	MMP3	TNF-RII	IL-1RA	IL-6R	IL-17	Positive*

*** Positive control; ** Negative control; *** Notched corner**

C

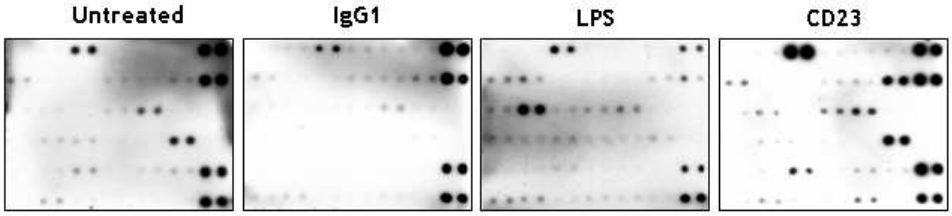

D

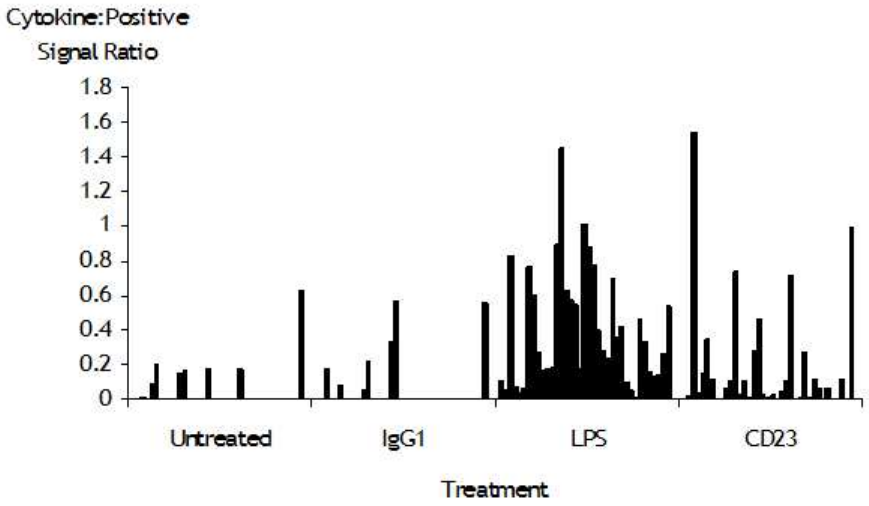

Figure 4.2 Validation of cytokine arrays for the simultaneous detection of 36 cytokines

(A) Schematic diagram of the cytokine array process. Supernatant from stimulated cells was cleared by centrifugation and incubated with the cytokine array membrane. The nitrocellulose membrane has antibodies for specific cytokines attached at defined positions, as shown by the template guide. (B) The membrane was incubated with cleared supernatant for 2 hours, washed and incubated with biotinylated antibodies to specific cytokines. Binding of these biotinylated primary antibodies was detected using streptavidin conjugated to HRP. The blot was incubated with chemiluminescent substrate and the membrane exposed to x-ray film. (C) Cytokine arrays showing the global cytokine array responses for positive (LPS and CD23) and negative (Untreated cells and IgG1 stimulation) controls. The patterns were recorded and analysed using ImageJ software. Signal intensity was calculated as a ratio relative to the positive control signal intensity, to standardize for exposure differences (D). The response to IgG1 is included as a representative example. All antibody isotypes were tested (IgG1, IgG2a, IgG2b and IgG3) and gave responses equivalent to IgG1.

Table 4-1 Antibody pairs used to determine response to integrin binding

INTEGRIN	ANTIBODY	EPITOPE*
αV	AMF7	Non-RGD
	LM142	Non-RGD
αVβ3	23C6	RGD
	LM609	RGD**
αVβ5	P1F6	RGD
	15F11	Non-RGD
β2	PAH9	Non-RGD
	MEM48	Non-RGD
αMβ2	Clone44	RGD
	ICO-GMI	Non-RGD
αXβ2	Clone3.9	RGD
	HC1.1	RGD

*RGD signifies that the antibody inhibits or blocks the adhesive function of the integrin; Non-RGD indicates that the antibody does not inhibit adhesion
** Blocks adhesion via an allosteric site, i.e. does not bind directly to the RGD site

A

	a	b	c	d	e	f	g
1	Apo1/Fas	Leptin	RANTES	ICAM-1	IL-12	IL-7	Positive* (***)
2	CTLA	MIP-1α	TGF-β	VCAM-1	IL-3	IL-8	Positive*
3	Eotaxin	MIP-1β	IFN-γ	VEGF	IL-1	IL-10	Negative**
4	GM-CSF	MIP-1	TNF-α	IL-1α	IL-5	IL-12p40	Negative**
5	EGF	MIP-5	TNF-RI	IL-1β	IL-6	IL-15	Positive*
6	IP-10	MMP3	TNF-RII	IL-1RA	IL-6R	IL-17	Positive*

*** Positive control; ** Negative control; *** Notched corner**

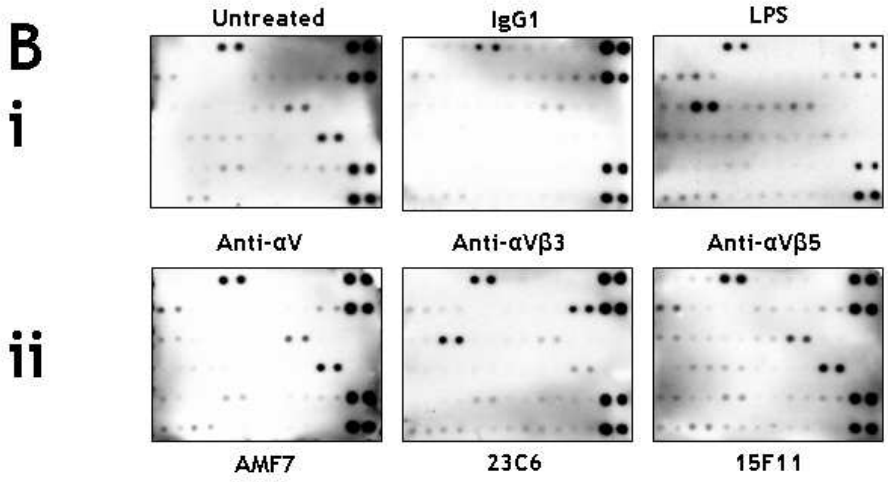

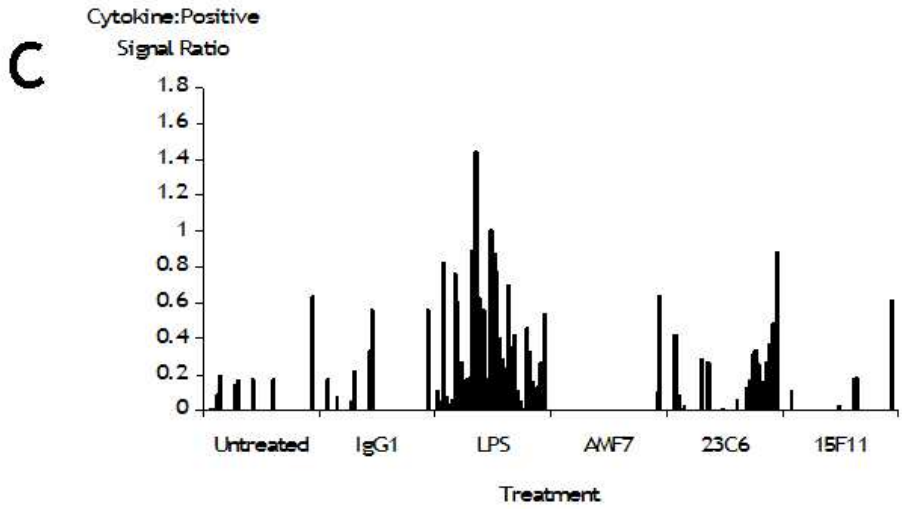

Figure 4.3 Cytokine Arrays for THP-1 treated with antibodies to αV integrins
(A) Cytokine array template showing location of antibodies to specific cytokines on the nitrocellulose membrane. (B) Cytokine array profile of the cleared supernatant from THP-1 cells treated with controls (Bi) or antibodies to members of the αV integrin family (Bii). The integrin isoform targeted in each array is indicated above the blot, while the clone name corresponding to the antibody used is detailed below the individual blots. Cytokines bound to the membrane were detected with specific biotinylated antibodies, which in turn were detected using HRP-congujated streptavidin and chemiluminescent based detection. (C) Densitometric analysis of cytokine array pattern, showing the ratio of all of the individual cytokine signal intensities to the positive control signal. All 36 cytokines are displayed together in the bar chart to yield a global, semi-quantitative representation of the response to each treatment. The response to IgG1 is included as a representative example. All antibody isotypes were tested (IgG1, IgG2a, IgG2b and IgG3) and gave responses equivalent to IgG1.

A

	a	b	c	d	e	f	g
1	Apo1/Fas	Leptin	RANTES	ICAM-1	IL-12	IL-7	Positive* (***)
2	CTLA	MIP-1α	TGF-β	VCAM-1	IL-3	IL-8	Positive*
3	Eotaxin	MIP-1β	IFN-γ	VEGF	IL-1	IL-10	Negative**
4	GM-CSF	MIP-1	TNF-α	IL-1α	IL-5	IL-12p40	Negative**
5	EGF	MIP-5	TNF-RI	IL-1β	IL-6	IL-15	Positive*
6	IP-10	MMP3	TNF-RII	IL-1RA	IL-6R	IL-17	Positive*

*** Positive control; ** Negative control; *** Notched corner**

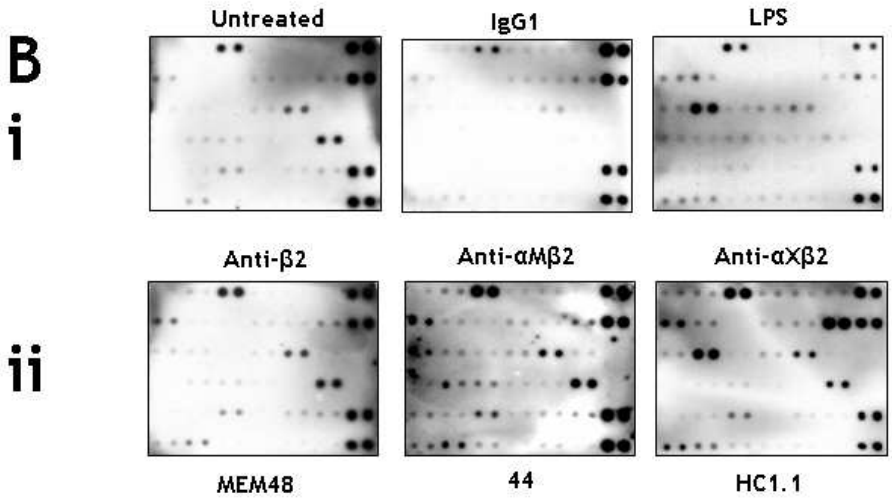

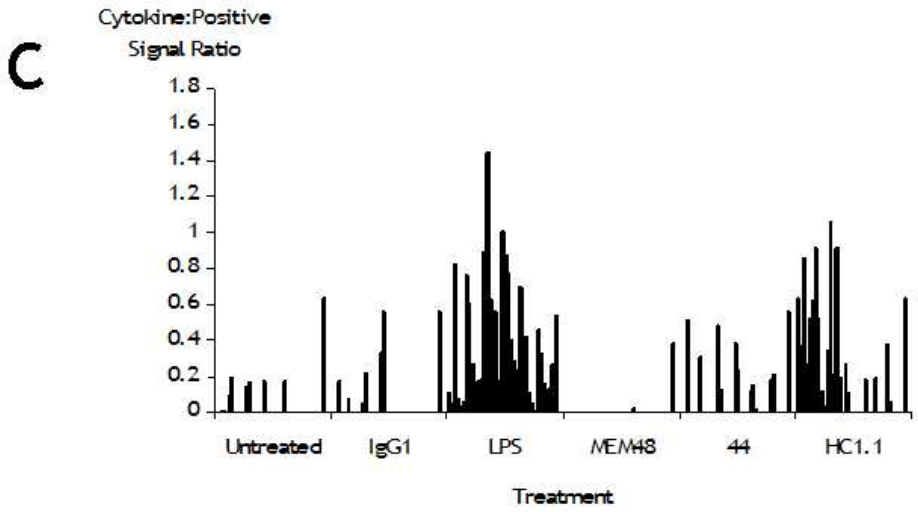

Figure 4.4 Cytokine Arrays for THP-1 treated with antibodies to β2 integrins
(A) Cytokine array template showing location of antibodies to specific cytokines on the nitrocellulose membrane. (B) Cytokine array profile of the cleared supernatant from THP-1 cells treated with controls (Bi) or antibodies to members of the β2 integrin family (Bii). The integrin isoform targeted in each array is indicated above the blot, while the clone name corresponding to the antibody used is detailed below the individual blots. Cytokines bound to the membrane were detected with specific biotinylated antibodies, which in turn were detected using HRP-congujated streptavidin and chemiluminescent based detection. (C) Densitometric analysis of cytokine array pattern, showing the ratio of all of the individual cytokine signal intensities to the positive control signal. All 36 cytokines are displayed together in the bar chart to yield a global semi-quantitative representation of the response to each treatment. The response to IgG1 is included as a representative example. All antibody isotypes were tested (IgG1, IgG2a, IgG2b and IgG3) and gave responses equivalent to IgG1.

4.2.3 Quantitative analysis of the cytokine output in response to integrin binding

ELISAs were used to detect the presence of MIP-1β, IL-8 and RANTES in the supernatant of THP-1 cells treated with antibodies against integrins (Table 4-1). The ELISAs were validated for our purpose using positive and negative stimulations in a dose-response experiment (Figure 4-5). The response of THP-1 cells to treatment with an isotype control (IgG1), RGDS and vitronectin was tested. The positive control selected was the 23C6 antibody specific for αVβ3 that gave a large signal in the global cytokine array. A dose-dependent increase in cytokine production was observed for 23C6 (anti-αV antibody) but not for any of the other stimulations. The THP-1 cultures did not produce a significant amount of IL-8 and MIP-1β in response to treatment with IgG1 or the RGDS peptide or the ECM protein, vitronectin, even at the highest concentrations of 5μg/mL. A high constitutive level of RANTES production, as detected in the cytokine arrays, was observed with untreated THP-1 cells and was slightly enhanced by stimulation of THP-1 cells with anti-αVβ3 antibody but not with any of the other treatments (Figure 4-5).

We used these ELISAs to evaluate the role of different integrin families, subunits and epitopes in cytokine production using specifically selected antibodies. Figure 4-6 shows the production of IL-8, MIP-1β and RANTES by the model monocytic cell line THP-1 after stimulation with antibodies against individual integrins. The data are displayed as stimulation index, which represents the fold elevation of cytokine production over the untreated cells (accounting for any constitutive expression). A fold stimulation value below 1 indicates a decrease in the cytokine output in response to a specific stimulus compared to the untreated control, while a fold stimulation value above 1 indicates an increase in the cytokine output in response to a specific stimulus compared to the untreated cells. THP-1 cells constitutively produced RANTES, but not IL-8 or MIP-1β. The concentration ranges for cytokines produced in response to stimulations were as follows: RANTES 1 000-10 000 pg/mL; IL-8 100-1 000pg/mL and MIP-1β 200-2 000pg/mL.

Figure 4-6 shows the production of IL-8 (A), MIP-1ß (B) and RANTES (C) by THP-1 cell cultures in response to stimulation with anti-integrin antibodies (Table 4-1).

The responses of THP-1 cells to antibodies against the αV integrin family are shown in the left hand panel (labelled Ai, Bi and Ci) and those to antibodies against the ß2 family are shown on the left hand panel (labelled Aii, Bii, and Cii). No stimulation of cytokine production was observed with any of the control treatments for THP-1. IgG1, RGDS peptide and vitronectin failed to induce cytokine production and therefore have a fold stimulation equal to or below 1.

Figure 4-6Ai shows the production of IL-8 by THP-1 cells induced by antibodies directed against members of the αV integrin family. Treatment of THP-1 cells with antibodies AMF7 and LM142, which are directed against the common αV subunit, produced a statistically significant increase in the production of IL-8 production. Both treatments induced a similar fold stimulation of ~8-fold and ~11-fold for AMF7 and LM142, respectively. For the αVβ3 and αVβ5 integrins, only one of the pairs of antibodies induced a significant response from the THP-1 cells. For the αVβ3 integrin, a fold stimulation of ~9-fold was obtained for treatment with the 23C6 antibody, whereas the LM609 clone did not produce a statistically significant increase in IL-8 production by THP-1 cells. For the αVβ5 heterodimer, the P1F6 antibody induced an equivalent ~9-fold increase over baseline IL-8 levels, while the 15F11 antibody, whilst still producing a statistically significant increase in IL-8 secretion, induced a much lower response (~3-fold stimulation).

Figure 4-6Aii shows the IL-8 responses of THP-1 cells following stimulation with antibodies against members of the β2 family of integrins. THP-1 cells did not show any increase in IL-8 concentration over baseline in response to antibodies directed against the common β2 subunit. Neither the P4H9 nor the MEM48 antibody induced any production of IL-8. An increase in the levels of IL-8 produced was observed for treatment of the THP-1 cells with the Clone44 antibody (directed against αMβ2) and the Clone 3.9 antibody (directed against αXβ2). The fold stimulations were ~7-fold and ~22-fold, respectively. The other antibody directed against αMβ2 (ICO-GM1) did not induce a statistically significant increase in IL-8 production.

Figure 4-6B shows the data for the production of MIP-1ß by THP-1 cells under exactly the same set of conditions. A striking similarity is observed for the fold-stimulation pattern of THP-1 cells in response to αV and β2 antibodies for the production of IL-8 and MIP-1β (compare Figures 4-6A and B). Exactly the same trend in stimulation is observed for IL-8 and MIP-1β production by stimulated THP-1 cells. A large increase in MIP-1β production was observed when THP-1 cells were treated with AMF7, LM142, 23C6 and P1F6 antibodies (~5-fold, ~9-fold, ~6-fold and ~7-fold, respectively). THP-1 cells also significantly increased production of MIP-1β in response to Clone44 (~10-fold), and Clone3.9 (~28-fold). In this case, the response to ICO-GMI was determined to be statistically significant, although it was much lower than that observed for Clone44 or Clone3.9 treatment. Again, treatment of THP-1 cells with antibodies against β2 integrins resulted in a greater response, although the range of response was more limited than that observed with the αV antibodies.

Figure 4-6C shows the production of RANTES by THP-1 cells in response to integrin binding. No statistically significant increase in cytokine production was seen with any of the controls for THP-1 cells. THP-1 cells were shown previously to produce RANTES constitutively. There was no significant stimulation over this background level in response to stimulation with any of the negative controls-IgG1, RGDS or vitronectin. Treatment with the anti-αV antibodies, AMF7 and LM142, and the anti-αVβ3 antibody, 23C6, produced small yet significant increases in RANTES production. Treatment with the anti-αXβ2 integrin antibody Clone3.9 induced a small but significant increase in RANTES production. Analysis of RANTES production was complicated by the high constitutive production by THP-1 cells.

Overall, treatment of THP-1 cells with anti-αXß2 antibody Clone3.9 lead to the greatest increase in IL-8 and MIP-1β production (~22-fold and ~28-fold respectively), although the cells responded to a greater range of antibodies directed against the αV family of integrins than the β2 family of integrins. The THP-1 cells failed to produce IL-8 or MIP-1β in response to binding the common ß2 chain of the ß2 family of integrins, but ligation of the common αV subunit stimulates cytokine release to a level similar that noted following binding of antibodies to the heterodimers αVß3 or αVß5.

Figure 4-7 shows the data for the production of IL-8, MIP-1β and RANTES by U937 cells treated in the same manner as the THP-1 cell experiments. U937 cells did not show a statistically significant increase in IL-8 levels in response to treatment with any of the anti-αV antibodies. A modest increase in IL-8 production of approximately 2-fold was observed after treatment with the αXβ2 antibody, Clone3.9. Treatment of U937 cells with the LM142 and 23C6 antibodies resulted in statistically significant increases in MIP-1β (2-fold and 4-fold respectively). U937 cells did not show a significant increase in RANTES production in response to treatment with antibodies against αV or β2 integrins.

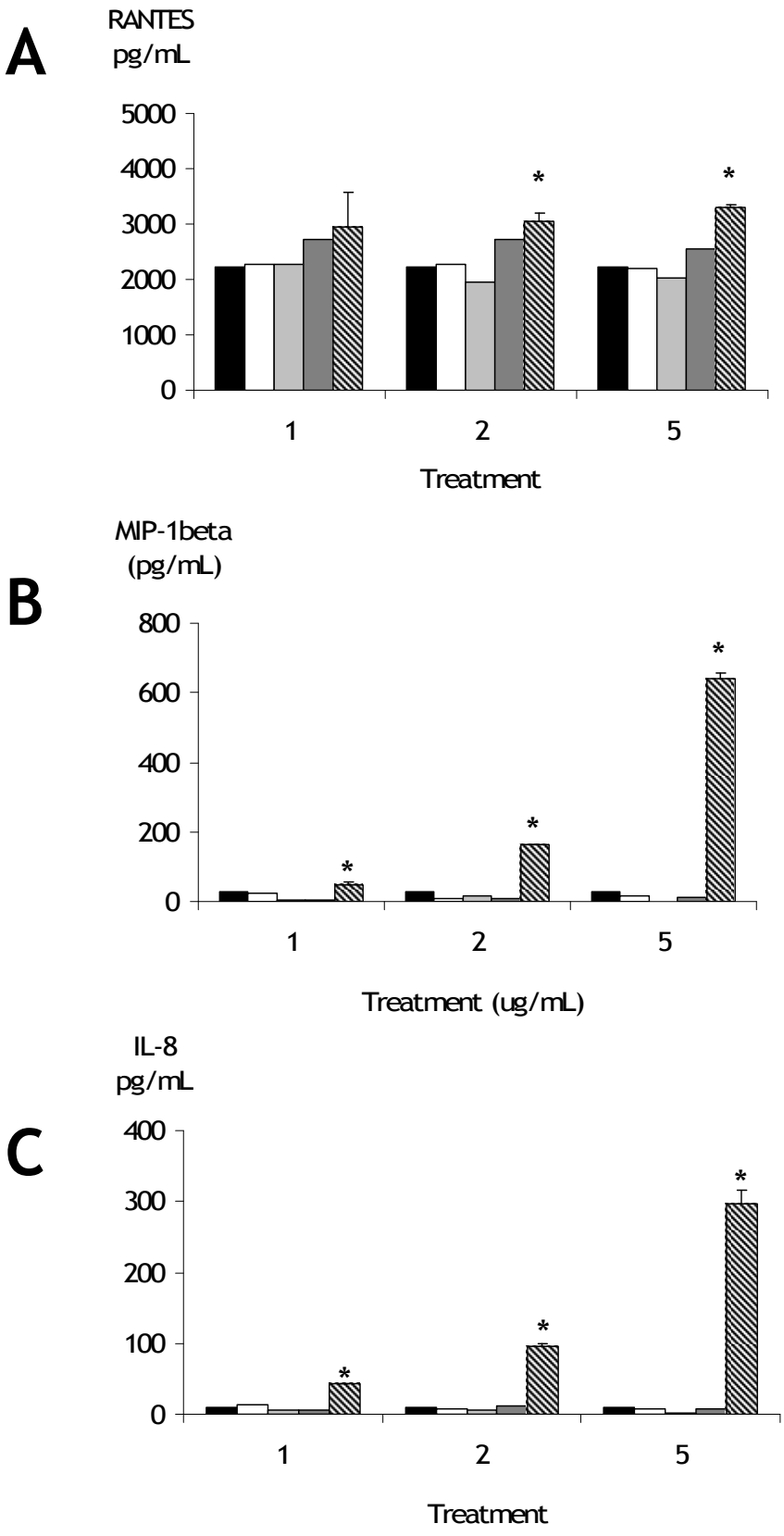

Figure 4.5 Cytokine production by THP-1 cells is not induced by binding controls

THP-1 cells were treated overnight as indicated below and the presence of RANTES (A), MIP-1β (B) and IL-8 (C) in the cleared supernatant determined by ELISA. Untreated cells:black bars; Vitronectin:white bars; RGDS:light grey bars; IgG1:dark grey bars; diagonal-striped bars:anti-αVβ3 23C6 Statistical analysis was performed using Student's *t*-test *p<0.05. Data are representative of at least 3 separate experiments. The error bars indicate standard deviations (SD). The response to IgG1 is included as a representative example. All antibody isotypes were tested (IgG1, IgG2a, IgG2b and IgG3) and gave responses equivalent to IgG1.

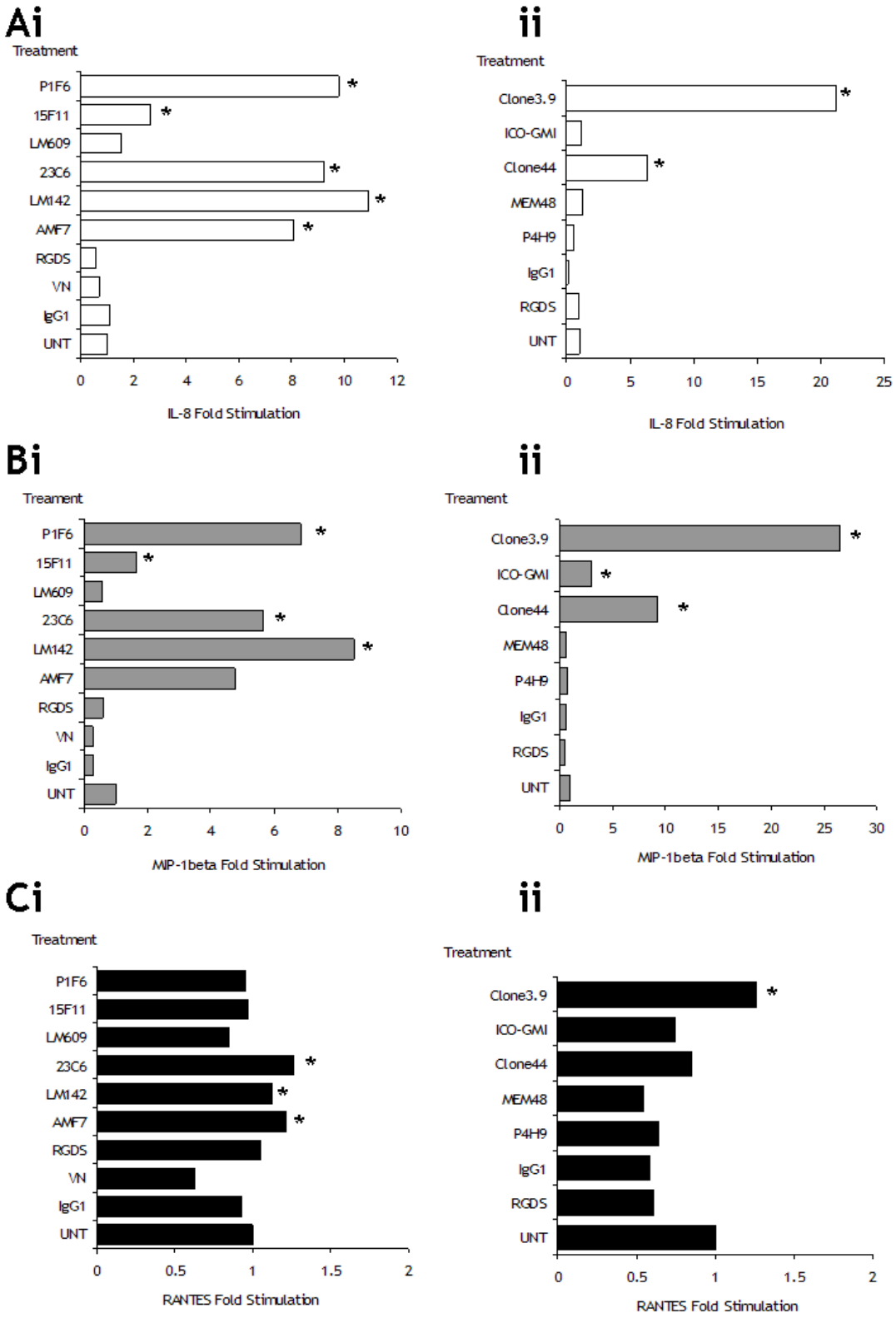

Figure 4.6 Cytokine production by THP-1 cells in response to integrin ligation

Supernatants from THP-1 cells stimulated with anti-αV antibodies (Ai, Bi and Ci) or anti-β2 antibodies (Aii, Bii and Cii) were tested for the presence of IL-8 (Ai and Aii; white bars), MIP-1β (Bi and Bii; grey bars) and RANTES (Ci and Cii; black bars) using ELISA. Fold-stimulation represents the ratio of the cytokine concentration produced by the integrin-stimulated sample after treatment with the differentiating agent relative to the integrin-stimulated untreated cells. Unt:Untreated cells; IgG1:Isotype control; RGDS: RGDS peptide; VN:vitronectin; AMF7:anti-αV; LM142:anti-αV; 23C6:anti-αVβ3; LM609: anti-αVβ3; 15F11:anti-αVβ5; P1F6:anti-αVβ5; P4H9:anti-β2; MEM48: anti-β2; Clone44:anti-αMβ2; ICO-GM1:anti-αMβ2; Clone3.9:anti-αXβ2. Statistical analysis was performed using Student's *t*-test *p<0.05. Data are representative of at least 3 separate experiments. The response to IgG1 is included as a representative example. All antibody isotypes were tested (IgG1, IgG2a, IgG2b and IgG3) and gave responses equivalent to IgG1.

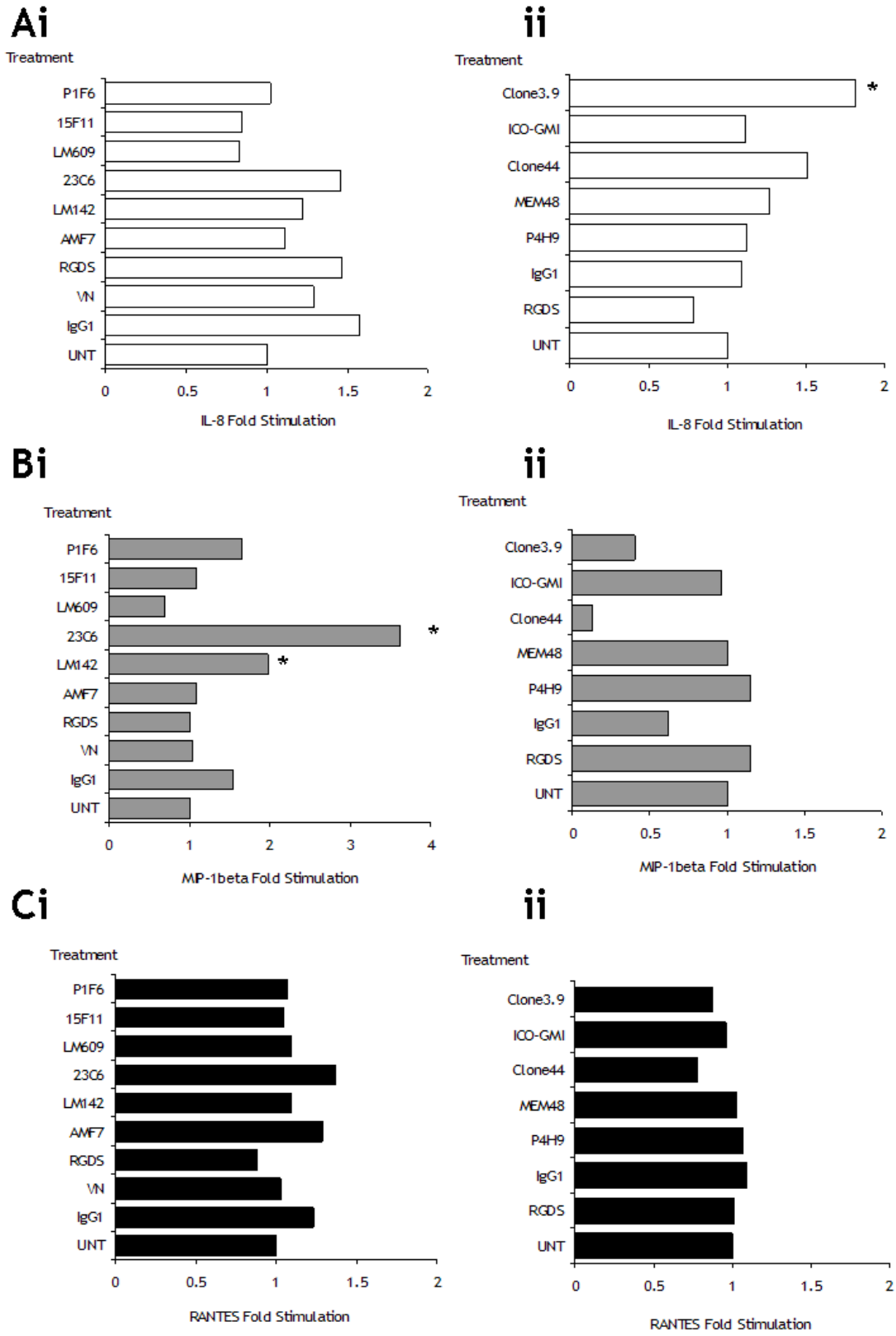

Figure 4.7 Cytokine production by U937 cells in response to integrin binding
Supernatants from U937 cells stimulated overnight with anti-αV antibodies (Ai, Bi and Ci) or anti-β2 antibodies (Aii, Bii and Cii) were tested for the presence of IL-8 (Ai and Aii; white bars), MIP-1β (Bi and Bii; grey bars) and RANTES (Ci and Cii; black bars) using ELISA. Fold-stimulation represents the ratio of the cytokine concentration produced by the integrin-stimulated sample after treatment with the differentiating agent relative to the integrin-stimulated untreated cells. Unt:Untreated cells; IgG1:Isotype control; RGDS: RGDS peptide; VN:vitronectin; AMF7:anti-αV; LM142:anti-αV; 23C6:anti-αVβ3; LM609: anti-αVβ3; 15F11:anti-αVβ5; P1F6:anti-αVβ5; P4H9:anti-β2; MEM48: anti-β2; Clone44:anti-αMβ2; ICO-GM1:anti-αMβ2; Clone3.9:anti-αXβ2. Statistical analysis was performed using Student's *t*-test *p<0.05. Data are representative of at least 3 separate experiments. The response to IgG1 is included as a representative example. All antibody isotypes were tested (IgG1, IgG2a, IgG2b and IgG3) and gave responses equivalent to IgG1.

4.2.4 Effect of integrin expression levels on cytokine production by THP-1 and U937 cells

THP-1 and U937 cells were tested for their cytokine responses to stimulation by CD23-binding integrins (Figures 4-6 and 4-7). Stimulation of different integrins induced distinct patterns of production of IL-8, RANTES and MIP-1ß by the two cell lines. To establish whether this was due to the levels of these integrins on the cell lines we examined the integrin expression levels on THP-1 and U937 cells and related this to the levels of cytokines produced in response to binding a specific heterodimer (Figure 4-9).

Figure 4-9A shows the expression of the four CD23 binding integrin heterodimers on the surface of U937 (Figure 4-9Ai) and THP-1 cell lines (Figure 4-9Aii). THP-1 and U937 cells express similar levels of these integrin heterodimers. There was no significant difference between the different cell lines. Within an individual cell line, the most highly expressed integins were the αVβ3, αVβ5 and αXβ2 heterodimers, with only low levels of αMβ2 integrin expressed. However, the cytokine production in response to stimulation of a particular heterodimer was markedly different between the cell lines (despite the equivalent integrin expression levels).

Figure 4-9B shows the relationship between the relative expression of the different integrins on THP-1 cells (Figure 4-9Bi) and the levels of cytokines produced by stimulating them (Figure 4-9Bii). Of the β2 integrins, the β2 subunit is expressed to the highest level on the surface of THP-1 cells (black line), followed by the αXβ2 isoform (blue line) and then the αMβ2 heterodimer (red line). The hierarchy of cytokine production indicated that stimulation of cells with anti-αXß2 antibodies (Clone3.9, blue arrow) resulted in the highest level of MIP-1ß release. Stimulation of the cells with anti-αMß2 (Clone44, red arrow) induced a moderate level of MIP-1ß production, while binding of the ß2 subunit did not result in the production of detectable levels of MIP-1ß (black arrows). Integrin expression level alone in this case was unlikely to be the major determinant of concentrations of cytokines produced in response to integrin stimulation, either between cell lines or within different integrin isoforms on the same cell line.

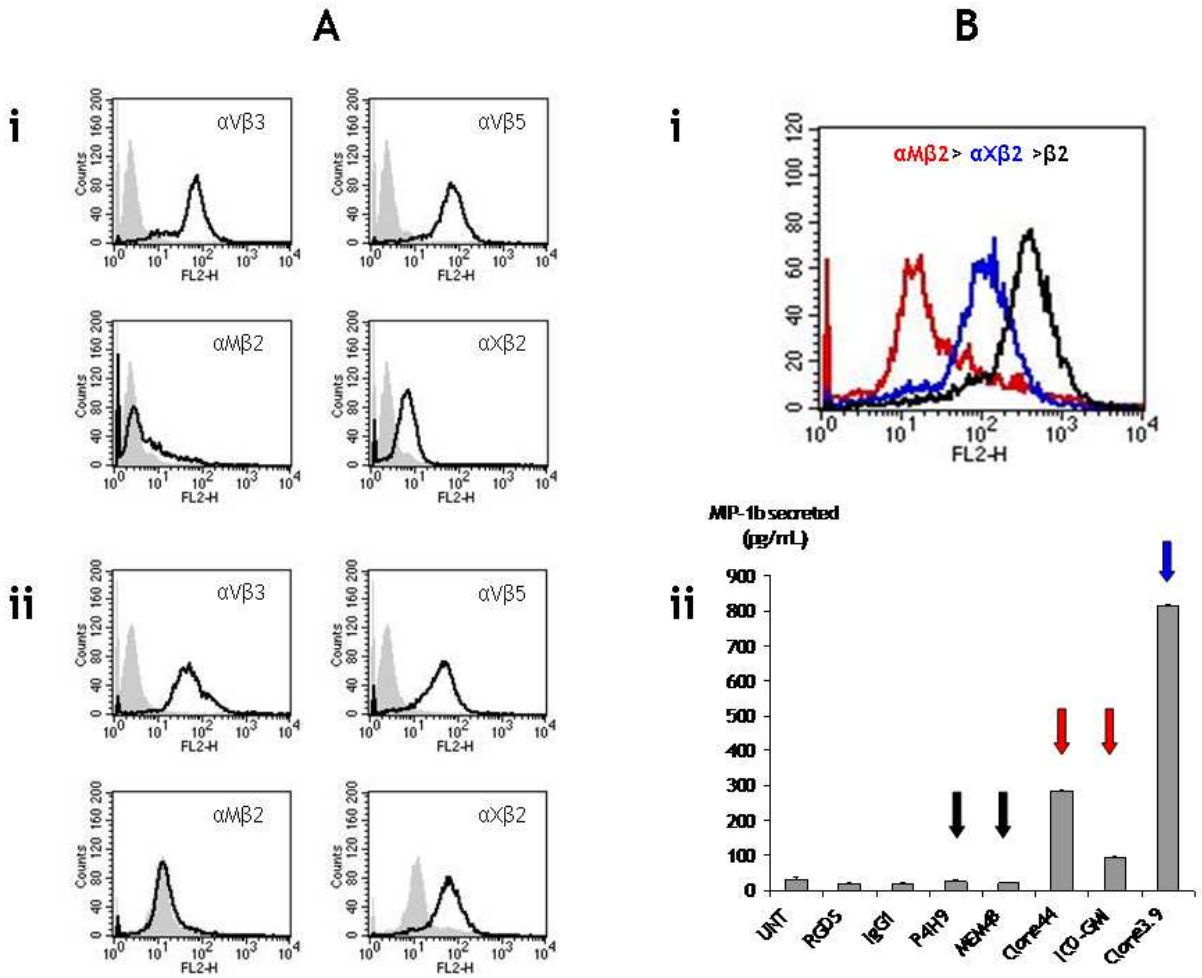

Figure 4.8 Integrin expression level alone does not determine cytokine output

(A) Expression levels of integrins on U937 (Ai) and THP-1 cells (Aii) was determined by flow cytometry. (B) Expression levels of different isoforms of β2 integrins on THP-1 cells was determined by flow cytometry. Integrin staining is shown as a solid black line and isotype staining is shown as grey shading (Bi) and the corresponding levels of MIP-1β production by binding those isoforms was determined by ELISA (Bii). Red line/arrow:αMβ2; Blue line/arrow:αXβ2; Black line/arrow:β2.Data are representative of at least 3 separate experiments. The error bars indicate standard deviations (SD).

4.2.5 Cytokine response after differentiation of THP-1 cells

A difference in cytokine production in response to the same stimulus was observed between the two cell lines THP-1 and U937. These two cell lines represent monocytic cell lines at different maturation stages. U937 is more similar to an early blood monocyte [166], whereas the THP-1 cell line is more monocyte/macrophage in nature [165]. To investigate further the role of cell differentiation state on integrin-mediated cytokine production, we treated THP-1 cells with differentiating agents and compared the cytokine response to antibody-mediated stimulation of specific integrins.

THP-1 cells were treated for 3 days with macrophage colony stimulating factor (M-CSF/CSF-1), granulocyte/macrophage colony stimulating factor (GM-CSF) and dibutryl-cyclic adenosine monophosphate (db-cAMP). The cells were washed and integrin expression and cytokine production in response to integrin binding determined (Figures 4-9, 4-10 and 4-11, respectively). Expression of integrins was determined by flow cytometry. The integrin staining observed for untreated cells is shown in grey shading and the equivalent staining for M-CSF, GM-CSF or db-cAMP-differentiated cells is shown as a black line. The cytokine production was determined by ELISA and is represented as fold-stimulation. This represents the ratio of the cytokine (RANTES, IL-8 or MIP-1ß) concentration produced by the integrin-stimulated sample after treatment with the differentiating agent relative to the integrin-stimulated untreated cells.

Figure 4-9 shows the comparison of the integrin expression levels (Figure 4-9A) and cytokine production level (Figure 4-9B) from untreated and M-CSF-treated THP-1 cells. THP-1 cells that were treated with 10ng/mL M-CSF for 3 days did not show any appreciable change in the expression levels of the αVβ3, αVβ5, αMβ2 or αXβ2 integrins (Figure 4-9A). A slight, non-specific increase was observed for RANTES production by untreated cells and in response to all stimulations. There was no increase in the IL-8 levels in response to any of the stimulations. An increase in the fold-stimulation for the production of MIP-1β was observed in response to stimulation with the anti-αMβ2 antibody, but not with any of the other stimulations.

Figure 4-10 shows the effect of treatment of THP-1 cells with 1ng/mL GM-CSF for 3 days. Treatment of THP-1 cells with GM-CSF did not considerably alter the expression of any of the CD23-binding integrins compared to the untreated cells (Figure 4-10A). There was no substantiated increase in the production of RANTES, IL-8 or MIP-1β for any of the stimulations tested (Figure 4-10B).

Figure 4-11 shows the expression levels and cytokine production characteristics of THP-1 cells that had been treated with db-cAMP for 3 days prior to stimulation. An increase in the expression levels of the αXβ2 integrin upon treatment with db-cAMP was noted, while there was no change in expression of αVβ3, αVβ5 or αMβ2. A general reduction in the secretion of RANTES was observed for untreated cells and in response to all stimulations. There was an increase in the fold stimulation for IL-8 and MIP-1β production in response to αVβ5 binding, but not for stimulation with any other integrin-directed antibody.

Differentiation of THP-1 cells with db-cAMP led to changes in expression levels of specific integrin heterodimers. This change in expression, however, did not necessarily correlate with the levels of cytokines produced as a consequence of integrin stimulation. For example, treatment of THP-1 cells with M-CSF did not influence the expression levels of integrins compared to untreated THP-1 cells, but led to an increase in the production of IL-8 in response to 23C6 treatment. Although the expression levels of αVβ5 did not change, treatment of the THP-1 cell line with db-cAMP led to an increase in the production of IL-8 and MIP-1β in response to stimulation with the anti-αVβ5 antibody. The cell line U937 had similar surface expression of integrins to the THP-1 line, but responded differently to integrin stimulation (i.e. did not produce cytokines).

Integrins play an important role in modulating the effects of other surface receptors and so we analysed the expression of other surface receptors after treatment of THP-1 cells with M-CSF, GM-CSF or db-cAMP. We hypothesised that cytokine production involved an additional receptor (apart from the integrin) and that the levels of this receptor may explain the discrepancies between expression level and cytokine production. The $F_c\gamma$ receptors are immunoreceptors that recognise the constant region of immunoglobulins and have an important role in cytokine

production by monocytes. We also assessed the levels of CD47 (integrin associated protein). CD47 is part of the αVβ3 signalling complex and therefore its expression levels might influence cytokine production.

Figure 4-12 shows the expression of the $F_c\gamma$ receptors, CD16, CD32, CD64 and the integrin associated protein CD47, on U937 cells and on THP-1 cells before and after treatment with M-CSF, GM-CSF or db-cAMP. There was no change in the expression of CD16, CD32, CD64 or CD47 by THP-1 cells that had been treated with M-CSF (Figure 4-12B), GM-CSF (Figure 4-12C) or db-cAMP (Figure 4-12D) compared with untreated THP-1 cells (Figure 4-12A). There was, however, a difference in the expression levels of the $F_c\gamma$ receptors on the U937 cell line compared with the THP-1 cell line. U937 cells did not express CD16 or CD32 and only expressed low levels of CD64 and CD47, compared with the THP-1 cells. We also tested the primary blood monocytes for the expression of these receptors. The cells stained positive for all 4 receptors, although at lower levels than found on THP-1 cells.

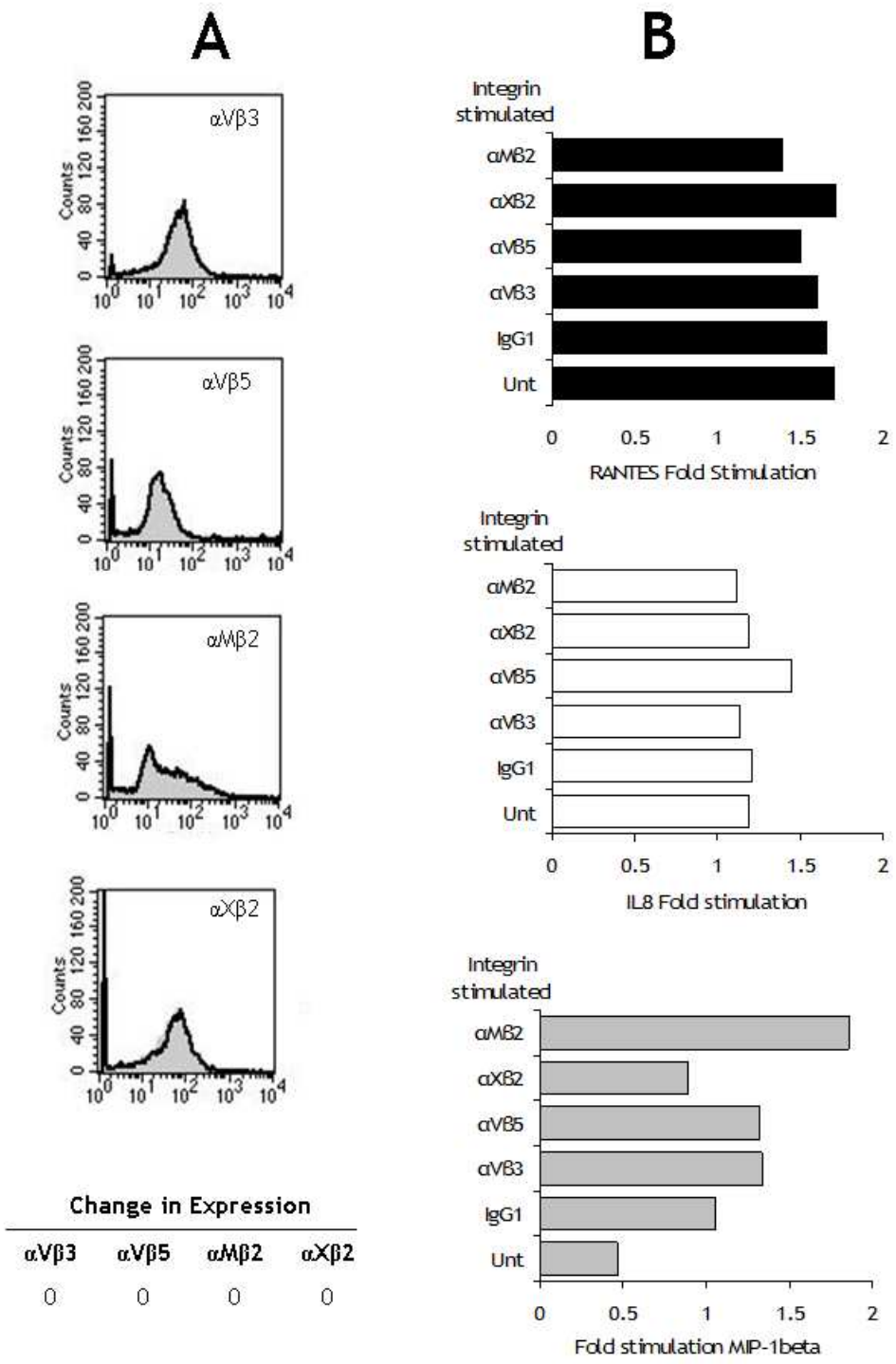

Figure 4.9 Integrin expression and cytokine profile of THP-1 cells after differentiation with M-CSF

THP-1 cells were cultured with or without 10ng/mL M-CSF for 3 days before analysis of integrin expression and cytokine production. (A) Untreated cells (grey shading) and M-CSF treated cells (black line) were stained for integrin expression by flow cytometry. (B) The cytokine production was determined by ELISA and is represented as fold stimulation. This represents the ratio of the cytokine (RANTES, IL-8 and MIP-1β) concentration produced by the integrin-stimulated sample after treatment with the differentiating agent relative to the integrin-stimulated untreated cells. Statistical analysis was performed using Students *t*-test. Data are representative of at least 3 separate experiments. The response to IgG1 is included as a representative example. All antibody isotypes were tested (IgG1, IgG2a, IgG2b and IgG3) and gave responses equivalent to IgG1.

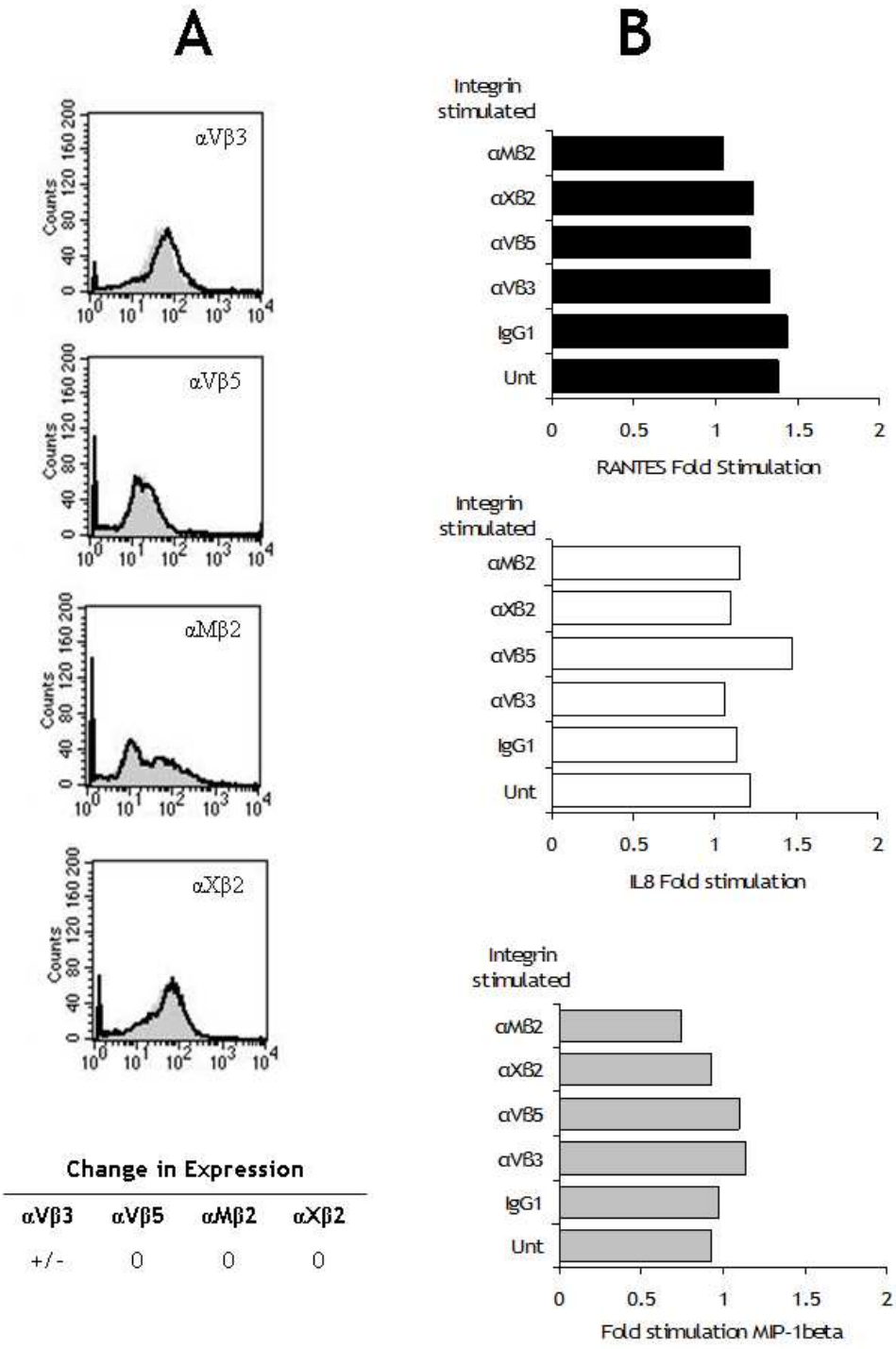

Figure 4.10 Integrin expression and cytokine profile of THP-1 cells after differentiation with GM-CSF

THP-1 cells were cultured with or without 1ng/mL GM-CSF for 3 days before analysis of integrin expression and cytokine production. (A) Untreated cells (grey shading) and GM-CSF treated cells (black line) were stained for integrin expression by flow cytometry. (B) The cytokine production was determined by ELISA and is represented as fold stimulation. This represents the ratio of the cytokine (RANTES, IL-8 and MIP-1β) concentration produced by the integrin-stimulated sample after treatment with the differentiating agent relative to the integrin-stimulated untreated cells. Statistical analysis was performed using Students *t*-test. Data are representative of at least 3 separate experiments. The response to IgG1 is included as a representative example. All antibody isotypes were tested (IgG1, IgG2a, IgG2b and IgG3) and gave responses equivalent to IgG1.

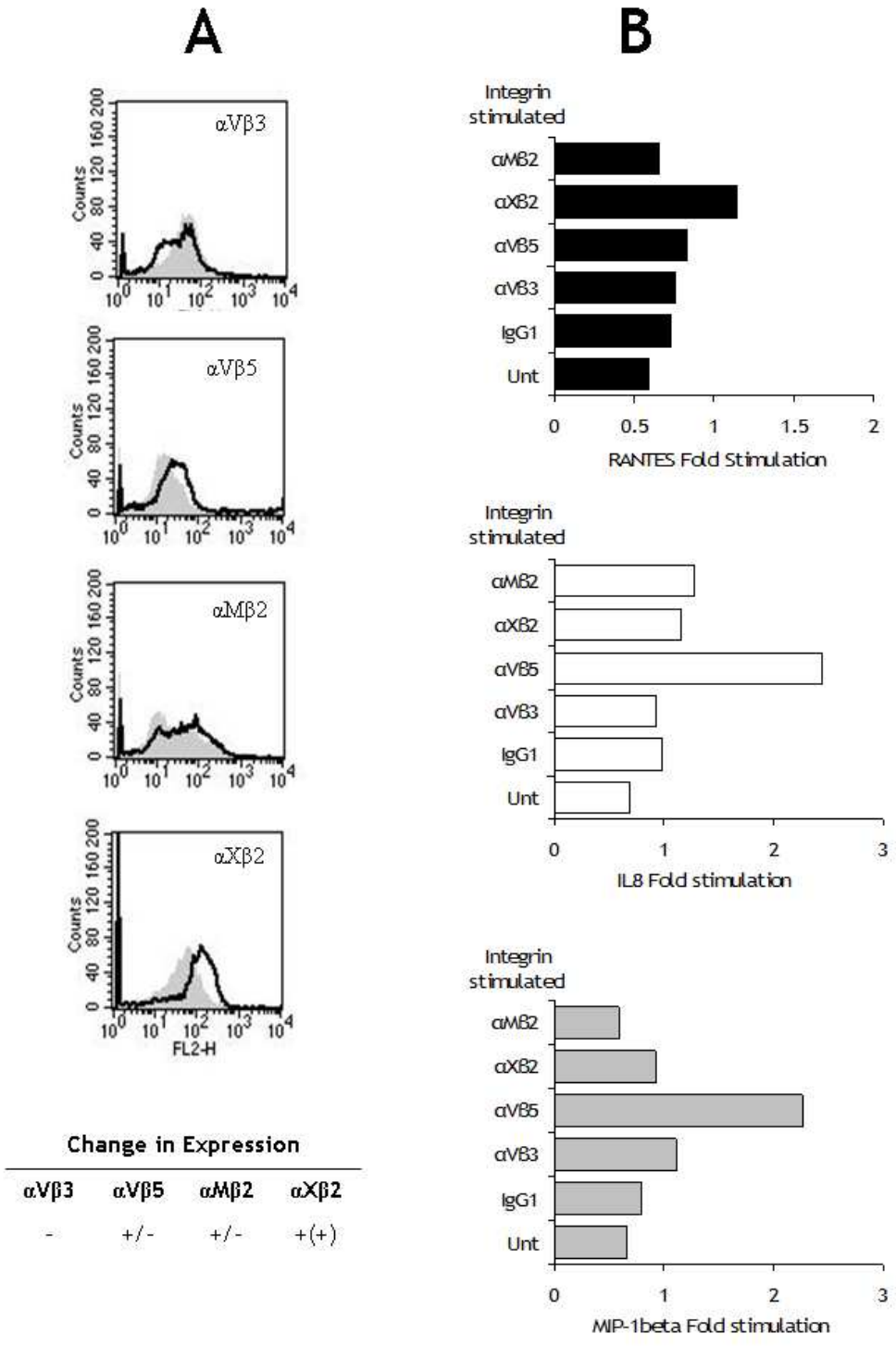

Figure 4.11 Integrin expression and cytokine profile of THP-1 cells after differentiation with dibutryl-cyclic AMP (db-cAMP)

THP-1 cells were cultured with or without 100mM db-cAMP for 3 days before analysis of integrin expression and cytokine production. (A) Untreated cells (grey shading) and db-cAMP treated cells (black line) were stained for integrin expression by flow cytometry. (B) The cytokine production was determined by ELISA and is represented as fold stimulation. This represents the ratio of the cytokine (RANTES, IL-8 and MIP-1β) concentration produced by the integrin-stimulated sample after treatment with the differentiating agent relative to the integrin-stimulated untreated cells. Statistical analysis was performed using Students *t*-test. Data are representative of at least 3 separate experiments. The response to IgG1 is included as a representative example. All antibody isotypes were tested (IgG1, IgG2a, IgG2b and IgG3) and gave responses equivalent to IgG1.

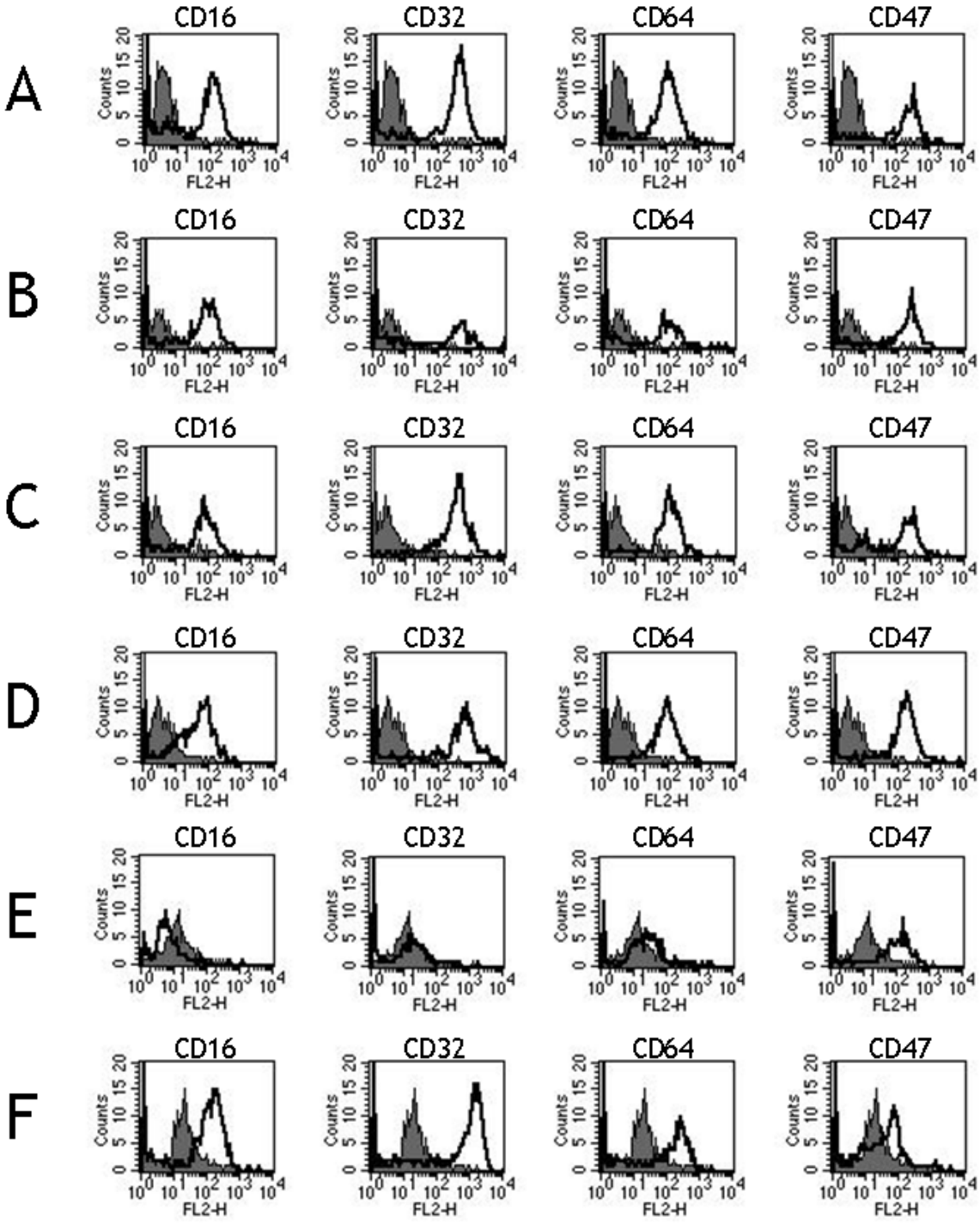

Figure 4.12 Expression of integrin associated receptors on monocytic cells
THP-1 cells (with or without treatment with differentiating agents), U937 and $CD14^+$PBMC were assessed for their expression of $F_c\gamma$ receptors (CD16, CD32 and CD64) and CD47 (integrin associated protein) by flow cytometry. Isotype control staining is shown as grey shading and antibody staining is shown as a solid black line. The identity of the protein detected is indicated above the individual histograms. A: THP-1 cells in OptiMEM, B: THP-1 cells in OptiMEM with M-CSF, C: THP-1 cells in OptiMEM with GM-CSF D: THP-1 cells in OptiMEM with db-cAMP, E: U937 in OptiMEM, F: $CD14^+$ blood monocytes.

4.2.6 Cooperation between different integrin heterodimers

The data in Figures 4-2 to 4-11 have shown that specific integrins can regulate cytokine production by monocytic cells when stimulated with antibodies against specific integrin isoforms, subunits and epitopes. Cross-talk amongst different integrins has been reported and so we investigated the response of monocytes to simultaneous stimulation with antibodies against multiple integrins. The production of RANTES, MIP-1ß and IL-8 was monitored by ELISA after overnight stimulation with multiple antibodies as indicated in figure legends.

We selected the anti-αVß3 antibody 23C6 and the anti-αXß2 antibody Clone3.9 for these analyses as they had induced high levels of cytokine production in the previous experiments. We examined the ability of the two antibodies to influence the cytokine production of the other when supplied at a suboptimal concentration. Figure 4-13A shows the response of THP-1 cells to incubation with increasing concentrations of Clone3.9 (0.2 – 1.0 µg/mL) in the absence (white bars) or presence (black bars) of a fixed suboptimal concentration of 23C6 (0.4µg/mL). The sub-optimal concentration of 23C6 was titrated in a dose-response experiment. The concentration of 23C6 at which cytokine production was half of the maximum concentration of cytokine produced by the cell line, was selected as the sub-optimal concentration (*data not shown*). A dose-dependent increase in the levels of RANTES, IL-8 and MIP-1β was observed with the increasing Clone3.9 concentration. Cytokine production was enhanced at all concentrations by the addition of 0.4µg/mL 23C6 antibody. Figure 4-13B shows the data for the reverse situation, where THP-1 cells were stimulated with increasing concentrations of 23C6 antibody alone (white bars) or in the presence of concentration of Clone3.9 (0.4µg/mL; black bars) and tested for the production of RANTES, IL-8 and MIP-1ß. A dose-dependent increase in the production of all of these cytokines was observed with increasing 23C6 concentration. The levels of RANTES, IL-8 and MIP-1ß produced at all concentrations of 23C6 were enhanced by the addition of suboptimal concentrations of Clone3.9. These data indicated that simultaneous binding of the αVß3 and αXß2 integrins enhanced cytokine production, and so we tested if any of the other integrins could influence the levels of cytokines produced in response to 23C6 or Clone3.9 stimulation.

Figure 4-14 shows the effect of incubation of THP-1 cells with the 23C6 antibody (0.2µg/mL) and increasing concentrations of antibodies against other αV integrins (anti-αV antibodies AMF7 and LM142 and anti-αVß5 antibody P1F6). Figure 4-15 shows the response of THP-1 cells to stimulation with 23C6 (anti-αVß3 antibody) in conjunction with antibodies against members of the ß2 integrin family (anti-αß2 antibodies Clone44 and ICO-GMI and anti-ß2 antibody P4H9). The data are represented as stimulation index (SI). The stimulation index is the fold-stimulation of cytokine production when using 23C6 and another antibody together, over the level of cytokine produced by treatment with 23C6 alone. There was no statistically significant enhancement or inhibition of the levels of RANTES, IL-8 or MIP-1ß produced by THP-1 cells in response to 23C6 when co-incubated with any of the antibodies AMF7 (αV), LM142 (αV) or P1F6 (αVß5). Similarly, there was no statistically significant increase or decrease in stimulation index for the production of RANTES, IL-8 and MIP-1ß when cells were treated with 23C6 (αVß3) and the ß2 family antibodies, ICO-GMI (αMß2), Clone44 (αMß2) and P4H9 (ß2). The co-stimulation of THP-1 cells with 23C6 and the anti αMß2 antibody ICO-GMI did appear to cause a modest, dose-dependent increase in the stimulation index for the production of IL-8, although these data were outside the confidence interval to be statistically significant ($p=0.055$ using Student's t-test).

Figure 4-16 and Figure 4-17 show the equivalent data for the treatment of THP-1 cells with Clone 3.9 (αXß2) and other antibodies against αV and ß2 integrins, respectively. THP-1 cells were treated with the Clone3.9 antibody (0.2µg/mL) and increasing concentrations of antibodies against αV integrins (anti-αV antibodies AMF7 and LM142 and anti-αVß5 antibody P1F6) and ß2 integrins (anti-αMß2 antibodies Clone44 and ICO-GMI and anti-ß2 antibody P4H9). The data are represented as stimulation index (SI). The stimulation index is the fold stimulation of cytokine concentration determined when treating cells with Clone3.9 in conjunction with another antibody over the concentration of cytokine produced by treatment with Clone3.9 alone. There was no statistically significant change in the stimulation index for IL-8, RANTES or MIP-1ß when THP-1 cells were stimulated with Clone3.9 in conjunction with any of the antibodies tested (Figures 4-16 and 4-17).

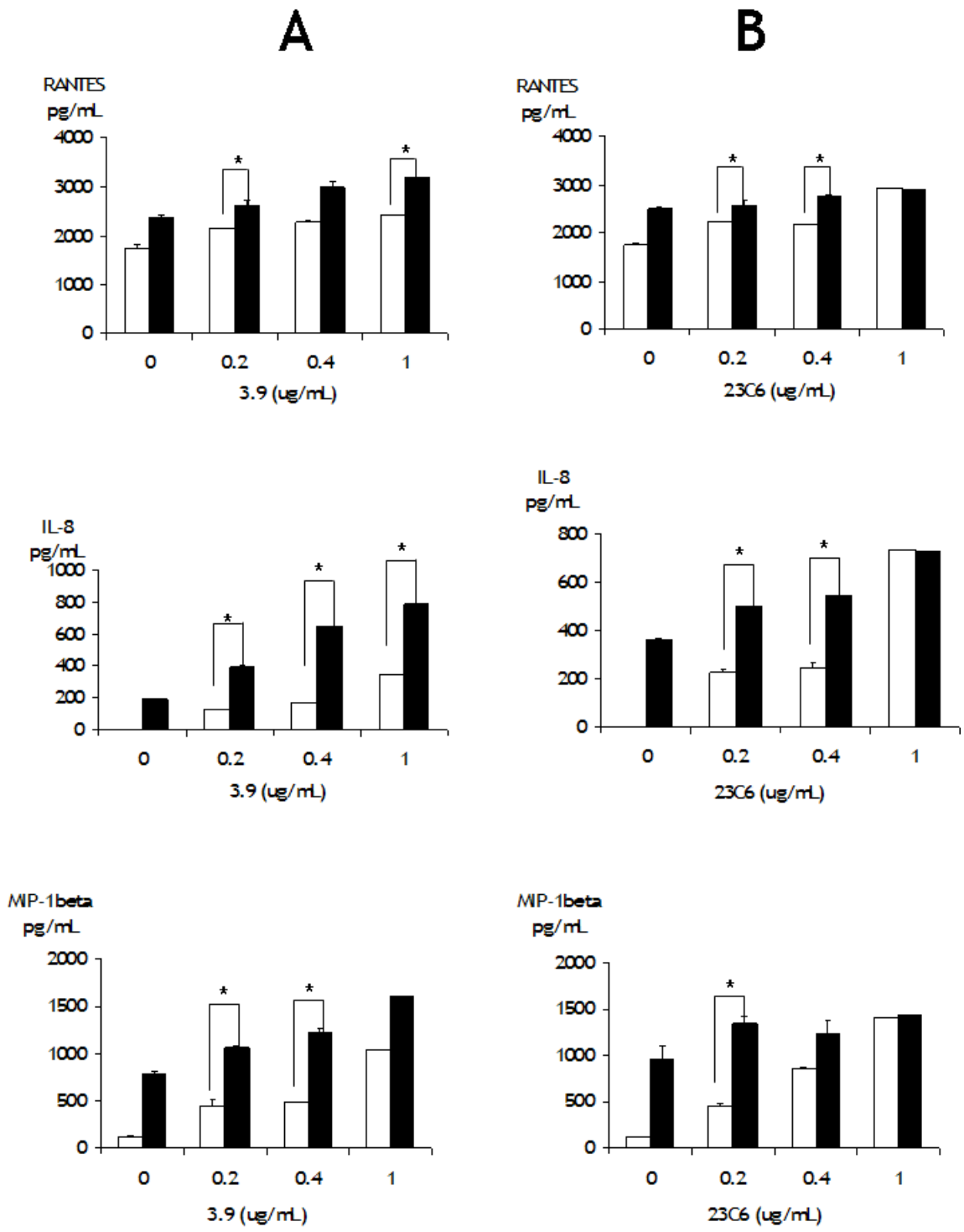

Figure 4.13 Cytokine production in response to simultaneous ligation of αVβ3 and αXβ2

THP-1 cells were stimulated overnight with (A) 0.4μg/mL 23C6 (anti αVβ3 antibody) alone (white bars) or with varying concentrations of Clone3.9 (anti-αXβ2 antibody) (black bars) or (B) 0.4μg/mL of Clone3.9 (anti αXβ2 antibody) alone (white bars) or varying concentrations of 23C6 (anti-αVβ3 antibody) (black bars). Cleared supernatants were tested for the presence of cytokines by ELISA. Statistical analysis was performed using Student's *t*-test *p<0.05. Data are representative of at least 3 separate experiments. The error bars indicate standard deviations (SD).

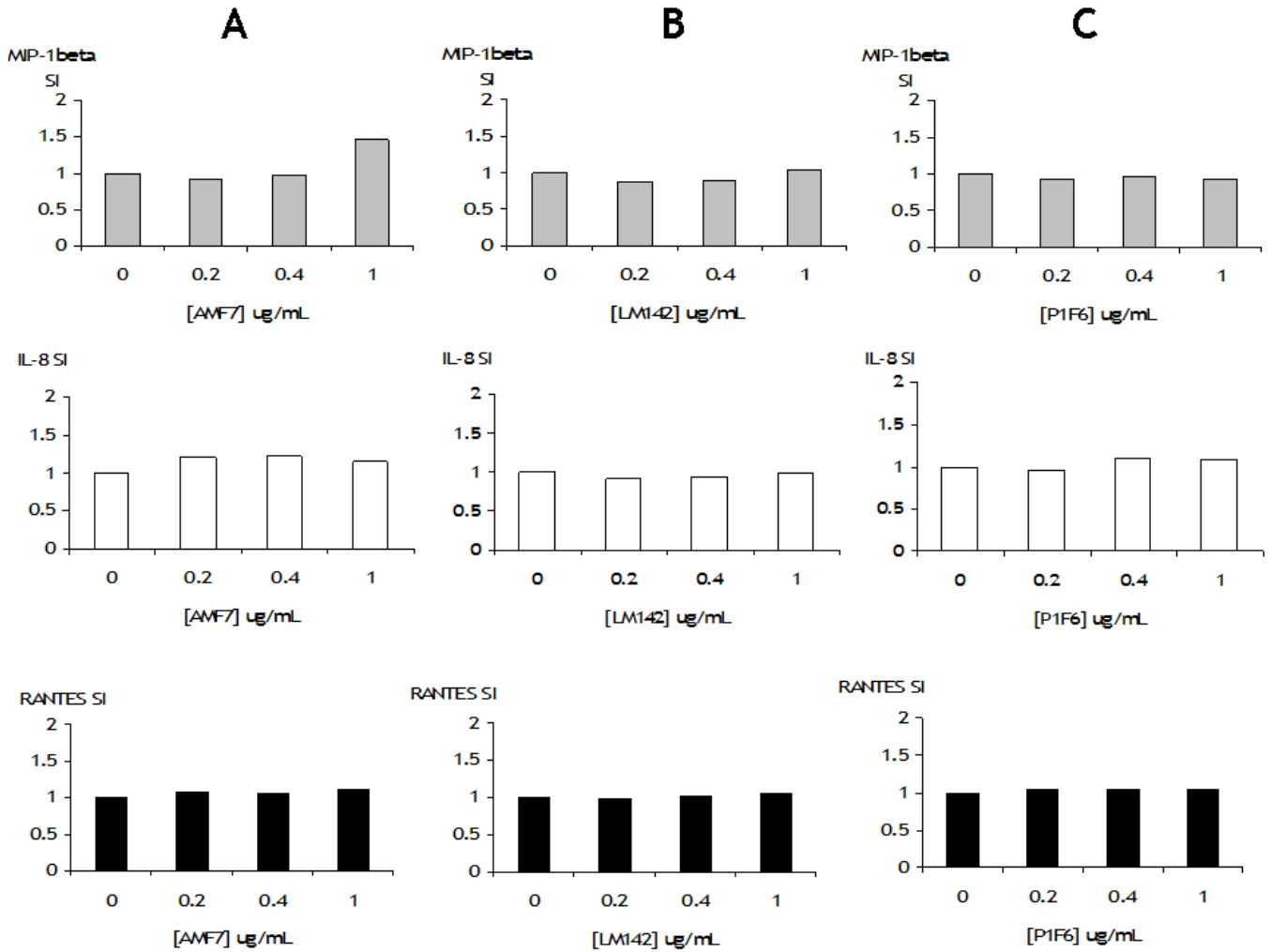

Figure 4.14 Effect of simultaneous ligation of αVβ3 and other αV integrins on cytokine production by THP-1 cells

THP-1 cells were incubated overnight with 23C6 (0.2µg/mL) alone or in conjunction with increasing concentrations of (A) AMF7 (anti-αV antibody), (B) LM142 (anti αV antibody) or (C) P1F6 (anti-αVβ5 antibody). Cytokine production was analysed by ELISA. Statistical analysis was performed using Student's *t*-test. Data are representative of at least 3 separate experiments

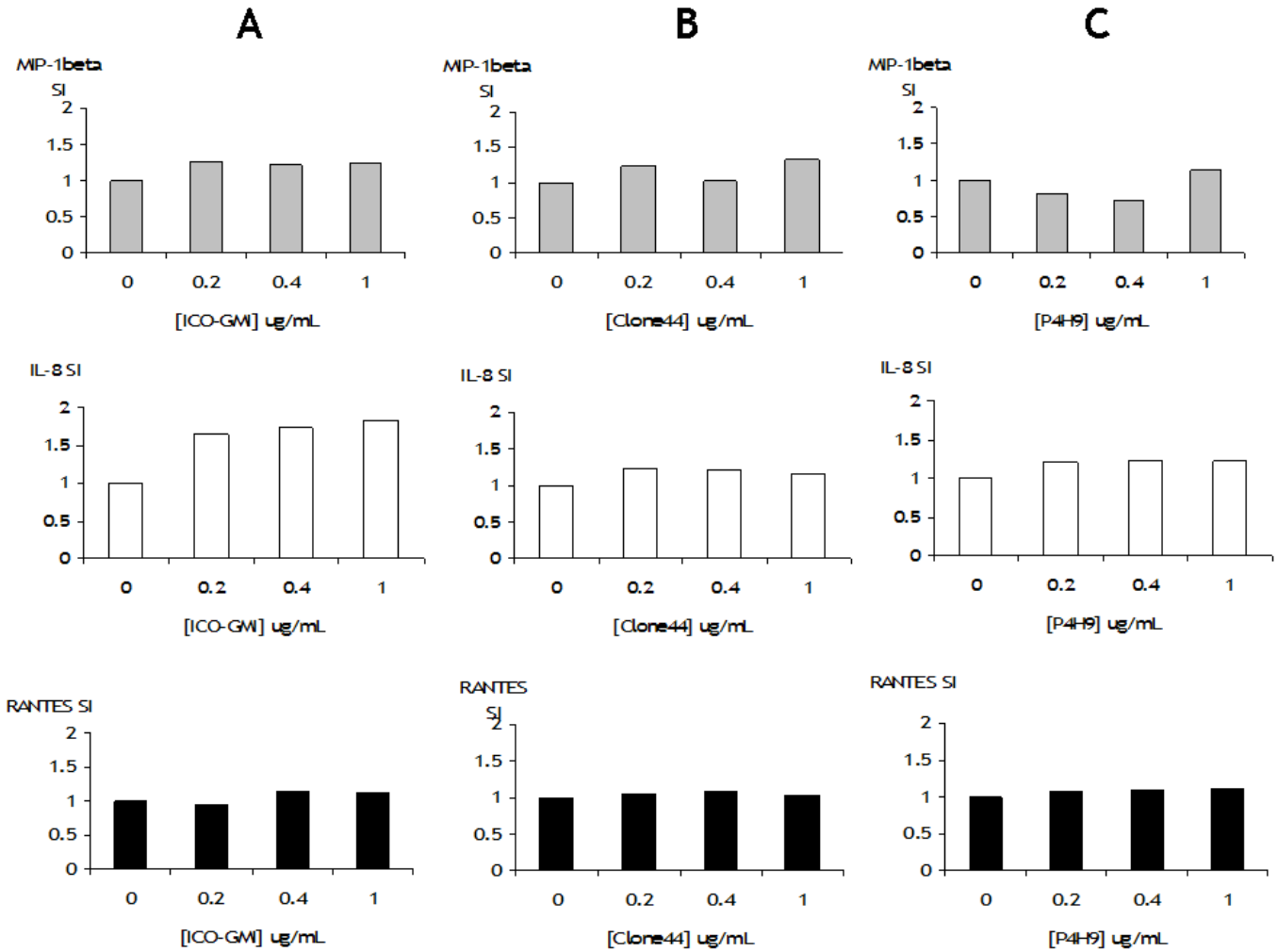

Figure 4.15 Effect of simultaneous ligation of αVβ3 and β2 integrins on cytokine production by THP-1 cells

THP-1 cells were incubated overnight with 23C6 (0.2µg/mL) alone or in conjunction with increasing concentrations of (A) ICO-GMI (anti-αXβ2 antibody), (B) Clone44 (anti αMβ2 antibody) or (C) P4H9 (anti-β2 antibody). Cytokine production was analysed by ELISA. Statistical analysis was performed using Student's *t*-test. Data are representative of at least 3 separate experiments.

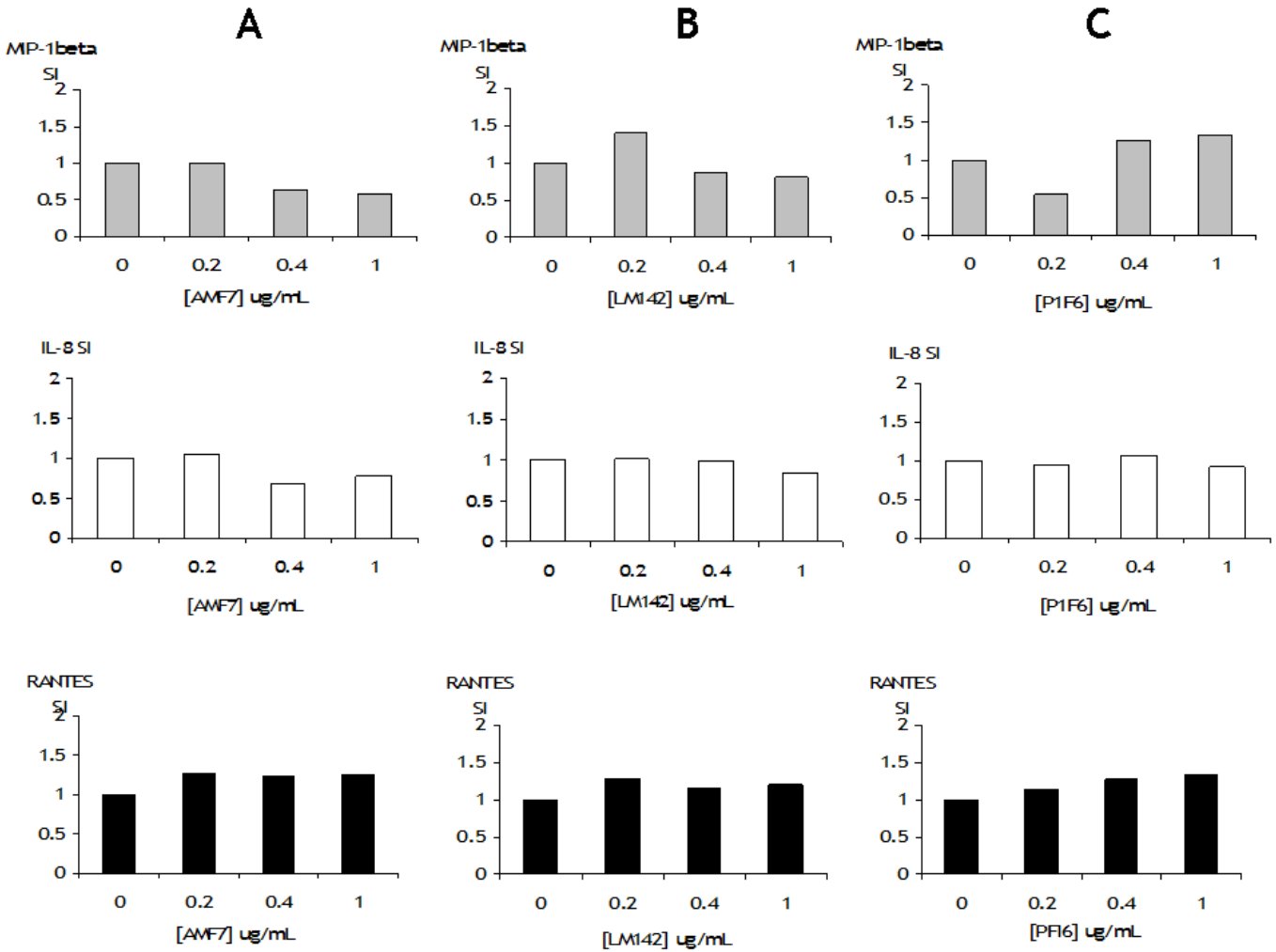

Figure 4.16 Effect of simultaneous ligation of αXβ2 and αV integrins on cytokine production by THP-1 cells

THP-1 cells were incubated overnight with Clone3.9 (0.2µg/mL) alone or in conjunction with increasing concentrations of (A) AMF7 (anti-αV antibody), (B) LM142 (anti αV antibody) or (C) P1F6 (anti-αVβ5 antibody). Cytokine production was analysed by ELISA. Statistical analysis was performed using Student's *t*-test. Data are representative of at least 3 separate experiments.

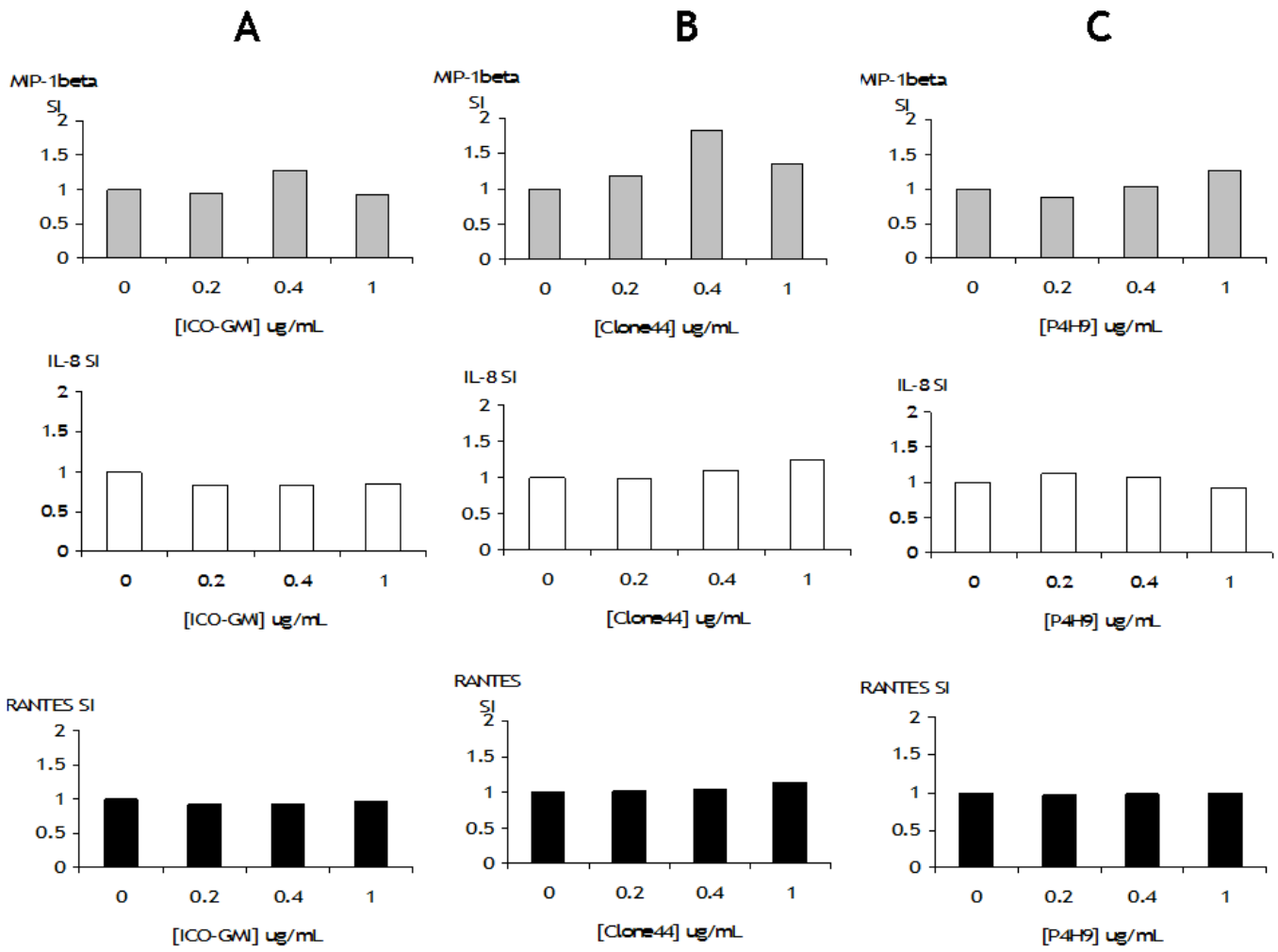

Figure 4.17 Effect of simultaneous ligation of αXβ2 and other β2 integrins on cytokine production by THP-1 cells

THP-1 cells were incubated overnight with Clone3.9 (0.2µg/mL) alone or in conjunction with increasing concentrations of (A) ICO-GMI (anti-αXβ2 antibody), (B) Clone44 (anti αMβ2 antibody) or (C) P4H9 (anti-β2 antibody). Cytokine production was analysed by ELISA. Statistical analysis was performed using Student's *t*-test. Data are representative of at least 3 separate experiments.

4.2.7 Effect of serum on cytokine production by integrin stimulation

All of the integrin stimulation experiments described thus far have been conducted in serum-free, OptiMEM medium. Given the role of integrins in cell adhesion and the presence of adhesive integrin ligands (such as vitronectin) in serum, we tested the effect of serum on cytokine production by 23C6 (αVβ3) and Clone3.9 (αXβ2).

Figure 4-18 shows the production of RANTES, IL-8, MIP-1β and VEGF by THP-1 cells stimulated with increasing concentrations of 23C6 in OptiMEM alone (white bars) or OptiMEM supplemented with 5% serum (white bars). Serum does not negatively affect cytokine production by THP-1 cells in response to 23C6 treatment. In most cases, except for the production of RANTES, serum has a positive effect on cytokine production, leading to a slight but statistically significant increase in the levels of IL-8, MIP-1β and VEGF.

Figure 4-19 shows the corresponding data for the stimulation of THP-1 cells with increasing concentrations of Clone3.9 in OptiMEM alone (white bars) or OptiMEM supplemented with FCS (grey bars). The presence of serum does not inhibit the production of RANTES, IL-8, MIP-1β and VEGF by THP-1 cells in response to Clone3.9 stimulation. In the case of MIP-1β and VEGF, inclusion of serum in the reaction leads to a statistically significant increase in concentration in response to stimulation by Clone3.9.

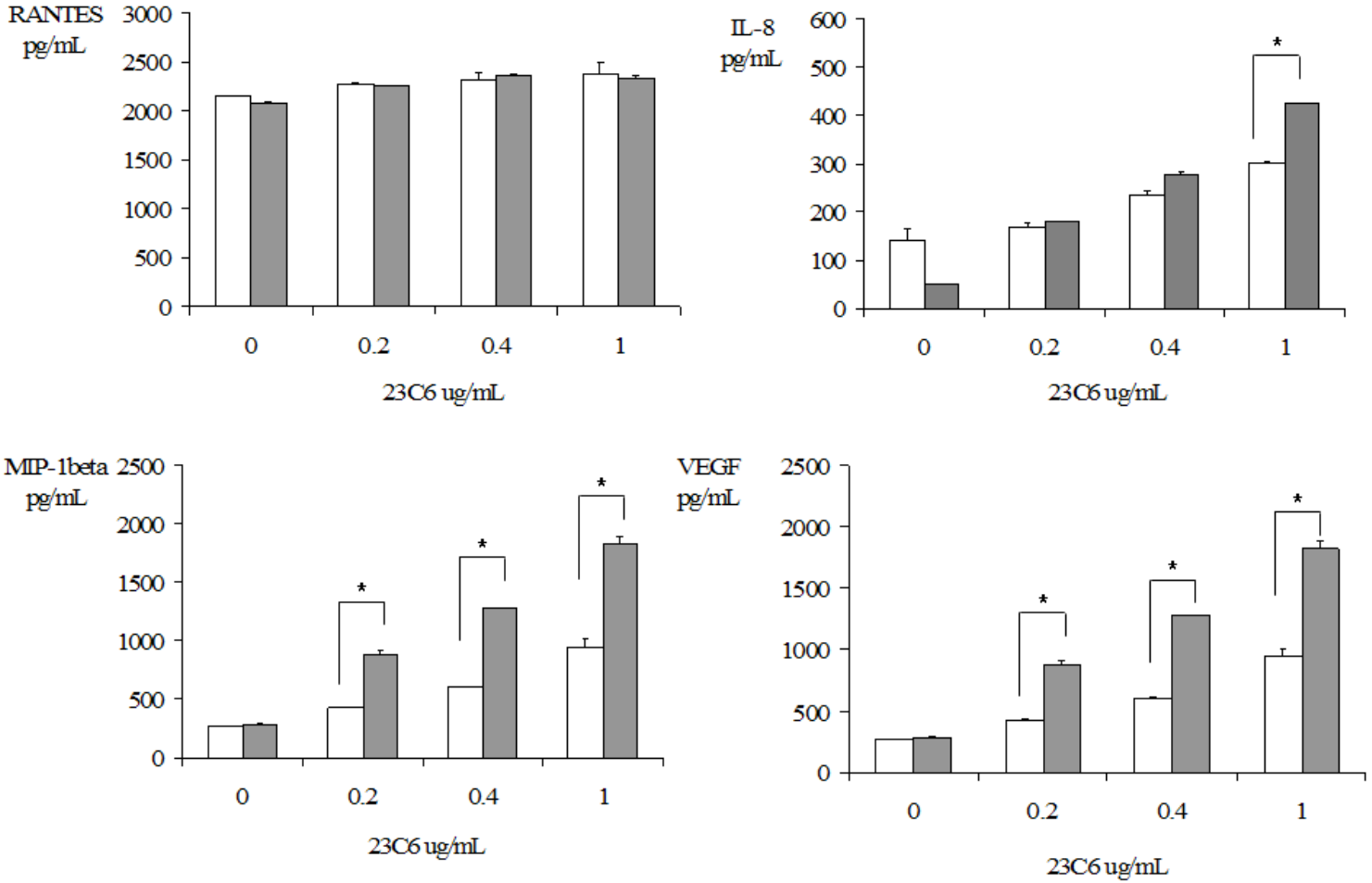

Figure 4.18 Effect of serum on αVβ3 induced cytokine production

THP-1 cells were stimulated with increasing concentrations of 23C6 (anti-αVβ3 antibody) in the presence (grey bars) and absence (white bars) of 5% FCS and cytokine production detected by ELISA. Statistical analysis was performed using Student's *t*-test *p<0.05. Data are representative of at least 3 separate experiments. The error bars indicate standard deviations (SD).

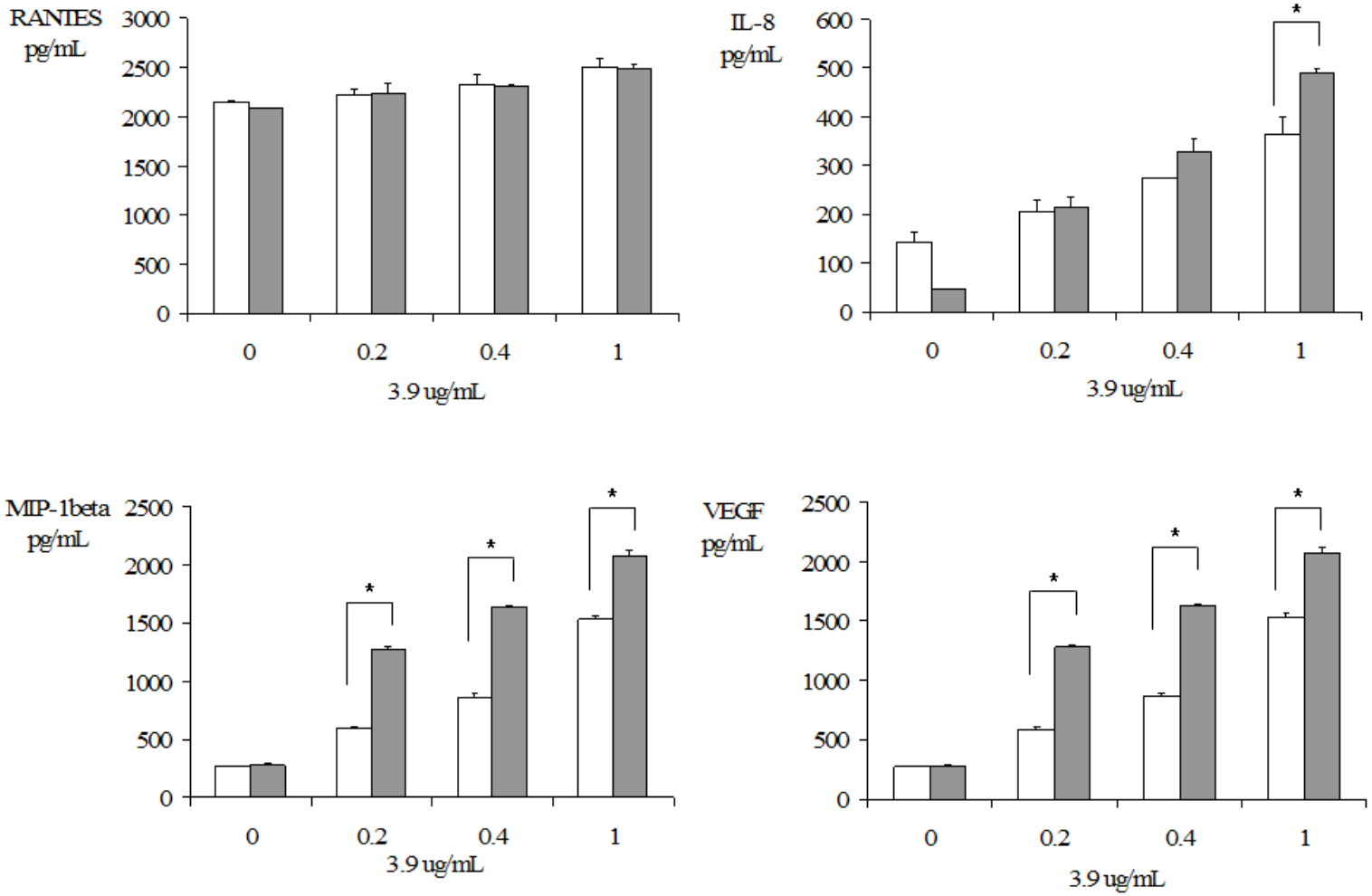

Figure 4.19 Effect of serum on αXβ2 induced cytokine production

THP-1 cells were stimulated with increasing concentrations of Clone3.9 (anti-αXβ2 antibody) in the presence (grey bars) and absence (white bars) of FCS and cytokine production detected by ELISA. Statistical analysis was performed using Student's *t*-test *p<0.05. Data are representative of at least 3 separate experiments. The error bars indicate standard deviations (SD).

4.2.8 Analysis of the responses to integrin stimulation in primary human monocytes

The THP-1 and U937 cells are cell lines derived from patients with leukaemia [165, 166]. The changes associated with these diseases may influence the cytokine responses of the cells. To confirm that integrin stimulation results in cytokine production under non-diseased, physiological conditions, we tested the responses of primary human $CD14^+$ monocytes and human primary bone marrow monocytes. Primary $CD14^+$ human monocytes from peripheral blood ($CD14^+$PBMC) and bone marrow-derived monocytes (BMDM) were cultured in RPMI-1640 medium supplemented with 1% serum and 10ng/mL M-CSF for 3 days before staining for surface expression of integrins and determination of integrin-induced cytokine production.

Figure 4-20 shows the expression of CD23-binding integrins on primary BMDM and $CD14^+$PBMC as determined by flow cytometry. The BMDM and the $CD14^+$PBMC both expressed the αVβ3, αMβ2 and αXβ2 integrins, while $CD14^+$PBMC also expressed the αVβ5 integrin.

Figures 4-21 and 4-22 show the responses of primary human BMDM and $CD14^+$PBMC to integrin stimulation. The primary cells were stimulated under the same conditions used for stimulation of THP-1 cells and cytokines released into the supernatant quantified by ELISA. The cytokine production is shown as fold stimulation over the untreated sample, where a fold stimulation of 1 indicates that there was no cytokine produced over constitutive levels (BMDM and $CD14^+$PBMC constitutively produced high levels of IL-8).

Integrin stimulation had no effect on the levels of RANTES and IL-8 produced by $CD14^+$PBMC. There was a statistically significant increase in the TNF-α production by $CD14^+$PBMC in response to stimulation with Zymosan and with antibodies against the β2 heterodimers, αMβ2 (Clone44) and αXβ2 (Clone3.9). The $CD14^+$PBMC did not produce TNF-α in response to stimulation with an antibody against the common β2 chain (P4H9). There was no TNF-α response observed for $CD14^+$PBMC stimulated with any of the anti-αV antibodies.

The BMDM showed a similar IL-8 profile to the $CD14^{+}$PBMC; there was no effect on IL-8 levels by any of the integrin treatments. A statistically significant increase in the levels of RANTES, MIP-1β and TNF-α was observed for BMDM treated with the anti-αVβ3 antibody (23C6) and the anti-αXβ2 antibody (Clone3.9). αMβ2 stimulation with the ICO-GMI antibody also led to a statistically significant increase in the production of MIP-1β. The BMDM were the most similar to the THP-1 cell line in their cytokine responses to integrin stimulation.

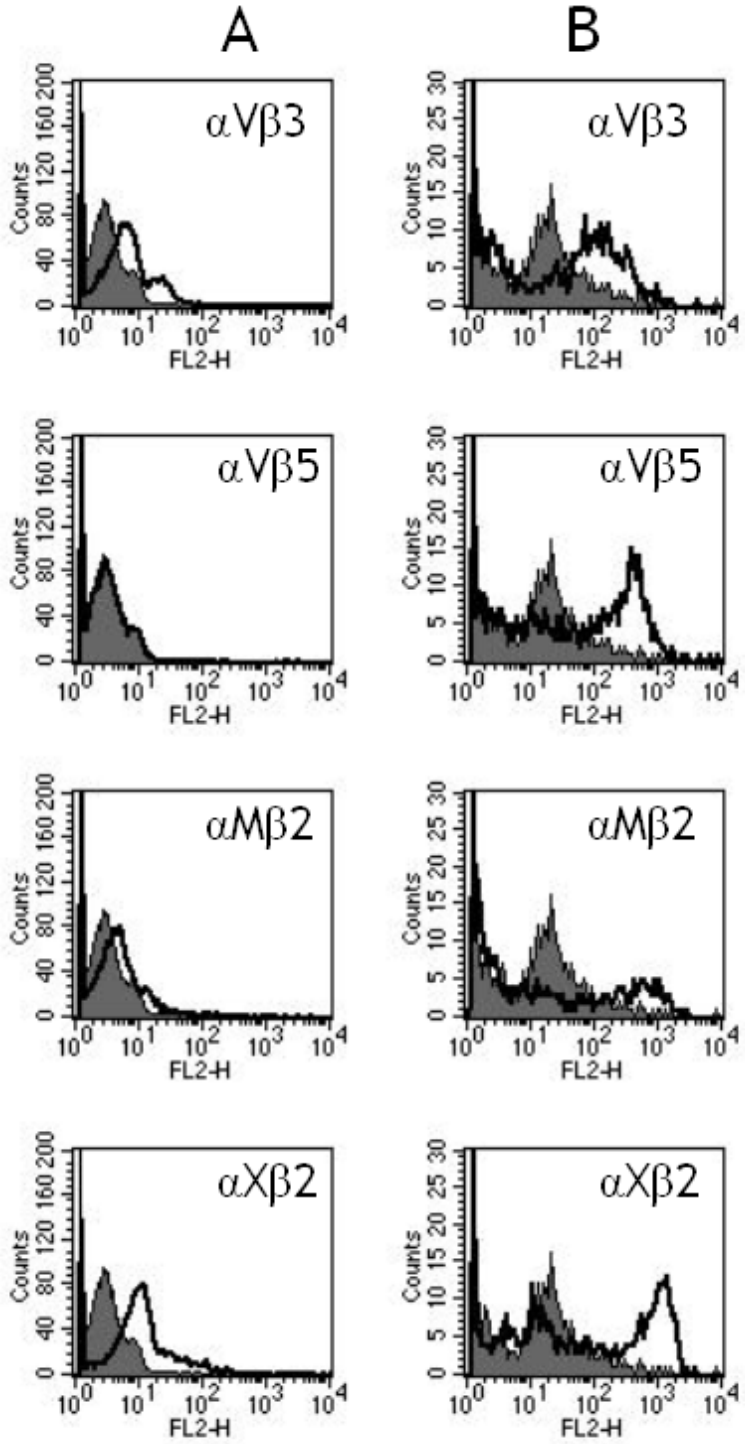

Figure 4.20 Expression of integrins on primary human bone marrow and CD14+ blood monocytes

Primary human monocytes from bone marrow (A) or peripheral blood (B) were incubated with anti-integrin antibodies on ice and binding of these primary antibodies was detected by binding of a secondary antibody conjugated to PE. The integrin heterodimer targeted is indicated in the top right corner of the plot. Isotype control is shown as grey shading and the antibody binding is shown as a black line.

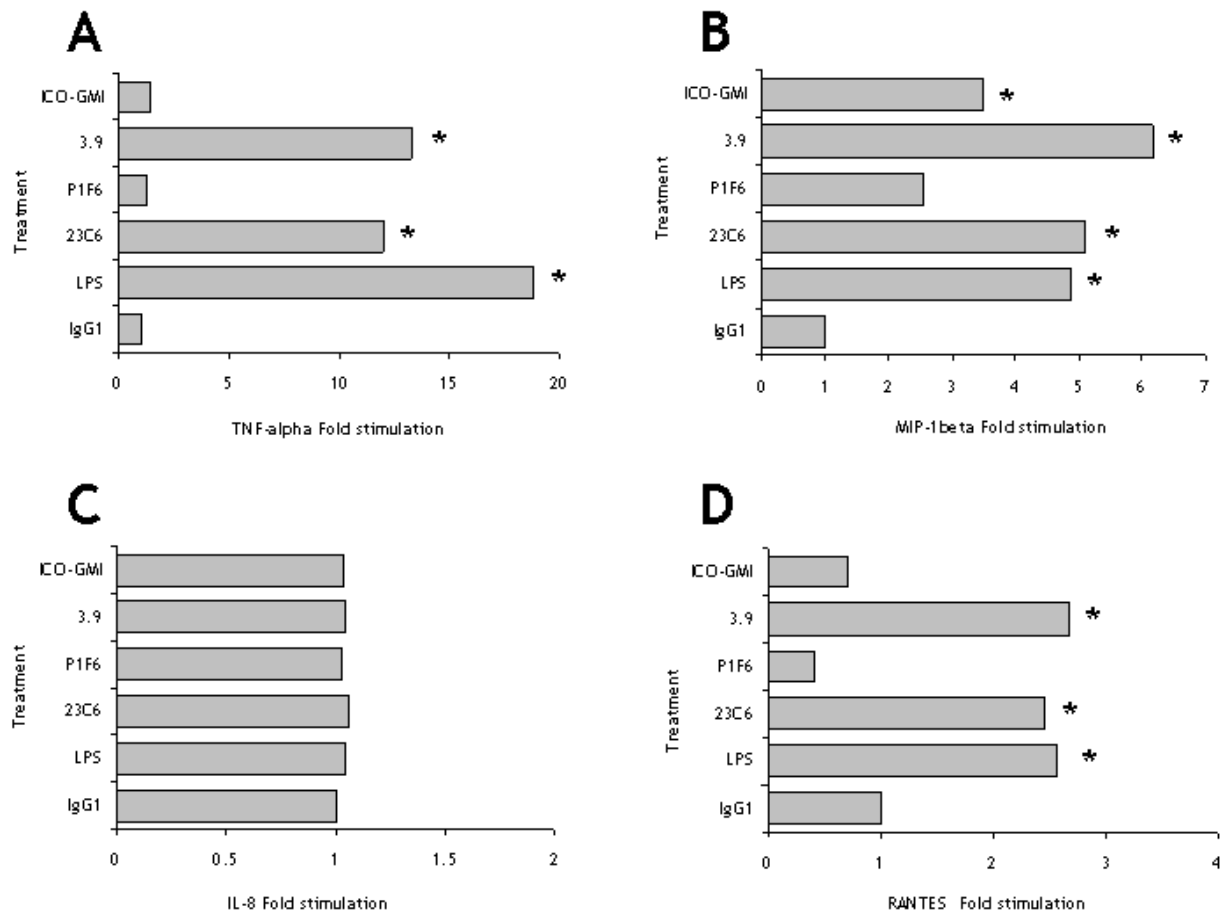

Figure 4.21 Production of cytokines by primary human bone monocytes in response to integrin stimulation

Primary human bone marrow monocytes were stimulated overnight with antibodies against integrins. The cytokine production was detected by ELISA and is represented as fold stimulation. This represents the ratio of the cytokine (TNF-α, RANTES, IL-8 and MIP-1β) concentration produced by the integrin-stimulated sample relative to the unstimulated/untreated cells. IgG1:Isotype control; RGDS:RGDS peptide; VN:vitronectin; AMF7:anti-αV; LM142:anti-αV; 23C6:anti-αVβ3; LM609:anti-αVβ3; 15F11:anti-αVβ5; P1F6:anti-αVβ5; P4H9:anti-β2; MEM48:anti-β2; Clone44:anti-αMβ2; ICO-GM1:anti-αMβ2; Clone3.9:anti-αXβ2. Statistical analysis was performed using Student's *t*-test *p<0.05. The response to IgG1 is included as a representative example. All antibody isotypes were tested (IgG1, IgG2a, IgG2b and IgG3) and gave responses equivalent to IgG1.

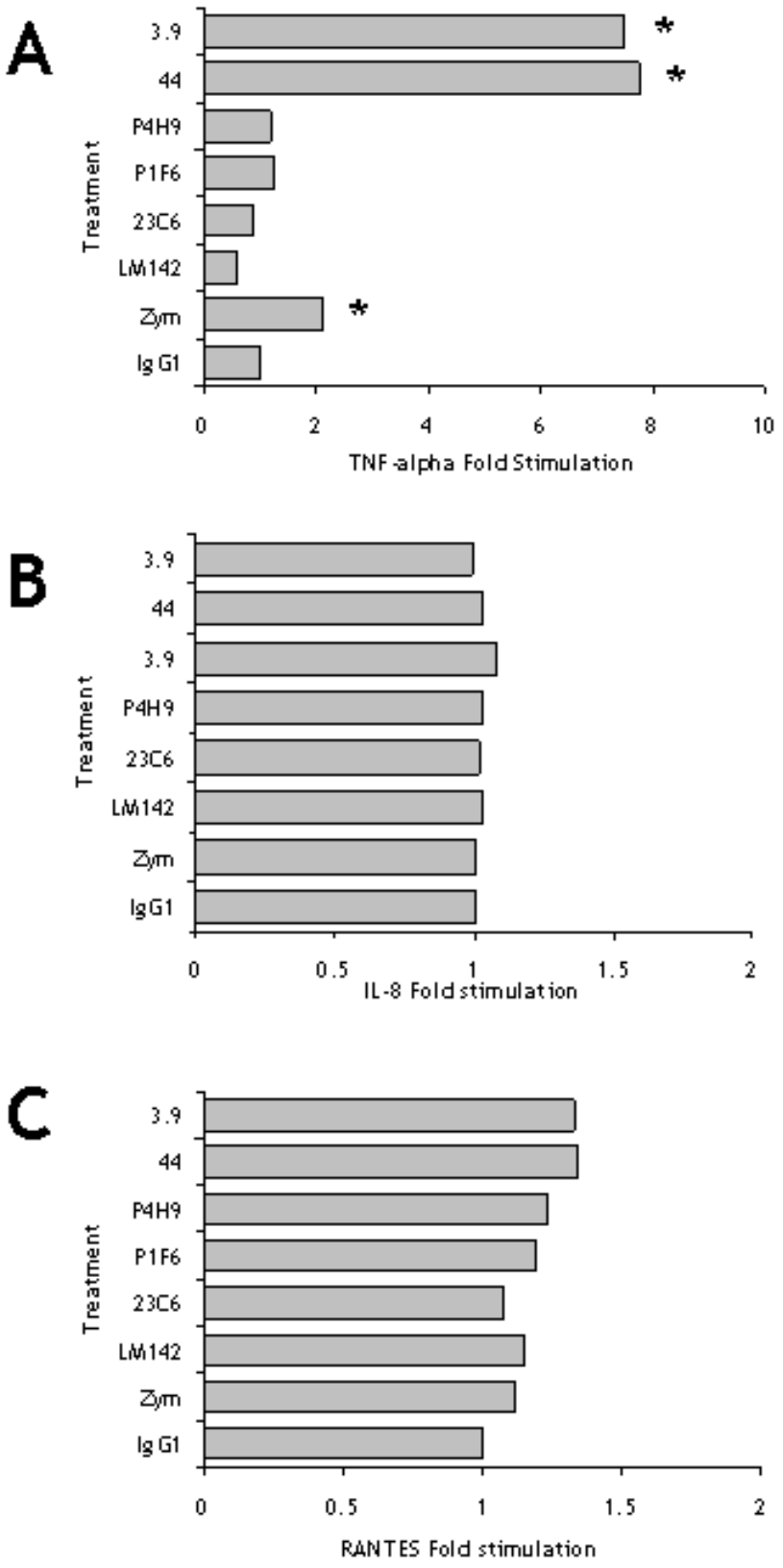

Figure 4.22 Cytokine production by primary CD14+ blood monocytes

Primary human $CD14^+$ peripheral blood monocytes were stimulated overnight with antibodies against integrins. The cytokine production was detected by ELISA and is represented as fold stimulation. This represents the ratio of the cytokine (TNF-α, IL-8 and MIP-1β) concentration produced by the integrin-stimulated sample relative to the unstimulated/untreated cells. IgG1:Isotype control; RGDS:RGDS peptide; VN:vitronectin; AMF7:anti-αV; LM142:anti-αV; 23C6:anti-αVβ3; LM609:anti-αVβ3; 15F11:anti-αVβ5; P1F6:anti-αVβ5; P4H9:anti-β2; MEM48:anti-β2; Clone44:anti-αMβ2; ICO-GM1:anti-αMβ2; Clone3.9:anti-αXβ2. Statistical analysis was performed using Student's *t*-test *p<0.05. The response to IgG1 is included as a representative example. All antibody isotypes were tested (IgG1, IgG2a, IgG2b and IgG3) and gave responses equivalent to IgG1.

4.3 Discussion

CD23 induces cytokine production by monocytic cells through an interaction with integrins [40, 41, 84]. There are four integrins which bind CD23, two from the αV family, namely αVß3 and αVß5, and two from the ß2 family, namely αMß2 and αXß2. We have investigated the individual contribution of these integrins to cytokine production by monocytes, using antibodies directed against these integrins. This approach has been used to a limited extent by some laboratories to investigate the role of the ß2 integrins [41, 84], but has not been previously performed for the role of CD23-binding αV integrins.

Antibodies were selected to investigate the role of the different integrin families (e.g. αV vs ß2 integrins); to analyse the role of different heterodimer isoforms (e.g. αV vs αVß3 vs αVß5); and to investigate the role of specific epitopes within a particular isoform (e.g. different antibody clones against the same integrin/subunit) (Table 4-1). We used two monocytic cell lines to address the role of cell differentiation state on cytokine production.

The preliminary analysis was conducted using a global cytokine array technique. This allowed the detection of 36 different cytokines in one supernatant in a simultaneous assay. We selected the particular cytokine array based on previous investigations into the types of cytokines produced by monocytes in response to CD23. Although this technique was qualitative, it was possible to use densitometry to produce standardised data that allowed comparison of the responses of different stimulating antibodies. Visual observation alone of the arrays could be misleading due to exposure differences between individual blots, which influenced signal intensity. The positive control signals on each blot are independent of integrin treatment and therefore were used to standardise the signal intensity between blots.

At the outset of the analysis, we were uncertain whether each treatment would result in a very different cytokine profile. We therefore used the cytokine arrays to perform the preliminary qualitative analysis and assess the production of a wide range of cytokines, from which we could subsequently select specific cytokines for quantitative analysis. Analysis of the cytokine array profiles from THP-1 cells treated with antibodies against CD23-binding integrins indicated that

the cytokine profile produced did not differ significantly between different integrin families or isoforms. We did not find that one family regulated a particular group or groups of cytokines, as we may have hypothesised. Our analyses suggested that, although the cytokine *profile* may be similar, the *concentration* of cytokines produced was influenced by integrin family, integrin isoform and integrin epitope targeted.

We selected three chemokines RANTES, IL-8 and MIP-1ß for the quantitative analysis. These chemokines were selected on the basis of the qualitative arrays and also because they have similar roles in the biology of the immune system. They are all chemotactic cytokines involved in the recruitment and activation of immune cells to the site of infection and, in the case of RANTES and MIP-1ß, they share a common receptor (CCR5). We attempted to define a hierarchy of importance for the CD23 binding integrins in the production of these cytokines by monocytic cells.

Using the quantitative ELISAs, we determined that cytokine production by THP-1 cells in response to integrin binding results in the production of physiologically-relevant levels of cytokines. The concentrations of cytokines detected in our analyses were similar to the concentrations observed in human serum in physiological and pathological conditions (Table 6-2). The interaction was specific and influenced by the integrin family, the subunit composition of the heterodimer and by the epitope bound on the heterodimer. It was not simply sufficient to have a high level of expression of a particular heterodimer to induce cytokine production; a precise signal was required.

4.3.1 Role of integrin family on cytokine production

Both CD23-binding members of the αV and ß2 family of integrins induced cytokine synthesis by THP-1 cells. Cytokine production in response to binding of αVß3, αMß2 and αXß2 have been published previously by other groups [40, 74]. Our group has recently identified the αVß5 integrin as a new receptor for CD23 [75]. This thesis is the first to identify cytokine production by monocytic cells in response to stimulation with antibodies against the αVß5 integrin. Stimulation of THP-1 cells with an antibody against αVß5 (P1F6) induced synthesis of RANTES, IL-8 and MIP-1ß.

Using antibodies against different isoforms within the αV and ß2 families we investigated the role of individual heterodimer isoforms in cytokine production. Within the αV family of integrins, both antibodies selected against the αV subunit (AMF7 and LM142) were able to induce synthesis of RANTES, IL-8 and MIP-1ß. Antibodies 23C6 and P1F6 directed against αVß3 and αVß5, respectively, were able to induce cytokine synthesis. Similarly, antibodies against the αMß2 and αXß2 integrins induced cytokine production (antibodies Clone44 and Clone3.9, respectively). However, stimulation of THP-1 cells with antibodies against the common ß2 subunit using antibodies MEM48 or P4H9 failed to induce synthesis of cytokines. Taken together, these data suggest that the important determinant of integrin-mediated cytokine production could be the integrin α subunit. All of the stimulations involving the α subunit of the heterodimer resulted in cytokine production, even if only the α subunit (i.e. not the heterodimer) was targeted. Ligation of the α subunit alone was sufficient to induce cytokine production, while the ß subunit alone was not. The binding site for CD23 on integrins remains to be identified, although a number of groups have suggested that the binding site for CD23 on integrins and thus the site responsible for inducing cytokine production, is located on the α chains of the integrins [40, 83]. This may be important in regulating the signalling pathways that arise from integrin ligation, as both the α and ß subunits contact cytoplasmic signalling molecules and are capable of inducing signalling cascades in the cytoplasm. In the case of αVß3, the phosphorylation of the ß3 tail relies on the presence of the αV subunit [187].

It was interesting to find two distinct families of integrins (αV and ß2) both influencing cytokine production by monocytic cells. The production of cytokines is specific and therefore it is possible that these different families of integrin regulate cytokine production under different conditions or environments. For example, the ß2 integrin family is expressed exclusively on leukocytes and not on other cell types in the body. As such, ß2-mediated cytokine production may be important for processes that are specific to leukocytes, such as extravasation and oxidative burst. The αV integrins, however, are expressed by a variety of cell types, such as fibroblasts, in addition to leukocytes. Therefore, their role in cytokine production will not be limited to those functions related to leukocytes. The αV-mediated cytokine production may substitute for ß2 integrins on other cell types. The expression pattern of particular integrins is developmentally

regulated and specific to certain cell types. Therefore, the ability of individual integrins to induce cytokine production may be regulated at the level of integrin expression. Additionally, integrins are known to cooperate with other receptors, including other integrins, as we have shown with the αVβ3 and αXβ2 integrins (See Figures 4-12 to 4-16). Stimulation of cells with antibodies against both integrins led to an increase in cytokine production over the levels produced by stimulation of a single integrin. Therefore, the cytokine output of a particular cell will also be influenced by the different types of integrins expressed on the cell surface.

4.3.2 Role of integrin isoform

Cytokine output was influenced by the heterodimer within the integrin family that was targeted. Stimulation of the cells with antibodies against the αVβ3 and αVβ5 integrins induced similar cytokine responses by monocytic cells. The αVβ3 and αVβ5 integrins were expressed at comparable levels and induced a similar increase in the fold stimulation of cytokine production by THP-1 cells. In contrast, the αMβ2 integrin induced lower levels of cytokines than the αXβ2 integrin. THP-1 cells express significantly lower levels of αMβ2 than αXβ2, although the expression level alone of a particular integrin was not sufficient to influence the production of cytokines. In the presence of the correct signal to induce cytokine production, however, expression levels may influence the concentration of cytokines released. This may account for the difference observed in the concentrations of cytokine produced by stimulation of αMβ2 versus αXβ2. Although treatment of the THP-1 cells with GM-CSF led to an increase in the expression of αMβ2, we did not observe an increase in αMβ2-mediated cytokine production. This may indicate, again, that expression levels of an integrin are not the major determinant of its ability to induce cytokine production. We cannot exclude the possibility though that there may have been changes other than in αMβ2 expression in the cell line after GM-CSF treatment that we did not observe, but which would explain the discrepancy between integrin level and cytokine production.

4.3.3 Role of integrin epitope

We investigated the role of the integrin epitope on the production of cytokines by integrin stimulation using paired antibodies against the same heterodimer. We observed that there was an epitope effect, since for both the αV and β2 heterodimers, only one of the paired antibodies elicited a response. Therefore, the site at which the integrin is bound is important for inducing cytokine production. This comparison is independent of concentration as both antibodies bind the same heterodimer and gives an indication of the specificity of the interaction. For the αVβ3 integrin, the 23C6 antibody induced high levels of cytokine synthesis by THP-1 cells. The other αVβ3 antibody used in the analysis, LM609, failed to induce the production of the cytokines studied. This suggests that the 23C6 clone may recognise the site on the heterodimer required to activate this integrin to induce cytokine production, while LM609 did not. The mechanism of this interaction will need to be determined; 23C6 may activate αVβ3 by binding to the critical site or through an allosteric mechanism. This remains to be determined. In addition, an analysis of the affinities of the individual antibodies should be undertaken, to ensure that the responses observed are not solely due to the strength of the interaction.

4.3.4 Role of cell differentiation status

We tested two monocytic cells lines, THP-1 and U937, for their ability to produce cytokines in response to integrin binding. THP-1 cells are derived from the peripheral blood of a patient suffering with acute myeloid leukaemia [165]. U937 cells were derived from a patient with histiocytic lymphoma [166]. Both cell lines are routinely used as model cell systems for analysis of monocytic/macrophage responses.

The two lines expressed similar levels of CD23-binding integrins, but responded differently to equivalent stimulation. This suggests that cell differentiation state may influence cytokine production in response to integrin stimulation. These data were supported by the studies involving the differentation of THP-1 cells using M-CSF, GM-CSF and db-cAMP. In these cases, a change in the expression level of the integrins did not correlate with an increase in cytokine production in response to integrin binding. It may be however, that THP-1 cells are already too

differentiated to observe any changes in response to treatment with the different agents. These experiments should have rather been conducted on the less differentiated U937 cell line.

It is possible that there was an increase in integrin activation without a change in expression levels that led to the increases in cytokine production. This is a difficult parameter to measure in the context of this interaction. The integrin stimulation in these experiments was performed using soluble ligands with cells in suspension and therefore it is difficult to define integrin activation under these conditions. Most analyses define integrin activation in terms of adhesion, and consequently the reagents available for the study of integrin activation (conformational antibodies), are based on the adhesive/RGD-binding abilities of integrins. We anticipate that the site on the integrin that modulates cytokine production is independent of the RGD site, although we have yet to identify it. It seems unlikely therefore, that activation of an integrin in the "classical adhesion-based" sense would enhance cytokine production. Our hypothesis is supported by the fact that the inclusion of FCS (which contains RGD-containing ligands) does not inhibit or dampen the cytokine response. Inclusion of FCS in the medium led to a statistically significant increase in cytokine production. Chemokines are known to activate integrins, this may lead to RGD binding and enhancement of the cytokine response. ECM proteins alone cannot induce cytokine response in solution. Alternatively, it may simply be due to the fact that the cells are better adapted and less stressed in media containing serum. The possible interplay between adhesive and non-adhesive integrin signalling will be addressed as more information regarding the role of integrins in non-adhesion based signalling becomes available.

4.3.5 Cooperation between integrins and other receptors

The role of integrins as modulators of the activity of other surface receptors is an example of adhesion-independent integrin-based signalling. Integrins are signalling molecules in their own right, but have also been shown to show synergy with other surface receptors. Cell differentiation is often associated with changes in activity and changes in the expression levels of surface proteins. The production of cytokines by integrins, therefore, may rely on the expression of an additional surface receptor that is developmentally regulated.

We analysed the expression of the $F_c\gamma$ receptors, a family of immunoreceptors which play a key role in cytokine production by monocytes [188]. Three $F_c\gamma$ receptors are expressed on monocytes, CD16, CD32 and CD64. CD64 is the high affinity receptor, which is capable of binding monomeric IgG, while the CD16 and CD32 receptors only bind IgG as part of an immune complex. Fc receptors have an important role in a number of integrin-mediated immune functions [189-192], which might influence cytokine production. As we were using antibodies, it was plausible that $F_c\gamma$ receptors may be involved in the interaction.

We did not find any change in the levels of $F_c\gamma$ receptors on the differentiated THP-1 cells that could explain the discrepancies between integrin expression levels and cytokine production. Interestingly, U937 cells, which did not produce significant quantities of cytokines in response to integrin binding, did not express CD16 or CD32 and only expressed low levels of CD64. The precise role of the $F_c\gamma$ receptors in integrin-induced cytokine production would need to be addressed using the corresponding Fab fragments that lack the Fc portion of the antibody, as opposed to whole immunoglobulin molecule. Isotype controls were used to control for the contribution of $F_c\gamma$ receptors, although they are not necessarily a true representation of the immune complexes required to induce cytokine production by $F_c\gamma$ receptors. A better approach would have been to use $F_c\gamma$ receptor blockers in conjunction with the specific antibodies. However, even if $F_c\gamma$ receptors are involved in the mechanism of integrin-mediated cytokine production, the interaction was still specific, as it was only observed in specific cases (such as 23C6), not with any antibody (such as LM609).

We also analysed the expression of CD47 on the differentiated THP-1 cells. CD47 is a component of the αVβ3 signalling complex and therefore an increase in CD47 levels may lead to an increase in αVβ3-mediated signalling without altering αVβ3 levels. There was no change in the expression of CD47 on the differentiated THP-1 cells or U937 cells that could explain the differences between change in expression level and cytokine production. It is still possible, however, that an additional, as yet unidentified, receptor is regulating integrin-mediated cytokine production.

We did not observe cooperativity between different integrins during cytokine production. Co-stimulation of THP-1 cells with the 23C6 and Clone3.9 antibody

led to higher levels of cytokine production, than when used alone at equivalent concentrations. This indicates that the pathways that lead from αVß3 and αXß2 integrins during cytokine production are not opposing and lead to a similar outcome. We would anticipate that both integrins activate the same pathway, possibly via a common co-receptor, although we do not currently have the data to support this conclusion. To observe cooperativity between the integrins, we would have expected an antibody that did not normally induce cytokine production (such as P4H9) to enhance the cytokine production of a suboptimal level of 23C6 or Clone3.9. We did not observe a statistically significant effect with any of the co-stimulations tested.

4.3.6 Integrin-mediated cytokine production by primary cells

Although used as a model for monocytic cells, the THP-1 cell line is derived from a patient suffering from acute myeloid leukaemia and carries the MLL-AF9 mutation [165]. It may be a better model for integrin-mediated cytokine production during pathology than in physiological conditions. We analysed the cytokine responses of primary cells (BMDM and $CD14^+$PBMC) to integrin stimulation. The $CD14^+$PBMC produced cytokines upon ß2 ligation, but did not produce cytokines in response to stimulation with antibodies against αV integrins. The BMDM gave the most similar response to THP-1 cells and produced cytokines in response to both αV and ß2 antibodies. This was unexpected as THP-1 cells are routinely used as a model for macrophage/monocytic cells and therefore it was anticipated that the $CD14^+$PBMC would be the most similar in response to THP-1. These data would suggest that in fact, THP-1 cells are more similar to BMDM in their integrin-mediated cytokine responses. These data further suggest that differentiation state is crucial for integrin-mediated cytokine synthesis.

We have analysed the importance of stimulation of different CD23-binding integrins in cytokine production by monocytic cells. This analysis has indicated that integrin-mediated cytokine production is specific and influenced by integrin family, isoform and epitope targeted. The production of these chemokines may have a role in the biology of the immune system and the monocytes themselves. CD23 itself also induces maturation/activation of monocytes via its interactions with ß2 integrins [74, 193].

5 ROLE OF αVβ3 INTEGRIN IN MONOCYTE DIFFERENTIATION

5.1 Introduction

5.1.1 The αVß3 integrin

The αVß3 integrin is a member of the vitronectin receptor family, integrins which all contain the αV subunit in a non-covalent association with one of 5 ß chains, namely ß1, ß3, ß5, ß6 or ß8, and have the capacity to bind vitronectin [194]. The αVß3 integrin is expressed at low levels in most normal tissues including intestinal, vascular and smooth muscle, although in general, the other αV isoforms are more widely expressed in normal tissues. High levels of αVß3 expression *in vivo* are observed in bone, placenta, inflammatory sites and invasive malignancies (including melanoma, glioma, ovarian and breast tumours). Specifically, cell types which express high levels of the αVß3 integrin are mature osteoclasts (bone resorbing cells), activated macrophages, angiogenic endothelial cells and migrating smooth muscle cells [195].

The aVβ3 integrin is one of the most well studied of the integrins, with the recent information on the general structure and conformational regulation of integrin activation being based on the published crystal structures of the extracellular domain of the αVβ3 integrin [94, 98]. The αVβ3 integrin plays an important role in adhesion and non-adhesion based interactions in cells. As a cell adhesion receptor it binds a wide range of ECM proteins in addition to vitronectin, including fibronectin, fibrinogen, osteopontin and thrombospondin. These interactions are mediated via recognition of the RGD motif in the various ECM proteins. These adhesive interactions are important during osteoclastogenesis and in the case of metastatic cancers. The αVβ3 integrin also functions as a receptor for a number of viruses during entry into cells. These interactions are both RGD-dependent and RGD-independent (Table 6-1).

In addition to its role in cell adhesion and migration processes, αVβ3 associates with and modulates the activity of a number of growth factor receptors, including the platelet-derived growth factor (PDGF) receptor [196-198], basic fibroblast growth factor (BFGF) receptor [137, 199-203], transforming growth factor-β (TGFβ) receptor [204-206], insulin growth factor (IGF) receptor[140, 207] and vascular endothelial growth factor (VEGF) receptor [137, 196, 197, 208]. The αVβ3 integrin has also been shown to associate with the M-CSF receptor, c-FMS, during osteoclast

development and macrophage activation [142, 209, 210]. The combined expression patterns and functions of αVβ3 make it an attractive target for therapies against a number of inflammatory disorders, rheumatic diseases and cancers [194, 211-216].

5.1.2 Macrophage differentiation and activation

Macrophages are a highly heterogeneous population that fulfil a range of functions in the immune system. They are the precursors for a number of terminally differentiated cells with specialised functions in the body, including osteoclasts and dendritic cells. Macrophages develop when blood monocytes move into the tissues in response to cues from the local environment. Macrophages can be activated by a number of different stimuli, each of which results in a macrophage that is polarised to exhibit specific characteristics. Activated macrophages can be classified as having undergone either a classical or alternative programme of activation.

5.1.2.1 Classically Activated Macrophages (M1)

Classically activated macrophages develop in response to treatment with IFN-γ and TNF-α. These macrophages are pro-inflammatory and produce high levels of pro-inflammatory cytokines, including TNF-α, IL-1 and IL-6 [217]. This type of macrophage is traditionally associated with Th1 responses that result in inflammation and the destruction and clearance of intracellular pathogens and tumour cells [217].

5.1.2.2 Alternatively Activated Macrophages (M2)

Alternatively activated macrophages are generally classed as anti-inflammatory and are usually identified due to their high expression of IL-10 and lack of IL-12 expression [6]. M2 macrophages can be further sub-classified into M2a (also known as alternatively activated), M2b (also known as type II activated) and M2c (also known as deactivated) macrophages, according to the activating signals under which they arise and their subsequent cytokine production profiles. M2a macrophages develop in response to treatment with agents including IL-4, IL-13 and glucocorticoids, while M2b develop in response to TLR or IL-1R ligation and immune complexes, and M2c macrophages develop in response to IL-10

treatment. M2 macrophages are associated with anti-inflammatory, tissue remodelling and pro-cancer activity. M2b macrophages are distinct in that they continue to produce the pro-inflammatory cytokine TNF-α, in addition to the anti-inflammatory IL-10 [16].

5.1.3 Activated macrophages and disease

Activated macrophages play an important role in the development and progression of a number of diseases [2]. Both pro-inflammatory M1 activated macrophages and anti-inflammatory M2 macrophages can contribute to human disease. Pro-inflammatory M1 activated macrophages are a hallmark of a number of inflammatory diseases, including rheumatoid arthritis [194, 217]. The production of cytokines (such as TNF-α, IL-6 and IL-1) by M1 macrophages is responsible for inflammation observed during these diseases. Anti-inflammatory M2 macrophages also have a role in human pathology, most likely as tumour-associated macrophages (TAM) [218]. TAMs are a M2 population of activated macrophages recruited to tumour sites, which do not destroy tumours, but rather contribute to their survival and development. TAMs aid in the establishment of a favourable tumour microenvironment by the release of pro-tumourgenic and pro-angiogenic mediators, including factors like VEGF and IL-8 [219].

5.2 Results

5.2.1 Integrin signalling during cytokine production

Stimulation of THP-1 cells with an anti-αVß3 antibody 23C6 led to the production of high levels of cytokines. We examined the early signalling events that occurred in the THP-1 cells after integrin stimulation with 23C6. Activation of the ß3 integrin has been shown to induce phosphorylation of the cytoplasmic tail at different sites [220-224]. To test if 23C6 was inducing cytoplasmic signalling by the αVβ3 (i.e., 23C6 was activatory as opposed to inhibitory), we examined the phosphorylation state of the ß3 tail in THP-1 cells after treatment with increasing concentrations of 23C6. Figure 5-1 shows Western blots for the phosphorylation of the ß3 cytoplasmic domain at residues Tyr773 or Tyr785. In the absence of treatment, there was no phosphorylation of the ß3 tail at either residue (Tyr773 or Tyr785). Ligation of αVβ3 with the 23C6 antibody led to detectable phosphorylation of the ß3 tail at Tyr773 at concentrations ranging from 0.25µg/mL – 5µg/mL antibody. There was no detectable phosphorylation of Tyr785 of the β3 cytoplasmic tail at any concentration of 23C6 treatment.

Integrins are known to activate the mitogen-activated protein kinase (MAPK) pathway in many cell lineages [84, 225-228]. We tested if treatment of THP-1 cells with the anti-αVβ3 antibody 23C6 in solution led to activation of the MAPK pathway and subsequent phosphorylation of extracellular signal-regulated kinase (ERK). Figure 5-2 shows the Western analysis for the phosphorylation of ERK in THP-1 cells treated with 23C6. Actin was used as a loading control and densitometry was performed using the *ImageJ* program, although using total ERK levels as a loaded control would have been more accurate. Figure 5-2A shows the phosphorylation of ERK in THP-1 cells treated with increasing concentrations of 23C6 for 30 min. Figure 5-2B shows the response of THP-1 cells treated with 1µg/mL of 23C6 at different time points. Phosphorylation of ERK was observed when THP-1 cells were stimulated with 23C6.

We analysed the importance of ERK activation in integrin-mediated production of cytokines using the mitogen-activated ERK-kinase (MEK) inhibitor U0126. MEK directly phosphorylates ERK during MAPK signalling [229]. THP-1 cells were stimulated to induce cytokine production using LPS (positive control), 23C6 (anti-αVβ3 integrin) or Clone3.9 (anti-αXβ2) in the absence and presence of the MEK inhibitor U0126, and cytokines (RANTES, MIP-1β and IL-8) released into the supernatant were detected by ELISA (Figure 5-3). THP-1 cells stimulated with LPS, 23C6 or Clone3.9 in the absence of U0126 produced high levels of RANTES (Figure 5-3A white bars), IL-8 (Figure 5-3B white bars) and MIP-1β (Figure 5-3C white bars). THP-1 cells were stimulated with the same treatments in the presence of the MEK inhibitor, U0126. Inclusion of the MEK inhibitor in the reaction lead to a statistically significant reduction in the concentrations of RANTES (Figure 5-3A grey bars), IL-8 (Figure 5-3B grey bars) and MIP-1β (Figure 5-3C grey bars) produced in response to integrin stimulation with either 23C6 or Clone3.9. LPS-induced RANTES production was statistically reduced by U0126 treatment, while LPS-induced IL-8 and MIP-1β concentrations did not differ significantly in the presence or absence of U0126. The MEK inhibitor did not completely inhibit cytokine production, as low levels of RANTES, IL-8 and MIP-1β were still released in the presence of U0126. In general, αXβ2-stimulated cytokine production was inhibited to a greater degree than the αVβ3-mediated cytokine production. Interestingly, treatment of cells with U0126 also inhibted the constitutive expression of RANTES observed previously with THP-1 cells.

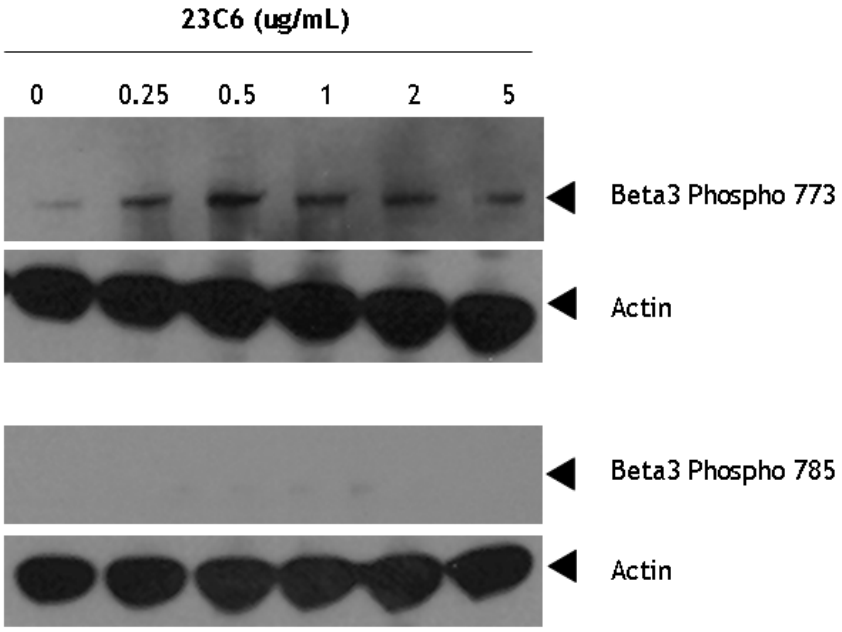

Figure 5.1 Phosphorylation of β3 tail in response to binding of anti-αVβ3 antibody to THP-1 cells

THP-1 cells were incubated with increasing concentrations of 23C6 (anti-αVβ3) antibody for 30mins. Lysates prepared were resolved by SDS-PAGE and probed for the presence of specific phosphorylation of the β3 integrin using antibodies to residues phosphotyrosine 773 and phosphotyrosine 785. Actin was used as a loading control. Data are representative of at least 3 separate experiments.

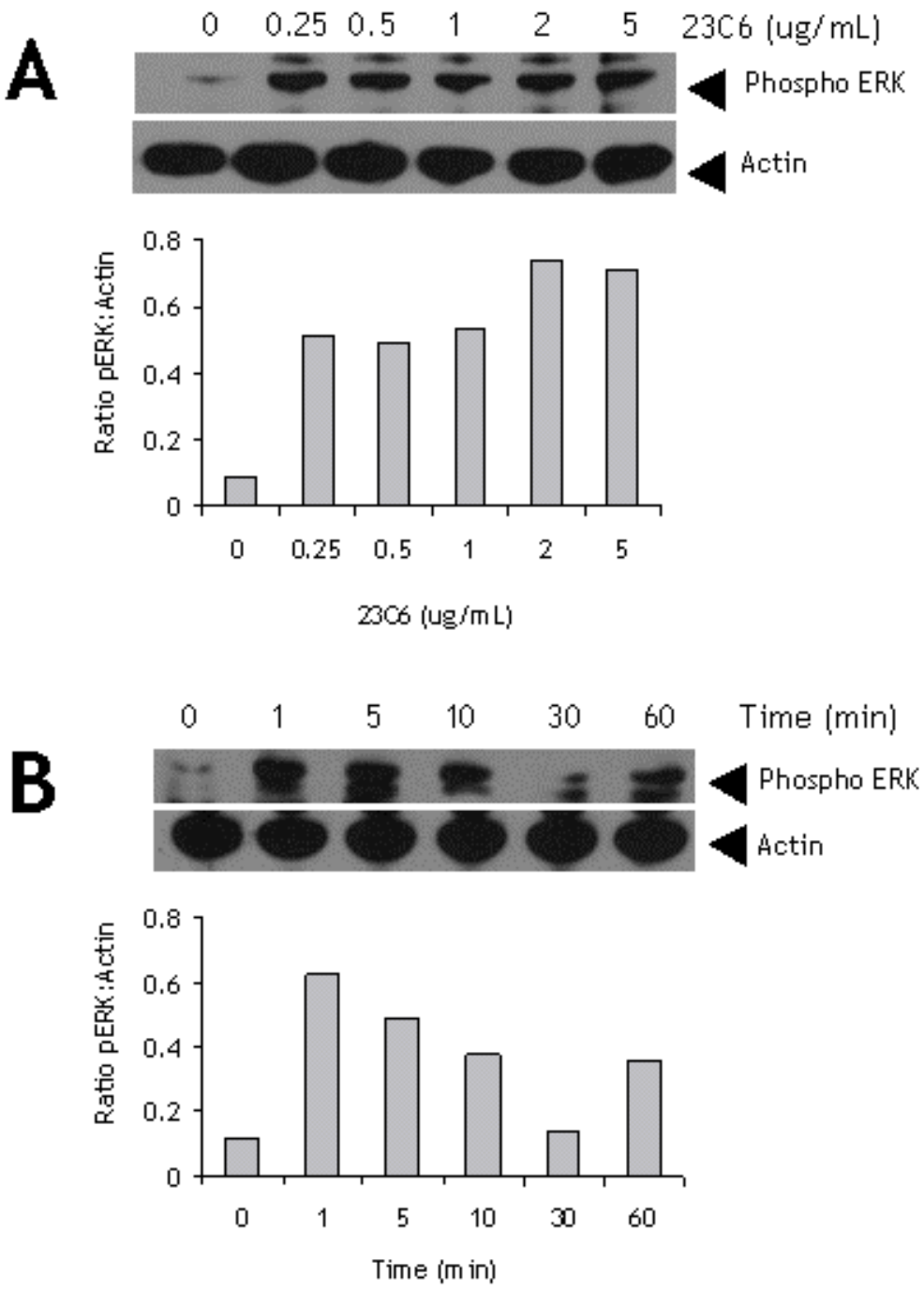

Figure 5.2 Integrin binding induces ERK phosphorylation

(A) THP-1 cells in OptiMEM were stimulated with increasing concentrations of 23C6 (anti-αVβ3 antibody) for 30mins. (B) THP-1 cells in OptiMEM were incubated with 1µg/mL of 23C6 (anti-αVβ3 antibody) and samples taken at specific time points. Cell lysates were analysed for expression of phosphorylated ERK and actin (loading control) by SDS-PAGE and Western blotting. Signal intensity was quantified by densitometry and represented as a ratio of pERK:Actin to standardise for loading inaccuracies. Data are representative of at least 3 separate experiments.

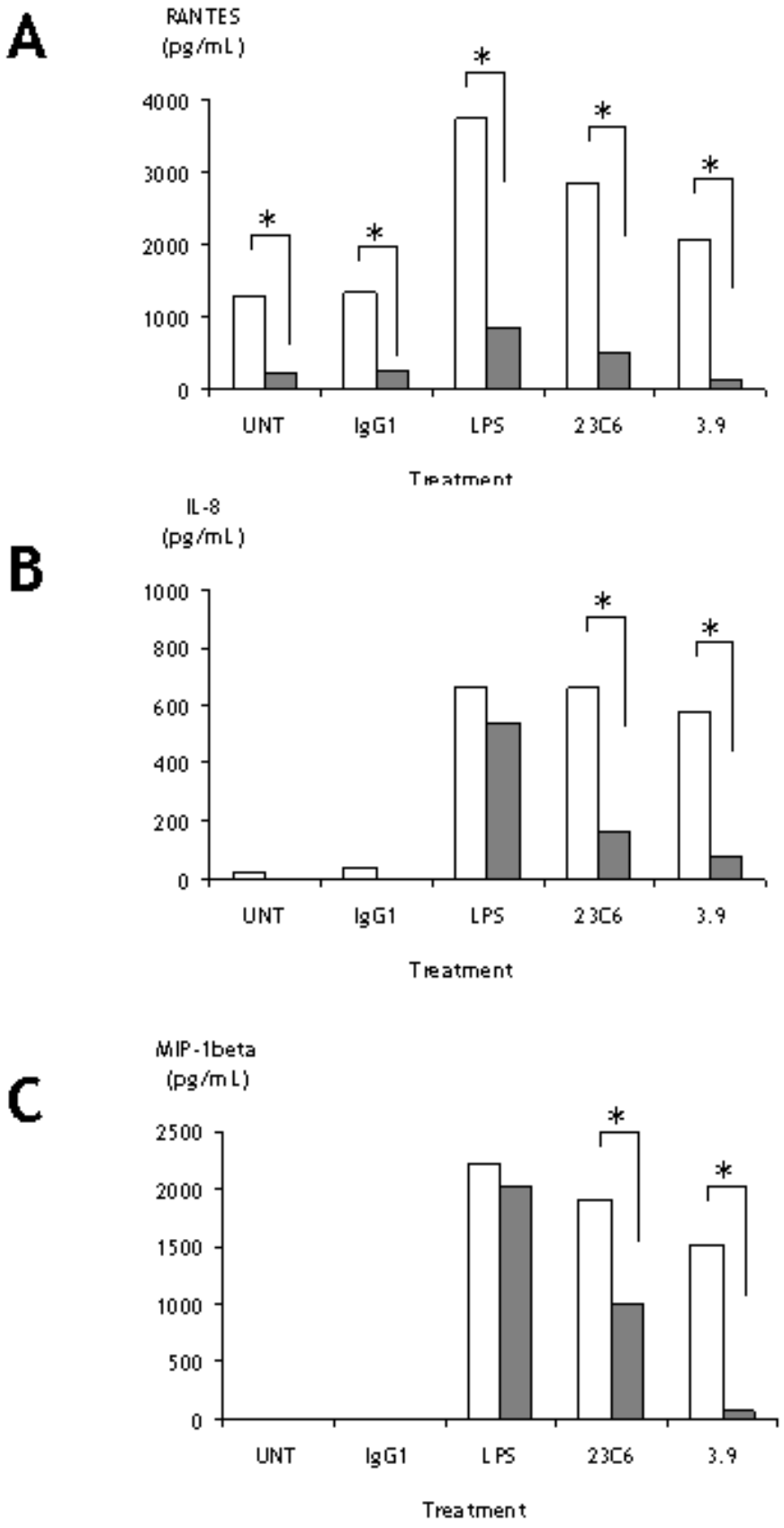

Figure 5.3 Inhibition of MEK blocks integrin-mediated cytokine production
Cytokine production by THP-1 cells was determined in the presence (grey bars) and absence (white bars) of the MEK inhibitor U0126 (10 μM). Cytokines released into the supernatant were detected by ELISA. Unt:untreated; IgG1:isotype control; LPS:positive control; 23C6:anti-αVβ3 antibody; 3.9:anti-αXβ2 antibody. Statisitical analysis was performed using Student's *t*-test*p<0.05. Data are representative of at least 3 separate experiments. The response to IgG1 is included as a representative example. All antibody isotypes were tested (IgG1, IgG2a, IgG2b and IgG3) and gave responses equivalent to IgG1.

5.2.2 Analysis of the effects of cytokines produced by integrin ligation upon migration of THP-1 cells

RANTES, IL-8 and MIP-1β are all involved in migratory responses of leukocytes *in vivo* and *in vitro* [12, 230-234]. We therefore analysed the chemotactic ability of the supernatant containing chemokines produced by THP-1 cells in response to integrin binding.

THP-1 cells were treated with different agents overnight and cleared supernatants collected. These supernatants were subsequently used as the chemotactic stimulus in transwell migration assays using unstimulated THP-1 cells. The concentrations of IL-8, RANTES, VEGF and MIP-1ß in the supernatants were quantified prior to use in the transwell assays. Consistent levels of cytokines were detected in all supernatants used in the analysis (*data not shown*). The transwell migration assays are conducted in multiwell plates that contain an upper and lower chamber separated by a polycarbonate membrane. Supernatants from THP-1 cells treated with stimulating agents (LPS, 23C6 or Clone3.9) were cleared by centrifugation and filtration and the levels of RANTES, IL-8 and MIP-1β quantified by ELISA. Untreated THP-1 cells in OptiMEM were placed in the upper chamber of the transwell plate and cleared supernatants in the lower chamber. The plate was incubated for 3 hours at 37^0C and cells that had migrated from the upper chamber across the membrane into the lower chamber were collected and quantified by flow cytometry.

The migration of unstimulated THP-1 cells across the transwell membrane was tested in response to OptiMEM or supernatant from stimulated THP-1 cells (Figure 5-4). A small number of cells migrated in response to OptiMEM. This can be considered due to random migration. There was a statistically significant increase in the number of migratory cells when cleared supernatant from 23C6-stimulated or Clone3.9-stimulated cells was used instead of OptiMEM (Figure 5-4A). There was no statistically significant increase in migration observed with cleared supernatant from LPS-stimulated supernatants over OptiMEM alone. 23C6-stimulated supernatant induced the greatest migration of THP-1 cells.

To determine if the increase in migration was due to the concentration of chemokines in the supernatant, we analysed the migratory response of THP-1 cells to serial dilutions of the cleared supernatant from 23C6-stimulated THP-1 cells. Cleared supernatant from 23C6-treated THP-1 cells was diluted (1 in 2, 1 in 5 and 1 in 10) with fresh OptiMEM and used in transwell migratory assays. Figure 5-4B shows that THP-1 cells migrated in response to undiluted supernatant from 23C6-treated cells (dilution factor=1). The dilution of the cleared supernatant in the transwell assay led to a statistically significant, dose-dependent decrease in migration of THP-1 cells. The greater the dilution of the supernatant, the fewer cells migrated across the membrane, although, even at 10-fold dilution, an increase in migration over the background (OptiMEM) was observed.

As migration across the membrane is an active process involving adhesion reactions, we measured the effect of coating the transwell polycarbonate membrane with proteins on the migration of THP- 1 cells to the same stimulus (Figure 5-4C). The transwell plate was incubated with the coating proteins at 37^0C for 1 hour. The chambers were washed with OptiMEM and used in transwell migration assays using cleared supernatant from 23C6-treated cells as the chemotactic stimulus. Bovine serum albumin (BSA) was used to control for the presence of non-specific protein on the membrane. This was compared with the migration of THP-1 cells across polycarbonate membranes coated with foetal calf serum (FCS), vitronectin (VN) or fibrinogen (FBGN). A statistically significant increase in migration was observed for membranes coated with FCS and VN, compared to BSA. The membrane coated with FBGN did not lead to a statistically significant increase in cell migration across the membrane compared with BSA (Figure 5-4C).

We tested the ability of the supernatants to influence the migration of other cells in the immune system. We compared the migration of THP-1 cells with the T cell line, Jurkat, and the B cell line, IB4. Figure 5-5 shows that cleared supernatant from THP-1 cells treated with 23C6 could positively influence the migration of Jurkat and IB4 cell lines in addition to THP-1 cells (Figure 5-5A). Although the greatest number of migratory cells was observed with THP-1 cells compared to Jurkat or IB4 cells, the fold stimulation over the number of randomly migrating cells was similar for all the cell lines (Figure 5-5B).

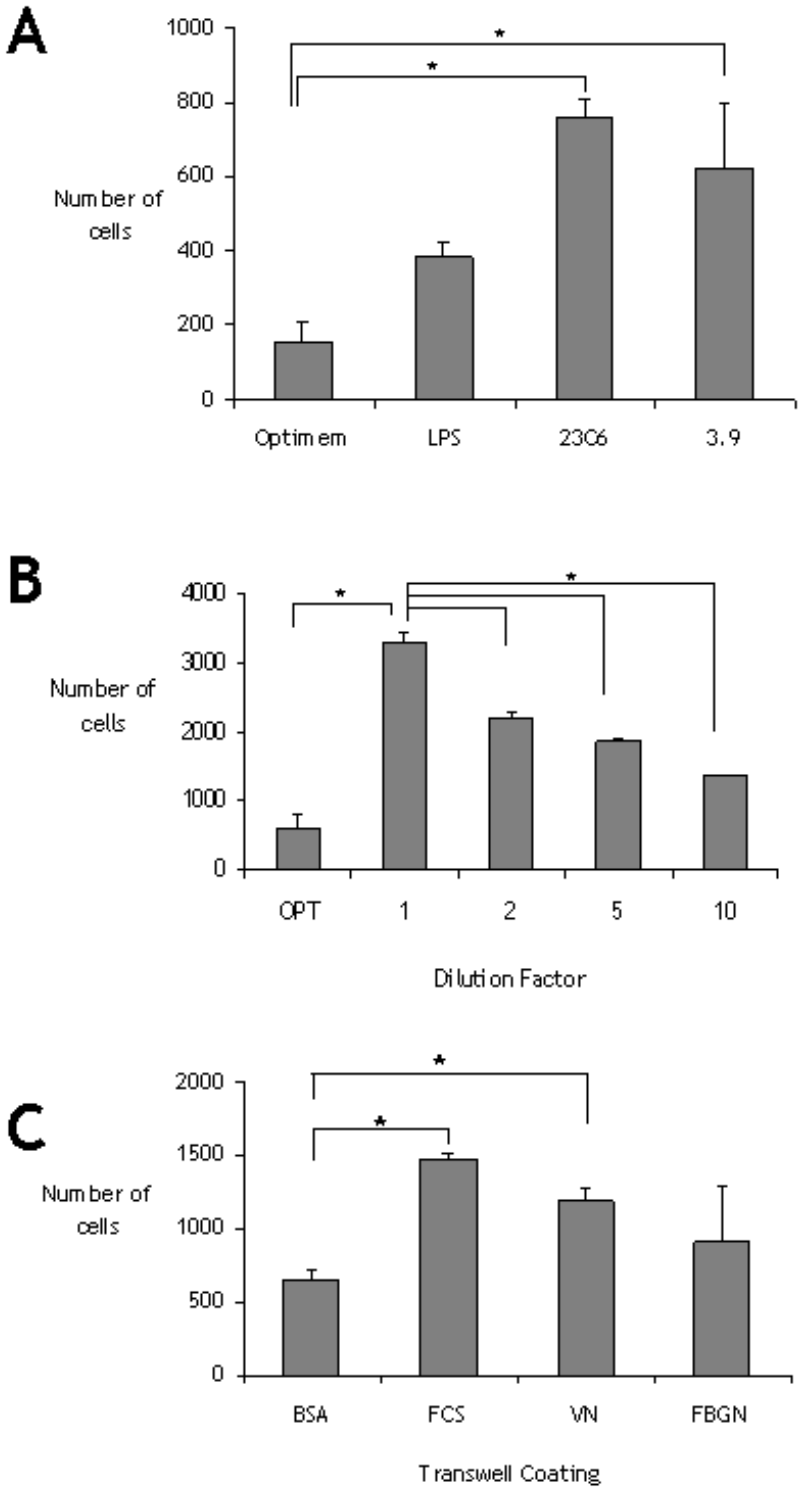

Figure 5.4 Migration of THP-1 cells in transwell assays

(A) Migration of cells towards Optimem (OPT) or cleared supernatants from LPS, 23C6 (anti-αVβ3) or 3.9 (anti-αXβ2) treated cells. (B) Effect of dilution of 23C6 (anti-αVβ3) supernatant on cell migration. (C) Effect of coating of transwell polycarbonate membrane with proteins on cell migration. Wells were coated with bovine serum albumin (BSA), foetal calf serum (FCS), vitronectin (VN) or fibrinogen (FBGN) for at least 1 hour at 37^0C prior to migration assays. Cells ($1x10^{-5}$) were placed in the upper transwell chamber and cleared supernatant from treated THP-1 cultures was placed in the lower chamber of transwell plates. The plates were incubated at 37^0C, in 5% CO_2 for 3 hours, whereupon cells that had migrated across the membrane into the lower chamber were collected by centrifugation, washed and resuspended in equivalent volumes of PBS/formalin. Cell counts in duplicate were determined by flow cytometry. Data represent mean of at least 3 independent experiments. Statistical analysis was performed using Students *t*-test, *$p<0.05$. The error bars indicate standard deviations (SD).

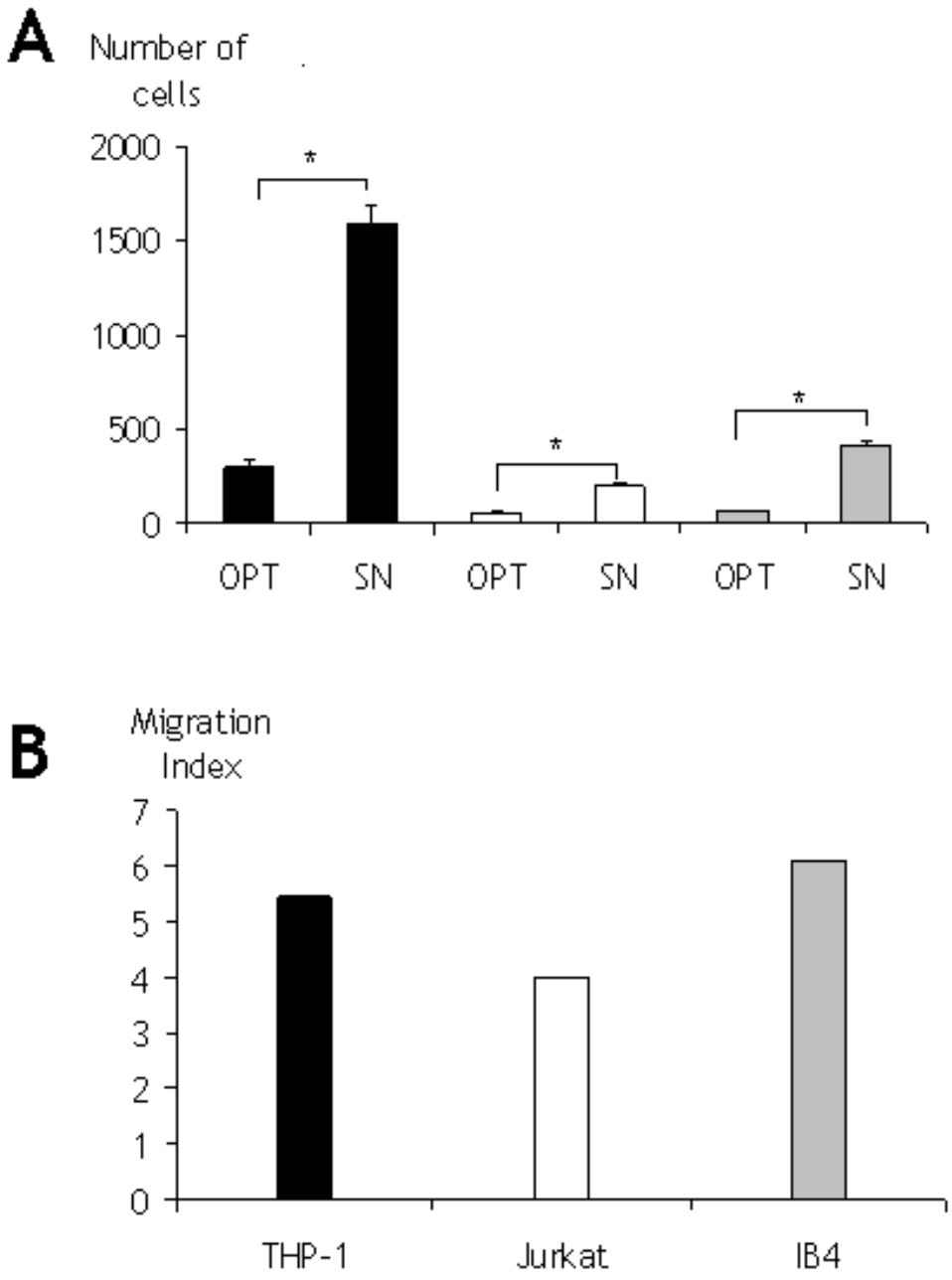

Figure 5.5 Comparison of migration of different cell types in transwell assay
(A) Migration of THP-1 (black bars), Jurkat (white bars) and IB4 (grey bars) cell lines to untreated Optimem medium (OPT) or cleared supernatant (SN) from 23C6 (anti-αVβ3) treated THP-1 cultures. (B) The migration index, representing fold-stimulation of migration in response to 23C6 (anti-αVβ3) supernatant relative to migration in response to Optimem. Migration of cells was measured using transwell plate assays. Cells that had migrated across the membrane into the lower chamber were collected by centrifugation, washed and resuspended in equivalent volumes of PBS/formalin. Cell counts in duplicate were determined by flow cytometry. Data represent mean of at least 3 separate experiments. Statistical analysis was performed using Students *t*-test, *$p<0.05$. The error bars indicate standard deviations (SD).

5.2.3 αVβ3-mediated monocyte differentiation/activation

Monocytic cells are the precursors for a number of essential cells in the body. Monocytes develop into cells such as macrophages, dendritic cells and osteoclasts when treated with different stimuli. CD23 has been shown to mediate monocyte activation via an interaction with ß2 integrins [74, 193].

We had previously analysed the response of THP-1 cells to acute (<24 hours) stimulation with anti-integrin antibodies. Stimulation of THP-1 cells with specific antibodies led to the production of cytokines over this time period. We were therefore interested in investigating the potential activation of THP-1 cells in response to chronic stimulation with these antibodies (>3 days).

Monocyte activation requires multiple signals, one of which is often a priming step induced by cytokines such as M-CSF. We tested the ability of selected antibodies to induce monocyte activation in conjunction with the myeloid growth factor, M-CSF (Figure 5-6). THP-1 cells were incubated in OptiMEM supplemented with 10ng/mL M-CSF and selected antibodies for 5 days and observed for changes in morphology associated with monocyte activation (such as increases in size and adherence). Any changes in cell morphology associated with monocyte differentiation were recorded by phase contrast microscopy (Figure 5-6).

Unstimulated cells cultured in OptiMEM/M-CSF retained a small, rounded morphology, although there was a minor increase in the degree of adherence to the plastic culture dish observed (Figure 5-6A). LPS treatment was used as a positive control for monocyte activation. LPS-stimulated THP-1 cells cultured in OptiMEM/M-CSF displayed an altered morphology characterised by a larger, adherent phenoytpe with a number of spiky cytoplasmic extensions characterisitc of activated macrophages (Figure 5-6B). There was no change in morphology for THP-1 cells treated with IgG1, MEM48 (ß2) or P1F6 (αVß5) in the presence of M-CSF (Figure 5-6C, D and F, respectively). The cells treated in this manner appeared similar to the untreated cells (Figure 5-6A). Treatment of THP-1 cells with the anti-integrin antibodies Clone44 (αMß2) and Clone3.9 (αXß2) induced a degree of change in THP-1 morphology that was similar but less extreme than that observed for the LPS-treated THP-1 cells (Figure 5-6 G and H,

respectively). By contrast, 23C6 induced a significant change in the morphology of THP-1 cells. These changes were more pronounced than those observed for LPS-treated THP-1 cells. The THP-1 cells became adherent and increased significantly in size, with a large number of spiky cytoplasmic extensions. In certain cases, 23C6/M-CSF-treated cells were observed to have multiple nuclei by Giemsa staining. Given this pronounced phenotype, we elected to analyse further the 23C6-mediated activation of THP-1 cells.

We investigated whether 23C6 could mediate this activation in the absence of the M-CSF growth factor. THP-1 cells in OptiMEM were incubated with 23C6 alone or in conjunction with the cytokine M-CSF for 3-7 days and observed for any changes in morphology (Figure 5-7). Stimulation of THP-1 cells with anti-$\alpha V\beta 3$ antibody alone led to the distinct changes in morphology. The THP-1 cells, which are usually small, rounded suspension cells (Figure 5-7A) formed clumps in solution and a number of cells became adherent and enlarged, with significant spiky processes. Treatment with 23C6 alone was sufficient to induce this change in morphology of THP-1 cells (Figure 5-7C), although the number of cells showing the differentiated morphology and the extent of the differentiation was enhanced by the presence of M-CSF (Figure 5-7D). Equivalent concentrations of M-CSF alone caused changes in morphology of the cells associated with maturation of monocytic cells to a more macrophage-like phenotype. Cells became slightly larger and adherent, but lacked the large number of spiky protuberances observed with the 23C6-treated cells. The 23C6-treated cells (with and without M-CSF) were significantly larger, more adherent and had a greater number of spiky extensions compared to those treated with M-CSF alone. The cytoplasm appeared to be highly granular or vesicular in nature (Figure 5-7).

We investigated the effect of 23C6 and M-CSF on the morphology of primary human monocytes derived from peripheral blood ($CD14^+$PBMC) or bone marrow (BMDM). Figure 5-8 shows the differentiation of BMDM in response to M-CSF (A and B), 23C6 and M-CSF (C and D) and LPS and M-CSF (E and F). Treatment of BMDM with M-CSF led to a change in morphology associated with a more macrophage-like phenotype, with cells being adherent, rounded and flattened in appearance. Treatment of BMDM with 23C6 in conjunction with M-CSF led to a similar adherent phenotype, together with the development of numerous spiky processes. A similar change in morphology was observed with BMDM treated with

LPS and M-CSF, although in this case, the LPS treated cells had fewer spiky processes than the 23C6-treated cells.

Figure 5-9 shows the differentiation of $CD14^+$PBMC in OptiMEM alone (Figure 5-9A) or supplemented with M-CSF (Figure 5-9B), 23C6 (Figure 5-9C) or 23C6 and M-CSF (Figure 5-9D). The difference in morphology is less obvious, as $CD14^+$PBMC are adherent even when unstimulated. However, closer observation of cultures suggested a change in morphology when $CD14^+$PBMC were treated with 23C6, either in the presence or absence of M-CSF. Treatment with 23C6 in the presence or absence of M-CSF induced a change in morphology, where the cells became enlarged, with a stellate morphology and a number of projections. A number of cells appeared to have multiple nuclei. Cells treated with M-CSF alone generally had an enlongated morphology.

Monocytic cells are known to differentiate into a number of different cell types, including but not limited to macrophages, dendritic cells and osteoclasts. The morphological changes observed in the THP-1 cells upon treatment with 23C6 and M-CSF were potentially consistent with the differentiation of the monocytic cells into one of these cell types. Each of these cell types has a characteristic set of surface markers and cytokine outputs that are defined by their nature.

We first investigated whether the THP-1 cells were acquiring an osteoclast-like phenotype. Osteoclasts are large, adherent, multinuclear cells derived from macrophages. The αVβ3 integrin and the cytokine M-CSF are associated with osteoclast development *in vivo* and *in vitro*. Therefore, given the morphology of the 23C6/M-CSF-treated cells (large, adherent, multinucleated), and the stimulus used to induce differentiation (anti-αVβ3 antibody and M-CSF), we hypothesised that the THP-1 cells may developing into osteoclasts. Osteoclasts can be identified by staining for the osteoclast marker, tartrate-resistant acid phosphatase (TRACP), which should give a pink colour due to the activity of the TRACP enzyme. Figure 5-10 shows the TRACP staining for 23C6/M-CSF-treated cells. The cells stained yellow with the TRACP assay. No pink colour was observed, even with the large, multinucleated cells (Figure 5-10B). This suggested that the stimulated THP-1 cells did not acquire an osteoclast-like nature, as defined by TRACP staining.

In light of the above result, we proposed that the change in morphology of the THP-1 cells was an indication of macrophage activation. Macrophages are a naturally heterogeneous population and there are multiple mechanisms which lead to macrophage activation [7, 8, 235]. Each of these mechanisms defines a specific type of macrophage, each of which has a characteristic expression of surface markers and cytokine profiles (summarised in Table 5-1). To investigate whether 23C6/M-CSF treatment of THP-1 cells was initiating a specific programme of activation, we analysed the changes in surface marker expression and monitored the cytokine profile of the differentiated cells during a 5-day stimulation.

After stimulation with M-CSF and 23C6 for 5 days, the THP-1 cells were assessed for the presence of specific cell surface markers by flow cytometry (Figure 5-11). These markers have been correlated with a specific type of macrophage activation mechanism (Table 5-1) [7]. The expression levels of selected markers on untreated THP-1 cells cultured in OptiMEM for 5 days (Figure 5-11A) was compared to the expression of the same markers after treatment of cells with 23C6 and M-CSF for 5 days (Figure 5-11B). A general increase in the background staining was observed for 23C6/M-CSF-treated cells compared to untreated cells. There was no significant change in the expression levels of CD86, HLA-DR, CD23 or CD14 between untreated THP-1 cells and 23C6/M-CSF stimulated THP-1 cells. There was also no change in the expression level of CD25, IFNγ-R1, TLR-2, CD64 or CD47. 23C6/M-CSF-stimulated THP-1 cells expressed lower levels of the $F_c\gamma$ receptors CD16 and CD32, but slightly upregulated expression of the chemokine receptor CCR5. Figure 5-12 shows the expression of integrins on unstimulated and 23C6/M-CSF-stimulated THP-1 cells. THP-1 cells treated with 23C6/M-CSF expressed lower levels of the αV subunit and the individual αVβ3 and αVβ5 heterodimers. The expression of the β1 integrin, β2 integrin, αMβ2 and αXβ2 were roughly equivalent between the stimulated and unstimulated THP-1 cells

Figure 5-13 shows the production of RANTES, MIP-1β, IL-8, TNF-α, IFN-γ, IL-12p40, IL-10, IL-4 and VEGF by the 23C6/M-CSF-treated THP-1 cultures over the 5 day stimulation period. THP-1 cells in OptiMEM were treated for 5 days with 23C6 and M-CSF and supernatant samples were analysed for the presence of cytokines by ELISA at specific time points.The cytokines IL-12p40 and IL-4 were not detected in the cell supernatant at any time during the stimulation. The

stimulated THP-1 cells produced high levels of RANTES, MIP-1ß, IL-8, TNF-α and VEGF during differentiation. For all these cytokines, there was a sustained proportional increase in cytokine production with the length of stimulation. The stimulated cultures transiently released IFN-γ and IL-10. A peak in IFN-γ and IL-10 levels was observed after 24 hours, but levels were reduced to zero after 48 hours after stimulation and did not increase later in the experiment.

The data from the above analyses are summarised in Table 5-1, along with the corresponding data collected for specific types of macrophage activation. Table 5-1 indicates the details determined for different mechanisms of macrophage activation, classical (M1) and alternative (M2 which can be sub-divided in M2a, M2b and M2c). The cytokine profile and surface marker expression of 23C6/M-CSF-treated THP-1 cells did not correlate significantly with any of the specific macrophage activation mechanisms. However, the upregulation of other markers, such as CCR5, and the production of cytokines, suggests that the stimulated THP-1 cells may still be classified as activated macrophages.

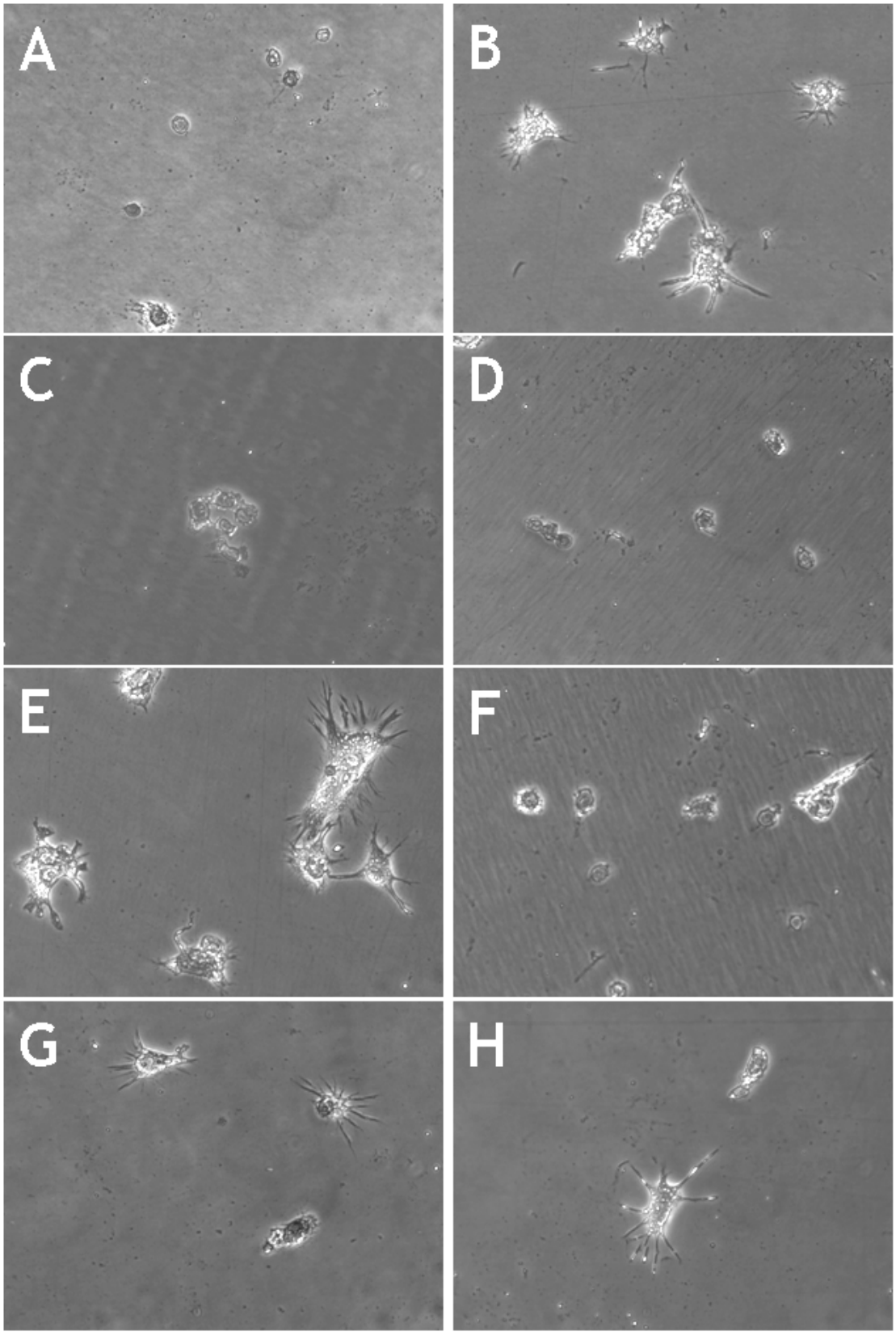

Figure 5.6 Screen of antibodies for monocyte activation
Antibodies known to induce cytokine production were screened for their ability to induce monocyte activation in the presence of M-CSF. Monocyte activation was measured by morphological changes, including increased size and adherence. THP-1 cells were treated with 10ng/mL M-CSF along with A: untreated, B: LPS, C: IgG1, D: MEM48, E: 23C6, F: P1F6, G: Clone44, H: Clone3.9. Data are representative of at least 3 separate experiments. The response to IgG1 is included as a representative example. All antibody isotypes were tested (IgG1, IgG2a, IgG2b and IgG3) and gave responses equivalent to IgG1.

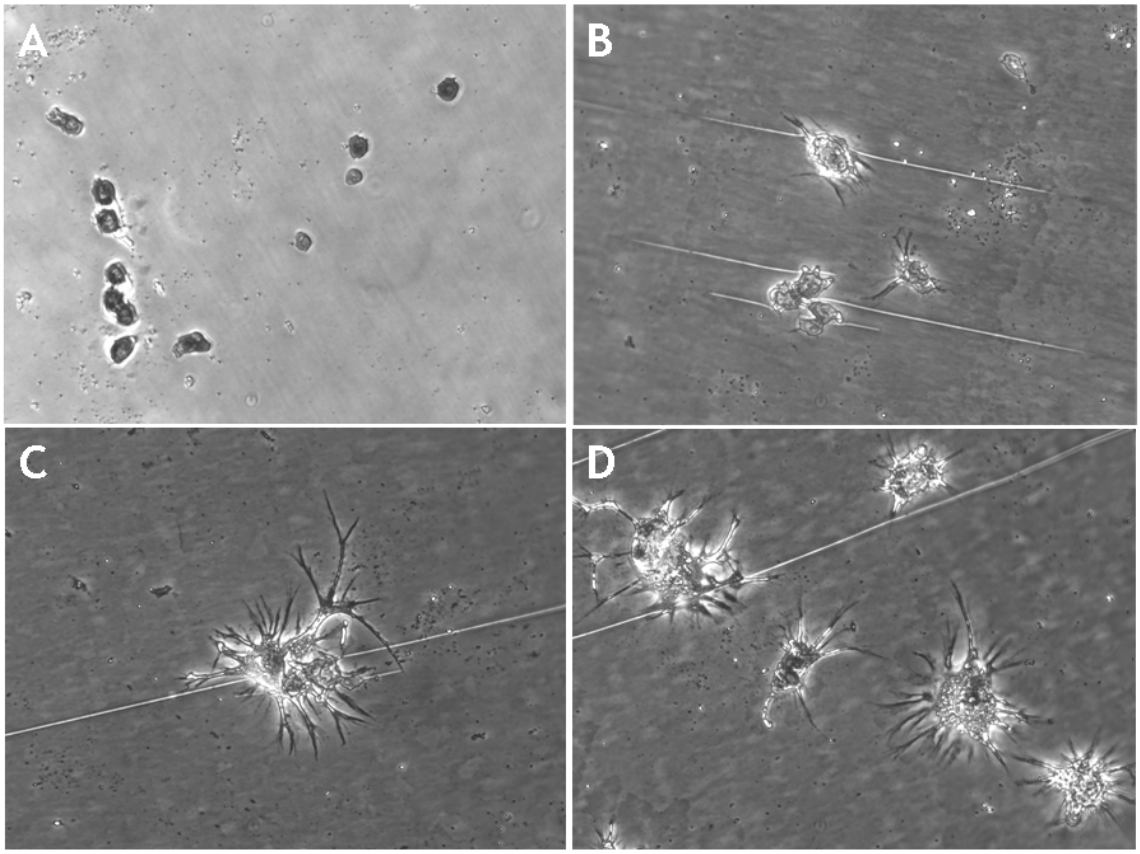

Figure 5.7 Integrin-mediated activation of THP-1 cells
THP-1 cells were grown for 5 days in Optimem medium (A) without supplementation, (B) with 10ng/mL M-CSF, (C) with 1µg/mL 23C6 (anti-αVβ3) antibody or (D) 10ng/mL M-CSF and 1µg/mL 23C6 (anti-αVβ3) antibody. Phase contrast photomicrographs (magnification x320) of cell morphology were taken using the Zeiss Axiovert microscope. Data are representative of at least 3 independent experiments.

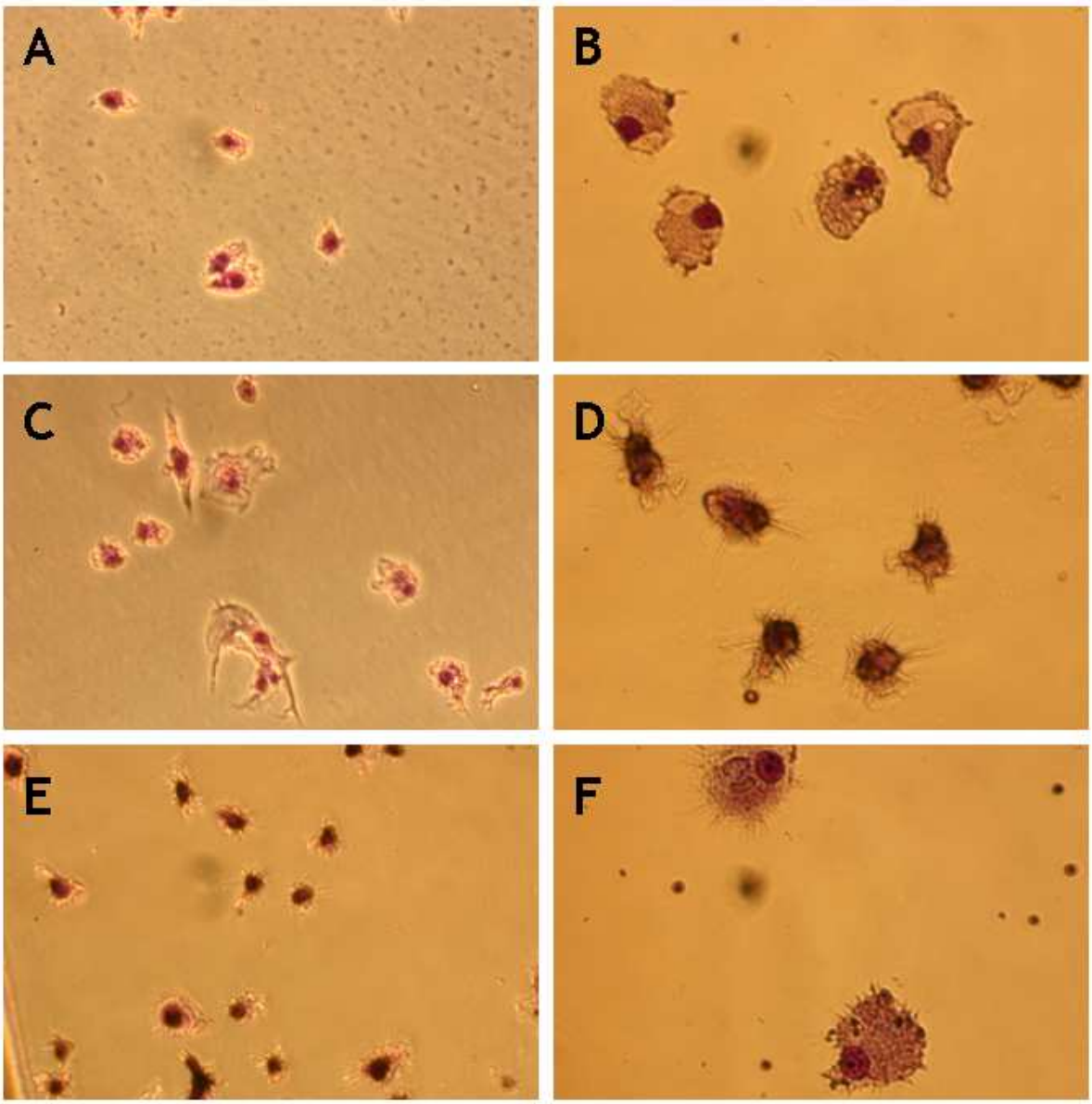

Figure 5.8 Differentiation of bone marrow derived monocytes in response to treatment with 23C6 and M-CSF

Bone marrow monocytes were stimulated with 5ng/mL M-CSF (A and B), 5ng/mL M-CSF and 23C6 (C and D) and LPS (E and F). Pictures A, C and E are 200x magnification and B, D and F are 320x magnification. Cells were fixed and stained with Giemsa stain and images captured using a Canon EOS300 digital camera attached to a Zeiss Axiovert S100 microscope.

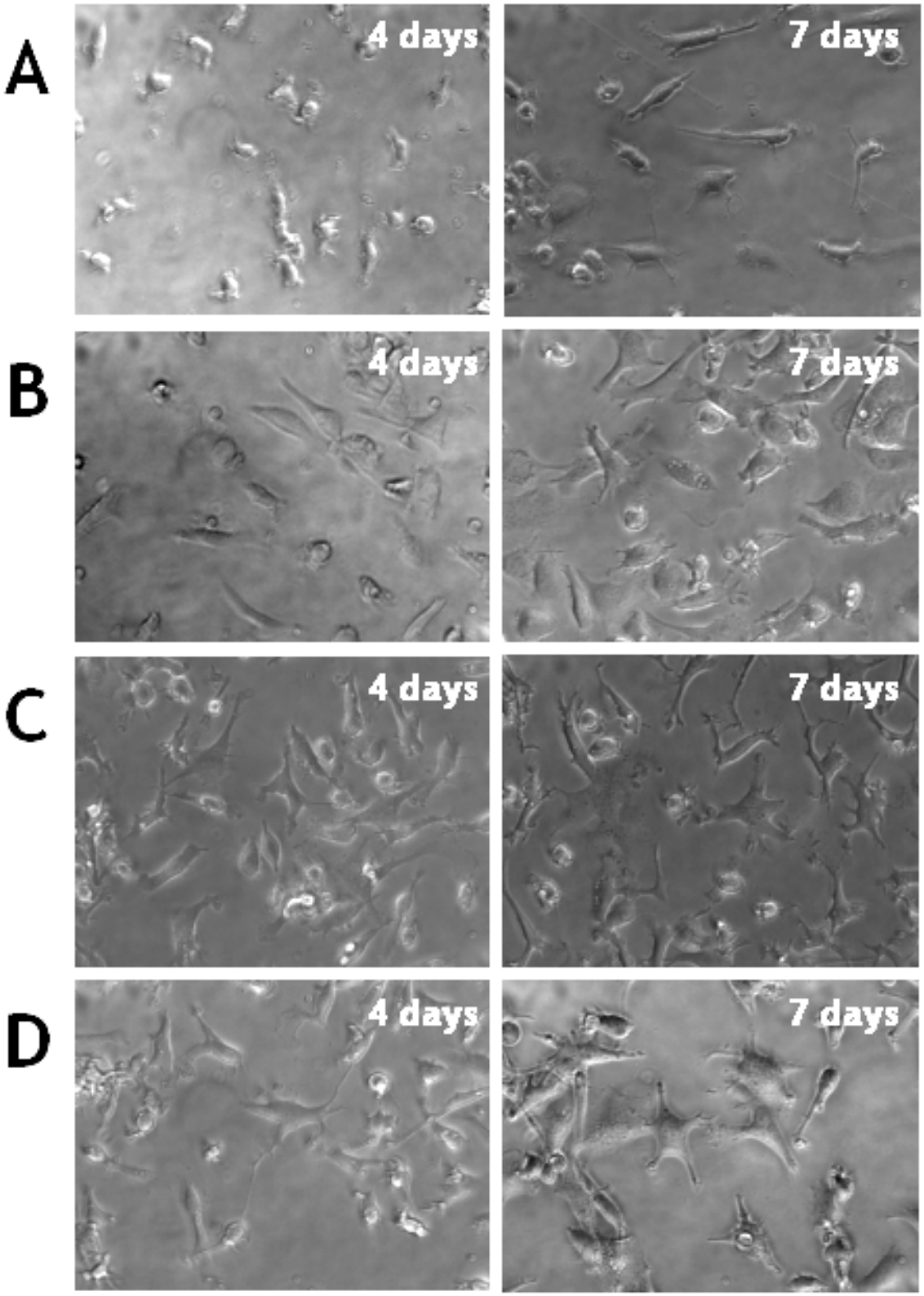

Figure 5.9 Differentiation of CD14+ blood monocytes in response to treatment with 23C6 and M-CSF

CD14+ peripheral blood monocytes were cultured in OptiMEM with 1% FCS (A) or OptiMEM with 1% FCS supplemented with 10ng/mL M-CSF (B) or 23C6 1µg/mL (C) or a combination of 10ng/mL M-CSF and 1µg/mL 23C6 (D). Phase contrast photomicrographs (magnification x320) of cell morphology were taken using the Zeiss Axiovert microscope.

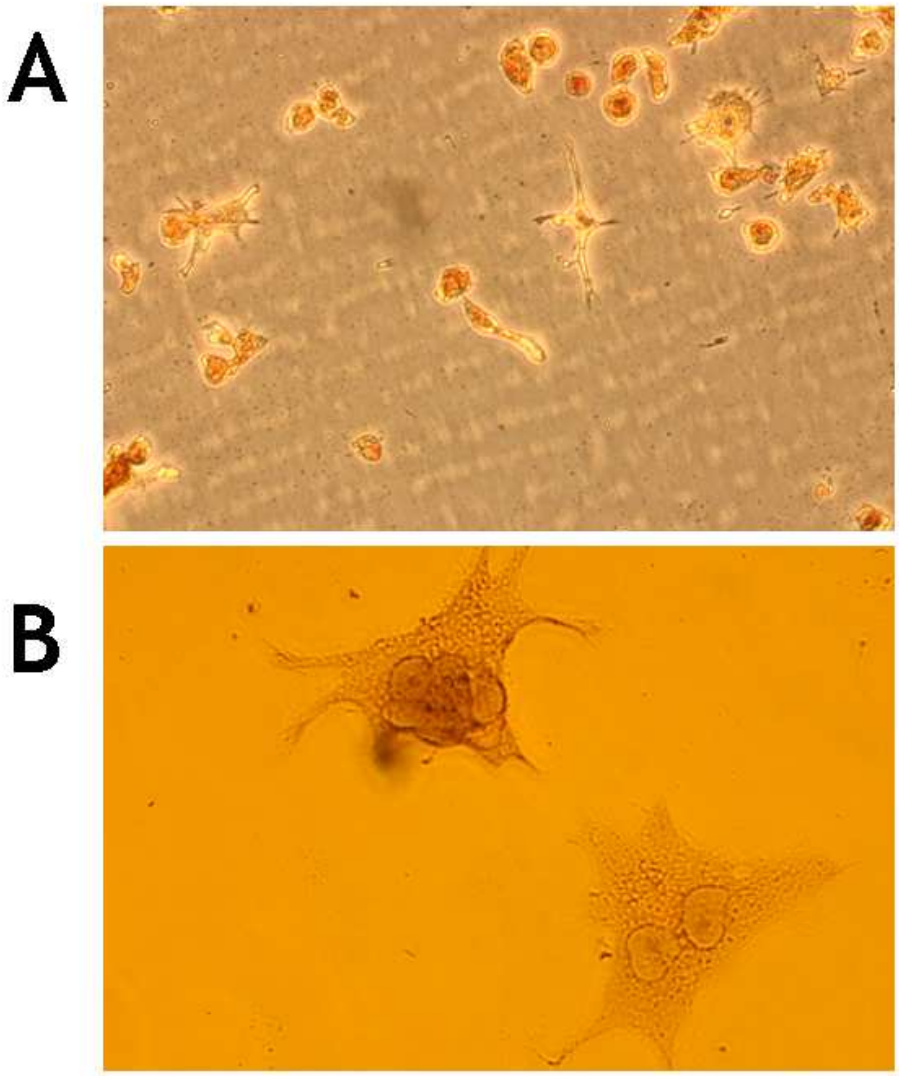

Figure 5.10 Staining of 23C6/M-CSF treated THP-1 cells for the osteoclast marker TRACP

THP-1 cells were treated with 23C6 and M-CSF for 5 days before being fixed and stained for the osteoclast marker, TRACP. Images at different magnifications (A is x200 and B is x320) were captured using a Canon EOS300 digital camera attached to a Zeiss Axiovert S100 microscope.

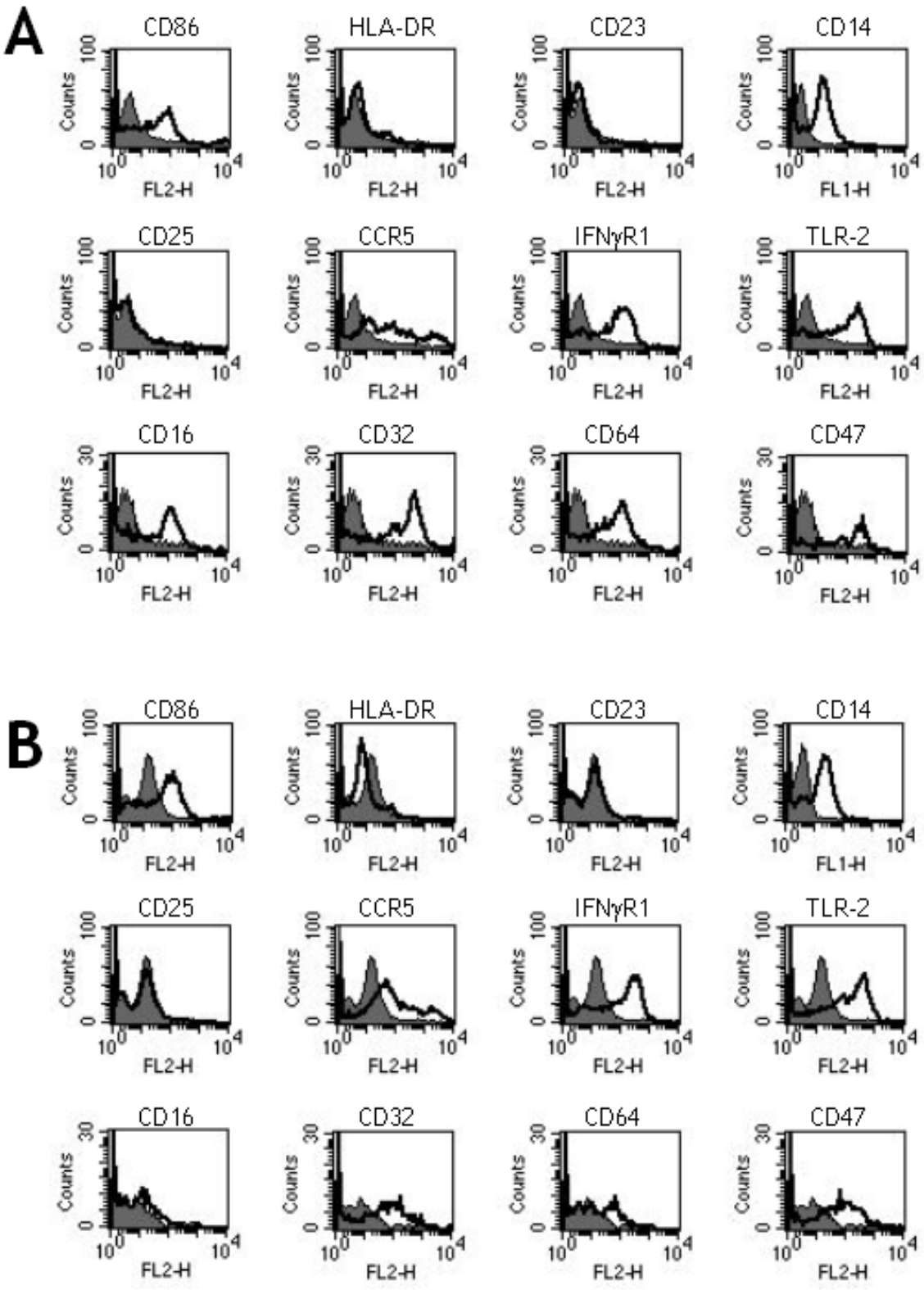

Figure 5.11 Analysis of THP-1 cells for surface markers of macrophage activation

THP-1 cells were grown in OptiMEM (A) or OptiMEM supplemented with 23C6 and M-CSF for 5 days (B) and then analysed for the expression of markers characteristic of macrophage activation by flow cytometry. Isotype control staining is shown as grey shading and antibody staining as a black line. The antigen targeted is indicated above the individual plots. Data are representative of at least 3 separate experiments.

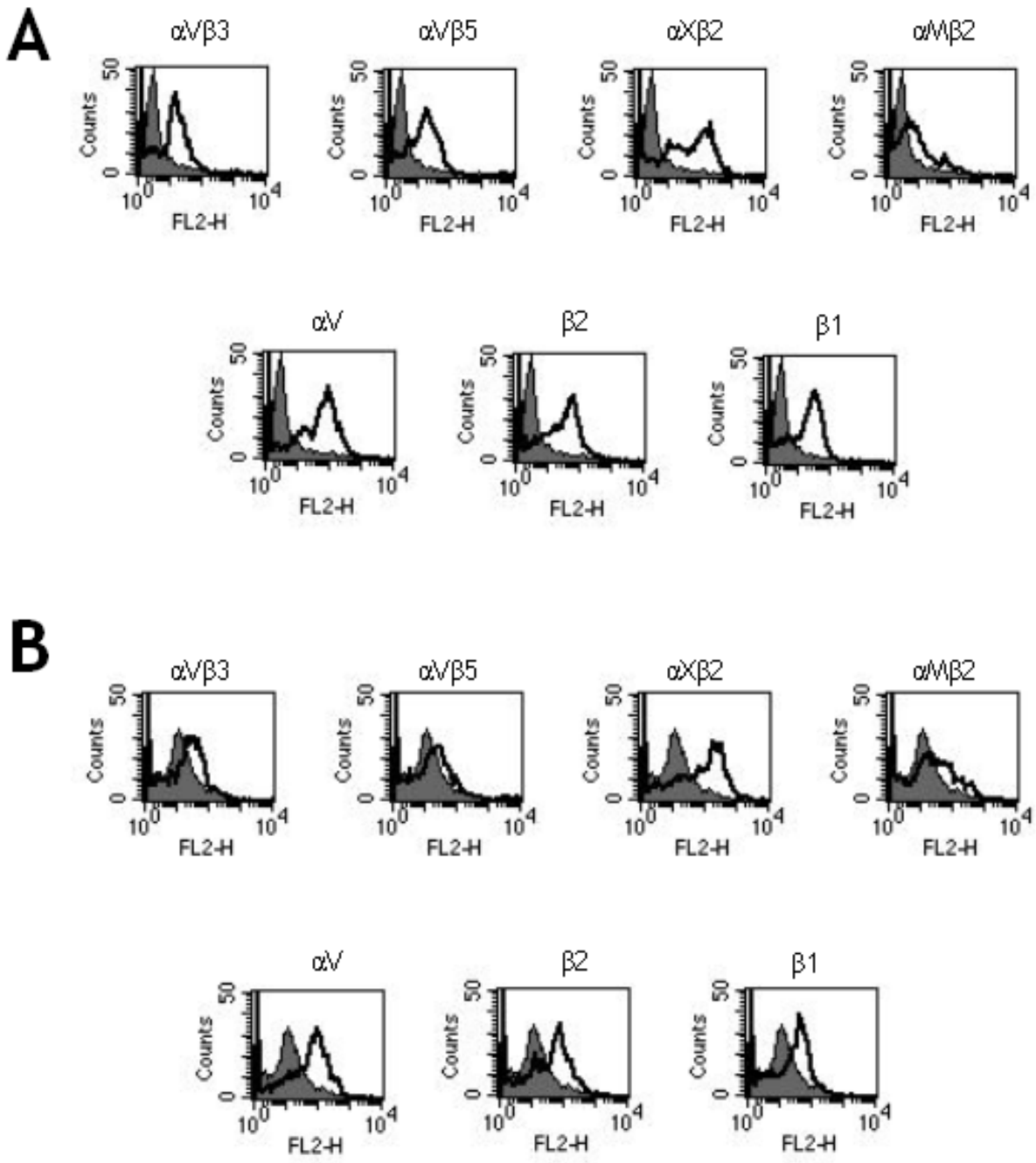

Figure 5.12 Analysis of expression of integrins on THP-1 cells before and after treatment with 23C6 and M-CSF

THP-1 cells were grown in OptiMEM (A) or OptiMEM supplemented with 23C6 and M-CSF for 5 days and then analysed for the expression of integrins by flow cytometry. Isotype control staining is shown as grey shading and antibody staining as a black line. The antigen targeted is indicated above the individual plots. Data are representative of at least 3 separate experiments.

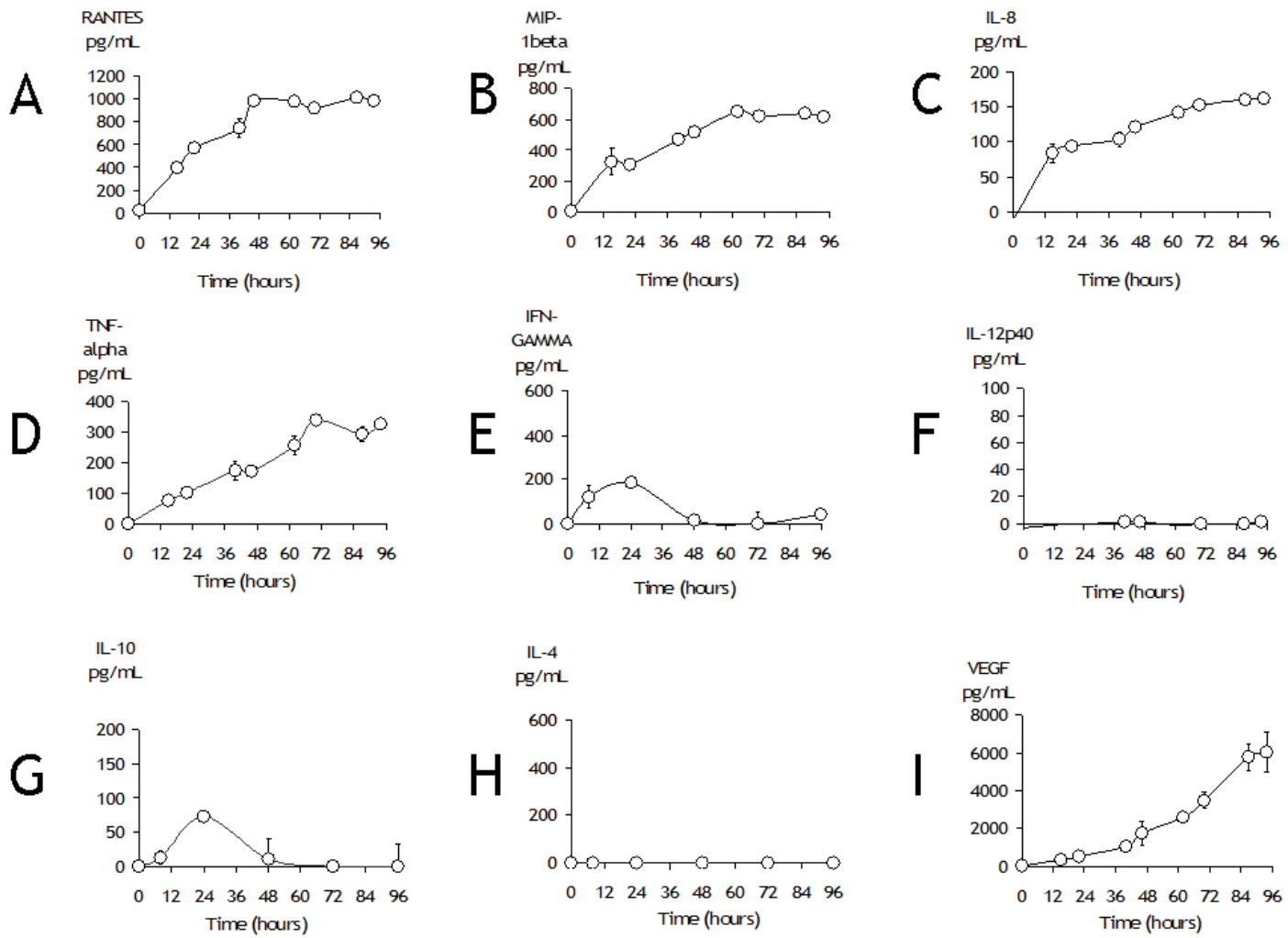

Figure 5.13 Cytokine production during THP-1 differentiation/activation by M-CSF and 23C6

THP-1 cells were stimulated with M-CSF and 23C6 for 5 days. Supernatant samples were collected at intervals and assessed for the production of cytokines by ELISA. Data are representative of at least three independent experiments.

Table 5-1 Characteristics of activated macrophages (adapted from[6, 7, 16, 236])

DETAIL	CLASSICAL (M1)	ALTERNATE (M2)			**INTEGRIN MEDIATED**
		M2a	M2b	M2c	
Activating signals	IFN-γ TNF-α	IL-4 glucocorticoids	Immune complexes/ TLR/IL-1R ligands	IL-10	**αVβ3 binding** **M-CSF**
Cytokines secreted	TNF-α IL-12 IL-1 IL-6	IL-1RA IL-10	TNF-α IL-10 IL-6	TGF-β IL-10	**TNF-α** **Transient IL10** **Transient IFN-γ**
Growth factors		VEGF***	VEGF***	VEGF***	**VEGF**
Markers	UP: MHC-II CD86 DOWN: Mannose receptor	UP: MHC-II Mannose receptor Scavenger receptor CD23 DOWN: CD14 CD163 MS-1	UP: MHC-II CD86 DOWN: Mannose receptor	UP: SLAM Mannose receptor DOWN: CD14 CD163 MS-1	**UP** **CCR5** **UNCHANGED:** **CD86** **CD14** **CD23 (not expressed)** **HLA-DR** **NOT ANALYSED:** **Mannose receptor** **Scavenger receptor** **CD163** **MS-1**
Killer molecules	NO, O_2^-	NONE	None/*NO, O_2^-	NONE	**NONE**
Chemokines	MCP-1 MIP-1 IP-10	AMAC	**ND	AMAC	**IL-8** **RANTES** **MIP-1Β**

* High levels of IL-10 block radicals
**ND - not determined
***in the context of tumour associated macrophages (TAM)[236-238]

5.2.4 Role of the receptors αVβ3, c-FMS and TLR-2 during macrophage activation

Toll-like receptors (TLRs) are immunoreceptors that play in important role in the innate immune response, particularly with respect to detection of pathogens. Binding of TLRs on macrophages can lead to their activation, either directly or via TLR-induced cytokine production. These TLRs often associate with other surface receptors, including integrins, to achieve these functions. The LPS signalling complex, for example, is composed of CD14, TLR-4 and the CD18 integrin. We hypothesised that the αVβ3-mediated macrophage activation and cytokine production involved a similar signalling complex that included TLR-2 and the M-CSF receptor c-FMS.

THP-1 cells were shown to be activated by stimulation of the αVβ3 integrin with the 23C6 antibody (Figure 5-1). This activation was enhanced by the presence of the cytokine M-CSF. M-CSF is known to exhibit its effects by binding to its receptor, c-FMS. We had previously shown that THP-1 cells express the αVβ3 integrin and so we examined the cells for the expression of the M-CSF receptor c-FMS. Figure 5-14 shows the western blot and densitometric analysis using actin as a loading control of the expression of c-FMS in THP-1 and U937 whole cell lysates. THP-1 was shown to express the c-FMS receptor, as indicated by a band at ~170 kDa. The U937 cell lysate did not express the c-FMS receptor. U937 cells failed to differentiate under treatment conditions similar to those causing the morphology changes in THP-1 cells. U937 cells did not respond with an altered morphology, but instead the cultures failed to survive for the 3-7 day treatment with 23C6 and M-CSF (*data not shown*).

The stimulatory effect of 23C6 and M-CSF on THP-1 cells was determined to be dose-dependent, with respect to both 23C6 concentration and M-CSF concentration (Figure 5-15). Figure 5-15 shows the dose-dependent differentiation of the THP-1 cells in response to changing concentrations of 23C6 and a constant M-CSF concentration (Ai), and to changing concentrations of M-CSF and a fixed concentration of 23C6 (Bi). Cells were treated with the indicated concentrations of 23C6 and M-CSF and the number of cells exhibiting the altered morphology per microscope field was counted. Three fields were randomly selected and the number of differentiated cells counted in duplicate wells

(Figure 5-15 A and B ii). An increase in either 23C6 concentration at a fixed M-CSF concentration (Figure 5-15A) or M-CSF at a fixed 23C6 concentration (Figure 5-15B) led to an increase in the number of differentiated cells per field and an increase in the degree of change of morphology.

We continued to examine the relationship between 23C6 and M-CSF in the processes of cytokine production and activation of the THP-1 cells. The 23C6 antibody was previously shown to induce high levels of cytokines in THP-1 cells, which could be responsible for the morphological changes and monocyte differentiation phenotype. We observed a dose-dependent enhancement of THP-1 differentiation as measured by changes in cell morphology in response to suboptimal concentrations of 23C6 or M-CSF by M-CSF and 23C6, respectively. We therefore examined the effect of M-CSF on 23C6-mediated cytokine production (Figure 5-16) and ERK phosphorylation (Figures 5-17 and 5-18).

Figure 5-16 shows the enhancement of 23C6-mediated RANTES, IL-8 and MIP-1ß production stimulated by increasing concentrations of M-CSF (Figure 5-16A, B and C respectively). M-CSF alone (white bars) did not induce release of RANTES, IL-8 or MIP-1β by THP-1 cells at any concentration tested. Cytokine production by THP-1 cells treated with a suboptimal level of 23C6 (when M-CSF is absent) was enhanced by the addition of M-CSF (5-25ng/mL), in a dose-dependent manner (black bars). Increasing concentrations of M-CSF led to an increase in the cytokine output for the fixed concentration of 23C6.

The enhancement of cytokine production was associated with an enhancement of 23C6-mediated ERK phosphorylation by the presence of M-CSF. We previously determined that 23C6 induces a signalling pathway that involves ERK phosphorylation in THP-1 cells. Figures 5-17 and 5-18 show data collected to examine the effect of M-CSF on this ERK phosphorylation.

Figure 5-17 shows the western blot (A) and densitometry analysis (B) for the effect of increasing M-CSF concentrations on ERK phosphorylation. THP-1 cells were treated with increasing concentrations of M-CSF with or without 23C6 for 30 min and lysates probed for the phosphorylation of ERK by Western blotting. M-CSF treatment alone led to phosphorylation of ERK at a concentration of 50ng/mL, but not at the lower concentrations (0-20ng/mL). Treatment of THP-1 cells with 23C6 alone at a concentration of 0.5µg/mL induced ERK

phosphorylation. This 23C6-mediated ERK phosphorylation was enhanced by addition of M-CSF, even at the lower concentrations of 10ng/mL and 20ng/mL, where M-CSF alone failed to induce ERK phosphorylation.

We analysed the kinetics of ERK phosphorylation in response to 23C6 and M-CSF treatment (Figure 5-18). THP-1 cells were incubated with M-CSF alone, 23C6 alone or a combination of 23C6 and M-CSF for different time periods. Lysates were probed for phosphorylation of ERK by Western blot using actin as a loading control. Treatment of THP-1 cells with M-CSF alone led to phosphorylation of ERK that was observed after 10 min of treatment and peaked at 60 min after stimulation. Treatment of THP-1 cells with 23C6 led to weak phosphorylation of ERK that was observed after 5 min of treatment and peaked at 60 min after stimulation. Treatment of THP-1 cells with 23C6 and M-CSF led to a stronger phosphorylation of ERK that was observed after 5min of treatment and peaked at 30 min after stimulation.

We next examined the expression of TLR-2 on THP-1 and U937 cell lines. Both THP-1 and U937 expressed high levels of TLR-2 (Figure 5-19). We compared the morphology of the 23C6/M-CSF-treated THP-1 cells with THP-1 cells activated by a TLR-2 ligand, yeast zymosan. Figure 5-20 shows the morphology of untreated THP-1 cells (A and B), compared with THP-1 cells treated with zymosan (C and D) and 23C6/M-CSF treated THP-1 cells (E and F). Untreated THP-1 cells were small, non-adherent and rounded in culture. Zymosan and 23C6/M-CSF treated cells both acquired a similar morphology, large and adherent, with spiky projections. The 23C6/M-CSF treatment appeared to induce larger cells with a greater number of projections than zymosan-treated cells. We assessed the ability of the TLR-2 ligand zymosan to induce cytokine production by THP-1 cells (Figure 5-21). Zymosan-treated cells produced high levels of MIP-1β and IL-8, as observed with 23C6 and 23C6/M-CSF treatment. This suggested that a TLR-2-induced response was consistent with the activation and cytokine profile observed for 23C6 treated THP-1 cells.

We had previously established that the M-CSF receptor was essential for the 23C6-mediated THP-1 activation, as U937 cells which did not express c-FMS did not activate/differentiate in response to 23C6 or 23C6/M-CSF treatment (*data not shown*). We attempted to identify the role of TLR-2 in cytokine production

using a blocking antibody. THP-1 cells were pre-treated with a neutralising antibody against TLR-2 or an RGDS peptide and then stimulated with the 23C6 antibody. Cytokines released into the supernatant were quantified by ELISA (Figure 5-22). The production of MIP-1ß, RANTES, IL-8 and VEGF was not inhibited by the pre-incubation and inclusion of the RGDS peptide. The inclusion of the neutralising TLR-2 antibody, however, led to a statistically significant reduction in the production of all four cytokines. This supported a role for TLR-2 in the 23C6-mediated cytokine production by THP-1 cells.

TLRs are capable of two signalling mechanisms, one dependent on the MyD88 (myeloid differentiation factor 88) molecule and the other independent of this protein. TLR-2-based signalling is dependent on MyD88; no MyD88-independent signalling pathway has been identified for TLR-2. We therefore investigated the effect of blocking MyD88 signalling on cytokine production by THP-1 cells in response to 23C6 binding (Figure 5-23). THP-1 cells were incubated with the MyD88 inhibitory peptide[239] or control peptide for 24 hours or anti-TLR-2 antibody for 1 hour prior to stimulation with 23C6 or the TLR-2 ligand zymosan. Treatment of the THP-1 cells with the control peptide did not inhibit release of IL-8, RANTES or MIP-1ß produced in response to 23C6 or zymosan treatment (Figure 5-23, black bars). Pre-incubation of THP-1 cells with the neutralising TLR-2 antibody led to a statistically significant reduction in RANTES, IL-8 and MIP-1ß concentrations in response to stimulation with either 23C6 or zymosan (Figure 5-23, white bars). Treatment of THP-1 cells with the MyD88 inhibitory peptide caused a statistically significant reduction in the levels of IL-8 and MIP-1ß, but not RANTES, produced in response to zymosan treatment. MyD88 inhibition did not affect the production of IL-8, MIP-1ß or RANTES in response to 23C6 stimulation (Figure 5-23, grey bars).

We extended this analysis to test the effect of the anti-TLR-2 antibody and the MyD88 peptide on the transcription of the cytokine genes. Using IL-8 as a model, we investigated the production of mRNA in response to 23C6-mediated stimulation using semi-quantitative PCR. Total RNA was extracted from THP-1 cells that had been stimulated with 23C6 or zymosan after being incubated with the anti-TLR-2 antibody or the MyD88 inhibitory peptide. The RNA was used in semi-quantitative RT-PCR reactions for the detection of IL-8 transcripts, using GAPDH as an internal standard (Figure 5-24). RNA from untreated THP-1 cells did

not contain any detectable IL-8 transcript. Transcripts for IL-8 were observed in cells treated with the control peptide and the MyD88 inhibitory peptide, and stimulated with 23C6 or zymosan. The signal for the IL-8 transcript was not reduced compared to the control cells treated with zymosan. Pre-treatment of THP-1 cells with the anti-TLR-2 antibody prior to stimulation with 23C6 or zymosan led to a decrease in the expression of the IL-8 transcript relative to the GAPDH signal. These data were consistent with the reduction in cyoktine production by inhibition of TLR-2, but not by inhibition of MyD88, observed in the ELISA analysis (Figure 5-23).

As TLR signalling leads to activation of the NFκB transcription factors, we investigated whether 23C6/M-CSF treatment could lead to activation of this pathway. We performed gel shift assays (EMSAs) to detect the presence of activated transcription factors in nuclear extracts from THP-1 cells treated with 23C6. Nuclear extracts were prepared from untreated THP-1 cells, THP-1 cells treated with 23C6, and THP-1 cells treated with 23C6 and anti-TLR-2 antibody. These extracts were assessed for their ability to bind the radioactively labelled NFκB consensus oligonucleotide in electrophoretic mobility shift assays/EMSAs (Figure 5-25A). Untreated THP-1 nuclear extract did not bind the NFκB oligo. Nuclear extracts from THP-1 cells treated with 23C6 or 23C6 and M-CSF antibody bound the radioactively-labelled NFκB consensus oligonucleotide, as indicated by the presence of a low mobility band on the autoradiogram (Figure 5-25A, arrow). This was deemed to be a specific interaction, as it could be prevented by competition with a cold/unlablled NFκB consensus oligonucleotide. We were unable to identify the member of the NFκB family by supershift analysis, but we attempted to analyse the translocation of p65 to the nucleus using immunofluorescence staining and confocal microscopy (Figure 5-25B). There was no difference observed for the expression levels or subcellular localisation of p65 in untreated or 23C6/M-CSF-treated THP-1 cells (Figure 5-25B).

We next examined the activation of the signalling pathway leading to activation of the NFκB transcription factors. The TLR-mediated pathway involves signalling factors such as TRAF-6 and IRAK-1. We examined the expression of IRAK-1 in response to 23C6, M-CSF and zymosan treatment by confocal microscopy. Untreated THP-1 cells or THP-1 cells treated with M-CSF alone did not express detectable levels of IRAK-1. Treatment of THP-1 cells with 23C6 induced low levels of IRAK-1, which was enhanced by the addition of M-CSF. The IRAK-1 staining for 23C6 and M-CSF was similar to that observed for the TLR-2 ligand zymosan, which induced a strong IRAK signal in THP-1 cells (Figure 5-26).

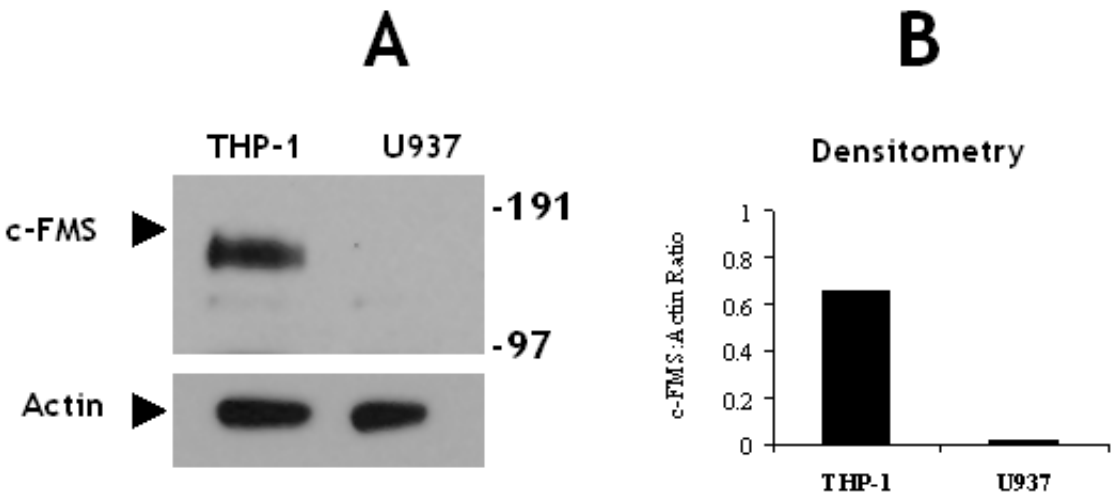

Figure 5.14 Expression of c-FMS by THP-1 and U937 cell lines
Expression of the M-CSF receptor c-FMS in THP-1 and U937 cell lines as determined by western blotting. Whole cell lysates from THP-1 and U937 cells were resolved by SDS-PAGE and c-FMS detected by Western blotting (A) and the signal quantified by densitometry against an actin loading control using the *ImageJ* program (B). The data are representative of at least 3 independent experiments.

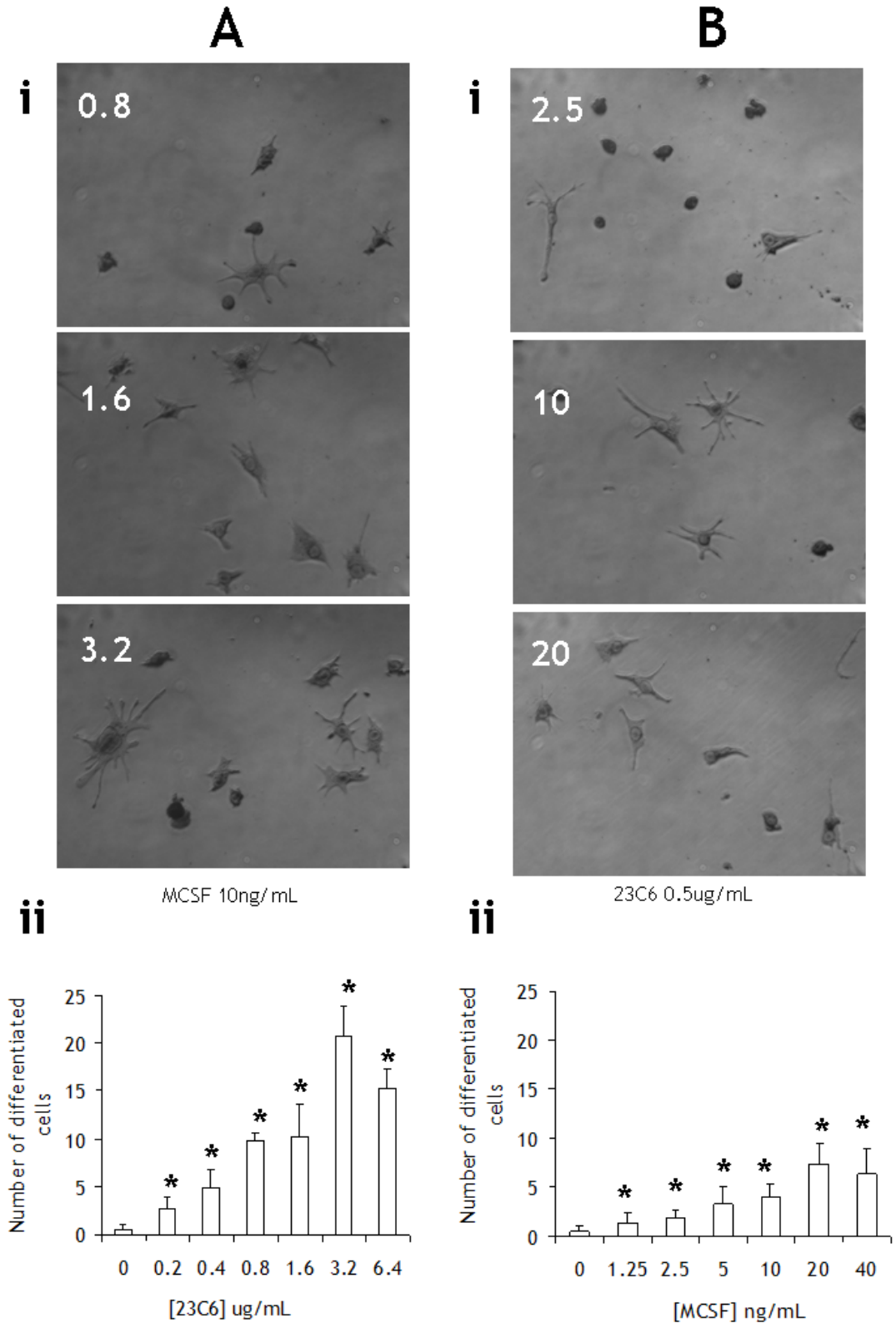

Figure 5.15 Integrin-mediated differentiation and activation of THP-1 is dose-dependent

THP-1 cells were grown for 5 days in Optimem medium (A) with M-CSF (10ng/mL) and increasing concentrations of 23C6 (anti-αVβ3) antibody or (B) with 23C6 (anti-αVβ3) antibody at 0.5µg/mL and increasing concentrations of M-CSF. Numbers in the top right corners indicate concentrations of 23C6 (anti-αVβ3) antibody in µg/mL (A) or M-CSF in ng/mL (B). (A)i and (B)i show photomicrographs of cell morphology and (A)ii and (B)ii show the quantitation of the numbers of differentiated cells with increasing concentration of 23C6 (anti-αVβ3) antibody and M-CSF, respectively. Data shown are representative of at least three independent experiments. Statistical analysis was performed using Students *t*-test, *p<0.05. The error bars indicate standard deviations (SD).

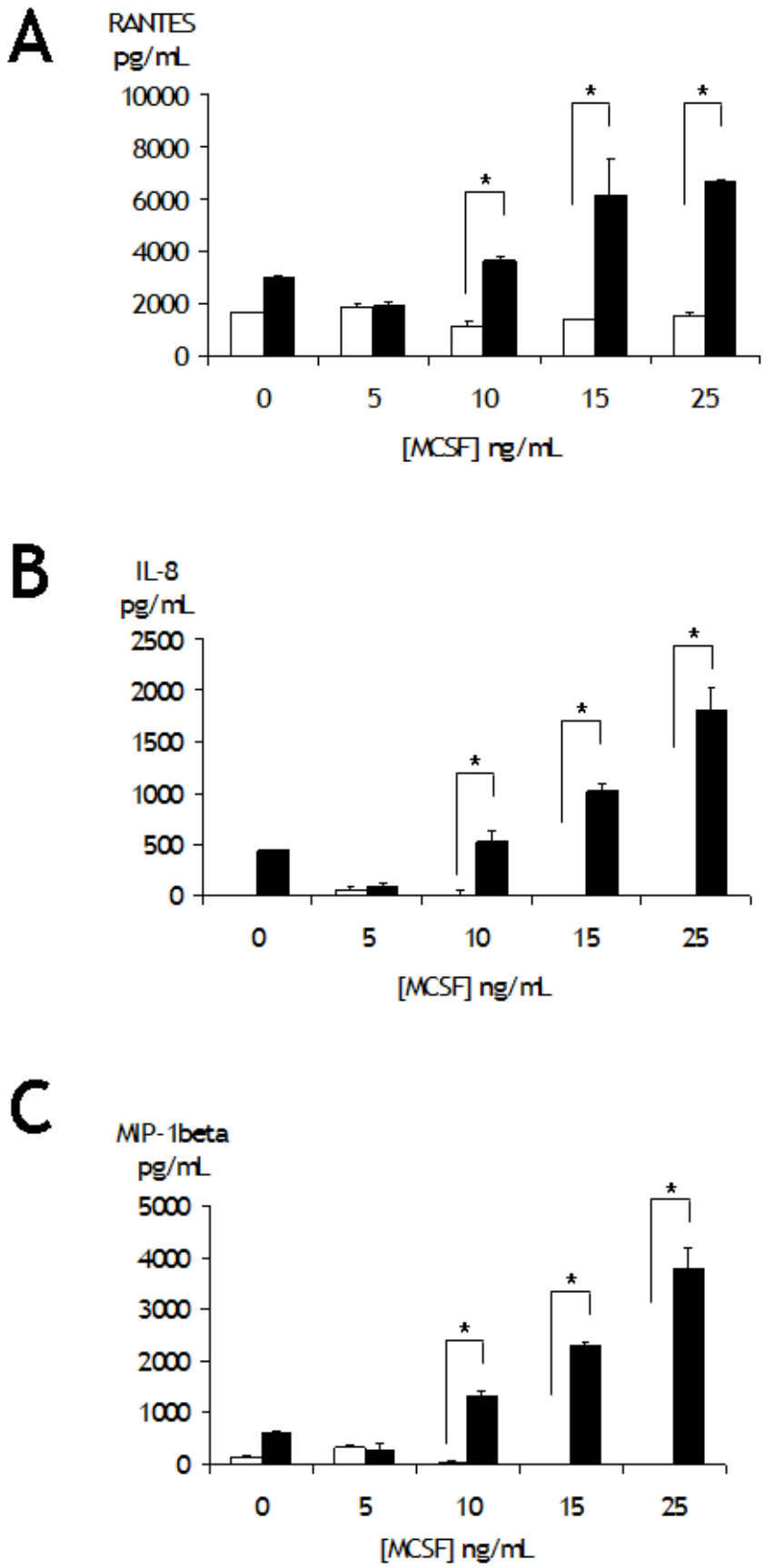

Figure 5.16 Enhancement of 23C6-mediation cytokine production by M-CSF
Cells were incubated with increasing concentrations of M-CSF alone (white bars) or M-CSF with a fixed concentration of 0.5µg/mL of 23C6 (anti-αVβ3) antibody (black bars) overnight at 37^0C. Cytokines released into the supernatant were quantified by ELISA. Data are representative of at least 3 independent experiments. Statistical analysis was performed using Students *t*-test, *p<0.05. The error bars indicate standard deviations (SD).

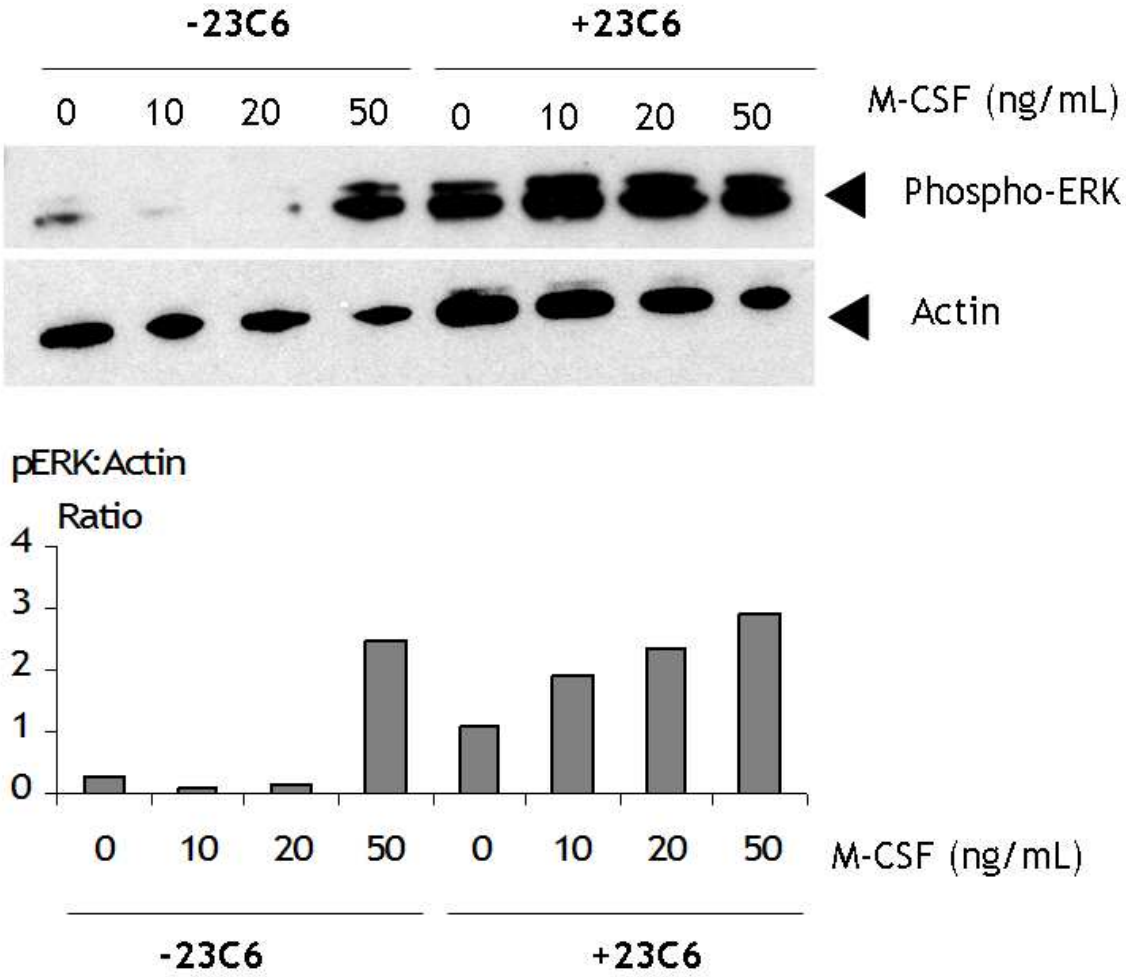

Figure 5.17 Enhancement of ERK phosphorylation by M-CSF for a given concentration of 23C6.

Cells were incubated with increasing concentrations of M-CSF alone or M-CSF with a fixed concentration of 0.5µg/mL of 23C6 (anti-αVβ3) antibody for 30min at 37^0C. ERK phosphorylation was detected by SDS-PAGE and Western blotting, with actin as a loading control. Band intensity was quantified by densitometry using *ImageJ* graphics software. Data are representative of at least 3 independent experiments.

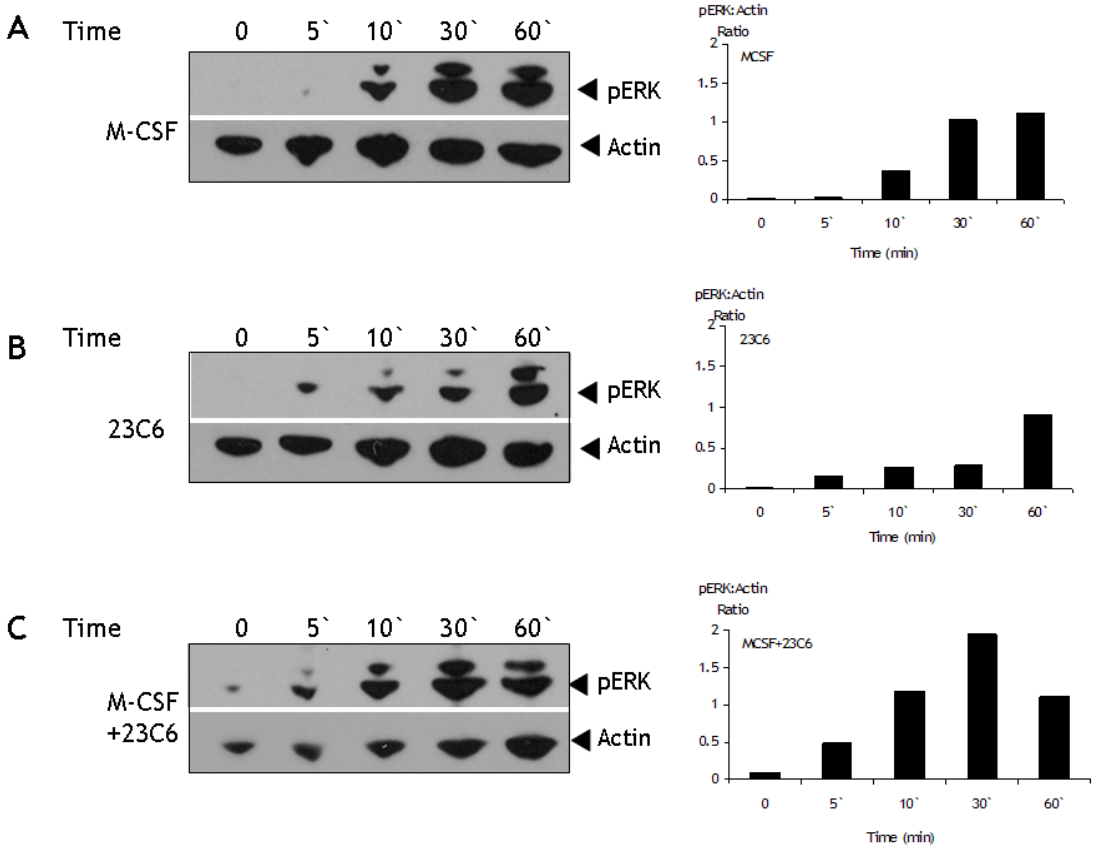

Figure 5.18 Kinetics of ERK phosphorylation in 23C6/M-CSF-treated cells
Cells were incubated with M-CSF alone (50ng/mL), 23C6 alone (0.5µg/mL) or a combination of M-CSF (50ng/mL) and 23C6 (0.5µg/mL) at 37^0C. Samples were collected at time points indicated and ERK phosphorylation was detected by SDS-PAGE and Western blotting, with actin as a loading control. Band intensity was quantified by densitometry using *ImageJ* graphics software. Data are representative of at least 3 independent experiments.

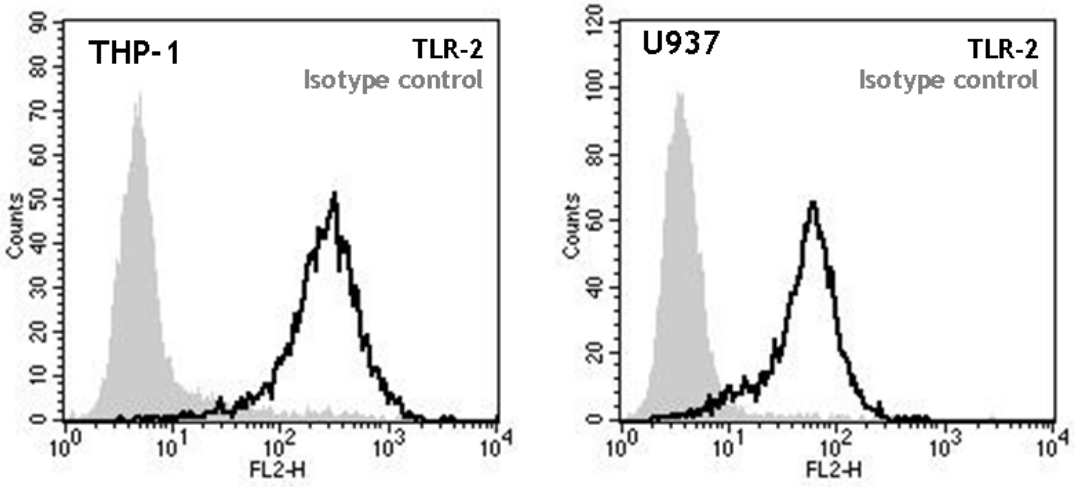

Figure 5.19 Expression of TLR-2 by THP-1 and U937 cell lines

THP-1 and U937 cells were incubated with anti-TLR-2 antibody (black line) or isotype matched control (grey shading). Primary antibody binding was detected by secondary antibody conjugated to the fluorescent label PE. The data are representative of at least 3 independent experiments.

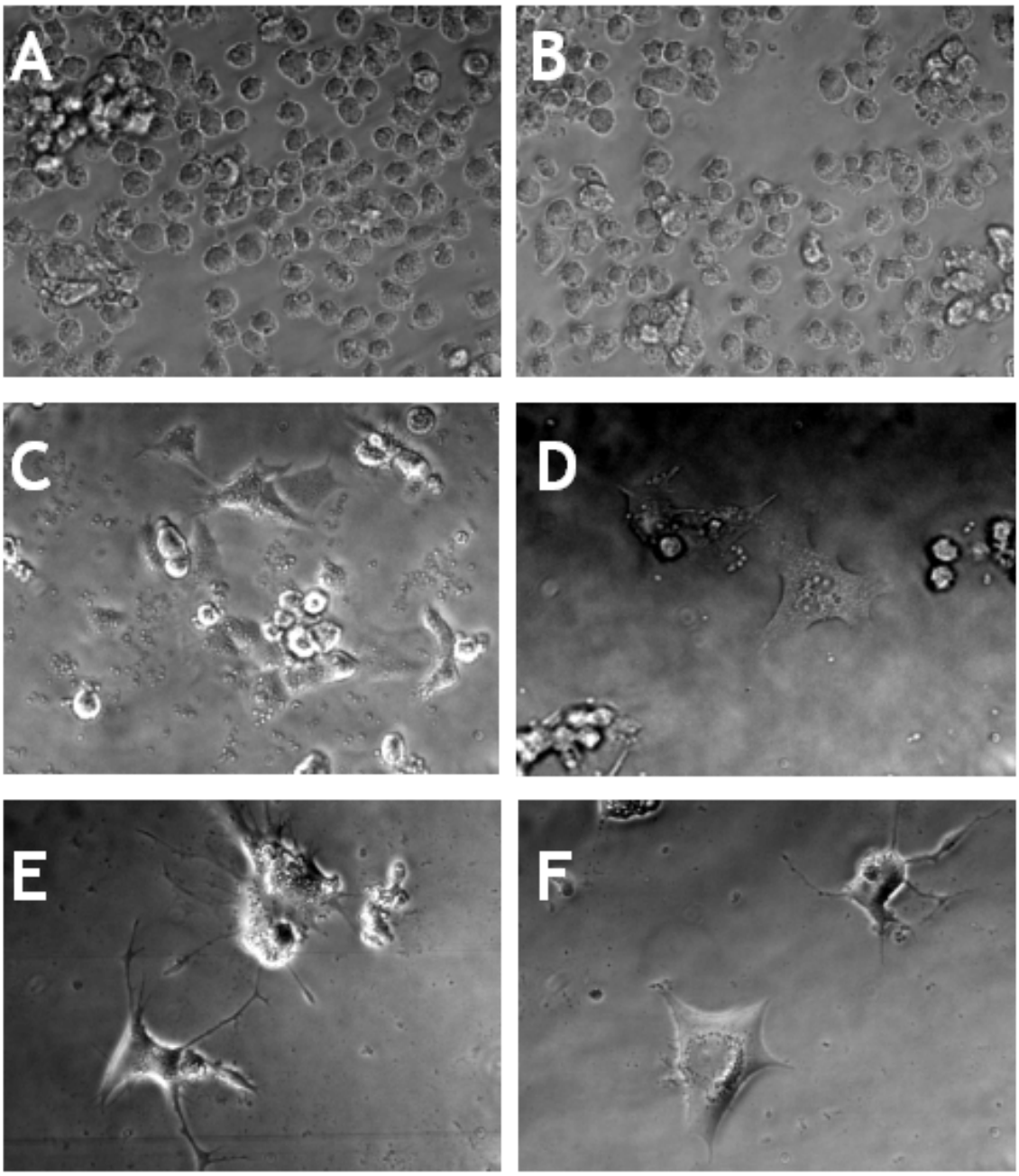

Figure 5.20 Comparison of morphologies of zymosan-treated and 23C6/M-CSF-treated THP-1 cells

THP-1 cells were grown for 5 days in Optimem medium (A and B) without supplementation, (C and D) with 10µg/mL Zymosan A (E and F) with 10ng/mL M-CSF and 1µg/mL 23C6 (anti-αVβ3) antibody. Phase contrast photomicrographs (magnification x320) of cell morphology were taken using the Zeiss Axiovert microscope. Data are representative of at least 3 independent experiments.

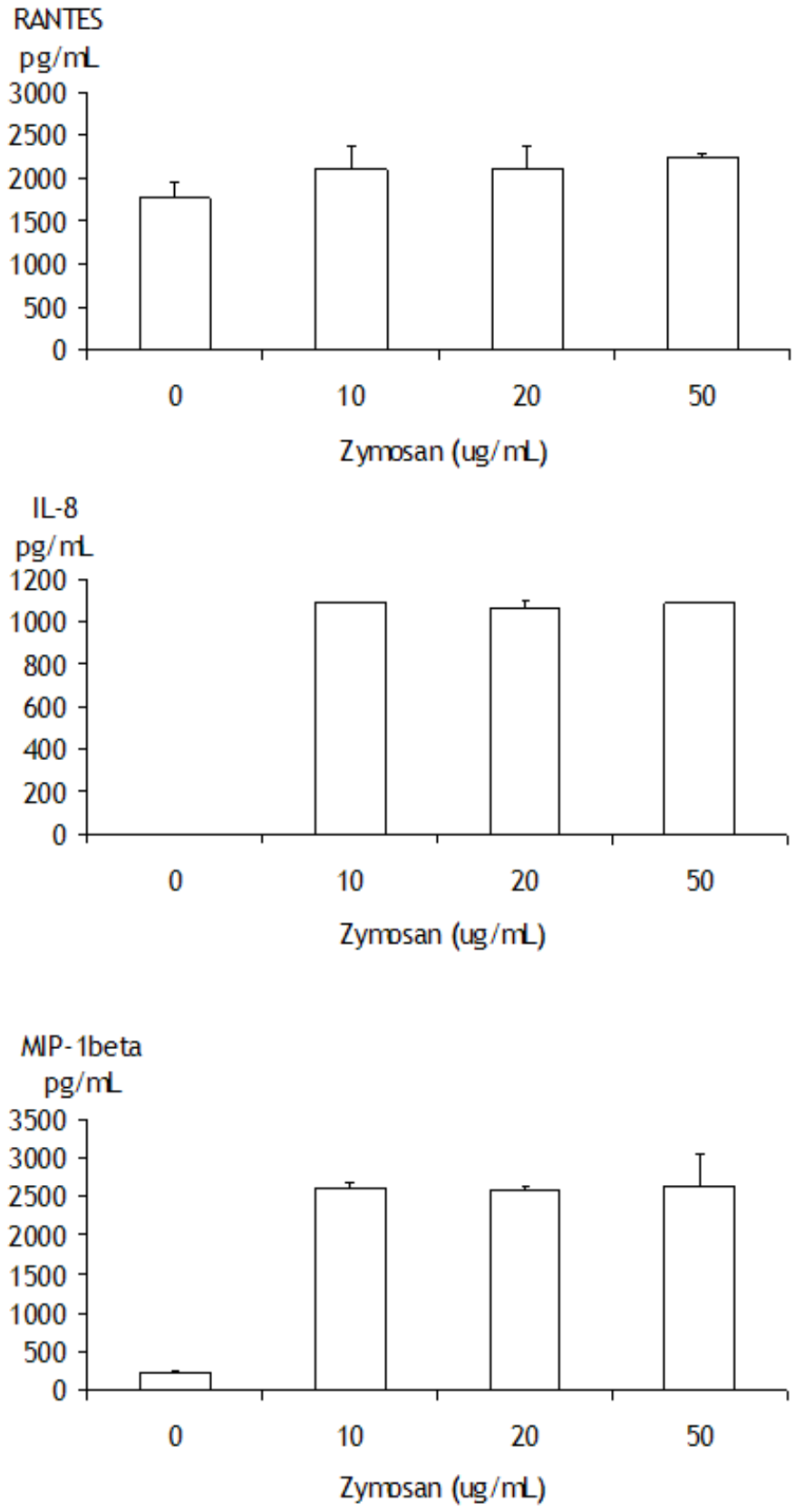

Figure 5.21 Cytokine responses of THP-1 cells to the TLR-2 ligand, Zymosan
THP-1 cells ($1x10^6$/mL) in Optimem were exposed to increasing concentrations of yeast zymosan A and incubated overnight at 37^0C in 5% CO_2. Cytokines released into the supernatant were quantified by ELISA. The data are representative of at least 3 independent experiments. The error bars indicate standard deviations (SD).

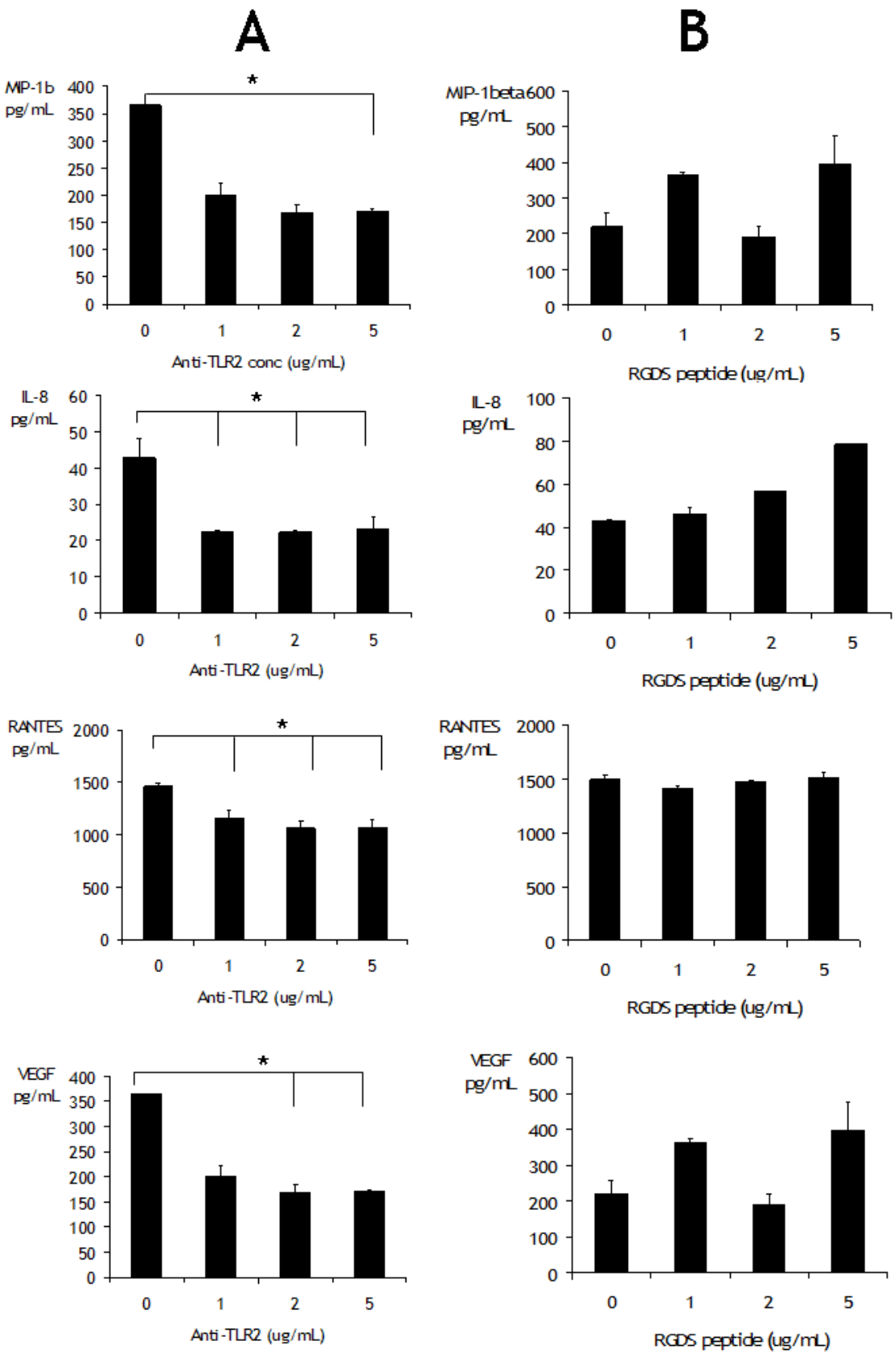

Figure 5.22 Reduction in 23C6 induced cytokine levels in response to anti-TLR-2 antibody, but not RGDS peptide

THP-1 cells were incubated with increasing concentrations of anti-TLR-2 antibody or β3 blocking peptide for 30min prior to stimulation with 23C6 (anti-αVβ3) antibody (1µg/mL) overnight at 37^0C and 5% CO_2. Cytokines released into the supernatant were quantified by ELISA. Data are representative of at least 3 independent experiments. Statistical analysis was performed using Students *t*-test, *p<0.05. The error bars indicate standard deviations (SD).

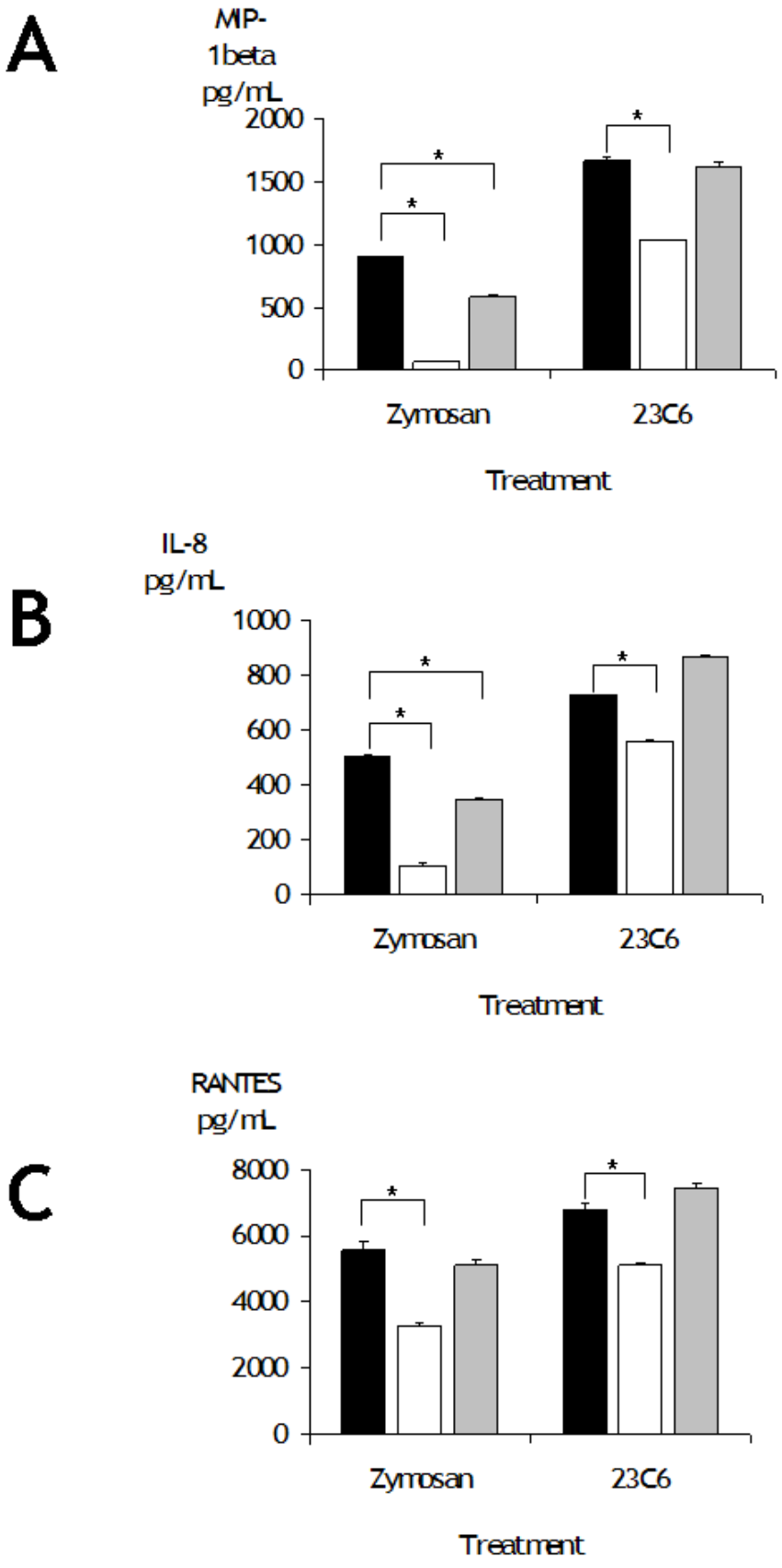

Figure 5.23 Cytokine production in cells treated with anti-MyD88 peptide
THP-1 cells were incubated with control peptide (black bars), anti-TLR2 antibody (white bars), anti-MyD88 signalling peptide (grey bars) before being stimulated with zymosan or 23C6. MIP-1β (A), IL-8 (B) and (C) RANTES released into the supernatant were detected using ELISA. Data are representative of at least 3 independent experiments. Statistical analysis was performed using Students *t*-test, *p<0.05. The error bars indicate standard deviations (SD).

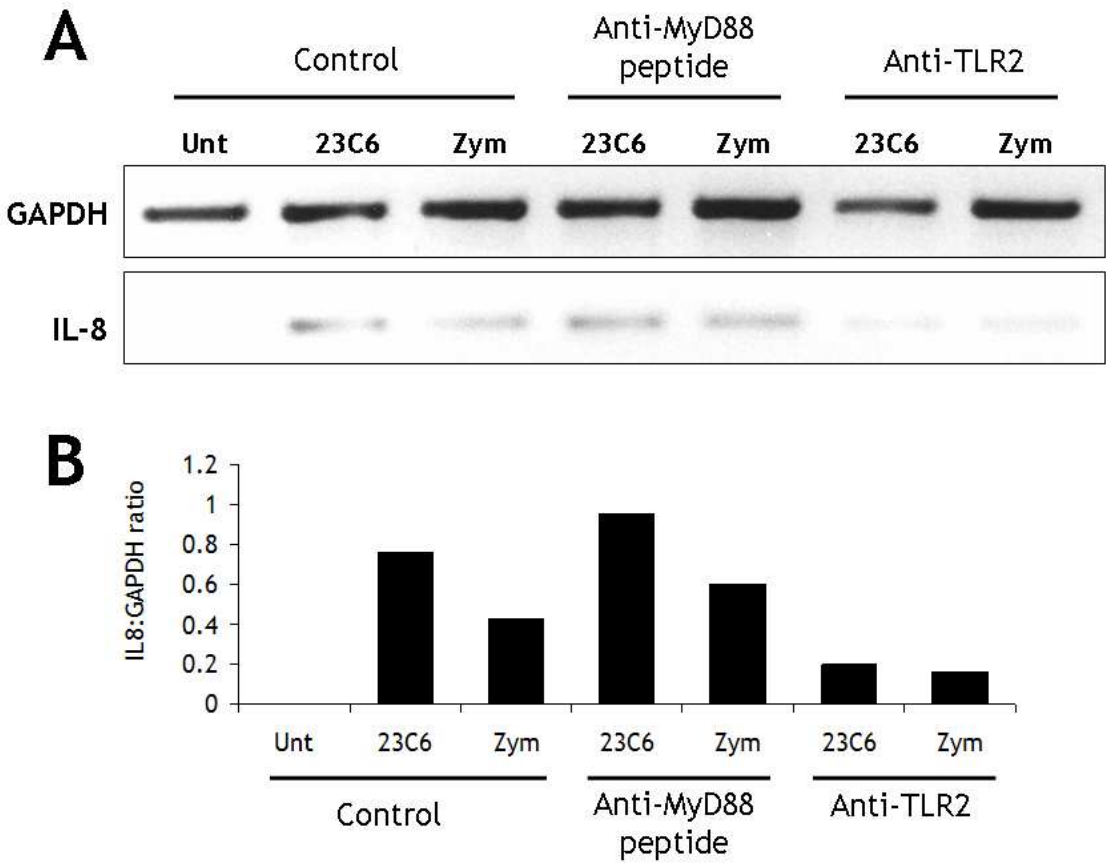

Figure 5.24 Reduction in integrin induced IL-8 mRNA expression by blocking TLR-2, but not MyD88

(A) THP-1 cells were untreated or treated with either anti-MyD88 peptide or TLR-2 blocking antibody prior to stimulation with 23C6 (anti-αVβ3) antibody or TLR-2 ligand, zymosan for 6 hours at 37^0C. Total RNA was Trizol extracted and used in semi-quantitative RT-PCR reactions to detect the presence of IL-8 and GAPDH mRNA. Densitometric analysis of bands was acheived using *ImageJ* software. The data are representative of at least 2 independent experiments.

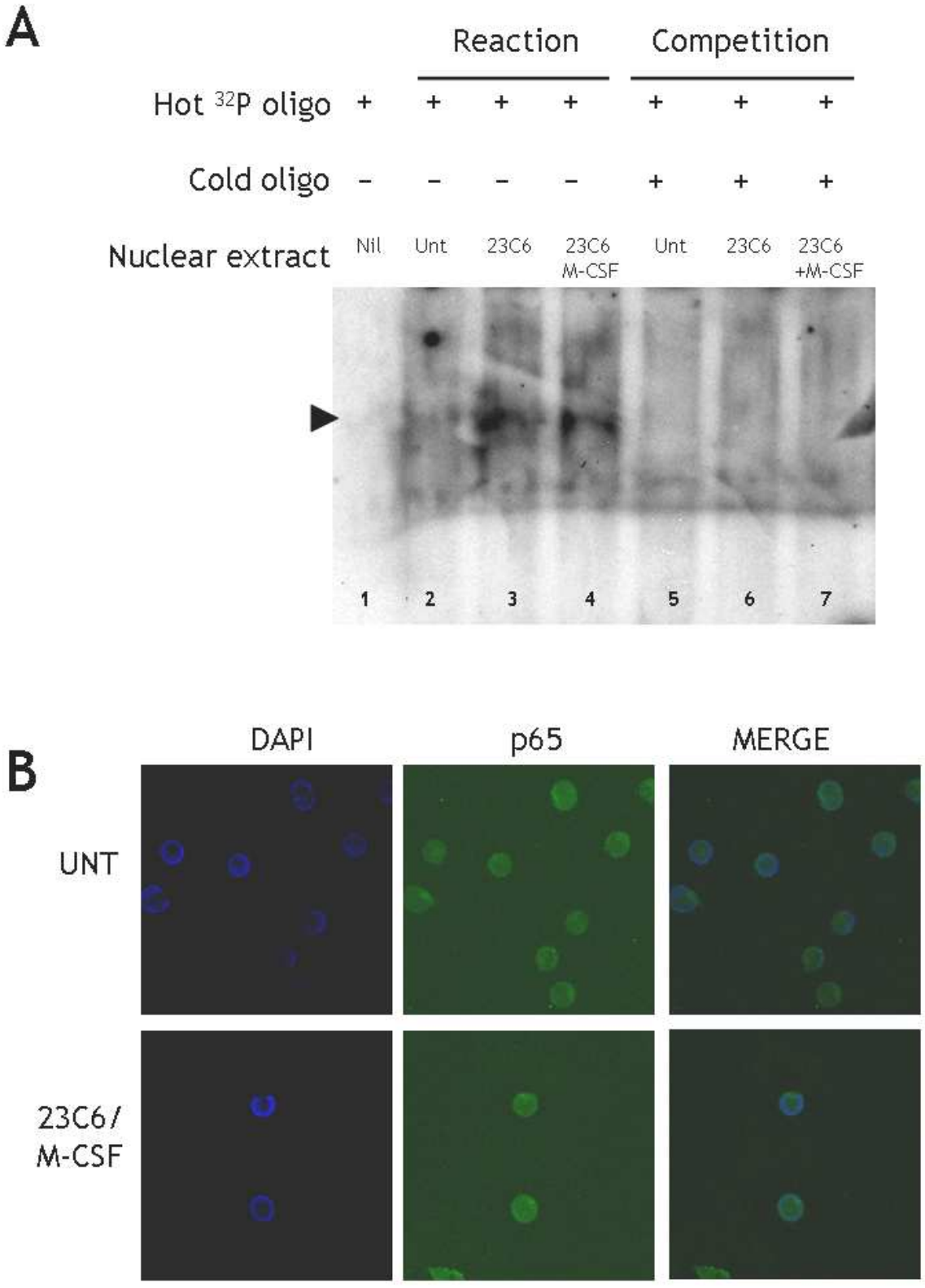

Figure 5.25 Analysis of NFκB activation in 23C6-treated THP-1 cells
(A) Nuclear extracts were prepared from untreated THP-1 cells, THP-1 cells treated overnight with 23C6 and THP-1 cells treated overnight with 23C6 and M-SF and assessed for the activation of NFκB by EMSA. (B) Localisation and expression of p65 before and after 23C6 /M-CSF treatment was analysed by confocal microscopy. Primary anti-p65 was detected using Secondary antibody conjugated to FITC. DAPI was used to stain nuclei and images captured using the Zeiss LSM 510 Microscope (magnification x320).

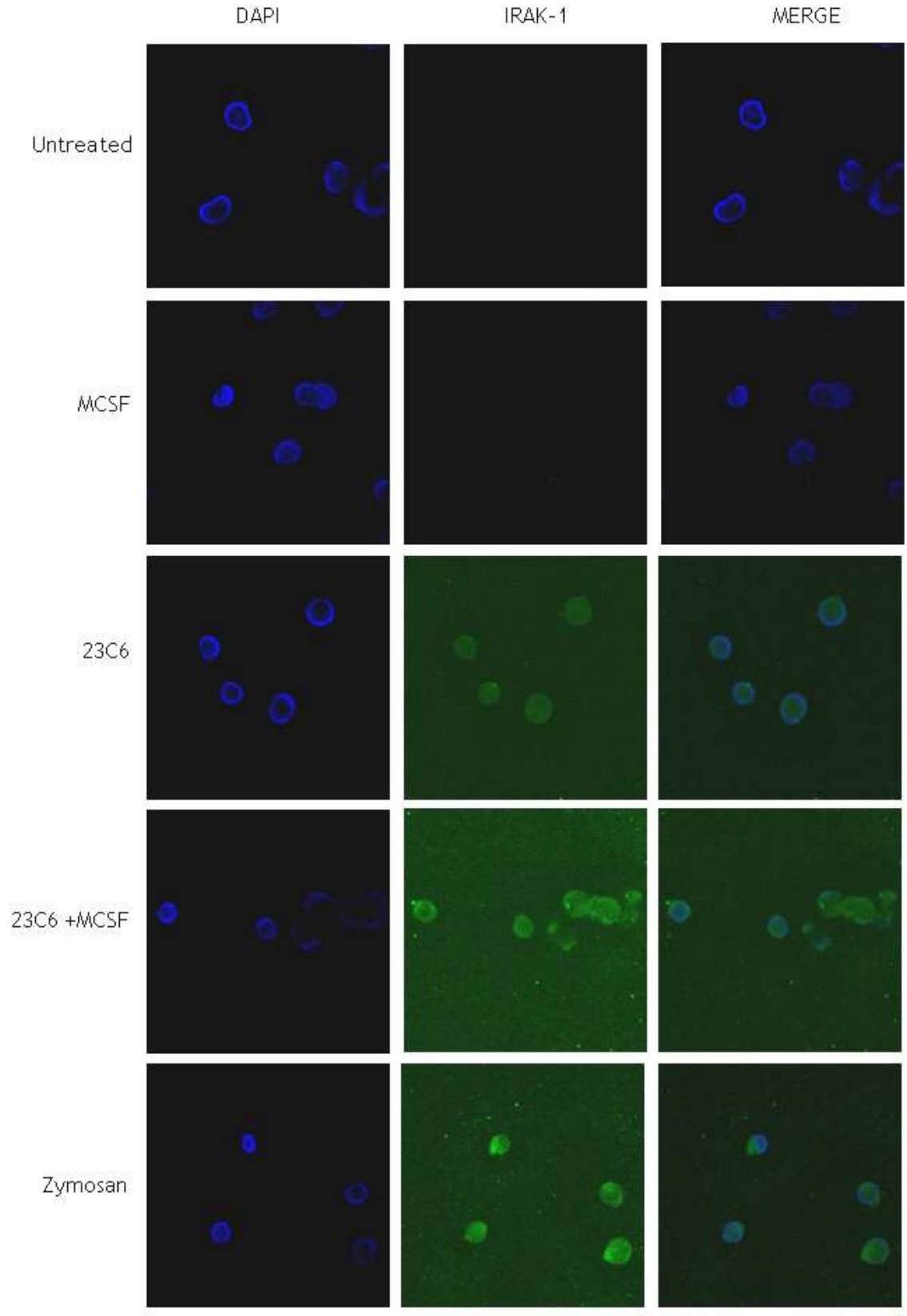

Figure 5.26 IRAK-1 expression in response to anti-αVβ3 integrin and M-CSF treatment

THP-1 cells were treated with agents indicated in left panel for 3 hours at 37^0C, prior to being fixed with acetone/methanol and stained for the presence of IRAK-1. Primary anti-IRAK-1 was detected using Secondary antibody conjugated to FITC. DAPI was used to stain nuclei and images captured using the Zeiss LSM 510 Microscope (magnification x320).

5.3 Discussion

Treatment of THP-1 cells with the αVβ3 antibody 23C6 was shown to induce high levels of cytokine release by these cells. We analysed further the role of the 23C6 antibody in monocyte differentiation. We observed that 23C6 ligation led to the phosphorylation of the β3 cytoplasmic tail and activation of the ERK signalling pathway in THP-1 cells during cytokine production. Chemokines produced by αVβ3 ligation with 23C6 were capable of inducing monocyte migration *in vitro* and possibly contributed to 23C6-mediated monocyte activation. Treatment of THP-1 cells with the 23C6 antibody was enhanced by the addition of M-CSF and led to distinct changes in cell morphology, consistent with a more macrophage-like phenotype. The 23C6/M-CSF-activation and cytokine production of THP-1 cells was influenced by the presence of the M-CSF receptor c-FMS and partially inhibited by the blockage of the TLR-2 receptor using an anti-TLR-2 antibody, but not an inhibitor of MyD88-dependent signalling.

5.3.1 23C6 treatment of THP-1 cells induces signalling

The 23C6 antibody induced the production of high levels of cytokines by THP-1 cells. Antibodies may be defined as neutralising if they block the function of the antigen receptor to which they bind, or activating if they stimulate the function of their target antigen. We analysed the signalling events induced by αVβ3 ligation by 23C6.

Binding of the anti-αVβ3 integrin antibody 23C6 to THP-1 cells was shown to induce phosphorylation of the β3 cytoplasmic domain on the Tyr773 residue. Phosphorylation of this residue activates the integrin and is required for firm adhesion of αVβ3 to vitronectin [220-222]. This is considered to be an early event in the adhesion of leukocytes and is associated with the activation of the Rho signalling pathway and reorganisation of the actin cytoskeleton to form adhesive contacts. The phosphorylation of the β3 tail at this residue is consistent with the morphological changes associated with long term exposure of THP-1 cells to 23C6. Under these conditions, the THP-1 cells became enlarged and adhered to the plastic tissue culture dish. The stimulation of THP-1 cells with 23C6 was conducted in a short time period (30 min), during which the cells were still in

suspension and had not acquired an adherent morphology. This indicated that a soluble ligand for αVß3, namely the 23C6 antibody in solution, was capable of activating the adhesive function of the integrin. Phosphorylation of ß3 on this site is known to activate the Rho/ROCK signalling pathway, which would account for the morphological changes observed [222], although further analysis would be required to conclusively link 23C6 ligation with an activation of the Rho/ROCK pathway. However, these data suggest that the effects of ligation of αVß3 are due to direct signalling via this integrin, as opposed to indirect activation of other signalling pathways (i.e. where neutralisation of αVß3 allows signalling via an alternative pathway to proceed).

Ligation of αVß3 by the 23C6 antibody in THP-1 cells led to the activation of the MAPK pathway and ERK phosphorylation. An increase in ERK phophorylation was observed with increasing concentrations of 23C6 and with increased length of stimulation. Cytokine production by THP-1 cells in response to 23C6 binding required ERK phosphorylation, as treatment of cells with the MEK inhibitor U0126 reduced cytokine production in response to stimulation with this antibody. Cytokines also induce activation of MAPK pathways via interactions with their receptors on cells, although, the ERK phosphorylation assays were conducted over a 30 time period, prior to any detectable cytokine release in the supernatant. This indicated that the ERK phosphorylation observed was not a result of cytokine activation of THP-1 cells but rather due to direct integrin ligation by 23C6.

Integrin-mediated activation of ERK can occur by activation of the Ras/Raf/MEK/ERK pathway. This pathway can be activated either by FAK-dependent activation of SFKs in focal adhesions or by activation of Grb2 and Sos directly by SFK, such as Fyn and Shc. Both pathways are involved in the activation of genes controlling cell differentiation and cytokine production and are linked to the integrin-mediated phosphorylation of focal adhesion kinase (FAK). We attempted to detect FAK phosphorylation in the 23C6-stimulated THP-1 cells. Although we were unable to identify any phosphorylated FAK upon treatment of THP-1 cells with the 23C6 antibody, it is possible that activation of FAK did occur upon αVβ3 ligation with 23C6 and that the levels of FAK were below our detection limits, due to low expression levels in suspension cells which lack focal adhesions. Phosphorylated FAK can also activate Src which can

activate p190RhoGAP and inactivates its GAP function. P190RhoGAP catalyses the conversion of active RhoGTP to inactive RhoGDP and thus its inactivation could lead to an increase in active RhoGTP pools. This RhoGTP activates ROCK, which subsequently leads to reorganisation of the cytoskeleton, integrin clustering and adhesion. This mechanism would explain the signalling events from ß3 phosphorylation by the binding of 23C6 to the activation of the ERK pathway in THP-1 cells.

Other pathways, such as the JNK, p38 MAPK and PI3K pathways have been implicated in cytokine production by integrin ligation [240-244]. We are currently analysing the potential role of these pathways in the signalling from the αVβ3 integrin in this system. Preliminary investigations suggest that signalling via the PI3K pathway is not as important during integrin-mediated production of cytokines by THP-1 cells, as we have been unable to detect phosphorylated Akt in response to 23C6 treatment of THP-1 cells or to inhibit 23C6-mediated cytokine production by THP-1 cells using an inhibitor of PI3K (*data not shown*). Further analysis of these signalling events is underway.

5.3.2 The role of αVβ3-induced cytokines in monocyte migration

Treatment of THP-1 cells with 23C6 led to the production of a range of cytokines (as detailed in the previous chapters). A number of these cytokines, including IL-8, RANTES and MIP-1ß, are chemotatic cytokines known as chemokines. Chemokines are cytokines capable of influencing the migration of immune cells and are used in the body to recruit cells to specific sites at which they are required. This suggested a possible role for αVß3-induced cytokines in the regulation of migration of immune cells. However, different chemokine isoforms, concentrations and combinations will have different chemotactic abilities. Therefore, it was necessary to analyse the chemotactic ability of 23C6-stimulated THP-1 supernatants and not to merely assume that the presence of a specific chemokine equates to a high chemotactic effect. The ability of supernatants from 23C6-treated THP-1 cells to influence the migration of virgin/unstimulated cells was analysed *in vitro* using transwell migration assays. Cleared supernatants from THP-1 cells stimulated with 23C6 were capable of inducing the migration of unstimulated THP-1 monocytic cells, Jurkat T-cells and

IB4 B-cells. Chemokines are known to activate integrins to lead to adhesion and extravasation. Therefore, it is possible that the soluble signalling via the αVß3 integrin induces the production of chemokines which are subsequently capable of activating the adhesive functions of other integrins, as indicated by an increase in the migration of THP-1 cells across FCS or VN coated membranes transwells, as opposed to BSA-coated membranes. The increased migration of THP-1 cells on vitronectin to 23C6-treated supernatant suggests activation of the adhesive functions of αV integrins. The use of neutralising antibodies against different chemokines should have been included in the analysis. This would have allowed identification of the chemokine responsible for mediating cell migration under these conditions.

The ability of chemokines produced by αVß3 ligation to induce migration of immune cells may be important *in vivo* in physiological immune system function during infections and pathological states in which inflammation and infiltration of immune cells contributes to the pathology of inflammatory diseases, such as rheumatoid arthritis and certain cancers.

5.3.3 The role of αVβ3 and c-FMS during monocyte differentiation/ activation

CD23 stimulation of monocytic cells leads to the production of cytokines in response to interaction with its integrin receptors (αVβ3, αVβ5, αMβ2 and αXβ2). Acute stimulation (< 24 hours) with antibodies against these integrins can mimick the effect of CD23 and induce cytokine production in monocytic cells (Chapter 4) [40, 41, 84]. CD23 is also known to induce monocyte activation via its interactions with the β2 integrins, αMβ2 and αXβ2 [74, 193]. The ability of selected anti-integrin antibodies in conjunction with M-CSF to induce monocyte activation was tested over a 5 day assay period (chronic stimulation).

Long-term exposure of THP-1 to the anti-β2 antibodies, Clone44 and Clone3.9, led to changes in the THP-1 morphology to a more macrophage-like phenotype. The cells, originally small, rounded and in suspension, became enlarged and adherent with a number of spiky processes/extensions. A similar morphology was observed with LPS-treated THP-1 cells. CD23 is known to stimulate monocyte activation via an interaction with the β2 integrins, αMβ2 and αXβ2 [74, 193].

Therefore the morphological changes associated with treatment of THP-1 cells with the anti-β2 antibodies (and LPS) may have mimicked the effects of CD23 and led to activation of the THP-1 cells. LPS also binds to β2 integrins, as part of the LPS signalling complex [143, 245, 246].

Treatment of THP-1 cells with the 23C6 antibody led to similar distinct morphological changes to those observed with anti-αXβ2, anti-αMβ2 and LPS treatment. However, the changes in the morphology of 23C6-treated cells were more pronounced than those observed with either LPS-stimulation or treatment with the anti-β2 heterodimer antibodies. The 23C6-treated cells were larger and had a greater number and degree of cytoplasmic extensions than THP-1 cells treated with LPS, Clone3.9 or Clone44. Indeed, 23C6 alone (without M-CSF) was sufficient to induce the morphological changes in THP-1 cultures, while M-CSF was required for LPS and β2-mediated activation of THP-1 cells. It is possible that the cytokines produced in response to integrin ligation contributed to the development of the activated phenotype, especially considering THP-1 cells express at least some of the receptors for those cytokines (i.e., CCR5 and IFNγR) and that cytokine production preceded monocyte activation. However, it seems likely that there are other events controlling these morphological changes in the monocytic cells, as antibodies that induced a similar cytokine release profile did not induce the same level of monocyte activation. For example, the 23C6 and Clone3.9 antibodies induced the release of high levels of cytokines by THP-1 cells, but the 23C6-treated THP-1 cells acquired a more severe phenotype than the Clone3.9-treated cells. These morphological changes were associated with the continued synthesis of cytokines (TNF-α) and chemokines (IL-8, RANTES and MIP-1β), which indicated that the cells continued to be viable during the 5 day period.

There are few reports in the literature of the role of the αVβ3 integrin in the activation of monocytic/macrophage cells. The αVβ3 integrin is important in the development of osteoclasts, terminally differentiated bone-resorbing cells that arise from macrophages. Osteoclasts upregulate αVβ3 as they develop from macrophages under the influence of M-CSF and receptor activator for NFκB ligand (RANKL). Osteoclast can be identified as large, adherent, multinuclear cells that express high levels of the osteoclast marker, TRACP. The morphological changes observed with 23C6-treatment of THP-1 cells were

consistent with the development of osteoclasts (a number of cells with multiple nuclei were also observed in the THP-1 cells stained with Giemsa stain). However, 23C6-treated THP-1 cells were consistently negative for the osteoclast marker TRACP and, as opposed to upregulating αVβ3 as would be expected for developing osteoclasts, the cells appeared to downregulate this heterodimer during the 5 day assay period. However, TRACP staining can be technically difficult and in the absence of a positive control it is not possible to state conclusively that the cells are not osteoclasts. Measurement of the levels of IL-6 and TGF-β produced by these cells would also have aided in their identification.

An alternative hypothesis was that these morphological changes were an indication of the activation of the THP-1 cells into an activated macrophage phenotype in response to 23C6/M-CSF treatment. Monocyte/macrophage activation can occur via a number of mechanisms, each of which leads to a macrophage of a particular function and phenotype. These macrophages can be identified by the surface markers they express and their characteristic cytokine profiles. We analysed the expression of specific surface markers and the cytokine production profiles of 23C6/M-CSF-treated THP-1 cells, to identify the nature of this 23C6-mediated activation of THP-1 cells with reference to published markers of macrophage activation[7, 8, 247, 248]. Table 5-1 shows a summary of the cytokine profile and surface marker expression of THP-1 cells treated with 23C6 and M-CSF, compared with characteristics of specific populations of activated macrophages. The expression of selected surface markers on THP-1 cells did not correlate with the surface marker profile for a particular type of macrophage activation.

Specific cytokine profiles are also associated with macrophage activation mechanisms. Classical activation of macrophages (M1) is induced by treatment with IFN-γ and TNF-α and is characterised by the production of pro-inflammatory cytokines such as TNF-α and IL-12. Alternative activation of macrophages (M2) is characterised by the production of high levels of IL-10 and not IL-12 or TNF-α in response to exposure to stimuli such as IL-4, IL-10 and glucocorticoids. M2 macrophages can be further sub-divided into M2a, M2b and M2c sub-populations of alternatively activated macrophages (Table 5-1). M2a and M2c are similar in that they both produce high levels of anti-inflammatory agents, such as IL-10 and IL-1RA. M2b macrophages are a distinct population that develop in response

to exposure to immune complexes and to TLR ligation, and produce TNF-α in conjunction with high levels of IL-10 and low levels of IL-12.

THP-1 cells treated with 23C6 and M-CSF for 5 days produced a range of cytokines. High levels of TNF-α, RANTES, IL-8, MIP-1ß and VEGF were continuously released during the 5 day assay period. There was a transient release of IFN-γ and IL-10 detected after 24 hours, which had declined to zero after 48 hours. It is possible that this decline to zero was a result of autocrine uptake of these cytokines by the stimulated THP-1 cells. THP-1 cells express the receptor for IFN-γ (*data not shown*). Other authors have reported some morphological changes in THP-1 cells after treatment with IFN-γ and M-CSF [249]. It is also possible that release of IFN-γ and IL-10 was inhibited after 24 hours due to changes associated with the activation of THP-1 cells by 23C6 and M-CSF. No IL-4 or IL-12p40 was detected at any time during the 5 day assay.

The cytokine profiles, similar to the cell surface markers, did not correlate absolutely with a specific mechanism of macrophage activation. The cytokines produced in response to 23C6/M-CSF may provide autocrine activating signals for the cells or may be the consequence of a specific programme of macrophage activation.

It seems unlikely that the 23C6/M-CSF-treated THP-1 cells had undergone an M2a or M2c programme of alternative macrophage activation. The lack of IL-4 production, the transient IL-10 production and the levels of TNF-α produced by 23C6/M-CSF-treated THP-1 cells suggested that these are not M2a or M2c alternatively activated macrophages. Similarly, although the 23C6/M-CSF treated THP-1 cells produced IFN-γ (albeit transiently) and TNF-α, there was no production of IL-12, reactive nitrogen species (RNS) or reactive oxygen species (ROS) as would be expected of a classically activated macrophage (M1) population.

Based on the data, it was hypothesised that the 23C6/M-CSF-activated THP-1 cells were most similar in their profile to M2b activated macrophages. The levels of TNFα, lack of production of ROS and RNS, transient IL-10 production and lack of IL-12 production suggested this was the most likely macrophage activation phenotype for the 23C6/M-CSF treated THP-1 cells. These data were supported by the fact that M2b macrophage activation is induced by IgG

complexes and TLR ligands. It is possible that 23C6 antibody binding involved a TLR receptor (discussed later). In addition, the production of VEGF and IL-8 by the 23C6/M-CSF-treated THP-1 cells is also observed with tumour-associated macrophages (TAM), which are defined as an M2 macrophage population. TAM are a major component of many tumours and are proposed to actively contribute to the development, survival and metastasis of cancers.

Further analysis will be required to conclusively identify if these cells are indeed an activated macrophage population and that αVβ3-ligation in conjunction with M-CSF leads to macrophage activation. The data herein have tentatively identified 23C6/M-CSF-differentiated THP-1 cells as most similar to M2b macrophages. However, macrophages are a highly heterogenous population and it is plausible that not all the mechanisms leading to their activation have been described and that integrin-mediated activation represents a new type of macrophage activation mechanism. Similarly, it is equally possible that these *in vitro* experiments are lacking specific (unknown) factors that would result in the development of surface markers and cytokine profiles for 23C6/M-CSF-treated THP-1 cells identical to a specific type of activated macrophage. It may also be that these 23C6/M-CSF-treated THP-1 cells are arrested at a particular developmental point (such as a pre-osteoclast or osteoclast-like cell that has yet to express the TRACP osteoclast marker) and therefore, would differentiate further given the correct *in vivo* or *in vitro* environment. This, however, does not take away from the fact that ligation of the αVβ3 integrin by the 23C6 antibody in the presence or absence of the myeloid growth factor M-CSF has a profound effect on the morphology and activity of THP-1 cells.

5.3.4 Role of TLR-2 and c-FMS during αVβ3-mediated cytokine production by THP-1 cells

Chronic stimulation of THP-1 cells with the anti-αVß3 antibody, 23C6, led to morphological changes within the THP-1 cells. This 23C6-mediated activation in THP-1 cells was enhanced by simultaneous addition of M-CSF. This was reflected in the increased degree of the morphological changes induced by the presence of M-CSF. In addition, 23C6-mediated signalling via the MAPK pathway and cytokine production by THP-1 cells was enhanced by the addition of M-CSF. Treatment of THP-1 cells with 23C6 alone did not induce the expression of M-CSF mRNA as

measured by semi-quantitative RT-PCR (*data not shown*). This enhancement of ERK phosphorylation and cytokine production by the combination of suboptimal concentrations of 23C6 and M-CSF suggests a synergistic relationship between the αVß3 integrin and the M-CSF receptor c-FMS.

The importance of the c-FMS receptor (even in the absence of exogenously supplied M-CSF) was revealed by the fact that U937 cells, which express equivalent levels of the αVß3 integrin to THP-1 cells but do not express c-FMS, failed to differentiate in response to 23C6 or 23C6/M-CSF treatment. The αVß3 integrin and c-FMS receptors have been shown to associate with each other during osteoclast development from macrophages. It is possible that αVß3 and c-FMS also associate during other macrophage differentiation events, such as macrophage activation.

The authors who identified the interaction between αVβ3 and c-FMS proposed that the αVß3/c-FMS association is part of a larger signalling complex which includes other, as yet unidentified, receptors. Data presented herein suggest that the 23C6/M-CSF-treated THP-1 cells acquired a phenotype most similar to M2b activated macrophages. The mechanism of activation of M2b activated macrophage involves binding of TLR ligands (Table 5-1). Thus, it was hypothesised that one of the unidentified receptors in the αVβ3/c-FMS signalling complex was one of the TLR family of receptors. The LPS signalling complex is comprised of a similar group of receptors. This complex contains the LPS receptor, CD14, the αXß2 integrin and the TLR-4 isoform. ß2 integrins contain binding sites for LPS. Therefore, given the existence of this complex, it is plausible to suggest the existence of other integrin/TLR complexes.

Zymosan, a yeast-derived ligand for TLR-2, also binds β2 integrins. Treatment of THP-1 cells with zymosan induced the production of similar cytokines to those observed with 23C6/M-CSF treatment of THP-1 cells. We observed similarities between the morphology of 23C6/M-CSF-treated cells and THP-1 cells treated with the TLR-2 ligand, zymosan, which led us to hypothesise that TLR-2 might be involved. A neutralising antibody against TLR-2 reduced the levels of 23C6/M-CSF-induced RANTES, IL-8, MIP-1β and VEGF to approximately half of those observed in the absence of the TLR-2 antibody, although the anti-TLR-2 antibody did not completely abolish cytokine production. Production of RANTES, IL-8 and

MIP-1β by THP-1 cells in response to 23C6/M-CSF treatment was inhibited by treatment of the cells with anti-TLR-2 but was not inhibited by the inclusion of an inhibitor of MyD88-based signalling. This was unexpected, as all TLR-2 signalling pathways described to date are dependent on the MyD88 molecule. The production of IL-8 and MIP-1β by THP-1 cells in response to zymosan was inhibited by the anti-TLR-2 antibody and by the inhibitor of MyD88 signalling (albeit to a lesser extent than the inhibition observed with the antibody). The levels of IL-8 mRNA detected in THP-1 cells treated with 23C6/M-CSF or zymosan were not inhibited by the MyD88 inhibitor but were inhibted by the anti-TLR-2 antibody.

Treatment of THP-1 cells with 23C6 or 23C6/M-CSF led to the activation of NFκB transcription factor, as indicated by EMSA analysis. We were unable to detect a supershift using an anti-p65 antibody and also failed to observe translocation of p65 to the nucleus after 23C6/M-CSF treatment. Therefore, it was not possible to identify the individual NFκB protein involved in the analysis, although it was unlikely to be p65. We were able to detect increases in the levels of the TLR signalling molecule IRAK-1 in the cytoplasm of 23C6, 23C6/M-CSF and zymosan treated THP-1 cells compared with M-CSF-treated or untreated THP-1 cells.

The data described above suggest that cytokine production by THP-1 cells in response to 23C6 and M-CSF treatment was reduced by binding of the exterior of the TLR-2 receptor but not by blocking the MyD88 molecule at the top (upstream) of the cytoplasmic TLR-2 signalling pathway. This may be due to the antibody blocking an association between αVβ3, c-FMS and TLR-2. However, increases in the expression of the IRAK-1 protein downstream of MyD88 in this pathway and activation of NFκB transcription factors were observed in 23C6/M-CSF and zymosan-treated cells, suggesting that signalling was proceeding via the TLR-2 pathway, despite the lack of dependence on MyD88.

Taken together, these data might suggest the possibility of a MyD88-independent pathway from TLR-2, which may function together with the MyD88-dependent pathway. In some cases, blockage of MyD88 appeared to increase the levels of cytokines produced, although these were not quantified and therefore no comment can be made on their significance. There have been reports of cross-talk between the FAK (integrin-mediated) and MyD88 (TLR-mediated) pathways.

The mechanism is poorly understood at present, but it has been suggested that FAK can mediate the phosphorylation-dependent activation of MyD88 and other TLR signalling intermediates [133]. It may be that integrin-dependent activation of TLR signalling intermediates (such as TIRAP/Mal) exist, although this still needs to be determined [129].

Alternatively, it could be hypothesised that TLR-2 plays a minor role in this complex and is important in external recognition and not internal signalling. Thus, the inclusion of TLR-2 in this complex may activate a signalling pathway other than that originating from TLR-2 itself, leading to the activation of similar transcription factors (NFκB). In this case, the signalling events may originate from the αVβ3 and c-FMS receptors and therefore could be modulated by the external complex which contains TLR-2 but would be independent of MyD88 signalling. A recent study suggested that the αMβ2 integrin was capable of signalling via the TLR pathway, by hijacking the signalling intermediates IRAK and TRAF, in a MyD88-independent process [250]. TLR-2 has also been shown to act as a scaffold for other signalling complexes. It is unfortunate that there are no data available from this analysis on the effect of the anti-TLR-2 antibody on the activation of NFκB transcription factors or the levels of IRAK-1 in THP-1 cells treated with 23C6 and M-CSF. Further analysis is underway to confirm the existence of and to investigate this potential complex, including immunoprecipitaion and co-localisation studies on these three receptors.

The reduction in cytokine production due to the blockage of TLR-2 was not associated with a complete change in the cell morphology in response to 23C6/M-CSF treatment. The 23C6/M-CSF treated cells still displayed a degree of change in morphology associated with 23C6 stimulation (*data not shown*), although these experiments need to be repeated to confirm the accuracy of these data. This suggests that the pathways leading to cytokine production and macrophage activation are distinct, although they may be overlapping, as indicated by synergy in cytokine production and differentiation phenotype upon addition of M-CSF. This is supported by the fact that antibodies that induce high levels of cytokine production do not necessarily induce the morphological changes in the THP-1 cells.

The data presented in this chapter suggest that the αVβ3 integrin may have an important role in the function of monocytic cells in the immune systems, both by regulating the production of inflammatory species such as cytokines and chemokines which may affect other cells in the body but also by directly influencing the biology of the monocyte itself.

6 DISCUSSION

6.1 CD23-Integrin Interaction

CD23 interacts with four integrins, αVβ3, αVβ5, αMβ2 and αXβ2. The data in this thesis describe the analysis of the *in vitro* interaction between CD23/CD23-derived peptides and the αV integrins, αVβ3 and αVβ5. We mapped the recognition site in CD23 for αVß3 and αVß5 to a set of peptides which all contained a common tripeptide motif RKC [75]. The classical recognition site for integrins is the RGD motif, which mediates adhesive reactions and is bound at the interface of the α and ß integrin subunits [101]. The interaction between the integrin and RKC containing peptides was determined to be cation-independent, salt-sensitive and occurred even in the presence of RGD-containing integrin ligands. In addition, the RKC peptide is basic in nature whereas the RGD-binding site of integrins mediates binding of acidic motifs. These combined features of the CD23-integrin interaction suggest that the binding site for the RKC containing peptides on the integrin is not the RGD-binding site. While the RGD sequence is a highly conserved recognition sequence, it is plausible to propose the existence of alternative sites on integrins for other ligands. This suggests that the RKC motif is a novel motif for integrins and that it binds to an alternative site to the binding of RGD. This alternative site may be more important in non-adhesion based, integrin signalling in response to soluble ligands.

Integrins are important receptors in adhesion reactions, but they also participate in complexes that could be considered “non-adhesive” signalling. There is now a growing body of evidence suggesting an alternative site for the binding of non-RGD based, soluble ligands in integrins, such as that observed between CD23-derived peptides and the αV integrins. These data support the findings of a number of studies that have proposed the existence of an alternative site on integrins for ligand recognition. In all of these cases, the interaction is between a soluble ligand and occurs at a site distinct from the RGD-binding site [75, 109, 114, 115].

The potential existence of an alternative integrin recognition site for soluble ligands will be important for the design of anti-integrin based drugs, especially since most drugs will be in solution *in vivo*. The majority of studies on integrins have been performed in adherent cells, although there is now a growing

appreciation of the participation of integrins in alternative modes of signalling. Most studies on the biological roles of integrins have been performed in adherent cell types. It is possible that the conclusions based on studies in adherent cells are not applicable to integrin-mediated signalling in suspension cells. The possibility of an alternative mode of signalling is particularly interesting in the context of haematopoietic cells, including monocytes, which are non-adherent, suspension cells, but nonetheless express a wide range of integrins and are the precursors of a number of adherent, terminally differentiated cells, such as macrophages and osteoclasts. Monocytes, therefore, are a model for the study of integrin-based signalling in soluble and adherent situations. Chronic treatment of THP-1 cells with the anti-αVβ3 antibody 23C6 in solution led to a change in morphology of the model cell line THP-1. The untreated THP-1 cells were small and rounded cells in suspension, which became enlarged and adherent after treatment with a soluble ligand, 23C6. This indicated that a soluble stimulus resulted in the activation of signalling pathways related to adhesion or that the pathways that have been previously described relating to adhesion are actually not exclusively reserved for adhesion based signalling. This further supports the suggestion that integrins participate in two different modes of signalling, and that it may or may not be possible to completely separate the adhesive and non-adhesive based functions of integrins.

6.2 A potential Integrin/Growth Factor Receptor/ TLR Complex

Integrins are well known modulators of signalling from other receptors, often being components of larger signalling complexes, such as the endotoxin signalling complex that is comprised of TLR-4/β2/CD14. We hypothesise that the αVβ3 integrin may form a similar complex with the M-CSF receptor, c-FMS, and TLR-2 and that this is one example of a range of complexes that involve integrins, TLRs and growth factor receptors.

Macrophages activate in response to the presence of pathogens, often through the binding of TLRs. TLRs are a group of evolutionarily conserved receptors that form an important part of the innate immune response via their recognition of conserved pathogen associated molecular patterns (PAMPs). A number of

pathogens that interact with TLRs, have also been shown to bind integrins as receptors for entry into the cell (Table 6-1). Many pathogen receptors incorporate an RGD sequence which they use to interact with integrins, although a number of pathogens also gain entry to cells by interactions with integrins that do not involve an RGD (or related) sequence and cannot be blocked by RGD containing ligands [251-255]. In this manner, these RGD-independent reactions with the integrins could be considered similar to the nature of the interaction observed with the interaction between CD23/CD23-derived peptides and the integrins *in vitro*.

Therefore, the existence of a pathogen response complex including a TLR and an integrin, along with additional macrophage activation receptors such as c-FMS, would couple the innate sensing mechanism (TLRs) with a mechanism for inducing activation of the cell and cytokine production (integrins and growth factor receptors). Indeed, such a complex exists for endotoxin sensing. This complex is composed of the LPS receptor, CD14, TLR-4 and β2 integrins and in this case LPS contains binding sites for β2 integrins, TLR-4 and CD14 (Figure 6-1). It is possible that the formation of this complex is one example of a group of similar complexes which associate in response to different stimuli. Just as there are known specific pairings between different TLRs, it may be that specific integrins form partnerships with particular TLRs and GFRs. Indeed, both LPS and zymosan have the ability to bind both integrins and TLRs [256, 257].

Our signalling data suggested that pathways activated by our proposed αVβ3/TLR-2/c-FMS complex during cytokine production are MyD88 independent. This indicates that in this case, the signalling is mediated not by the TLR-2 but rather by the integrin or indeed by integrin-mediated enhancement of c-FMS signalling. Therefore, both the integrin and the TLR are accessory proteins that provide the mechanism to sense and enhance the response to a potential pathogen. The most likely candidate for controlling the signalling pathways that connect ERK phosphorylation (from c-FMS and/or αVβ3) to NFκB (from the TLR-based signalling) is FAK, although this still needs to be determined conclusively. In certain cases, integrin signalling pathways have resulted in the activation of intermediates of other signalling pathways, including TLR pathways. This may represent a novel mechanism for integrin-mediated synergy with other existing cellular signalling pathways, which will become clear as investigations continue.

Table 6-1 Pathogens that bind TLRs and Integrins

Pathogen	TLR	Integrin	Reference
Adenovirus	TLR-9	αVβ3** αVβ5	258-261
Coxackievirus A9	*ND*	αVβ3*	253, 262
HIV	TLR-7/8 (ssRNA) TLR-4	αVβ3*	263-266
Hantavirus	*ND* *(potentially 3, 7, 9)*	αVβ3 αIIbβ3	252
Rotavirus	*ND*	αVβ3*	254
Candida albicans	TLR-2 TLR-4	αVβ3 β2	267-272
Bacterial LPS	TLR-4	β2	143, 273, 274
Fungal Zymosan	TLR-2	β2	256, 275, 276

*Entry is RGD-dependent
** RGD-dependent and RGD-independent strains identified
ND not determined

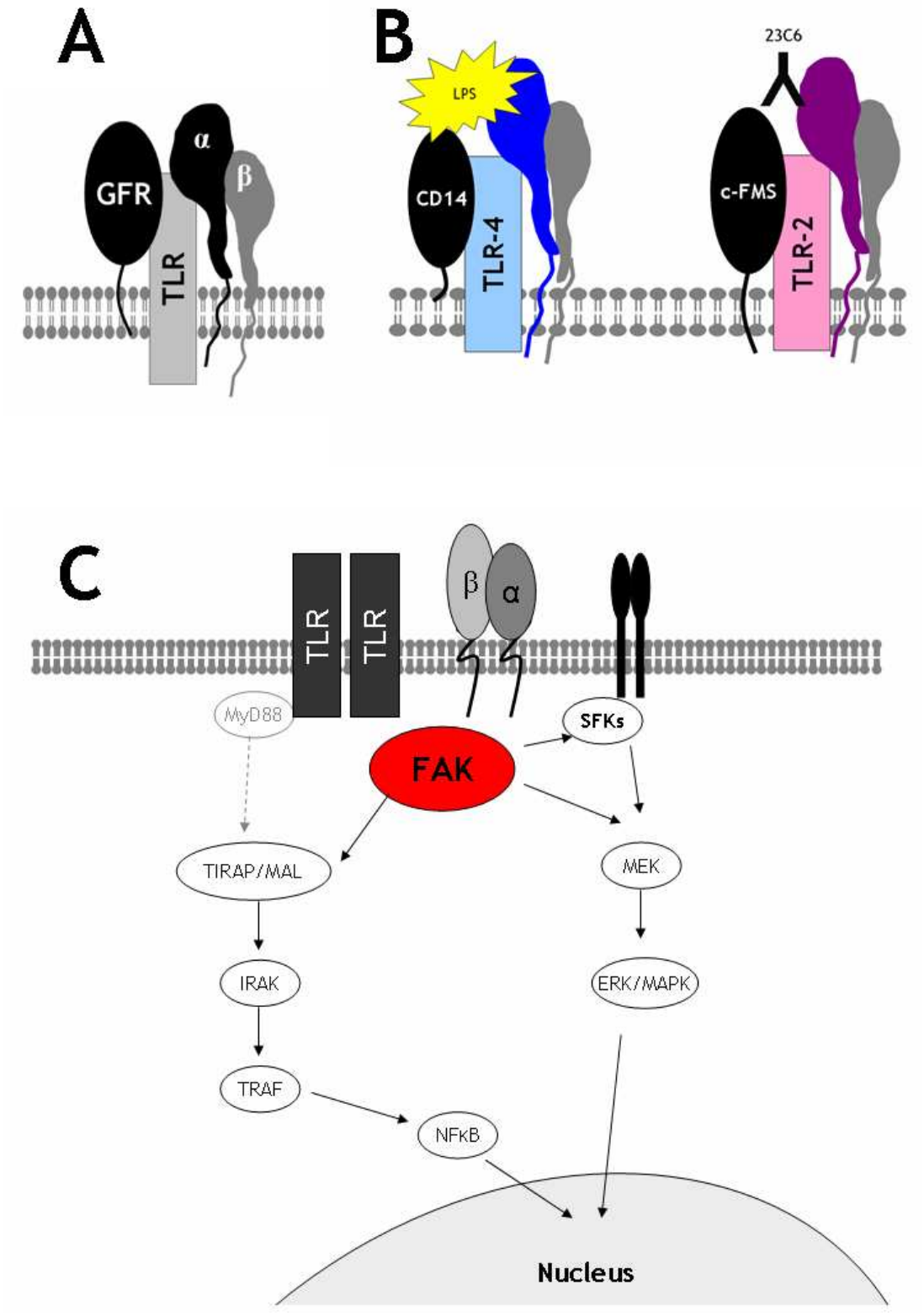

Figure 6-1 Potential Integrin/TLR/GFR receptor signalling complexes
(A) Proposed TLR, integrin and growth factor complexes involved in the control of innate immune responses. (B) Examples of specific integrin/TLR/GFR complexes with defined functions, such as the endotoxin signaling complex containing CD14/TLR-4 and β2 integrin and the complex of TLR-2/αVβ3/c-FMS proposed by this study. (C) Potential signalling pathways from the TLR/integrin/GFR complexes, connected by FAK.

6.3 Integrin-mediated cytokine production and the Immune System

The role of soluble CD23 in the production of cytokines by monocytic cells through interactions with the integrins aVß3, αMß2 and αXß2 is well established. This study included the first analysis of the role of the newly defined CD23-binding integrin receptor, αVß5 on monocytic cells. The data conclude that αVß5 is similar to the other integrin receptors for CD23 and is also involved in the regulation of production of cytokines by monocytic cells. Taken together, the data indicate that both the αV and β2 families of CD23-binding integrins control the production of the same types of cytokines in response to specific ligation. It therefore appears that there is no relative hierarchy between the different CD23 binding integrins during cytokine production. It may be that the response of a particular cell to CD23 treatment will therefore be controlled by the relative expression levels of the different integrins. This hypothesis could be addressed by evaluating the cytokine responses of cells with targeted depletion of specific integrin isoforms using techniques such as RNAi.

6.3.1 Induction of cytokine production is specific

Although no hierarchy between the different integrin families was observed, it was determined that cytokine production was specific with respect to the site on the individual integrin subunit. Only those antibodies that recognised a specific epitope were effective at inducing cytokine production. This again highlights the importance of specific, distinct epitopes during the regulation of integrin interactions and function. For example, ligation of the αVβ3 integrin with the 23C6 antibody led to the release of high levels of cytokines, whereas ligation of the same integrin with the LM609 antibody did not induce cytokine production. Both 23C6 and LM609 inhibit adhesion-dependent reactions of αVβ3, but the antibodies recognise different sites on the integrin. Integrins are associated with a range of different diseases, ranging from inflammatory diseases to certain cancers. The specificity of the different integrin recognition sites is especially relevant in the case where integrins are targeted as therapies for diseases [195, 277, 278].

Table 6-2 Cytokine levels detected in serum during human diseases

Disease	Chemokine and Concentration Range (pg/mL)		Ref
Normal/control levels	**IL-8** **MIP-1ß** **RANTES** **TNF-α** **IL-10** **VEGF**	**16.0** **60** **7900** **1-12** **44** **170**	279 280
Infectious disease			
Toxoplasmic retinochoroiditis (with vasculitis)	IL-8	35	279
Lyme Borreliosis	IL-8 MIP-1ß	100-800 100-300	281
Viral infection (HCV)	IL-8 TNF-α	10-10000 10-100	280
Inflammatory disease			
Multiple sclerosis	IL-8 RANTES	40-200 100-600	282
Rheumatoid Arthritis and Osteoarthritis *	IL-8 MIP-1ß RANTES	80-150 80-120 8000-12000	283
Systemic lupus erthymatosis *	IL-8 IL-10 TNF-α IFN-γ	40 10 10-300 10	284 285
Sjogren's Syndrome *	IL-8 RANTES MIP-1β TNF-α	3 1300 20 32	286
Inflammatory bowel disease/ Crohn's Disease	IL-10 VEGF	140 440	287 288

*Diseases associated with high serum levels of CD23

LM609 is the clone name for the anti-αVβ3 integrin antibody-based therapeutic known as Vitaxin [289]. This humanised anti-αVβ3 antibody was developed by the company MedImmune as a treatment for inflammatory diseases and certain cancers [194, 290-292]. However, Vitaxin failed to prove effective in clinical trials for inflammatory diseases (such as rheumatoid arthritis and psoriasis). MedImmune have subsequently discontinued the development of Vitaxin as an anti-inflammatory treatment, although it is still in trials for use as an anti-cancer agent [293]. In light of our data, it is tempting to speculate that the reason Vitaxin is ineffective as an anti-inflammatory agent is that, while it targets the correct integrin, αVβ3, it is directed against the wrong epitope on the integrin. From the data presented herein, the critical site that governs cytokine production by αVβ3 ligation is bound by 23C6 and not LM609. LM609 still inhibts adhesion and this may explain its continued potential to be effective in the prevention of cancer metastasis. This suggests that there are distinct sites on the integrin- one that mediates adhesive reactions and one that mediates cytokine production. These conclusions are consistent with the potential existence of distinct RGD and non-RGD based binding sites on the integrins, as observed with the interaction of the αV integrins and CD23-derived peptides. It is also interesting to note that the inflammatory disorders (such as rheumatoid arthritis and psoriasis) in which αVβ3 is being targeted are those which are correlated with high serum levels of soluble CD23 [294].

6.3.2 Role of cytokines in physiological and pathological immune function

Specific ligation of selected integrins led to the production of high levels of cytokines and chemokines by monocytic cells and the subsequent activation of these cells to develop a more macrophage-like phenotype. The chemokines produced were capable of inducing the migration of THP-1 cells, Jurkat T cells and IB4 B cells across a membrane in an *in vitro* assay for migration. The concentrations of cytokines observed during these experiments are similar to concentrations observed in a number of infectious and inflammatory challenges observed *in vivo* (Table 6-2).These combined functions are all important during the immune response under both physiological and pathological conditions.

Figure 6-2 suggests how the combined functions of integrin ligation could contribute *in vivo* to the establishment of inflammation during pathogen invasion and in inflammatory disease such as RA. The process can be considered as stages A-D which encompass the onset of cytokine production by specific ligation of the integrin (A), the recruitment and activation of immune cells from the bloodstream to the site of stimulation (B), autocrine signalling leads to activation of the resident macrophage population (C), and when the inflammatory environment is established (D), which may also lead to a change in the cytokine profile from the original stimulus.

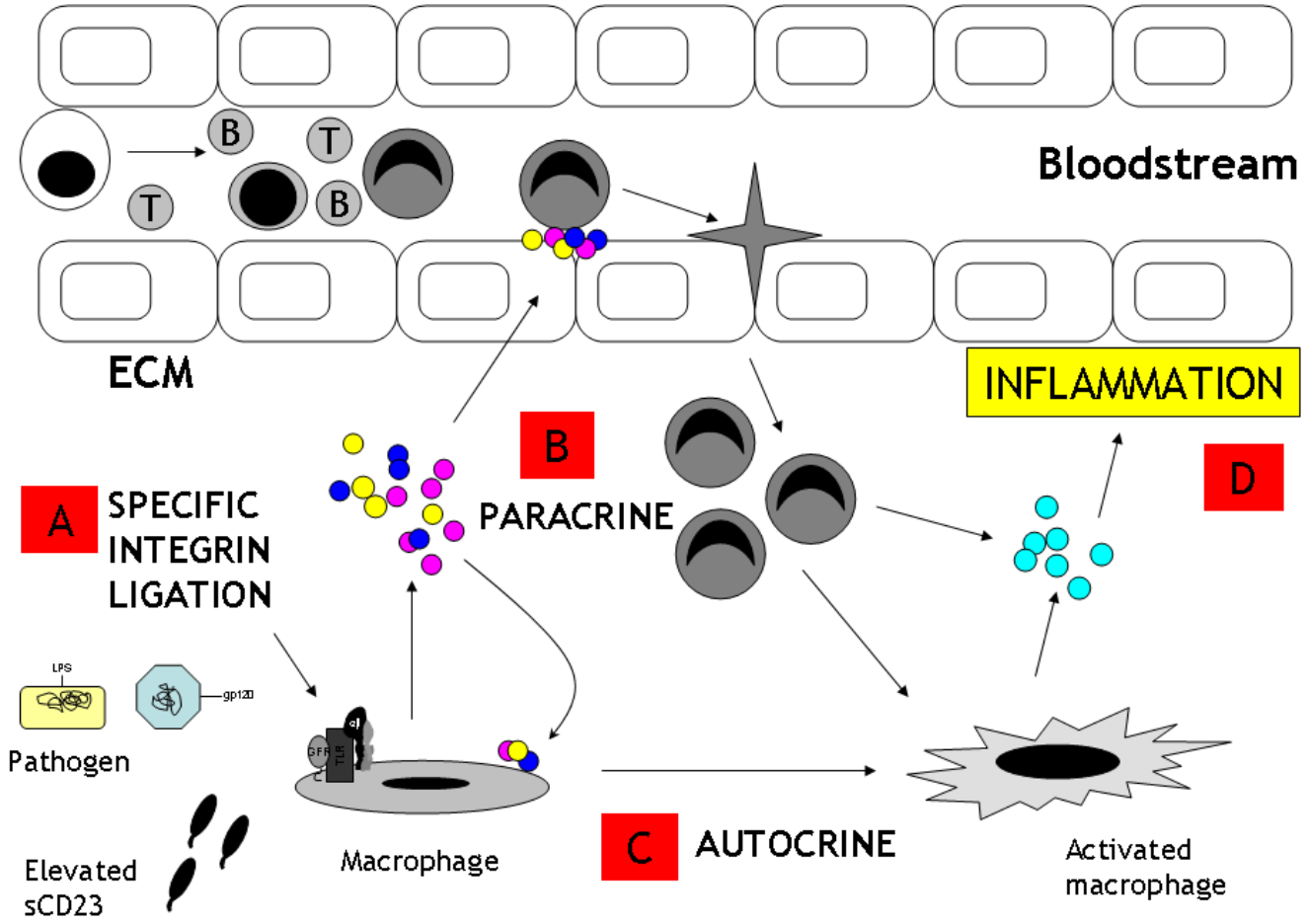

Figure 6-2 Schematic representation of the role of integrins in a model of inflammatory disease/infection

(A) Ligation of macrophage integrin by sCD23 or pathogen at the correct epitope triggers cytokine production. (B) Cytokines and chemokines have paracrine effects on surrounding cells and recruit immune cells from the bloodstream to the tissue. (C) Cytokines have autocrine effect on macrophage and lead to macrophage activation (D) Recruited cells and activated macrophages lead to establishment and maintenance of inflammation

Specific ligation of the integrin/integrin signalling complex on a macrophage induces high levels of cytokine release. In the case of an infection, this binding would be mediated by a pathogen receptor, such as LPS or zymosan, whereas in an inflammatory disorder, such as rheumatoid arthritis, the stimulus for cytokine production could be induced by the high levels of CD23 detected in serum. The production of TNF-α, IL-8, RANTES and MIP-1β can be considered as pro-inflammatory cytokines, which lead to the establishment of an inflammatory state.

The cytokines produced in response to integrin ligation will induce both paracrine and autocrine effects. The concentrations of cytokines and chemokines induced by integrin ligation are similar to the concentration ranges observed in the serum of patients with infectious and inflammatory diseases (Table 6-2). The chemokines diffuse into the surrounding tissues and recruit cells to the site of stimulation by activating integrins and inducing extravasation of immune cells from the bloodstream into the tissue. The integrin ligation and cytokines produced also have an autocrine effect on the original macrophage, which leads to activation and continued production of cytokines, to establish the inflammatory state. The activation of the macrophage by the initial stimulus may lead to a change in the cytokine profile. For example, under the conditions of our experiments, high levels of VEGF production were observed 48 hours after stimulation, suggesting that this may be a consequence of a change in the monocyte/macrophage biology. The initial stimulus will determine if the inflammation is productive, in the case of a pathogenic infection, or non-productive, in the case of an auto-immune/auto-inflammatory disorder such as rheumatoid arthritis.

6.4 Conclusion

This study has examined the interaction between CD23 and the αVβ3 and αVβ5 integrins and attempted to define the individual roles of individual CD23-binding integrins (αVβ3, αVβ5, αMβ2 and αXβ2) in the production of cytokines by monocytic cells and the activation of these cells. Further analysis of integrin-mediated signalling is challenging our view of these interesting receptors as mere adhesive structures. It is clear that integrins participate in a range of other modes of signalling in addition to those traditionally associated with adhesive or migratory functions. It is possible that these interactions will be mediated by an alternative site on the integrin that remains to be identified.

References

1. Janeway, C., Travers, P., Walport, M. & Shlomchik, M. J. Imunobiology, the immune system in health and disease (Garland Science Publishing, New York, 2005).
2. Gordon, S. The macrophage: past, present and future. Eur J Immunol 37 Suppl 1, S9-17 (2007).
3. Delneste, Y. et al. Interferon-gamma switches monocyte differentiation from dendritic cells to macrophages. Blood 101, 143-50 (2003).
4. Chomarat, P., Dantin, C., Bennett, L., Banchereau, J. & Palucka, A. K. TNF skews monocyte differentiation from macrophages to dendritic cells. J Immunol 171, 2262-9 (2003).
5. Fujikawa, Y., Quinn, J. M., Sabokbar, A., McGee, J. O. & Athanasou, N. A. The human osteoclast precursor circulates in the monocyte fraction. Endocrinology 137, 4058-60 (1996).
6. Gordon, S. Alternative activation of macrophages. Nat Rev Immunol 3, 23-35 (2003).
7. Mosser, D. M. The many faces of macrophage activation. J Leukoc Biol 73, 209-12 (2003).
8. Ma, J. et al. Regulation of macrophage activation. Cell Mol Life Sci 60, 2334-46 (2003).
9. Elenkov, I. J., Iezzoni, D. G., Daly, A., Harris, A. G. & Chrousos, G. P. Cytokine dysregulation, inflammation and well-being. Neuroimmunomodulation 12, 255-69 (2005).
10. Woo, P. Cytokine polymorphisms and inflammation. Clin Exp Rheumatol 18, 767-71 (2000).
11. Hanada, T. & Yoshimura, A. Regulation of cytokine signaling and inflammation. Cytokine Growth Factor Rev 13, 413-21 (2002).
12. Cinamon, G. et al. Novel chemokine functions in lymphocyte migration through vascular endothelium under shear flow. J Leukoc Biol 69, 860-6 (2001).
13. Taub, D. D. & Oppenheim, J. J. Chemokines, inflammation and the immune system. Ther Immunol 1, 229-46 (1994).
14. Mantovani, A. The chemokine system: redundancy for robust outputs. Immunol Today 20, 254-7 (1999).
15. Perretti, M. & Getting, S. J. Migration of specific leukocyte subsets in response to cytokine or chemokine application in vivo. Methods Mol Biol 225, 139-46 (2003).
16. Mantovani, A. et al. The chemokine system in diverse forms of macrophage activation and polarization. Trends Immunol 25, 677-86 (2004).
17. Bleul, C. C., Wu, L., Hoxie, J. A., Springer, T. A. & Mackay, C. R. The HIV coreceptors CXCR4 and CCR5 are differentially expressed and regulated on human T lymphocytes. Proc Natl Acad Sci U S A 94, 1925-30 (1997).
18. Zaitseva, M. et al. Expression and function of CCR5 and CXCR4 on human Langerhans cells and macrophages: implications for HIV primary infection. Nat Med 3, 1369-75 (1997).
19. Lu, Z. et al. Evolution of HIV-1 coreceptor usage through interactions with distinct CCR5 and CXCR4 domains. Proc Natl Acad Sci U S A 94, 6426-31 (1997).
20. De Clercq, E. & Schols, D. Inhibition of HIV infection by CXCR4 and CCR5 chemokine receptor antagonists. Antivir Chem Chemother 12 Suppl 1, 19-31 (2001).
21. D'Apuzzo, M. et al. The chemokine SDF-1, stromal cell-derived factor 1, attracts early stage B cell precursors via the chemokine receptor CXCR4. Eur J Immunol 27, 1788-93 (1997).
22. Bauer, J. W. et al. Elevated serum levels of interferon-regulated chemokines are biomarkers for active human systemic lupus erythematosus. PLoS Med 3, e491 (2006).
23. Vergunst, C. E., van de Sande, M. G., Lebre, M. C. & Tak, P. P. The role of chemokines in rheumatoid arthritis and osteoarthritis. Scand J Rheumatol 34, 415-25 (2005).
24. Allavena, P., Garlanda, C., Borrello, M. G., Sica, A. & Mantovani, A. Pathways connecting inflammation and cancer. Curr Opin Genet Dev (2008).
25. Barton, G. M. A calculated response: control of inflammation by the innate immune system. J Clin Invest 118, 413-20 (2008).
26. Kiyono, H., Kweon, M. N., Hiroi, T. & Takahashi, I. The mucosal immune system: from specialized immune defense to inflammation and allergy. Acta Odontol Scand 59, 145-53 (2001).
27. Bodolay, E., Koch, A. E., Kim, J., Szegedi, G. & Szekanecz, Z. Angiogenesis and chemokines in rheumatoid arthritis and other systemic inflammatory rheumatic diseases. J Cell Mol Med 6, 357-76 (2002).

28. Szekanecz, Z., Szucs, G., Szanto, S. & Koch, A. E. Chemokines in rheumatic diseases. Curr Drug Targets 7, 91-102 (2006).
29. Mossalayi, M. D., Arock, M. & Debre, P. CD23/Fc epsilon RII: signaling and clinical implication. Int Rev Immunol 16, 129-46 (1997).
30. Dugas, B., Mencia-Huerta, J. M. & Braquet, P. The low affinity receptor for IgE (CD23) in human: a multifunctional receptor/cytokine? Eur Cytokine Netw 3, 35-41 (1992).
31. Gordon, J. et al. CD23: a multi-functional receptor/lymphokine? Immunol Today 10, 153-7 (1989).
32. Bonnefoy, J. Y. et al. Structure and functions of CD23. Int Rev Immunol 16, 113-28 (1997).
33. Weskamp, G. et al. ADAM10 is a principal 'sheddase' of the low-affinity immunoglobulin E receptor CD23. Nat Immunol 7, 1293-8 (2006).
34. Lemieux, G. A. et al. The low affinity IgE receptor (CD23) is cleaved by the metalloproteinase ADAM10. J Biol Chem 282, 14836-44 (2007).
35. Marolewski, A. E. et al. CD23 (FcepsilonRII) release from cell membranes is mediated by a membrane-bound metalloprotease. Biochem J 333 (Pt 3), 573-9 (1998).
36. Arock, M. et al. Soluble CD23 increases IL-3 induction of histamine synthesis by human bone marrow cells. Int Arch Allergy Appl Immunol 96, 190-2 (1991).
37. Mossalayi, M. D. et al. Cytokine effects of CD23 are mediated by an epitope distinct from the IgE binding site. Embo J 11, 4323-8 (1992).
38. Armant, M., Ishihara, H., Rubio, M., Delespesse, G. & Sarfati, M. Regulation of cytokine production by soluble CD23: costimulation of interferon gamma secretion and triggering of tumor necrosis factor alpha release. J Exp Med 180, 1005-11 (1994).
39. Herbelin, A., Elhadad, S., Ouaaz, F., de Groote, D. & Descamps-Latscha, B. Soluble CD23 potentiates interleukin-1-induced secretion of interleukin-6 and interleukin-1 receptor antagonist by human monocytes. Eur J Immunol 24, 1869-73 (1994).
40. Hermann, P. et al. The vitronectin receptor and its associated CD47 molecule mediates proinflammatory cytokine synthesis in human monocytes by interaction with soluble CD23. J Cell Biol 144, 767-75 (1999).
41. Rezzonico, R., Imbert, V., Chicheportiche, R. & Dayer, J. M. Ligation of CD11b and CD11c beta(2) integrins by antibodies or soluble CD23 induces macrophage inflammatory protein 1alpha (MIP-1alpha) and MIP-1beta production in primary human monocytes through a pathway dependent on nuclear factor-kappaB. Blood 97, 2932-40 (2001).
42. Sutton, B. J. & Gould, H. J. The human IgE network. Nature 366, 421-8 (1993).
43. Schwarzmeier, J. D. et al. The role of soluble CD23 in distinguishing stable and progressive forms of B-chronic lymphocytic leukemia. Leuk Lymphoma 43, 549-54 (2002).
44. Saka, B. et al. Prognostic importance of soluble CD23 in B-cell chronic lymphocytic leukemia. Clin Lab Haematol 28, 30-5 (2006).
45. Kalil, N. & Cheson, B. D. Management of chronic lymphocytic leukaemia. Drugs Aging 16, 9-27 (2000).
46. Hamblin, T. J. Achieving optimal outcomes in chronic lymphocytic leukaemia. Drugs 61, 593-611 (2001).
47. Wagner, S. D. & Cwynarski, K. Chronic lymphocytic leukaemia: new biological markers for assessing prognosis. Hematol J 5, 197-201 (2004).
48. Chomarat, P., Briolay, J., Banchereau, J. & Miossec, P. Increased production of soluble CD23 in rheumatoid arthritis, and its regulation by interleukin-4. Arthritis Rheum 36, 234-42 (1993).
49. Fernandez-Gutierrez, B., Hernandez-Garcia, C., Banares, A. A. & Jover, J. A. CD23 hyperexpression in rheumatoid arthritis: evidence for a B cell hyperresponsiveness to cognate and noncognate T-cell signals. Clin Immunol Immunopathol 72, 321-7 (1994).
50. Rezonzew, R. & Newkirk, M. M. Impaired release of sCD23 by activated B-cells from RA patients. Clin Immunol Immunopathol 71, 156-63 (1994).
51. Bansal, A. S. et al. Increased levels of sCD23 in rheumatoid arthritis are related to disease status. Clin Exp Rheumatol 12, 281-5 (1994).
52. Massa, M. et al. Serum soluble CD23 levels and CD23 expression on peripheral blood mononuclear cells in juvenile chronic arthritis. Clin Exp Rheumatol 16, 611-6 (1998).
53. Vaiopoulos, G. et al. Hemoglobin levels correlate with serum soluble CD23 and TNF-Rs concentrations in patients with rheumatoid arthritis. Haematologia (Budap) 29, 89-99 (1998).
54. Kleinau, S., Martinsson, P., Gustavsson, S. & Heyman, B. Importance of CD23 for collagen-induced arthritis: delayed onset and reduced severity in CD23-deficient mice. J Immunol 162, 4266-70 (1999).
55. Ribbens, C. et al. Increased synovial fluid levels of soluble CD23 are associated with an erosive status in rheumatoid arthritis (RA). Clin Exp Immunol 120, 194-9 (2000).

56. De Miguel, S. et al. Mechanisms of CD23 hyperexpression on B cells from patients with rheumatoid arthritis. J Rheumatol 28, 1222-8 (2001).
57. Swendeman, S. L. & Thorley-Lawson, D. Soluble CD23/BLAST-2 (S-CD23/Blast-2) and its role in B cell proliferation. Curr Top Microbiol Immunol 141, 157-64 (1988).
58. Kijimoto-Ochiai, S. & Uede, T. CD23 molecule acts as a galactose-binding lectin in the cell aggregation of EBV-transformed human B-cell lines. Glycobiology 5, 443-8 (1995).
59. Liu, Y. J. et al. Recombinant 25-kDa CD23 and interleukin 1 alpha promote the survival of germinal center B cells: evidence for bifurcation in the development of centrocytes rescued from apoptosis. Eur J Immunol 21, 1107-14 (1991).
60. Dalloul, A. H., Fourcade, C., Debre, P. & Mossalayi, M. D. Thymic epithelial cell-derived supernatants sustain the maturation of human prothymocytes: involvement of interleukin 1 and CD23. Eur J Immunol 21, 2633-6 (1991).
61. Kijimoto-Ochiai, S. CD23 (the low-affinity IgE receptor) as a C-type lectin: a multidomain and multifunctional molecule. Cell Mol Life Sci 59, 648-64 (2002).
62. Hibbert, R. G. et al. The structure of human CD23 and its interactions with IgE and CD21. J Exp Med 202, 751-60 (2005).
63. Wurzburg, B. A., Tarchevskaya, S. S. & Jardetzky, T. S. Structural changes in the lectin domain of CD23, the low-affinity IgE receptor, upon calcium binding. Structure 14, 1049-58 (2006).
64. Beavil, A. J., Edmeades, R. L., Gould, H. J. & Sutton, B. J. Alpha-helical coiled-coil stalks in the low-affinity receptor for IgE (Fc epsilon RII/CD23) and related C-type lectins. Proc Natl Acad Sci U S A 89, 753-7 (1992).
65. Yokota, A. et al. Two forms of the low-affinity Fc receptor for IgE differentially mediate endocytosis and phagocytosis: identification of the critical cytoplasmic domains. Proc Natl Acad Sci U S A 89, 5030-4 (1992).
66. Yokota, A. et al. Two species of human Fc epsilon receptor II (Fc epsilon RII/CD23): tissue-specific and IL-4-specific regulation of gene expression. Cell 55, 611-8 (1988).
67. Moulder, K. The role of RGD in CD23-mediated cell adhesion. Immunol Today 17, 198-9 (1996).
68. Steiner, B., Trzeciak, A., Pfenninger, G. & Kouns, W. C. Peptides derived from a sequence within beta 3 integrin bind to platelet alpha IIb beta 3 (GPIIb-IIIa) and inhibit ligand binding. J Biol Chem 268, 6870-3 (1993).
69. Conrad, D. H. Fc epsilon RII/CD23: the low affinity receptor for IgE. Annu Rev Immunol 8, 623-45 (1990).
70. Aubry, J. P., Pochon, S., Graber, P., Jansen, K. U. & Bonnefoy, J. Y. CD21 is a ligand for CD23 and regulates IgE production. Nature 358, 505-7 (1992).
71. Aubry, J. P. et al. CD23 interacts with a new functional extracytoplasmic domain involving N-linked oligosaccharides on CD21. J Immunol 152, 5806-13 (1994).
72. Bjorck, P., Elenstrom-Magnusson, C., Rosen, A., Severinson, E. & Paulie, S. CD23 and CD21 function as adhesion molecules in homotypic aggregation of human B lymphocytes. Eur J Immunol 23, 1771-5 (1993).
73. Bonnefoy, J. Y. et al. Regulation of IgE synthesis by CD23/CD21 interaction. Int Arch Allergy Immunol 107, 40-2 (1995).
74. Lecoanet-Henchoz, S. et al. CD23 regulates monocyte activation through a novel interaction with the adhesion molecules CD11b-CD18 and CD11c-CD18. Immunity. 3, 119-125 (1995).
75. Borland, G. et al. alphavbeta5 integrin sustains growth of human pre-B cells through an RGD-independent interaction with a basic domain of the CD23 protein. J Biol Chem 282, 27315-26 (2007).
76. Sayers, I., Housden, J. E., Spivey, A. C. & Helm, B. A. The importance of Lys-352 of human immunoglobulin E in FcepsilonRII/CD23 recognition. J Biol Chem 279, 35320-5 (2004).
77. Bonnefoy, J. Y. et al. A new pair of surface molecules involved in human IgE regulation. Immunol Today 14, 1-2 (1993).
78. Yu, P., Kosco-Vilbois, M., Richards, M., Kohler, G. & Lamers, M. C. Negative feedback regulation of IgE synthesis by murine CD23. Nature 369, 753-6 (1994).
79. Fremeaux-Bacchi, V. et al. Soluble CD21 (sCD21) forms biologically active complexes with CD23: sCD21 is present in normal plasma as a complex with trimeric CD23 and inhibits soluble CD23-induced IgE synthesis by B cells. Int Immunol 10, 1459-66 (1998).
80. Beavil, R. L., Graber, P., Aubonney, N., Bonnefoy, J. Y. & Gould, H. J. CD23/Fc epsilon RII and its soluble fragments can form oligomers on the cell surface and in solution. Immunology 84, 202-6 (1995).
81. McCloskey, N. et al. Soluble CD23 monomers inhibit and oligomers stimulate IGE synthesis in human B cells. J Biol Chem 282, 24083-91 (2007).

82. Gould, H. J. & Sutton, B. J. IgE in allergy and asthma today. Nat Rev Immunol 8, 205-17 (2008).
83. Aubry, J. P. et al. The 25-kDa soluble CD23 activates type III constitutive nitric oxide-synthase activity via CD11b and CD11c expressed by human monocytes. J Immunol 159, 614-22 (1997).
84. Rezzonico, R., Chicheportiche, R., Imbert, V. & Dayer, J. M. Engagement of CD11b and CD11c beta2 integrin by antibodies or soluble CD23 induces IL-1beta production on primary human monocytes through mitogen-activated protein kinase-dependent pathways. Blood 95, 3868-77 (2000).
85. Conrad, D. H., Ford, J. W., Sturgill, J. L. & Gibb, D. R. CD23: an overlooked regulator of allergic disease. Curr Allergy Asthma Rep 7, 331-7 (2007).
86. Conrad, D. H., Kilmon, M. A., Studer, E. J. & Cho, S. The low-affinity receptor for IgE (Fc epsilon RII or CD23) as a therapeutic target. Biochem Soc Trans 25, 393-7 (1997).
87. Arnaout, M. A., Goodman, S. L. & Xiong, J. P. Structure and mechanics of integrin-based cell adhesion. Curr Opin Cell Biol 19, 495-507 (2007).
88. Arnaout, M. A., Mahalingam, B. & Xiong, J. P. Integrin structure, allostery, and bidirectional signaling. Annu Rev Cell Dev Biol 21, 381-410 (2005).
89. Yamada, S., Brown, K. E. & Yamada, K. M. Differential mRNA regulation of integrin subunits alpha V, beta 1, beta 3, and beta 5 during mouse embryonic organogenesis. Cell Adhes.Commun. 3, 311-325 (1995).
90. Guo, W. & Giancotti, F. G. Integrin signalling during tumour progression. Nat Rev Mol Cell Biol 5, 816-26 (2004).
91. Clark, R. A., Ashcroft, G. S., Spencer, M. J., Larjava, H. & Ferguson, M. W. Re-epithelialization of normal human excisional wounds is associated with a switch from alpha v beta 5 to alpha v beta 6 integrins. Br.J.Dermatol. 135, 46-51 (1996).
92. Issekutz, T. B. In vivo blood monocyte migration to acute inflammatory reactions, IL-1 alpha, TNF-alpha, IFN-gamma, and C5a utilizes LFA-1, Mac-1, and VLA-4. The relative importance of each integrin. J Immunol 154, 6533-40 (1995).
93. Humphries, M. J. Integrin structure. Biochem Soc Trans 28, 311-39 (2000).
94. Xiong, J. P. et al. Crystal structure of the extracellular segment of integrin alpha Vbeta3. Science 294, 339-345 (2001).
95. Shimaoka, M., Takagi, J. & Springer, T. A. Conformational regulation of integrin structure and function. Annu Rev Biophys Biomol Struct 31, 485-516 (2002).
96. Shi, M. et al. The Crystal Structure of the Plexin-Semaphorin-Integrin Domain/Hybrid Domain/I-EGF1 Segment from the Human Integrin {beta}2 Subunit at 1.8-A Resolution. J.Biol Chem 280, 30586-30593 (2005).
97. Adair, B. D. et al. Three-dimensional EM structure of the ectodomain of integrin {alpha}V{beta}3 in a complex with fibronectin. J.Cell Biol. 168, 1109-1118 (2005).
98. Xiong, J. P. et al. Crystal structure of the extracellular segment of integrin alpha Vbeta3 in complex with an Arg-Gly-Asp ligand. Science 296, 151-155 (2002).
99. Takagi, J., Isobe, T., Takada, Y. & Saito, Y. Structural interlock between ligand-binding site and stalk-like region of beta1 integrin revealed by a monoclonal antibody recognizing conformation-dependent epitope. J Biochem 121, 914-21 (1997).
100. Kamata, T., Handa, M., Sato, Y., Ikeda, Y. & Aiso, S. Membrane-proximal {alpha}/{beta} stalk interactions differentially regulate integrin activation. J Biol Chem 280, 24775-83 (2005).
101. Ruoslahti, E. RGD and other recognition sequences for integrins. Annu Rev Cell Dev Biol 12, 697-715 (1996).
102. Papadopoulos, G. K., Ouzounis, C. & Eliopoulos, E. RGD sequences in several receptor proteins: novel cell adhesion function of receptors? Int J Biol Macromol 22, 51-7 (1998).
103. Villard, V. et al. Synthetic RGD-containing alpha-helical coiled coil peptides promote integrin-dependent cell adhesion. J Pept Sci 12, 206-12 (2006).
104. Pfaff, M. et al. Selective recognition of cyclic RGD peptides of NMR defined conformation by alpha IIb beta 3, alpha V beta 3, and alpha 5 beta 1 integrins. J.Biol.Chem. 269, 20233-20238 (1994).
105. Pierschbacher, M. D. & Ruoslahti, E. Influence of stereochemistry of the sequence Arg-Gly-Asp-Xaa on binding specificity in cell adhesion. J Biol Chem 262, 17294-8 (1987).
106. Schaffner, P. & Dard, M. M. Structure and function of RGD peptides involved in bone biology. Cell Mol Life Sci 60, 119-32 (2003).
107. Takagi, J. Structural basis for ligand recognition by RGD (Arg-Gly-Asp)-dependent integrins. Biochem Soc Trans 32, 403-6 (2004).
108. Pedchenko, V., Zent, R. & Hudson, B. G. Alpha(v)beta3 and alpha(v)beta5 integrins bind both the proximal RGD site and non-RGD motifs within noncollagenous (NC1) domain of the alpha3 chain of type IV collagen: implication for the mechanism of endothelia cell adhesion. J Biol Chem 279, 2772-80 (2004).

109. Vogel, B. E. et al. A novel integrin specificity exemplified by binding of the alpha v beta 5 integrin to the basic domain of the HIV Tat protein and vitronectin. J.Cell Biol. 121, 461-468 (1993).
110. Tselepis, V. H., Green, L. J. & Humphries, M. J. An RGD to LDV motif conversion within the disintegrin kistrin generates an integrin antagonist that retains potency but exhibits altered receptor specificity. Evidence for a functional equivalence of acidic integrin-binding motifs. J Biol Chem 272, 21341-8 (1997).
111. Pfaff, M., McLane, M. A., Beviglia, L., Niewiarowski, S. & Timpl, R. Comparison of disintegrins with limited variation in the RGD loop in their binding to purified integrins alpha IIb beta 3, alpha V beta 3 and alpha 5 beta 1 and in cell adhesion inhibition. Cell Adhes.Commun. 2, 491-501 (1994).
112. Gupta, S., Li, H. & Sampson, N. S. Characterization of fertilin beta-disintegrin binding specificity in sperm-egg adhesion. Bioorg Med Chem 8, 723-9 (2000).
113. Evans, J. P. Fertilin beta and other ADAMs as integrin ligands: insights into cell adhesion and fertilization. Bioessays 23, 628-39 (2001).
114. Maeshima, Y., Colorado, P. C. & Kalluri, R. Two RGD-independent alpha vbeta 3 integrin binding sites on tumstatin regulate distinct anti-tumor properties. J Biol Chem 275, 23745-50 (2000).
115. Dong, L. J., Hsieh, J. C. & Chung, A. E. Two distinct cell attachment sites in entactin are revealed by amino acid substitutions and deletion of the RGD sequence in the cysteine-rich epidermal growth factor repeat 2. J Biol Chem 270, 15838-43 (1995).
116. ffrench-Constant, C. & Colognato, H. Integrins: versatile integrators of extracellular signals. Trends Cell Biol 14, 678-86 (2004).
117. Yee, K. L., Weaver, V. M. & Hammer, D. A. Integrin-mediated signalling through the MAP-kinase pathway. IET Syst Biol 2, 8-15 (2008).
118. Calderwood, D. A., Shattil, S. J. & Ginsberg, M. H. Integrins and actin filaments: reciprocal regulation of cell adhesion and signaling. J Biol Chem 275, 22607-10 (2000).
119. Calderwood, D. A. & Ginsberg, M. H. Talin forges the links between integrins and actin. Nat Cell Biol 5, 694-7 (2003).
120. Lad, Y., Harburger, D. S. & Calderwood, D. A. Integrin cytoskeletal interactions. Methods Enzymol 426, 69-84 (2007).
121. Humphries, M. J. et al. Integrin structure: heady advances in ligand binding, but activation still makes the knees wobble. Trends Biochem.Sci. 28, 313-320 (2003).
122. Calderwood, D. A. Talin controls integrin activation. Biochem Soc Trans 32, 434-7 (2004).
123. Calderwood, D. A. Integrin activation. J Cell Sci 117, 657-66 (2004).
124. van der Flier, A. & Sonnenberg, A. Function and interactions of integrins. Cell Tissue Res 305, 285-98 (2001).
125. Takagi, J. & Springer, T. A. Integrin activation and structural rearrangement. Immunol Rev 186, 141-63 (2002).
126. Gline, S. E., Cambier, S., Govaerts, C. & Nishimura, S. L. A 50-A separation of the integrin alpha v beta 3 extracellular domain C termini reveals an intermediate activation state. J.Biol.Chem. 279, 54567-54572 (2004).
127. Gottschalk, K. E., Gunther, R. & Kessler, H. A three-state mechanism of integrin activation and signal transduction for integrin alpha(v)beta(3). Chembiochem. 3, 470-473 (2002).
128. Giancotti, F. G. & Ruoslahti, E. Integrin signaling. Science 285, 1028-32 (1999).
129. Zeisel, M. B. et al. Cross talk between MyD88 and focal adhesion kinase pathways. J Immunol 174, 7393-7 (2005).
130. Barberis, L. et al. Distinct roles of the adaptor protein Shc and focal adhesion kinase in integrin signaling to ERK. J Biol Chem 275, 36532-40 (2000).
131. Renard, P. & Raes, M. The proinflammatory transcription factor NFkappaB: a potential target for novel therapeutical strategies. Cell Biol Toxicol 15, 341-4 (1999).
132. Lien, E. & Ingalls, R. R. Toll-like receptors. Crit Care Med 30, S1-11 (2002).
133. Semaan, N., Alsaleh, G., Gottenberg, J. E., Wachsmann, D. & Sibilia, J. Etk/BMX, a Btk Family Tyrosine Kinase, and Mal Contribute to the Cross-Talk between MyD88 and FAK Pathways. J Immunol 180, 3485-91 (2008).
134. Alam, N. et al. The integrin-growth factor receptor duet. J Cell Physiol 213, 649-53 (2007).
135. Lee, J. W. & Juliano, R. Mitogenic signal transduction by integrin- and growth factor receptor-mediated pathways. Mol Cells 17, 188-202 (2004).
136. Eliceiri, B. P., Klemke, R., Stromblad, S. & Cheresh, D. A. Integrin alphavbeta3 requirement for sustained mitogen-activated protein kinase activity during angiogenesis. J Cell Biol 140, 1255-63 (1998).

137. Barillari, G. et al. Inflammatory cytokines synergize with the HIV-1 Tat protein to promote angiogenesis and Kaposi's sarcoma via induction of basic fibroblast growth factor and the alpha v beta 3 integrin. J.Immunol. 163, 1929-1935 (1999).
138. Masson-Gadais, B., Houle, F., Laferriere, J. & Huot, J. Integrin alphavbeta3, requirement for VEGFR2-mediated activation of SAPK2/p38 and for Hsp90-dependent phosphorylation of focal adhesion kinase in endothelial cells activated by VEGF. Cell Stress Chaperones 8, 37-52 (2003).
139. Woodard, A. S. et al. The synergistic activity of alphavbeta3 integrin and PDGF receptor increases cell migration. J Cell Sci 111 (Pt 4), 469-78 (1998).
140. Maile, L. A. & Clemmons, D. R. The alphaVbeta3 integrin regulates insulin-like growth factor I (IGF-I) receptor phosphorylation by altering the rate of recruitment of the Src-homology 2-containing phosphotyrosine phosphatase-2 to the activated IGF-I receptor. Endocrinology 143, 4259-64 (2002).
141. Brooks, P. C. et al. Insulin-like growth factor receptor cooperates with integrin alpha v beta 5 to promote tumor cell dissemination in vivo. J.Clin.Invest 99, 1390-1398 (1997).
142. Faccio, R., Takeshita, S., Zallone, A., Ross, F. P. & Teitelbaum, S. L. c-Fms and the alphavbeta3 integrin collaborate during osteoclast differentiation. J Clin Invest 111, 749-58 (2003).
143. Flaherty, S. F., Golenbock, D. T., Milham, F. H. & Ingalls, R. R. CD11/CD18 leukocyte integrins: new signaling receptors for bacterial endotoxin. J Surg Res 73, 85-9 (1997).
144. Harris, E. S., McIntyre, T. M., Prescott, S. M. & Zimmerman, G. A. The leukocyte integrins. J Biol Chem 275, 23409-12 (2000).
145. Stewart, M., Thiel, M. & Hogg, N. Leukocyte integrins. Curr Opin Cell Biol 7, 690-6 (1995).
146. Dugas, B., Mossalayi, M. D., Damais, C. & Kolb, J. P. Nitric oxide production by human monocytes: evidence for a role of CD23. Immunol Today 16, 574-80 (1995).
147. Smith, J. W., Vestal, D. J., Irwin, S. V., Burke, T. A. & Cheresh, D. A. Purification and functional characterization of integrin alpha v beta 5. An adhesion receptor for vitronectin. J.Biol.Chem. 265, 11008-11013 (1990).
148. Charo, I. F., Nannizzi, L., Smith, J. W. & Cheresh, D. A. The vitronectin receptor alpha v beta 3 binds fibronectin and acts in concert with alpha 5 beta 1 in promoting cellular attachment and spreading on fibronectin. J.Cell Biol. 111, 2795-2800 (1990).
149. Hultenby, K., Reinholt, F. P., Heinegard, D., Andersson, G. & Marks, S. C., Jr. Osteopontin: a ligand for the alpha v beta 3 integrin of the osteoclast clear zone in osteopetrotic (ia/ia) rats. Ann N Y Acad Sci 760, 315-8 (1995).
150. Yokoyama, K., Zhang, X. P., Medved, L. & Takada, Y. Specific binding of integrin alpha v beta 3 to the fibrinogen gamma and alpha E chain C-terminal domains. Biochemistry 38, 5872-5877 (1999).
151. Denis, C., Williams, J. A., Lu, X., Meyer, D. & Baruch, D. Solid-phase von Willebrand factor contains a conformationally active RGD motif that mediates endothelial cell adhesion through the alpha v beta 3 receptor. Blood 82, 3622-3630 (1993).
152. Sriramarao, P., Mendler, M. & Bourdon, M. A. Endothelial cell attachment and spreading on human tenascin is mediated by alpha 2 beta 1 and alpha v beta 3 integrins. J.Cell Sci. 105 (Pt 4), 1001-1012 (1993).
153. Gao, A. G., Lindberg, F. P., Dimitry, J. M., Brown, E. J. & Frazier, W. A. Thrombospondin modulates alpha v beta 3 function through integrin-associated protein. J.Cell Biol. 135, 533-544 (1996).
154. Zhang, H., Li, Z., Viklund, E. K. & Stromblad, S. P21-activated kinase 4 interacts with integrin alpha v beta 5 and regulates alpha v beta 5-mediated cell migration. J.Cell Biol. 158, 1287-1297 (2002).
155. Horton, M. A. The alpha v beta 3 integrin "vitronectin receptor". Int.J.Biochem.Cell Biol. 29, 721-725 (1997).
156. Conforti, G., Calza, M. & Beltran-Nunez, A. Alpha v beta 5 integrin is localized at focal contacts by HT-1080 fibrosarcoma cells and human skin fibroblasts attached to vitronectin. Cell Adhes.Commun. 1, 279-293 (1994).
157. Panetti, T. S., Wilcox, S. A., Horzempa, C. & McKeown-Longo, P. J. Alpha v beta 5 integrin receptor-mediated endocytosis of vitronectin is protein kinase C-dependent. J.Biol.Chem. 270, 18593-18597 (1995).
158. van Leeuwen, R. L. et al. Attachment, spreading and migration of melanoma cells on vitronectin. The role of alpha V beta 3 and alpha V beta 5 integrins. Exp.Dermatol. 5, 308-315 (1996).
159. Felding-Habermann, B., Ruggeri, Z. M. & Cheresh, D. A. Distinct biological consequences of integrin alpha v beta 3-mediated melanoma cell adhesion to fibrinogen and its plasmic fragments. J.Biol.Chem. 267, 5070-5077 (1992).

160. Zimolo, Z. et al. Soluble alpha v beta 3-integrin ligands raise [Ca2+]i in rat osteoclasts and mouse-derived osteoclast-like cells. Am.J.Physiol 266, C376-C381 (1994).
161. Miyauchi, A. et al. Binding of osteopontin to the osteoclast integrin alpha v beta 3. Osteoporos Int 3 Suppl 1, 132-5 (1993).
162. Seftor, R. E. et al. Role of the alpha v beta 3 integrin in human melanoma cell invasion. Proc.Natl.Acad.Sci.U.S.A 89, 1557-1561 (1992).
163. Danen, E. H. et al. Emergence of alpha 5 beta 1 fibronectin- and alpha v beta 3 vitronectin-receptor expression in melanocytic tumour progression. Histopathology 24, 249-256 (1994).
164. Vellon, L., Menendez, J. A. & Lupu, R. alpha(V)beta(3) integrin regulates heregulin (HRG)-induced cell proliferation and survival in breast cancer. Oncogene (2005).
165. Tsuchiya, S. et al. Establishment and characterization of a human acute monocytic leukemia cell line (THP-1). Int J Cancer 26, 171-6 (1980).
166. Sundstrom, C. & Nilsson, K. Establishment and characterization of a human histiocytic lymphoma cell line (U-937). Int J Cancer 17, 565-77 (1976).
167. Schneider, U., Schwenk, H. U. & Bornkamm, G. Characterization of EBV-genome negative "null" and "T" cell lines derived from children with acute lymphoblastic leukemia and leukemic transformed non-Hodgkin lymphoma. Int J Cancer 19, 621-6 (1977).
168. Hurley, E. A., Klaman, L. D., Agger, S., Lawrence, J. B. & Thorley-Lawson, D. A. The prototypical Epstein-Barr virus-transformed lymphoblastoid cell line IB4 is an unusual variant containing integrated but no episomal viral DNA. J Virol 65, 3958-63 (1991).
169. Laemmli, U. K. Cleavage of structural proteins during the assembly of the head of bacteriophage T4. Nature 227, 680-5 (1970).
170. Myszka, D. G. Improving biosensor analysis. J Mol Recognit 12, 279-84 (1999).
171. Riener, C. K., Kada, G. & Gruber, H. J. Quick measurement of protein sulfhydryls with Ellman's reagent and with 4,4'-dithiodipyridine. Anal Bioanal Chem 373, 266-76 (2002).
172. Lecoanet-Henchoz, S. et al. CD23 regulates monocyte activation through a novel interaction with the adhesion molecules CD11b-CD18 and CD11c-CD18. Immunity 3, 119-25 (1995).
173. Kijimoto-Ochiai, S. & Noguchi, A. Two peptides from CD23, including the inverse RGD sequence and its related peptide, interact with the MHC class II molecule. Biochem Biophys Res Commun 267, 686-91 (2000).
174. White, L. J. et al. Inhibition of apoptosis in a human pre-B-cell line by CD23 is mediated via a novel receptor. Blood 90, 234-43 (1997).
175. Ruoslahti, E. & Pierschbacher, M. D. New perspectives in cell adhesion: RGD and integrins. Science 238, 491-7 (1987).
176. Gehlsen, K. R., Sriramarao, P., Furcht, L. T. & Skubitz, A. P. A synthetic peptide derived from the carboxy terminus of the laminin A chain represents a binding site for the alpha 3 beta 1 integrin. J Cell Biol 117, 449-59 (1992).
177. Ivaska, J. et al. A peptide inhibiting the collagen binding function of integrin alpha2I domain. J Biol Chem 274, 3513-21 (1999).
178. Wayner, E. A. & Carter, W. G. Identification of multiple cell adhesion receptors for collagen and fibronectin in human fibrosarcoma cells possessing unique alpha and common beta subunits. J Cell Biol 105, 1873-84 (1987).
179. Mayer, R. J. et al. CD23 shedding: requirements for substrate recognition and inhibition by dipeptide hydroxamic acids. Inflamm Res 51, 85-90 (2002).
180. Roman, V. et al. Characterization of a constitutive type III nitric oxide synthase in human U937 monocytic cells: stimulation by soluble CD23. Immunology 91, 643-8 (1997).
181. Gresham, H. D., Graham, I. L., Anderson, D. C. & Brown, E. J. Leukocyte adhesion-deficient neutrophils fail to amplify phagocytic function in response to stimulation. Evidence for CD11b/CD18-dependent and -independent mechanisms of phagocytosis. J Clin Invest 88, 588-97 (1991).
182. Shahan, T. A. et al. Identification of CD47/integrin-associated protein and alpha(v)beta3 as two receptors for the alpha3(IV) chain of type IV collagen on tumor cells. Cancer Res 59, 4584-90 (1999).
183. Fujimoto, T. T., Katsutani, S., Shimomura, T. & Fujimura, K. Thrombospondin-bound integrin-associated protein (CD47) physically and functionally modifies integrin alphaIIbbeta3 by its extracellular domain. J Biol Chem 278, 26655-65 (2003).
184. Gonzalez, M., Merino, R., Gonzalez, A. L. & Merino, J. The ability of B cells to participate in allogeneic cognate T-B cell interactions in vitro depends on the presence of CD4+ T cells during their development. J Immunol 155, 1091-100 (1995).
185. Paul-Eugene, N. et al. Ligation of CD23 triggers cAMP generation and release of inflammatory mediators in human monocytes. J Immunol 149, 3066-71 (1992).
186. Gadgil, H. S. et al. Proteome of monocytes primed with lipopolysaccharide: analysis of the abundant proteins. Proteomics 3, 1767-80 (2003).

187. Blystone, S. D., Lindberg, F. P., Williams, M. P., McHugh, K. P. & Brown, E. J. Inducible tyrosine phosphorylation of the beta3 integrin requires the alphaV integrin cytoplasmic tail. J Biol Chem 271, 31458-62 (1996).
188. Fernandez, N., Renedo, M., Garcia-Rodriguez, C. & Sanchez Crespo, M. Activation of monocytic cells through Fc gamma receptors induces the expression of macrophage-inflammatory protein (MIP)-1 alpha, MIP-1 beta, and RANTES. J Immunol 169, 3321-8 (2002).
189. Torsteinsdottir, I., Arvidson, N. G., Hallgren, R. & Hakansson, L. Monocyte activation in rheumatoid arthritis (RA): increased integrin, Fc gamma and complement receptor expression and the effect of glucocorticoids. Clin Exp Immunol 115, 554-60 (1999).
190. Reumaux, D., Kuijpers, T. W., Hordijk, P. L., Duthilleul, P. & Roos, D. Involvement of Fcgamma receptors and beta2 integrins in neutrophil activation by anti-proteinase-3 or anti-myeloperoxidase antibodies. Clin Exp Immunol 134, 344-50 (2003).
191. Nagahata, H., Sawada, C., Higuchi, H., Teraoka, H. & Yamaguchi, M. Fc receptor-mediated phagocytosis, superoxide production and calcium signaling of beta 2 integrin-deficient bovine neutrophils. Microbiol Immunol 41, 747-50 (1997).
192. Nagahata, H., Higuchi, H., Goji, N., Noda, H. & Kuwabara, M. Functional characteristics of enhanced Fc receptor expression of beta 2 integrin-deficient bovine mononuclear phagocytes. Microbiol Immunol 40, 389-95 (1996).
193. Lecoanet-Henchoz, S. et al. Mouse CD23 regulates monocyte activation through an interaction with the adhesion molecule CD11b/CD18. Eur J Immunol 27, 2290-4 (1997).
194. Wilder, R. L. Integrin alpha V beta 3 as a target for treatment of rheumatoid arthritis and related rheumatic diseases. Ann.Rheum.Dis. 61 Suppl 2, ii96-ii99 (2002).
195. Switala-Jelen, K. et al. The biological functions of beta3 integrins. Folia Biol (Praha) 50, 143-52 (2004).
196. Hutchings, H., Ortega, N. & Plouet, J. Extracellular matrix-bound vascular endothelial growth factor promotes endothelial cell adhesion, migration, and survival through integrin ligation. Faseb J 17, 1520-2 (2003).
197. Tsou, R. & Isik, F. F. Integrin activation is required for VEGF and FGF receptor protein presence on human microvascular endothelial cells. Mol Cell Biochem 224, 81-9 (2001).
198. Matsumoto, T. & Claesson-Welsh, L. VEGF receptor signal transduction. Sci STKE 2001, RE21 (2001).
199. Gloe, T., Sohn, H. Y., Meininger, G. A. & Pohl, U. Shear stress-induced release of basic fibroblast growth factor from endothelial cells is mediated by matrix interaction via integrin alpha(v)beta3. J Biol Chem 277, 23453-8 (2002).
200. Harwood, F. L., Goomer, R. S., Gelberman, R. H., Silva, M. J. & Amiel, D. Regulation of alpha(v)beta3 and alpha5beta1 integrin receptors by basic fibroblast growth factor and platelet-derived growth factor-BB in intrasynovial flexor tendon cells. Wound Repair Regen 7, 381-8 (1999).
201. Klein, S. et al. Basic fibroblast growth factor modulates integrin expression in microvascular endothelial cells. Mol Biol Cell 4, 973-82 (1993).
202. Liu, G., Eskin, S. G. & Mikos, A. G. Integrin alpha(v)beta(3) is involved in stimulated migration of vascular adventitial fibroblasts by basic fibroblast growth factor but not platelet-derived growth factor. J.Cell Biochem. 83, 129-135 (2001).
203. Mawatari, K., Liu, B. & Kent, K. C. Activation of integrin receptors is required for growth factor-induced smooth muscle cell dysfunction. J Vasc Surg 31, 375-81 (2000).
204. Asano, Y. et al. Increased expression of integrin alpha(v)beta3 contributes to the establishment of autocrine TGF-beta signaling in scleroderma fibroblasts. J Immunol 175, 7708-18 (2005).
205. Chin, S. L. et al. A role for alphaV integrin subunit in TGF-beta-stimulated osteoclastogenesis. Biochem Biophys Res Commun 307, 1051-8 (2003).
206. Scaffidi, A. K. et al. alpha(v)beta(3) Integrin interacts with the transforming growth factor beta (TGFbeta) type II receptor to potentiate the proliferative effects of TGFbeta1 in living human lung fibroblasts. J.Biol.Chem. 279, 37726-37733 (2004).
207. Kuemmerle, J. F. Occupation of alphavbeta3-integrin by endogenous ligands modulates IGF-I receptor activation and proliferation of human intestinal smooth muscle. Am J Physiol Gastrointest Liver Physiol 290, G1194-202 (2006).
208. Strieth, S. et al. Antiangiogenic combination tumor therapy blocking alpha(v)-integrins and VEGF-receptor-2 increases therapeutic effects in vivo. Int J Cancer 119, 423-31 (2006).
209. Ross, F. P. & Teitelbaum, S. L. alphavbeta3 and macrophage colony-stimulating factor: partners in osteoclast biology. Immunol Rev 208, 88-105 (2005).
210. Elsegood, C. L. et al. M-CSF induces the stable interaction of cFms with alphaVbeta3 integrin in osteoclasts. Int J Biochem Cell Biol 38, 1518-29 (2006).

211. Hofmeister, V., Schrama, D. & Becker, J. C. Anti-cancer therapies targeting the tumor stroma. Cancer Immunol Immunother 57, 1-17 (2008).
212. Harris, T. D. et al. Design, synthesis, and evaluation of radiolabeled integrin alpha v beta 3 receptor antagonists for tumor imaging and radiotherapy. Cancer Biother.Radiopharm. 18, 627-641 (2003).
213. Kumar, C. C. Integrin alpha v beta 3 as a therapeutic target for blocking tumor-induced angiogenesis. Curr.Drug Targets. 4, 123-131 (2003).
214. Rader, C., Popkov, M., Neves, J. A. & Barbas, C. F., 3rd. Integrin alpha(v)beta3 targeted therapy for Kaposi's sarcoma with an in vitro evolved antibody. Faseb J 16, 2000-2 (2002).
215. Gutheil, J. C. et al. Targeted antiangiogenic therapy for cancer using Vitaxin: a humanized monoclonal antibody to the integrin alphavbeta3. Clin Cancer Res 6, 3056-61 (2000).
216. Janssen, M. L. et al. Tumor targeting with radiolabeled alpha(v)beta(3) integrin binding peptides in a nude mouse model. Cancer Res. 62, 6146-6151 (2002).
217. Duffield, J. S. The inflammatory macrophage: a story of Jekyll and Hyde. Clin Sci (Lond) 104, 27-38 (2003).
218. Pollard, J. W. Tumour-educated macrophages promote tumour progression and metastasis. Nat Rev Cancer 4, 71-8 (2004).
219. Mantovani, A., Allavena, P. & Sica, A. Tumour-associated macrophages as a prototypic type II polarised phagocyte population: role in tumour progression. Eur J Cancer 40, 1660-7 (2004).
220. Chandhoke, S. K., Williams, M., Schaefer, E., Zorn, L. & Blystone, S. D. Beta 3 integrin phosphorylation is essential for Arp3 organization into leukocyte alpha V beta 3-vitronectin adhesion contacts. J.Cell Sci. 117, 1431-1441 (2004).
221. Boettiger, D., Huber, F., Lynch, L. & Blystone, S. Activation of alpha(v)beta3-vitronectin binding is a multistage process in which increases in bond strength are dependent on Y747 and Y759 in the cytoplasmic domain of beta3. Mol Biol Cell 12, 1227-37 (2001).
222. Butler, B., Williams, M. P. & Blystone, S. D. Ligand-dependent activation of integrin alpha vbeta 3. J Biol Chem 278, 5264-70 (2003).
223. Li, Z., Xi, X. & Du, X. A mitogen-activated protein kinase-dependent signaling pathway in the activation of platelet integrin alpha IIbbeta3. J Biol Chem 276, 42226-32 (2001).
224. Maile, L. A., Badley-Clarke, J. & Clemmons, D. R. Structural analysis of the role of the beta 3 subunit of the alpha V beta 3 integrin in IGF-I signaling. J.Cell Sci. 114, 1417-1425 (2001).
225. Zhang, B., Hirahashi, J., Cullere, X. & Mayadas, T. N. Elucidation of molecular events leading to neutrophil apoptosis following phagocytosis: cross-talk between caspase 8, reactive oxygen species, and MAPK/ERK activation. J Biol Chem 278, 28443-54 (2003).
226. Weyts, F. A., Li, Y. S., van Leeuwen, J., Weinans, H. & Chien, S. ERK activation and alpha v beta 3 integrin signaling through Shc recruitment in response to mechanical stimulation in human osteoblasts. J.Cell Biochem. 87, 85-92 (2002).
227. Moore, C., Shen, X. D., Fondevila, C. & Coito, A. J. Fibronectin-alpha4beta1 integrin interactions modulate p42/44 MAPK phosphorylation in steatotic liver cold ischemia-reperfusion injury. Transplant Proc 37, 432-4 (2005).
228. Bergh, J. J. et al. Integrin {alpha}V{beta}3 Contains a Cell Surface Receptor Site for Thyroid Hormone that is Linked to Activation of MAPK and Induction of Angiogenesis. Endocrinology (2005).
229. Crews, C. M., Alessandrini, A. & Erikson, R. L. The primary structure of MEK, a protein kinase that phosphorylates the ERK gene product. Science 258, 478-80 (1992).
230. McGettrick, H. M. et al. Chemokine- and adhesion-dependent survival of neutrophils after transmigration through cytokine-stimulated endothelium. J Leukoc Biol 79, 779-88 (2006).
231. Paoletti, S. et al. A rich chemokine environment strongly enhances leukocyte migration and activities. Blood 105, 3405-12 (2005).
232. Ji, J. F., He, B. P., Dheen, S. T. & Tay, S. S. Interactions of chemokines and chemokine receptors mediate the migration of mesenchymal stem cells to the impaired site in the brain after hypoglossal nerve injury. Stem Cells 22, 415-27 (2004).
233. Gillitzer, R. Inflammation in human skin: a model to study chemokine-mediated leukocyte migration in vivo. J Pathol 194, 393-4 (2001).
234. Ogata, M. et al. Chemotactic response toward chemokines and its regulation by transforming growth factor-beta1 of murine bone marrow hematopoietic progenitor cell-derived different subset of dendritic cells. Blood 93, 3225-32 (1999).
235. Helming, L. & Gordon, S. Macrophage fusion induced by IL-4 alternative activation is a multistage process involving multiple target molecules. Eur J Immunol 37, 33-42 (2007).

236. Mantovani, A., Schioppa, T., Porta, C., Allavena, P. & Sica, A. Role of tumor-associated macrophages in tumor progression and invasion. Cancer Metastasis Rev 25, 315-22 (2006).
237. Schoppmann, S. F. et al. Tumor-associated macrophages express lymphatic endothelial growth factors and are related to peritumoral lymphangiogenesis. Am J Pathol 161, 947-56 (2002).
238. Valkovic, T. et al. Correlation between vascular endothelial growth factor, angiogenesis, and tumor-associated macrophages in invasive ductal breast carcinoma. Virchows Arch 440, 583-8 (2002).
239. Loiarro, M. et al. Peptide-mediated interference of TIR domain dimerization in MyD88 inhibits interleukin-1-dependent activation of NF-{kappa}B. J Biol Chem 280, 15809-14 (2005).
240. Sekimoto, H., Eipper-Mains, J., Pond-Tor, S. & Boney, C. M. {alpha}V{beta}3 integrins and Pyk2 mediate IGF-I activation of Src and MAPK in 3T3-L1 cells. Mol.Endocrinol. (2005).
241. Bhattacharyya, S. P. et al. Both adhesion to immobilized vitronectin and FcepsilonRI cross-linking cause enhanced focal adhesion kinase phosphorylation in murine mast cells. Immunology 98, 357-62 (1999).
242. Armulik, A., Velling, T. & Johansson, S. The integrin beta1 subunit transmembrane domain regulates phosphatidylinositol 3-kinase-dependent tyrosine phosphorylation of Crk-associated substrate. Mol Biol Cell 15, 2558-67 (2004).
243. Lyman, S., Gilmore, A., Burridge, K., Gidwitz, S. & White, G. C., 2nd. Integrin-mediated activation of focal adhesion kinase is independent of focal adhesion formation or integrin activation. Studies with activated and inhibitory beta3 cytoplasmic domain mutants. J Biol Chem 272, 22538-47 (1997).
244. Danilkovitch, A., Skeel, A. & Leonard, E. J. Macrophage stimulating protein-induced epithelial cell adhesion is mediated by a PI3-K-dependent, but FAK-independent mechanism. Exp Cell Res 248, 575-82 (1999).
245. Flo, T. H. et al. Involvement of CD14 and beta2-integrins in activating cells with soluble and particulate lipopolysaccharides and mannuronic acid polymers. Infect Immun 68, 6770-6 (2000).
246. Troelstra, A. et al. Lipopolysaccharide-coated erythrocytes activate human neutrophils via CD14 while subsequent binding is through CD11b/CD18. J Immunol 162, 4220-5 (1999).
247. Abdelilah, S. G. et al. Molecular characterization of the low-affinity IgE receptor Fc epsilonRII/CD23 expressed by human eosinophils. Int Immunol 10, 395-404 (1998).
248. Martinez, F. O., Gordon, S., Locati, M. & Mantovani, A. Transcriptional profiling of the human monocyte-to-macrophage differentiation and polarization: new molecules and patterns of gene expression. J Immunol 177, 7303-11 (2006).
249. Kimball, E. S., Kovacs, E., Clark, M. C. & Schneider, C. R. Activation of cytokine production and adhesion molecule expression on THP-1 myelomonocytic cells by macrophage colony-stimulating factor in combination with interferon-gamma. J Leukoc Biol 58, 585-94 (1995).
250. Shi, C., Zhang, X., Chen, Z., Robinson, M. K. & Simon, D. I. Leukocyte integrin Mac-1 recruits toll/interleukin-1 receptor superfamily signaling intermediates to modulate NF-kappaB activity. Circ Res 89, 859-65 (2001).
251. Cornaglia-Ferraris, P., De Maria, A., Cirillo, C., Cara, A. & Alessandri, G. Adhesion of human neuroblasts to HIV-1 tat. Pediatr Res 38, 792-6 (1995).
252. Gavrilovskaya, I. N., Brown, E. J., Ginsberg, M. H. & Mackow, E. R. Cellular entry of hantaviruses which cause hemorrhagic fever with renal syndrome is mediated by beta3 integrins. J Virol 73, 3951-9 (1999).
253. Roivainen, M. et al. Entry of coxsackievirus A9 into host cells: specific interactions with alpha v beta 3 integrin, the vitronectin receptor. Virology 203, 357-365 (1994).
254. Guerrero, C. A. et al. Integrin alpha(v)beta(3) mediates rotavirus cell entry. Proc.Natl.Acad.Sci.U.S.A 97, 14644-14649 (2000).
255. Chu, J. J. & Ng, M. L. Interaction of West Nile virus with alpha v beta 3 integrin mediates virus entry into cells. J.Biol.Chem. 279, 54533-54541 (2004).
256. Au, B. T., Williams, T. J. & Collins, P. D. Zymosan-induced IL-8 release from human neutrophils involves activation via the CD11b/CD18 receptor and endogenous platelet-activating factor as an autocrine modulator. J Immunol 152, 5411-9 (1994).
257. Wong, K. F., Luk, J. M., Cheng, R. H., Klickstein, L. B. & Fan, S. T. Characterization of two novel LPS-binding sites in leukocyte integrin betaA domain. Faseb J 21, 3231-9 (2007).

258. Goldman, M. J. & Wilson, J. M. Expression of alpha v beta 5 integrin is necessary for efficient adenovirus-mediated gene transfer in the human airway. J.Virol. 69, 5951-5958 (1995).
259. Wickham, T. J., Filardo, E. J., Cheresh, D. A. & Nemerow, G. R. Integrin alpha v beta 5 selectively promotes adenovirus mediated cell membrane permeabilization. J.Cell Biol. 127, 257-264 (1994).
260. Wickham, T. J., Mathias, P., Cheresh, D. A. & Nemerow, G. R. Integrins alpha v beta 3 and alpha v beta 5 promote adenovirus internalization but not virus attachment. Cell 73, 309-319 (1993).
261. Jimenez-Martinez, M. C. et al. [Expression of B7 molecules and TLR-9 on corneal epithelial cells infected with adenovirus: clinico-pathological implications in viral keratoconjunctivitis]. Arch Soc Esp Oftalmol 81, 391-400 (2006).
262. Triantafilou, M., Triantafilou, K., Wilson, K. M., Takada, Y. & Fernandez, N. High affinity interactions of Coxsackievirus A9 with integrin alphavbeta3 (CD51/61) require the CYDMKTTC sequence of beta3, but do not require the RGD sequence of the CAV-9 VP1 protein. Hum Immunol 61, 453-9 (2000).
263. Lafrenie, R. M., Lee, S. F., Hewlett, I. K., Yamada, K. M. & Dhawan, S. Involvement of integrin alphavbeta3 in the pathogenesis of human immunodeficiency virus type 1 infection in monocytes. Virology 297, 31-8 (2002).
264. Tachado, S. D., Zhang, J., Zhu, J., Patel, N. & Koziel, H. HIV impairs TNF-alpha release in response to Toll-like receptor 4 stimulation in human macrophages in vitro. Am J Respir Cell Mol Biol 33, 610-21 (2005).
265. Meier, A. et al. MyD88-dependent immune activation mediated by human immunodeficiency virus type 1-encoded Toll-like receptor ligands. J Virol 81, 8180-91 (2007).
266. Heil, F. et al. Species-specific recognition of single-stranded RNA via toll-like receptor 7 and 8. Science 303, 1526-9 (2004).
267. Forsyth, C. B., Plow, E. F. & Zhang, L. Interaction of the fungal pathogen Candida albicans with integrin CD11b/CD18: recognition by the I domain is modulated by the lectin-like domain and the CD18 subunit. J Immunol 161, 6198-205 (1998).
268. Lavigne, L. M. et al. Integrin engagement mediates the human polymorphonuclear leukocyte response to a fungal pathogen-associated molecular pattern. J Immunol 178, 7276-82 (2007).
269. Sturtevant, J. & Calderone, R. Candida albicans adhesins: Biochemical aspects and virulence. Rev Iberoam Micol 14, 90-7 (1997).
270. Blasi, E. et al. Biological importance of the two Toll-like receptors, TLR2 and TLR4, in macrophage response to infection with Candida albicans. FEMS Immunol Med Microbiol 44, 69-79 (2005).
271. Corbucci, C. et al. Immune response to Candida albicans is preserved despite defect in O-mannosylation of secretory proteins. Med Mycol 45, 709-19 (2007).
272. Netea, M. G. et al. Toll-like receptor 2 suppresses immunity against Candida albicans through induction of IL-10 and regulatory T cells. J Immunol 172, 3712-8 (2004).
273. Perera, P. Y. et al. CD11b/CD18 acts in concert with CD14 and Toll-like receptor (TLR) 4 to elicit full lipopolysaccharide and taxol-inducible gene expression. J Immunol 166, 574-81 (2001).
274. Sabroe, I., Jones, E. C., Usher, L. R., Whyte, M. K. & Dower, S. K. Toll-like receptor (TLR)2 and TLR4 in human peripheral blood granulocytes: a critical role for monocytes in leukocyte lipopolysaccharide responses. J Immunol 168, 4701-10 (2002).
275. Petersen, M. M., Steadman, R. & Williams, J. D. Protein kinase C activation modulates tumour necrosis factor-alpha priming of human neutrophils for zymosan-induced leukotriene B4 release. Immunology 75, 275-80 (1992).
276. Steadman, R., Petersen, M. M. & Williams, J. D. CD11b/CD18-dependent stimulation of leukotriene B4 synthesis by human neutrophils (PMN) is synergistically enhanced by tumour necrosis factor alpha and low dose diacylglycerol. Int J Biochem Cell Biol 28, 771-6 (1996).
277. Hynes, R. O. A reevaluation of integrins as regulators of angiogenesis. Nat Med 8, 918-21 (2002).
278. Mazzone, A. & Ricevuti, G. Leukocyte CD11/CD18 integrins: biological and clinical relevance. Haematologica 80, 161-75 (1995).
279. Goncalves, R. M. et al. Increased serum levels of CXCL8 chemokine in acute toxoplasmic retinochoroiditis. Acta Ophthalmol Scand 85, 871-6 (2007).
280. Polyak, S. J., Khabar, K. S., Rezeiq, M. & Gretch, D. R. Elevated levels of interleukin-8 in serum are associated with hepatitis C virus infection and resistance to interferon therapy. J Virol 75, 6209-11 (2001).

281. Grygorczuk, S. et al. Concentrations of macrophage inflammatory proteins MIP-1alpha and MIP-1beta and interleukin 8 (il-8) in lyme borreliosis. Infection 32, 350-5 (2004).
282. Bartosik-Psujek, H. & Stelmasiak, Z. The levels of chemokines CXCL8, CCL2 and CCL5 in multiple sclerosis patients are linked to the activity of the disease. Eur J Neurol 12, 49-54 (2005).
283. Torikai, E., Kageyama, Y., Suzuki, M., Ichikawa, T. & Nagano, A. The effect of infliximab on chemokines in patients with rheumatoid arthritis. Clin Rheumatol 26, 1088-93 (2007).
284. al-Janadi, M., al-Balla, S., al-Dalaan, A. & Raziuddin, S. Cytokine profile in systemic lupus erythematosus, rheumatoid arthritis, and other rheumatic diseases. J Clin Immunol 13, 58-67 (1993).
285. Al-Mutairi, S. et al. Lupus patients with pulmonary involvement have a pro-inflammatory cytokines profile. Rheumatol Int 27, 621-30 (2007).
286. Szodoray, P., Alex, P., Brun, J. G., Centola, M. & Jonsson, R. Circulating cytokines in primary Sjogren's syndrome determined by a multiplex cytokine array system. Scand J Immunol 59, 592-9 (2004).
287. Kucharzik, T., Stoll, R., Lugering, N. & Domschke, W. Circulating antiinflammatory cytokine IL-10 in patients with inflammatory bowel disease (IBD). Clin Exp Immunol 100, 452-6 (1995).
288. Bousvaros, A. et al. Elevated serum vascular endothelial growth factor in children and young adults with Crohn's disease. Dig Dis Sci 44, 424-30 (1999).
289. Wu, H. et al. Stepwise in vitro affinity maturation of Vitaxin, an alphav beta3-specific humanized mAb. Proc Natl Acad Sci U S A 95, 6037-42 (1998).
290. Gramoun, A. et al. Effects of Vitaxin, a novel therapeutic in trial for metastatic bone tumors, on osteoclast functions in vitro. J Cell Biochem 102, 341-52 (2007).
291. Posey, J. A. et al. A pilot trial of Vitaxin, a humanized anti-vitronectin receptor (anti alpha v beta 3) antibody in patients with metastatic cancer. Cancer Biother.Radiopharm. 16, 125-132 (2001).
292. Coleman, K. R., Braden, G. A., Willingham, M. C. & Sane, D. C. Vitaxin, a humanized monoclonal antibody to the vitronectin receptor (alphavbeta3), reduces neointimal hyperplasia and total vessel area after balloon injury in hypercholesterolemic rabbits. Circ Res 84, 1268-76 (1999).
293. Rosenwald, M. S. in Washington Post E05 (Washington, 2004).
294. Bonnefoy, J. Y. et al. A new role for CD23 in inflammation. Immunol Today 17, 418-20 (1996).